
THE UNIVERSITY
*of* EDINBURGH

# Manipulating macrophages to enhance liver regeneration

Benjamin Mark Stutchfield

Submitted for the degree:

Doctor of Philosophy in Regenerative Medicine

University of Edinburgh

2014

# Abstract

Acute liver failure confers a high risk of death, with liver transplantation offering the only effective therapy for life-threatening cases. Hepatic macrophages are crucial for innate immune integrity and effective hepatocyte proliferation. The macrophage may therefore present a novel therapeutic target to enhance regeneration following acute liver injury.

In this thesis I describe the development and use of mouse models of liver injury including partial hepatectomy, partial hepatectomy plus chronic liver injury and paracetamol intoxication. I show the development of liver function assays in these models including quantification of hepatic clearance of indocyanine green by fluorescent imaging and assessment of hepatic phagocytic capacity using fluorescent microbeads. I then describe macrophage based therapeutic interventions in mouse models of liver injury. Firstly the direct administration of bone marrow derived macrophages in partial hepatectomy plus chronic liver injury. I then tested the administration of macrophage colony stimulating factor in mouse models of partial hepatectomy, partial hepatectomy plus chronic liver injury and paracetamol intoxication, describing the phenotype and exploring mechanisms of action.

Collaborating with others I assessed serum CSF1 levels in humans with liver injury due to partial hepatectomy or paracetamol intoxication. I show that in acute liver failure a high serum CSF1 level is predictive of survival, indicating a new mechanistic biomarker.

# Declaration

This thesis has been written by myself and represents my own work. Where work has been completed in collaboration with others this is acknowledged.

# Acknowledgements

I would like to thank my supervisors, Professors Stuart Forbes and Stephen Wigmore for all their help and guidance prior to starting this project and for their continued support throughout. I am indebted to Alison Mackinnon and Davina Wojtacha for their guidance and assistance in the laboratory.

I would like to thank Professors David Webb and Iain McInnes for the opportunity to work with the Scottish Translational Medicine and Therapeutics Initiative and the funding and support that this has resulted in.

I would like to thank all those who I have collaborated with in particular Professor David Hume, Ken Simpson, Dan Antoine, Michael Hughes, Stephen Jenkins, Calum Bain, Professor Kevin Park, Professor Allan Mowat and Professor Jeff Pollard.

Most importantly I would like to thank my wife Jo for all her support throughout this research period, listening to all the trials and tribulations and keeping me on track. My children, Rosie and Harry, have been a fantastic distraction from studies both day and night.

# Contents

# Table of Figures

# Table of Appendices

# List of Abbreviations

AFS98: Antibody against the CSF1 receptor

Balb/c: inbred mouse strain (white)

BM: bone marrow

C57Bl/6: in bred mouse strain (black)

CCl4: Carbon tetrachloride

CD: cluster of differentiation

CSF1: Macrophage colony stimulating factor

CSF2: Granulocyte macropage colony stimulating factor

CSF3: Granulocyte colony stimulating factor

CSF1R: Macrophage colony stimulating factor receptor; also known as CD115

DAB: Diaminobenzidine

ECM: Extracellular matrix

EGF: Epidermal growth factor

Fc: Fragment crystallisable region

FcRn: Neonatal Fc receptor

FXR: Farnesoid X receptor

GCSF: Granulocyte colony stimulating factor (CSF3)

GMCSF: Granulocyte macropage colony stimulating factor (CSF2)

GW2580: Pharmacological inhibitor of the CSF1 receptor

HPC: hepatic progenitor cell

HBS: Hepatobiliary scintigraphy

HSC: Hepatic stellate cell

ICG: Indocyanine green

Il: Interleukin

INOS: Inducible nitric oxide synthase

IVC: Inferior vena cava

LPS: lipopolysaccharide

LSECs: Liver sinusoidal endothelial cells

LPS: lipopolysaccharide

MCSF: Macrophage colony stimulating factor (CSF1)

MMP: Matrix metalloproteinase

MR: Mannose receptor

OATP: Organic anion transporter polypeptide

NAPQI: N-acetyl-p-benzoquinone imine

NK: natural killer cells

NKT: natural killer T cells

NTCP: Na+-taurocholate cotransporting polypeptide

PAMPs: Pathogen associated molecular patterns

Pan CK: pan cytokeratin

PH: Partial hepatectomy

PRRs: Pathogen recognition receptors

PV: portal vein

TGFβ: Transforming growth factor beta

TV: tail vein

uPA: urokinase plasminogen activator

WT: wild type

YAP: Yes-associated protein

# Hypotheses

1. Macrophages have a central role in liver regeneration

2. Manipulation of macrophages can enhance liver regeneration

# Aims

1. Develop preclinical models of liver regeneration

2. Develop functional assays with translational potential to assess liver regeneration in vivo

3. Trial macrophage based therapies to enhance liver regeneration

4. Relate findings to the clinical setting by analysis of patient samples

# Publications related to thesis

## Introduction section

I wrote the following two review articles in the lead up to my PhD period to gain a greater understanding of the field and decide where I should focus my research.

**1. Stutchfield, B.M**., Forbes, S.J. & Wigmore, S.J. Prospects for stem cell transplantation in the treatment of hepatic disease. Liver Transpl 16, 827-836 (2010).

**2. Stutchfield, B.M**., Rashid, S., Forbes, S.J. & Wigmore, S.J. Practical barriers to delivering autologous bone marrow stem cell therapy as an adjunct to liver resection. Stem Cells Dev 19, 155-162 (2010).

I contributed to this book chapter and these reviews during my PhD period.

**3.** Wigmore SJ, **Stutchfield BM,** Forbes SJ. Liver Functions and Failure. In. Garden OJ, Parks RW. Companion to Specialist Surgical Practice: Hepatobiliary and Pancreatic Surgery, 5/e.2014

**4.** Moore, J.K., **Stutchfield, B.M.** & Forbes, S.J. Systematic review: the effects of autologous stem cell therapy for patients with liver disease. Aliment Pharmacol Ther 39, 673-685 (2014).

**5. Stutchfield, B.M.** & Forbes, S.J. Liver sinusoidal endothelial cells in disease - And for therapy? J Hepatol 58, 178-180 (2013).

## Methods section

I developed a method of assessing indocyanine green clearance to test hepatic function which I contributed to this paper.

**6.** Fallowfield J, Hayden A, Snowdon V, Aucott R, **Stutchfield BM,** Mole D, Pellicoro A, Gordon-Walker T, Henke A, Schrader J, Trivedi P, Princivalle M, Fores S, Collins J, Iredale J. Relaxin modulates human and rat hepatic myofibroblast function and ameliorates portal hypertension *in vivo*. *Hepatology*, 59(4): 1492-504, 2014

## Results section

I explored the role of macrophage stimulation following injury models in mice and collaborated with researchers from Liverpool and Edinburgh University to explore serum dynamics of macrophage colony stimulating factor following liver injury in humans (7). I assisted in the analysis of the effects of CSF1 receptor stimulation in mice in the steady state (8, 9).

**7. Stutchfield BM,** Antoine DJ, Mackinnon AC, Gow D, Jenkins SJ, Hughes M, Wojtacha D, Man TY, Dear JW, Devey LR, Pollard JW, Park BK, Simpson KJ, Wigmore SJ, Hume DA, Forbes SJ. Macrophage colony stimulating factor enhances innate immune capacity during liver regeneration and predicts survival in human liver failure. *Submitted to Science Translational Medicine*

**8.** Gow DJ, Sauter KA, Pridans C, Moffat L, **Stutchfield BM,** Raza S, Beard PM, Sehgal A, Tsai YT, Bainbridge G, Boner PL, Fici G, Garcia-Tapia D, Martin RA, Oliphant T, Shelly JA, Tiwari R, Wilson TL, Smith LB, Forbes SJ, Mabbott NA, Hume DA. A novel CSF1-Fc

conjugate expands mononuclear phagocyte populations and indirectly promotes extensive hepatocyte proliferation. *Molecular Therapy (accepted)*

**9.** Sauter KA, Pridans C, Sehgal A, Bain CC, Scott C, Moffat L, **Stutchfield BM**, Davies CL, Donaldson BM, Renault K, McColl BW, Mowat AM, Serrels A, Frame MC, Mabbott NA, Hume DA. Autologous bone marrow-derived mesenchymal stem cell transplantation promotes liver regeneration after portal vein embolization in cirrhotic rats. *PLOSOne (accepted)*

# Chapter 1. Introduction

## 1.1 The clinical setting

Liver disease is a major cause of morbidity and mortality. Since the 1970's the death rate attributed to liver disease has increased exponentially, especially in the under 65 age group. This change is particularly concerning given gradual reduction in other leading causes of mortality (Figure 1.1). A wide range of conditions have been attributed to this increase, including viral hepatitis (B and C), alcohol, fatty liver disease and cancer. Liver transplantation currently offers the only effective therapy for life threatening liver failure. However the demand for donor organs does not meet the requirement and many patient die whilst awaiting liver transplantation. There are currently no therapies proven to enhance regeneration of the injured liver.

Regenerative demand is placed on the liver in a wide range of clinical settings, including partial hepatectomy to remove liver cancer and viral or toxin induced liver injury. In this section I review the clinical context in more detail, review the biology underpinning the regenerating liver, explore the consequences of a failing liver and then examine potential strategies to enhance liver regeneration.

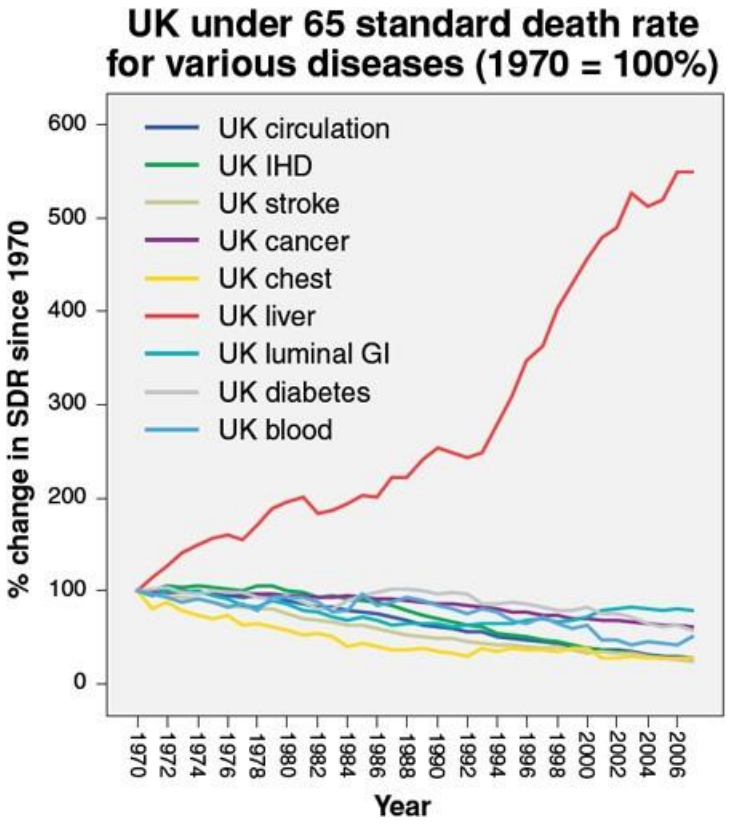


Figure 1.1: Change in death rate in the UK for various diseases between 1970 and 2006[1]

## Partial hepatectomy for liver cancer

Liver cancer can arise either following metastasis of an extrahepatic cancer or arise as a primary liver cancer, typically on a background of chronic liver disease (Figure 1.2). Colorectal liver metastasis is the commonest cause of hepatic malignancy leading to surgical resection[2]. However given the increase in chronic liver disease primary hepatic cancers, including hepatocellular carcinoma and cholangiocarcinoma, are also on the increase (Figure 1.3)[3].

A potentially curative treatment option for liver cancer is surgical removal of the cancer and the portion of the liver containing the cancer. Depending on the location, number and extent of the cancer up to around 75% of liver volume can be resected and the liver remnant will predictably regenerate over a period of weeks to months[2]. However, due to the rapid rise in liver cirrhosis and resulting hepatocellular carcinoma, it is now common for even relatively small tumours to be unresectable due to concerns over insufficient projected postoperative liver regeneration[4,5]. Multiple cancer foci's even in a normal liver may necessitate a radical resection (>75% volume to be resected), which may risk leaving an inadequate liver remnant and the development of liver failure. Preoperative chemotherapy may impair hepatic function[6], even in the absence of underlying chronic liver disease, so impairing regeneration and risking development of failure

One approach to the concern over the regenerative capacity of the liver remnant is to perform portal vein branch ligation or embolisation. This results in partial atrophy of the cancer bearing lobe and stimulates compensatory regeneration in the remaining lobe, thereby increasing future liver remnant volume preoperatively. However, in the common scenario of background liver fibrosis this may not be successful as underlying

liver disease can impair the regenerative response. If postoperative liver failure does ensue there is currently no available rescue therapy to enhance the regenerative response. Concern over regenerative capacity of the liver remnant means many patients are deemed unsuitable for surgery and are denied the option of a potentially curative intervention.

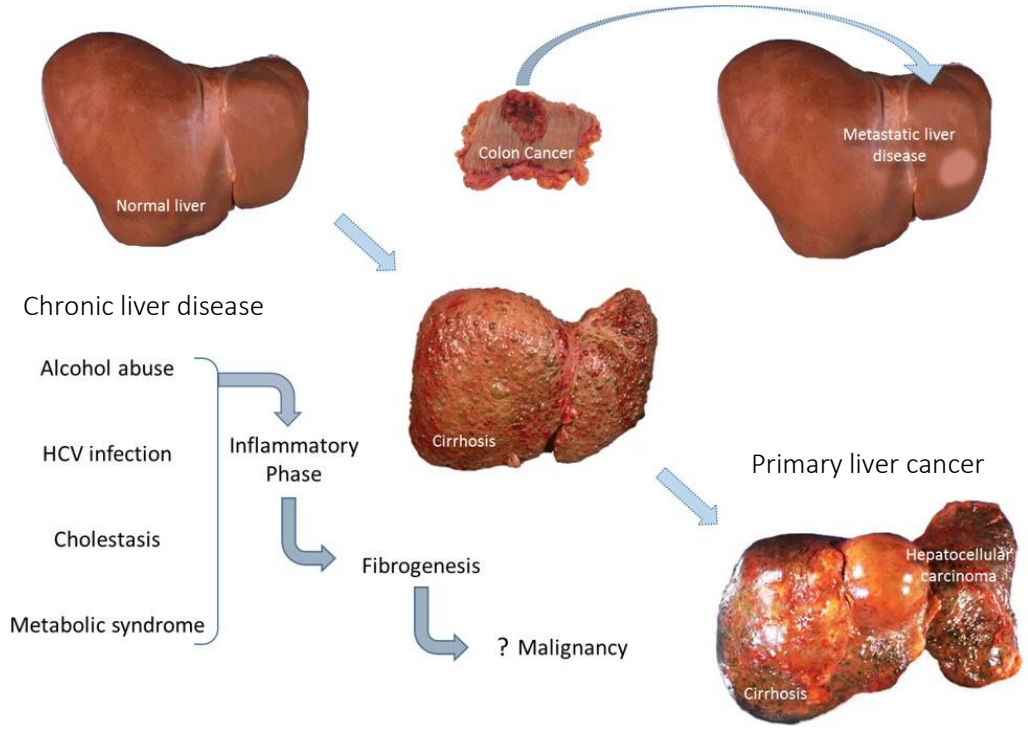


Figure 1.2: Schematic illustrating the occurrence of hepatic malignancy either via colorectal liver metastasis or on a background of chronic liver disease

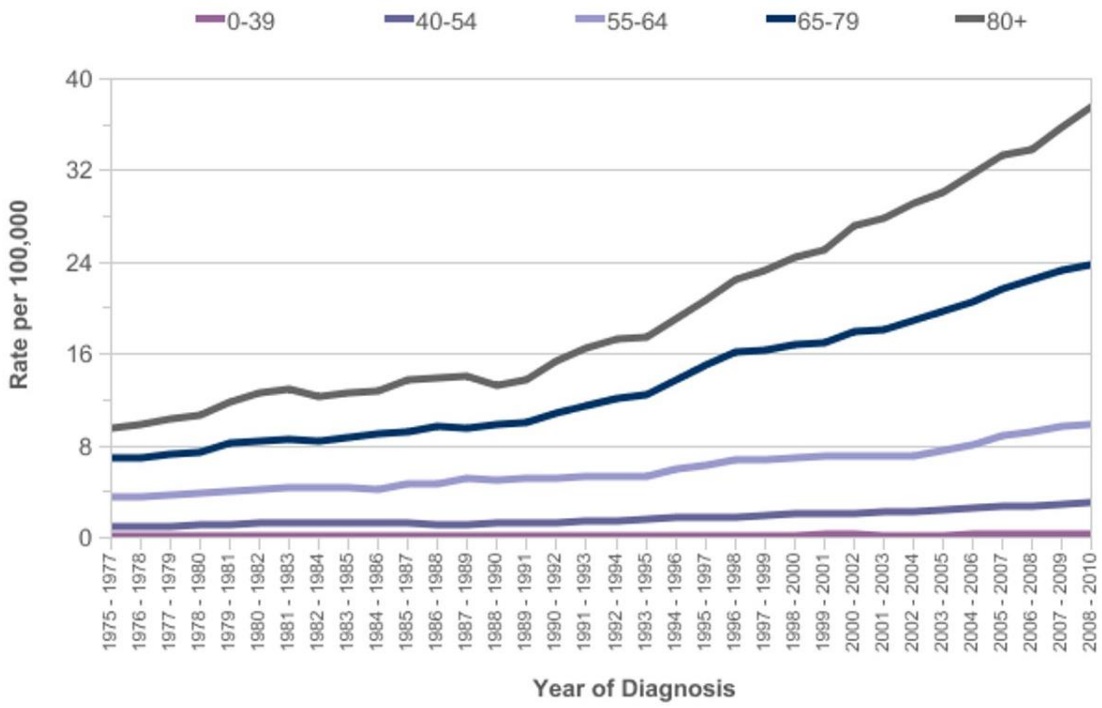


Figure 1.3: Incidence of primary liver cancer in the UK between 1975 and 2010[3]

Age standardised incidence rates per 100,000 population in the United Kingdom

## Acute liver injury

Aetiology of acute liver injury varies across the world, with viral causes predominant in the developing world and drug induced liver injury most prominent in Western Europe and the USA (Figure 1.4)[7]. The main viral causes worldwide include hepatitis A, B and E. Hepatitis A and E are spread mainly through the faecal-oral route and are typically self-limiting infections with low mortality, resolving over a period of weeks. Hepatitis A vaccination programmes have dramatically reduced its incidence. Hepatitis B is transmitted via exposure to body fluids of an infected individual. Mortality rate with hepatitis B is higher than A and E infections, but vaccination programmes and other public health measures have resulted in a substantial decrease in incidence and subsequent fall in the development of acute liver failure and mortality[8,9].

Drug induced liver failure in the USA and Western Europe is most commonly due to paracetamol intoxication[i] where the drug may be ingested with suicidal intent. In the UK the availability of paracetamol as an over-the-counter medication was thought to be a key factor in its selection by suicidal individuals. Legislation was introduced in 1998 to restrict the quantity of paracetamol that could be purchased at any one time. This change was associated with a 40% fall in admission to specialist liver units with paracetamol intoxication associated liver failure (up to 2004)[10]. However, this reduction has not necessarily been maintained and considerable regional variation exists. For example in Scotland there seems to have been little effect of the change in legislation on proportion of patients presenting with acute liver failure due to paracetamol intoxication[11] (Figure 1.5).

[i] Paracetamol is known also known as acetaminophen in the USA, Canada and Japan. It may also be referred to as APAP in reference to its chemical name N-acetyl-p-aminophenol. It is a widely available and used over-the-counter analgesic.

A wide spectrum of other drugs can cause acute liver failure, including non-steroidal anti-inflammatories, statins, antibiotics, antiepileptics, anti-tuberculosis drugs and toxins, e.g. *amanita phalloides* (mushroom). Ischemic injury can occur in cardiac failure or sepsis as a result of hypotension, metabolic liver disease (such as Wilson's disease[ii]), autoimmune hepatitis or Budd-Chiari syndrome[iii] [12,]. Partial hepatectomy to remove liver cancer can also induced acute liver failure as discussed in the previous section ("Partial hepatectomy for liver cancer").

In life threatening liver failure liver transplantation is currently the only effective therapy, although donor organ availability is limited and life-long immunosuppression is required in the majority of cases.

[ii] Wilson's disease is a autosomal recessive condition which is characterised by accumulation of copper in tissues. This can lead to a range of manifestations, including neurological disorders and chronic liver disease.

[iii] Budd-Chiari syndrome involves a triad of signs and symptoms including abdominal pain, ascites and hepatomegaly. It is caused by occlusion of the hepatic vein either by thrombosis within the vein (primary) or external occlusion of the vein (secondary, e.g. due to a tumour).

| | Drug | | Viral | | | Unknown | Other |
|---|---|---|---|---|---|---|---|
| | Paracetamol | Non-paracetamol | HAV | HBV | HEV | | |
| Spain 1992–2000[18] | 2% | 17% | 2% | 32% | .. | 35% | 12% |
| Sweden 1994–2003[19] | 42% | 15% | 3% | 4% | .. | 11% | 25% |
| UK 1999–2008[20] | 57% | 11% | 2% | 5% | 1% | 17% | 7% |
| Germany 1996–2005[21] | 15% | 14% | 4% | 18% | .. | 21% | 28% |
| USA 1998–2001[22] | 39% | 13% | 4% | 7% | .. | 18% | 19% |
| Australia 1988–2001[23] | 36% | 6% | 4% | 10% | .. | 34% | 10% |
| Pakistan 2003–05[24] | 0% | 2% | 7% | 20% | 60% | 7% | 4% |
| India 1989–96[25] | 0% | 1% | 2% | 15% | 44% | 31% | 7% |
| Sudan 2003–04[26] | 0% | 8% | 0% | 22% | 5% | 38% | 27% |

..=not reported. HAV=hepatitis A virus. HBV=hepatitis B virus. HEV=hepatitis E virus.

Figure 1.4: Aetiology of acute liver failure according to geographical location.

(adapted from Berry et al., 2010[7])

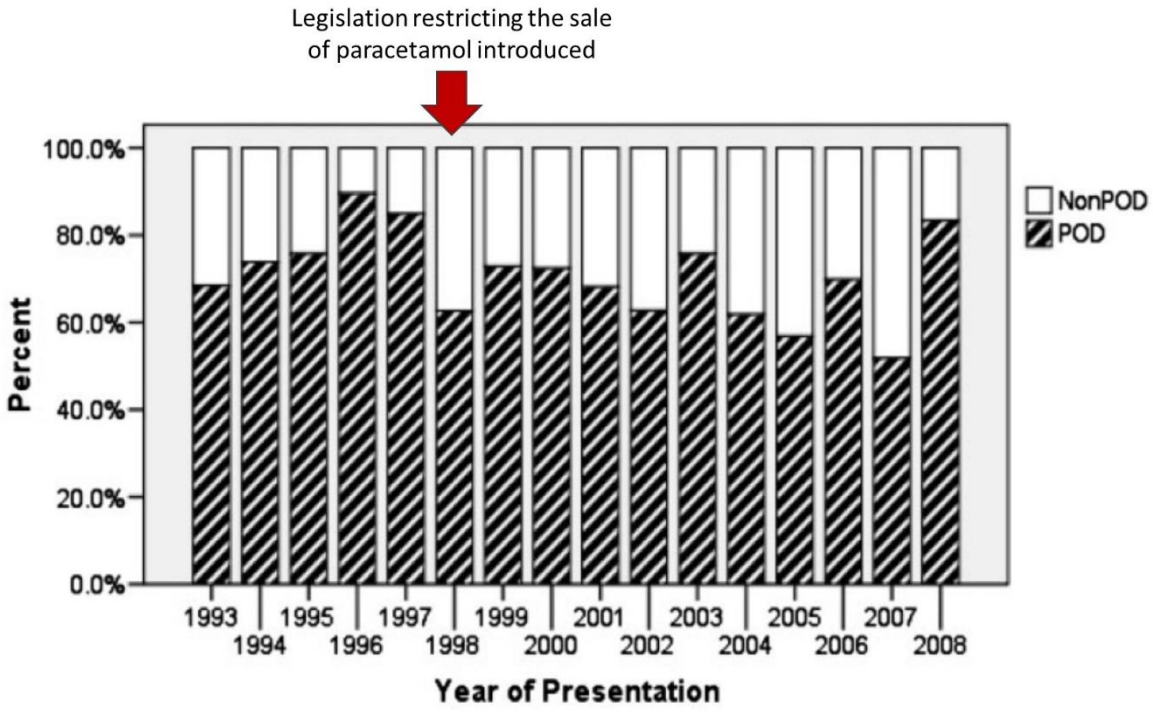


Figure 1.5: Proportion of yearly admissions attributed to paracetamol overdose in Scotland.

POD: paracetamol overdose; Non-POD: aetiology of acute liver failure other than POD.

(adapted from Bretherick et al., 2011[11])

## Acute on chronic liver failure

Acute liver failure may arise on a background of chronic liver disease, where an additional insult, such as infection, further toxic insult, or surgery tips the balance from compensated liver disease towards decompensation and liver failure. The patient with chronic liver disease may already be functioning on reserve capacity and it may not take much to tip this balance. Outcomes are particularly poor in this group of patients given the marked impairment in the liver's regenerative capacity.

Hepatic cirrhosis is the manifestation of end stage chronic liver disease. Cirrhosis has traditionally been regarded as an irreversible condition characterised by dense hepatic fibrosis, which surrounds regenerative nodules, induced by long term iterative liver injury. Common causes of chronic liver disease include hepatitis C and alcohol dependency. Non-alcoholic steatohepatitis is becoming an increasingly common cause of chronic liver disease, associated with rising levels of obesity[13]. Hepatitis C has long been regarded an incurable condition, however recent breakthroughs indicate that curative treatments are now becoming a reality[14] [iv]. Given reports indicating the potential reversibility of the fibrotic process in humans[15], it will be interesting to see how removal of the underlying viral cause influences established fibrosis.

[iv] Early clinical trial results indicate that 100% clearance of hepatitis C virus can be achieved using NS5A inhibitors which target steps in the viral replication cycle.

# 1.2 The biology of liver regeneration following acute injury

Liver regeneration is a complex process, involving multiple growth factors, cytokines and cell types. In experimental models acute liver injury is either induced by partial hepatectomy, toxic liver insult, or occurs on a background of chronic liver injury. In experimental models of partial hepatectomy liver lobes are removed, leaving an uninjured liver remnant which then regenerates rapidly. Acute toxic liver injury induces hepatocellular necrosis and apoptosis, with regeneration comprising both clearance of dead tissue, remodelling of liver architecture and restoration of hepatocyte mass. Chronic liver injury can lead to progressive hepatic fibrosis with acute injury in this context caused either by partial hepatectomy or toxins. The biology of regeneration in each of these contexts is discussed below.

## Regeneration following partial hepatectomy

Liver regeneration following partial hepatectomy reflects a compensatory hyperplasia of the liver remnant. The term 'regeneration' in this context is something of a misnomer. Liver regeneration in this context does not reflect a restoration of both form and function, as occurs in the out-budding of the salamander limb following limb removal for example[16], rather a process of liver remnant hypertrophy and hyperplasia characterised by rapid hepatocyte proliferation.

The majority of the mechanistic understanding of liver regeneration has come from partial hepatectomy in rodent models. Here the lobulated liver facilitates surgical resection, with the standard model being resection of 2/3 liver mass by the removal of the left and median liver lobes. Direct assessment of liver regeneration in humans is limited by the technical challenge and safety concerns of obtaining liver biopsies in the

postoperative period. Directly relating liver regeneration in rodents to that in humans may be difficult but it does allow identification of factors that may be beneficial or harmful in the clinical setting.

Liver regeneration in rodents is highly effective with liver weight returning to its preoperative weight by around day 7-10 following 2/3 PH. The ratio of liver weight to body weight is remarkably consistent, at around 5%. Factors governing liver size are unclear, but the change in flow dynamics through the liver remnant are thought to be central to this. There is no evidence that the liver can intrinsically "sense" its final size and final size does not appear to relate to metabolic demand[17].

Liver regeneration can be divided into four phases: Intiation, hepatocyte priming, hepatocyte proliferation and termination.

### Initiation

Alterations in cytokine expression are noted within 5 minutes following partial hepatectomy in mice, with an upregulation in urokinase plasminogen activator (uPa) across the whole liver[18]. There is evidence to suggest that the mechanical stress caused by changes in flow dynamics following loss of liver volume may induce this uPA activity[19,20]. The source of this uPA activity in the liver has not been characterised but by examining other systems it is likely that this is macrophage mediated. Sokabe et al. showed that shear stress can increase uPA gene expression in the vascular endothelium of carotid vessels, however this was related to turbulent flow and not laminar stress, which would be seen in the liver following PH[19]. However Yeh et al. showed that under sheer stress macrophages can upregulate uPA expression in coculture with chondrocytes[21]. uPAR is certainly highly expressed by macrophages[22] and macrophages

are abundant in the liver. Urokinase activity is known to induce matrix remodelling which fits with an early upregulation of MMP9 (from 30 minutes) gene expression following PH in mice[23]. Remodelling of hepatic matrix is required for the release and activation of hepatocyte growth factor (HGF, the main hepatocyte mitogen), which is bound to matrix via glycosaminoglycans[18]. TGFβ is well recognised as a mito-inhibitor and is bound to matrix decorin in the steady state, exerting a competing effect to HGF. Matrix remodelling releases TGFβ into the circulation where it binds to alpha-2-macroglobulin and is inactivated[24]. Figure 1.6 illustrates these early matrix remodelling events following partial hepatectomy.

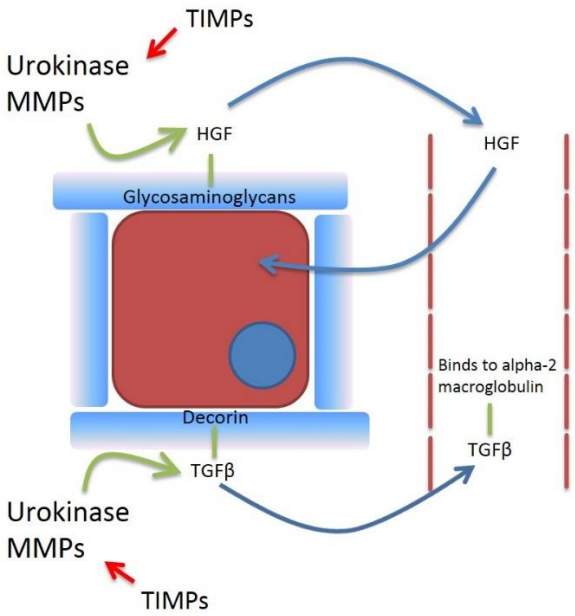


Figure 1.6: Matrix remodelling events and release of growth factors following partial hepatectomy.

Matrix remodelling is an early event following partial hepatectomy and is required for hepatocyte proliferation. The hepatocyte mitogen, HGF, and mito-inhibitor TGFβ are released from their matrix components (glycosaminoglycans and decorin respectively) by matrix metalloproteinases (MMPs) and urokinase activity. While HGF acts directly on hepatocytes to induce proliferation, TGFβ binds to alpha-2 macroglobulin limiting its ability to impair hepatocyte proliferation.

## Hepatocyte priming and proliferation

Tissue necrosis factor (TNF), Il6, serotonin and bile acids also increase in the circulation following partial hepatectomy and are required for effective regeneration through their priming effects on hepatocytes and effects on the hepatic environment[25-27]. Macrophage depletion studies in mice have demonstrated that TNF and Il6 are derived from macrophages, the depletion of which markedly impairs regeneration[28,29]. Indeed supplementary Il6 can both induce hepatocyte proliferation and promote liver regeneration following PH in rats with cirrhotic liver injury[30]. Platelet derived serotonin mediates vascular flow in mice following partial hepatectomy and its supplementation can facilitate regeneration in mouse models of maximal partial hepatectomy[31]. Bile acids accumulate in the circulation following partial hepatectomy and signal to the nuclear bile acid receptor on hepatocytes (FXR)[27]. Blockade of this receptor or a reduction of circulating bile acids in mice impairs regeneration[32].

Depletion of either natural killer t cells or eosinophils impairs regeneration and this is thought to be due to the direct effects of Il4 signalling on hepatocytes via Il4Rα[33,34]. Hepatic stellate cells can contribute to regeneration through the production of HGF and may have a role in catecholamine production which can promote hepatocyte proliferation[35]. Bone marrow derived liver sinusoidal progenitor cells are released from the bone marrow in response to rising granulocyte colony stimulating factor (GCSF) levels and contribute to regeneration in mice as they are a rich source of hepatocyte growth factor[36].

As well as HGF, the other main growth factor involved in liver regeneration is epidermal growth factor (EGF) which is produced by Brunner's glands in the duodenum[37]. These two growth factors (HGF and EGF) are known as direct hepatocyte mitogens as injection

of these growth factors alone can induce hepatocyte proliferation and hepatic enlargement. Figure 1.7 illustrates the phases required for effective liver regeneration. While these events are ongoing, beta catenin and Notch-1 intracellular domain appear in the hepatocyte nuclei, NFκB and Stat 3 activity is enhanced and hepatocytes enter the cell cycle[20]. Developmental morphogens, such as Hedgehog have also been related to liver regeneration, highlighting the link between development and regeneration. In the case of hedgehog signalling, blockade of this pathway markedly impaired liver regeneration in mice, related to reduced matrix deposition and the non-parenchymal cell proliferation which is required for hepatic remnant enlargement[38].

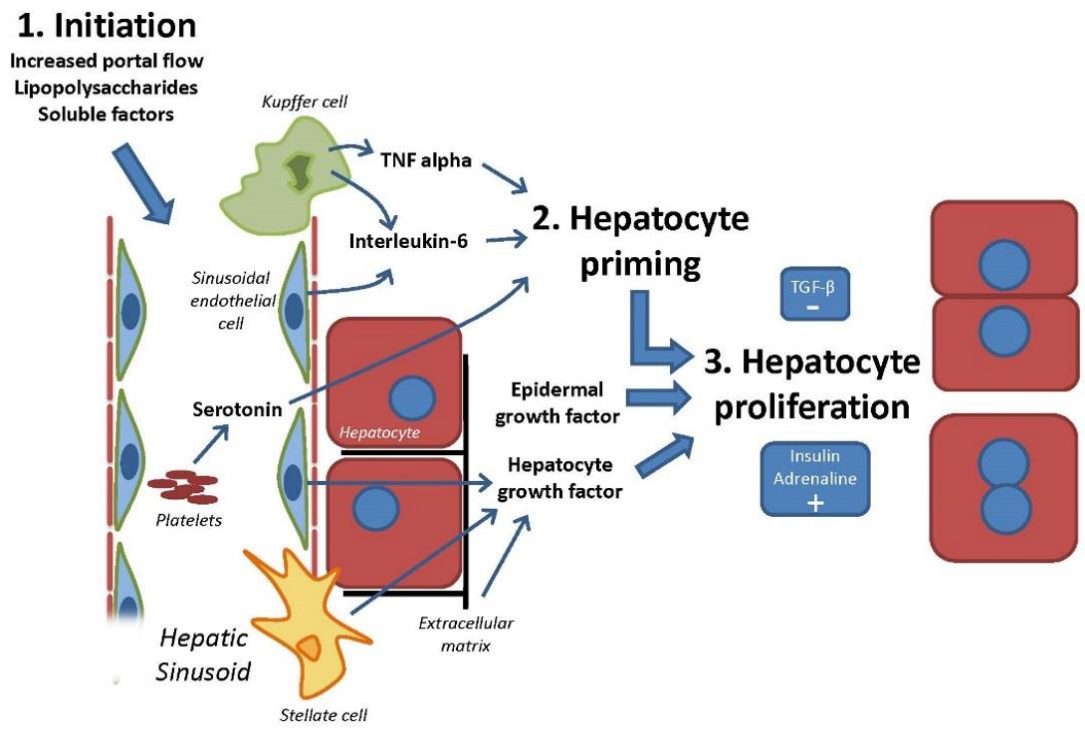


Figure 1.7: Summary of the initiation, priming and hepatocyte proliferation phases following partial hepatectomy.

Immediately following partial hepatecytomy portal flow increases to liver remnant with an increase in availability of gut derived substances, such as lipopolysaccharides, as a result of this increased flow. Combined with proinflammatory events, such as the release of TNF and Il-6 hepatocytes are primed to enter the cell cycle and proliferate.

## Termination of liver regeneration

While the initiation of liver regeneration has been studied in detail, mechanisms leading to its proper termination are poorly characterised. Dong et al. report the Hippo/YAP signalling pathway as a mechanism of universal size control in both drosphila and mammals[v]. The mouse experiments showed that transgenic induced YAP overexpression lead to liver growth characterised by widespread hepatocyte proliferation[39]. However as Yap is known to induce cellular proliferation to conclude that that the YAP/Hippo pathway regulates liver size may be erroneous especially as the proliferative stimulation also resulted in liver cancer. Rather, this experiment shows that overexpression of YAP can induce hepatocyte proliferation, which is essentially no different from the administration of a direct mitogen such as HGF.

There is often an overshoot in hepatocyte proliferation, which activates a small wave of apoptosis in hepatocytes when a similar liver size to that preoperatively is achieved[40]. The role of TGFβ1 in this setting has been considered. As mentioned earlier, TGFβ1 is a known inhibitor of hepatocyte proliferation, however the expression of TGFβ1 rises early following partial hepatectomy and remains elevated throughout the regenerative process[41]. In addition overexpression of TGFβ1 does not lead to widespread apoptosis, rather proliferating hepatocytes are scattered throughout the parenchyma[42] [vi]. Given the role of extracellular matrix (ECM) remodelling in the initiating events of liver regeneration, reconstitution of the ECM and associated signalling molecules may play an important role in the termination of liver regeneration[17]. As well as a source for growth

[v] The Hippo signalling pathway is highly conserved pathway present in drosphilia through to mammals. It has a key role in determining cellular apoptosis and proliferation. In drosphila it has been shown to be a regulator of organ size. YAP is an oncogene 39. Dong, J., *et al.* Elucidation of a universal size-control mechanism in Drosophila and mammals. *Cell* **130**, 1120-1133 (2007).

[vi] This paper also showed that TGFβ induced marked hepatic fibrosis (TGFβ is well recognised as a profibrotic agent). The overwhelming phenotype was that of TGFβ induced glomerulonephritis leading to renal failure.

factors the ECM contains signalling molecules which communicate with surrounding cells. Integrins mediate much of these signalling pathways. The role of integrins in mediating hepatocyte proliferation is illustrated by mice lacking integrin linked kinase. Here, in the steady state liver size was increased by nearly 60%[43]. The signals that facilitate appropriate remodelling however are unknown. Changes in flow dynamics and potentially vascular stress are likely to have a role to play given there is a reduction in these signals with increasing liver size. However conclusively demonstrating the series of events responsible for, rather than just associated with, termination of liver regeneration remains elusive.

## Regeneration following acute toxic liver injury

As with partial hepatectomy, much of our understanding of liver regeneration following acute toxic liver injury has come from the manipulation of rodent models. Common toxic agents to induce acute liver failure in rodents include paracetamol, carbon tetrachloride, and thioacetamide[44].

### Paracetamol

Paracetamol intoxication is one of the most clinically relevant of the injury models given this is one of the commonest causes of acute liver failure in the UK, USA and most of Europe[45]. There are three main pathways by which administered paracetamol is eventually metabolised. Over 90% undergoes either glucuronidation (addition of glucuronic acid) or sulfation (sulphate conjugation)[46]. These metabolites are then excreted via the kidneys. However a small percentage can form the toxic reactive intermediate N-acetyl-p-benzoquinone imine (NAPQI). This is detoxified by conjugation with glutathione. At high doses the glucuronidation and sulfation pathways can become saturated, forming excess NAPQI, depleting glutathione stores and binding to liver

proteins. This can lead to mitochondrial dysfunction, oxidative stress and activation of necrotic and apoptotic pathways. Glutathione concentrations are lowest in the centrilobular regions where tissue destruction is evident[47]. Following fasting the effects of paracetamol at toxic doses are considerably worse. This leads to a marked neutrophil infiltrate and increased severity of injury in mouse models of paracetamol intoxication[48]. Antoine et al., showed that fasting does not deplete glutathione levels or alter paracetamol metabolism, rather fasting depletes basal ATP which inhibits caspase-driven apoptosis resulting in predominant necrotic injury[48]. Following injury regeneration then relies upon CCR2 dependent monocyte and macrophage recruitment to clear necrotic debris[49,50]. In humans, monocytopenia is associated with the most severe injury[51,52]. Figure 1.8 summarises the process.

### Carbon tetrachloride

Carbon tetrachloride has been widely used as an agent to induce hepatic fibrosis following a chronic injury regimen. However a single high dose can be used to induce acute liver injury. Liver injury is induced by the formation of reactive intermediates via the cytochrome P-450 pathway and also alterations in calcium homeostasis[53,54]. Carbon tetrachloride induces a centrilobular injury.

### Thioacetamide

Thioacetamide forms the active metabolite TAA-S-oxide after biotransformation via the flavine adenine dinucleotide pathway[55]. At lower doses this can induce hepatocyte apoptosis but at high doses oxidative stress results in lipid peroxidation and centrilobular necrosis in mouse and rat liver[36].

Given the direct clinical relevance of paracetamol intoxication this model of liver injury has received the most research attention, particularly in recent years.

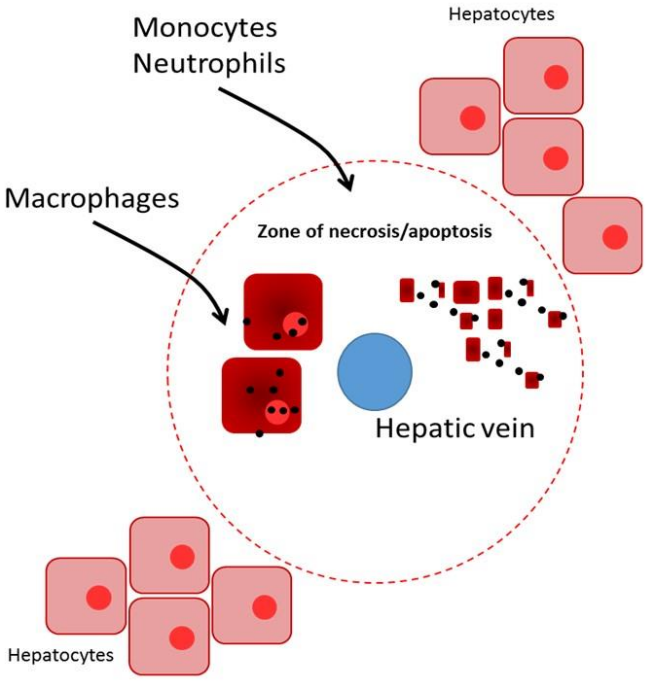


Figure 1.8: Schematic demonstrating tissue destruction following paracetamol intoxication.

## Regeneration following acute on chronic liver injury

Induction of chronic liver injury in mice and rats is typically performed by long term administration of carbon tetrachloride or thioacetamide. One of the earliest changes in the development of fibrosis is the loss of fenestrations in the liver sinusoidal endothelial cells and the formation of a basement membrane[56]. Hepatic stellate cells (the liver's fibroblasts) are the typical scar forming cells of the liver which then act with infiltrating monocyte populations to generate fibrotic scars[57]. Stellate cells interact with other mediators, such as platelet derived serotonin, which can enhance the fibrotic response[58]. The remodelling process is constantly active however with cellular populations having contrasting roles in both injury and resolution phases. For example depletion of monocyte/macrophage populations during injury reduces scar formation but depletion during recovery impairs scar resolution [59].

Acute liver injury can be applied to a background of chronic liver injury either by a high dose of toxin, such as carbon tetrachloride, or by partial hepatectomy. Following acute on chronic toxic liver injury the background hepatic fibrosis does exert a degree of protection from further acute injury, demonstrating the functional role of this process[60]. The mechanism underlying this protective effect was attributed to collagen mediated extracellular signalling such as ERK-1 (extracellular regulated kinase 1). Following partial hepatectomy on a background of chronic liver injury in rats, matrix remodelling is accelerated leading to a rapid reduction in fibrosis in the liver remnant[61]. This effect was attributed to increased expression of matrix metalloproteinases 9, 12 and 13.

# 1.3 The consequences of a failing liver

## Why do patients die from liver failure?

The failing liver can trigger a cascade of events, characterised by multiorgan dysfunction and sepsis, which can result in eventual death. Multi organ involvement markedly increases the risk of death, such that with three or more organs involved the chance of death approaches 80% versus less than 4% in patients with no extrahepatic involvement[62]. Typical manifestations include the development of bacterial infection, encephalopathy, gastrointestinal haemorrhage and ascites[62].

In chronic end stage liver disease the induction of acute liver failure by bacterial infection is the commonest cause of death[63]. Infection rates are increased following extended partial hepatectomy and sepsis complicates acute liver failure in over 30% of cases[2,64].

Hepatic encephalopathy, due to circulating ammonia and other neurotoxins, is often precipitated by infection and is associated with a profound inflammatory mediator response[65,66]. This can lead to cerebral oedema and intracranial hypertension manifesting with varying degrees of neuropsychiatric disturbances, from mild confusion to coma and subsequent death. Cerebral oedema accounts for around 20-25% of deaths from acute liver failure[67]. Gastrointestinal haemorrhage may relate to pre-existing vascular abnormalities, such as the development of oesophageal varices[vii], in combination with coagulopathy due to impaired hepatic synthetic function. Patient comorbidities may contribute to other causes of death relating to renal, respiratory and cardiac failure.

[vii] Oesophageal varices are dilated veins forming in the lower third of the oesophagus as a consequence of portal hypertension (increased pressure in the portal vasculature due to the circulatory abnormalities of chronic liver disease)

Clinical deterioration and death in liver failure is clearly a multifactorial process, with the development of sepsis and the inflammatory response major mediators. Given its position, directly downstream from the gut, the liver is an organ which exhibits predominant innate immunity[68]. The disruption of both liver architecture and function that occurs in liver injury can impair this immune barrier.

## The liver and innate immunity

The liver receives approximately 80% of its blood supply via the portal vein, with the remaining 20% supplied by the hepatic artery[68]. The liver therefore represents the last line of defence against gut derived pathogenic material arriving via the portal vein. The innate immune system is designed for rapid defence against pathogenic material. It is multi-layered, involving physical barriers, such as mucous membranes and skin, chemical barriers, such as stomach acid secretions, humoral factors, such as complement and interferons, lymphocytic cells, including natural killer cells and phagocytic cells, including neutrophils and macrophages.

The innate immune response relies on recognition of pathogens via "pathogen-recognition receptors" (PRRs) which detect "pathogen-associated molecular patterns" (PAMPs)[69]. Lipopolysaccharide is perhaps the best defined PAMP and relates to gram negative bacteria which predominate the gut flora. PRRs include membrane bound receptors (toll-like receptors and c-lectin receptors) and cytoplasmic PRRs (NOD-like receptors and RIG-1-like receptors)[69]. Gut-derived PAMPs first come into contact with the hepatic macrophage population, which filter the portal blood from their location extending into the hepatic sinusoids. The liver contains the body's largest populations of macrophages in direct contact with the blood and their location directly downstream of

the gut highlights the importance of this barrier (Figure 1.9)[68, viii]. As well as phagocytic functions, hepatic macrophages can endocytose smaller soluble macromolecules, such as lipopolysaccharide (LPS). Liver sinusoidal endothelial cells (LSECs) are also capable of eliminating soluble macromolecules and colloidal waste through endocytosis (such as LPS), but do not have phagocytic functionality. Other innate immune cells within the liver include natural killer (NK) cells and natural killer T cells (NKT). NK cells interact with other immune cells, in particular T cells, to regulate the immune response to pathogens involving cytokine release, priming other immune cells and subsequently influencing the adaptive immune response[70, ix]. Eosinophils and neutrophils are found in low numbers in the steady state liver but increase in number markedly following tissue injury.

There is mounting evidence that the impairment in hepatic innate immune function following injury is a major factor influencing the subsequent clinical outcome. In the context of experimental models of liver injury, hepatic bacterial clearance capacity is impaired, leading to increased systemic exposure to gut commensals[71]. Translocation of gut bacteria is a major cause of sepsis in chronic liver disease, which is thought to be linked to both a change in gut flora and also an alteration in gut integrity[72-74]. In experimental models of maximal partial hepatectomy (90%), marked bacterial translocation occurs 2 hours following surgery, associated with an overgrowth of Escheria coli in the distal intestine and dramatically reduced reticuloendothelial system function[75]. Hepatic phagocytic capacity in the clinical setting can be tested by measuring the rate of clearance of radiolabelled albumin microspheres from the circulation. Here clearance of these particles is markedly impaired in severe acute toxic liver injury, partial

[viii] Overall the gut hosts the body's largest population of macrophages, however these macrophages serve a barrier function relating to the intestinal lumen and are not positioned to serve as blood filters.

[ix] Adaptive immunity (also known as acquired immunity) refers to immune protection that develops in response to an antigen. It typically involves the development of antibodies, is mediated by T cells and B cells and can acquire "memory" such that subsequent insults with the same antigen lead to a more robust response.

hepatectomy and in chronic liver injury[76,77]. The importance of maintaining innate immune capacity following liver injury is clear and suggests an important link between the immune system and regeneration of the injured liver.

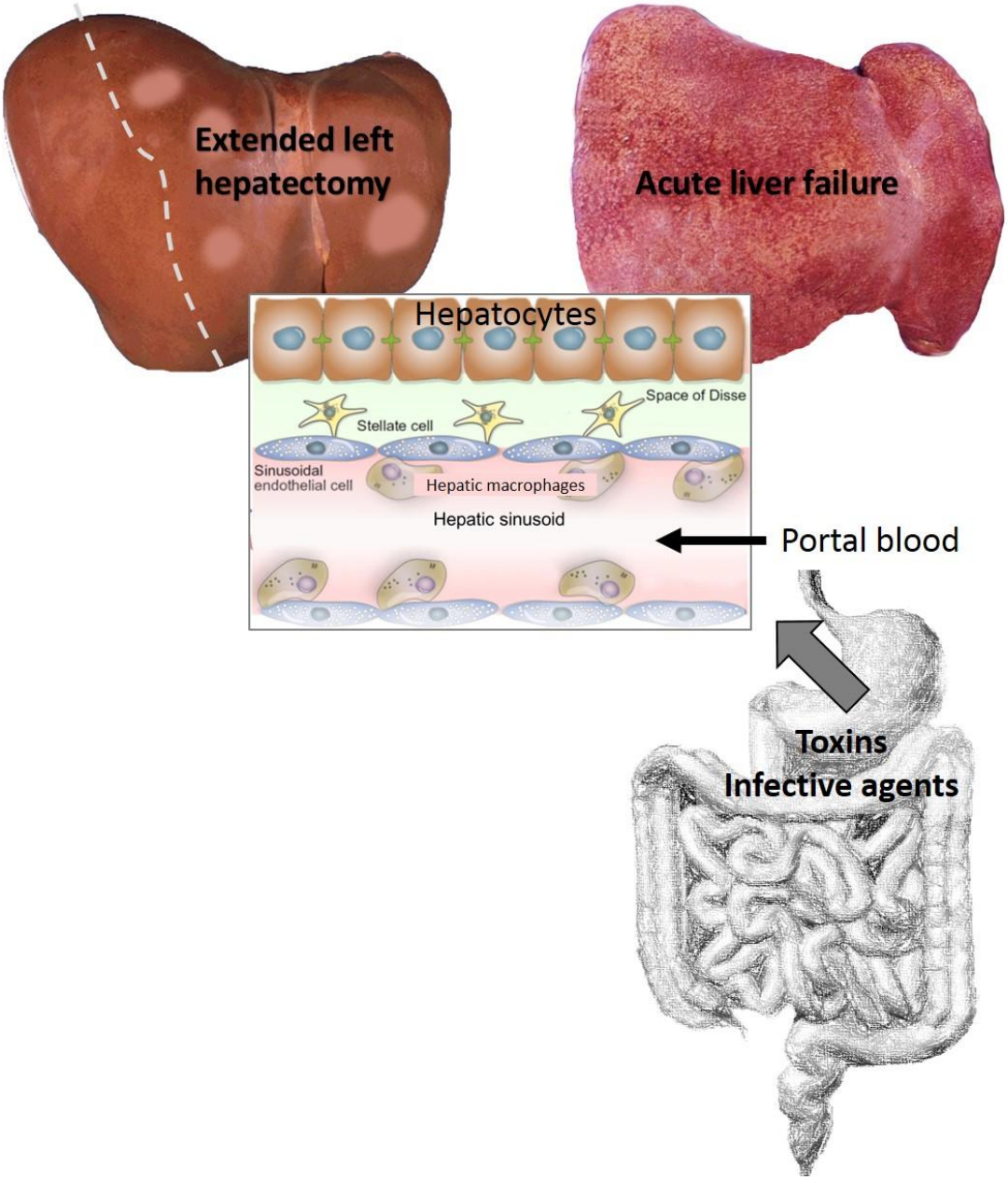


Figure 1.9: Relationship between the gut, portal blood, hepatic sinusoid and hepatic macrophage with illustrations of liver disease.

Central figure adapted from Stutchfield and Forbes, 2013[78].

## Linking hepatic regeneration and innate immunity

Innate immune cells have a central role in liver regeneration. During regeneration hepatic macrophages are important for hepatocyte priming and subsequent hepatocyte proliferation, while NK cells and eosinophils enable effective hepatocyte proliferation via Il-4 related signalling pathways (as discussed in "1.2 The biology of liver regeneration following acute injury") [28,33,34].

In the steady state it is the hepatic macrophage that is the predominant innate immune cell in the liver[68]. There is direct link between the number of mature hepatic macrophages and gut bacterial load, demonstrating the dynamic nature of this system[79]. Maintenance of hepatic macrophages is influenced by macrophage colony stimulating factor (CSF1)[80,81]. CSF1 is ubiquitously produced by many tissues[82,83], but hepatic macrophages serve as the major clearance site of CSF1 via receptor mediated endocytosis[84]. Hepatic regeneration following PH is stunted in CSF1 deficient mice (op/op) and reduction in hepatic macrophage number by blockade of macrophage colony stimulating factor significantly reduces hepatic size[85].

Hepatic macrophages have a protective effect following ischemia reperfusion injury of the liver involving a heme oxygenase-1 dependent mechanism[86]. In chronic liver injury macrophages have distinct roles during both injury and repair, important in the fibrogenesis phase after injury and equally important to facilitate remodelling and fibrosis resolution during recovery[59]. Indeed transplantation of ex vivo differentiated macrophages in a mouse model of fibrosis can reduce hepatic fibrosis by upregulating matrix remodelling[87].

NK cells can induce antifibrotic pathways following liver injury via effects on stellate cells, but may also mediate hepatocyte cytotoxicity dependent on the disease context[88,89]. In patients eosinophilia indicated a favourable outcome in drug induced liver injury although in experimental models eosinophils have a role in mediating the pathogenesis of drug induced liver injury although the mechanism was unclear[90,91].

Ultimately, maintaining an effective immune response in the presence of injury is a highly evolved process. The relationship between cells of innate immunity and liver regeneration is certainly complex, with evidence to suggest distinct roles in the pathogenesis, repair and resolution phases following liver injury. Rather than simply the presence of cells within the tissue being pathological, the context in which these cells find themselves appears to be the key determinant. Directing the immune response by targeting specific cells of the innate immune system could provide an effective therapeutic strategy to enhance recovery from liver injury.

## 1.4 Therapeutic strategies to facilitate liver regeneration

There is currently no therapy proven to enhance regeneration of the liver in clinical practice. Strategies to improve outcomes in liver failure currently focus on intensive care support as multiorgan failure and sepsis ensues. In life threatening liver failure, liver transplantation is currently the only therapy proven to improve survival in acute and acute-on-chronic liver failure[92,93]. The decision to undergo transplantation for acute liver failure in the UK is currently based on a series of clinical criteria which identifies those patients at greatest risk of death- the King's College Criteria[94] (Figure 1.10). While these criteria are designed to identify the sickest patients, active sepsis should be treated prior to transplantation[95]. The King's College Criteria are widely accepted as a prognostic algorithm reflecting marked clinical deterioration, although its sensitivity has been questioned[96].

The ability to accurately identify those patients who are likely to require transplantation prior to clinical deterioration would be highly desirable. Recent work has identified a range of biomarkers related to hepatic injury which show promise in predicting patients most likely to die or require liver transplantation, the most promising of these is acetyl-HMGB1which serves an indicator of necrosis[97,98]. If patients most likely to deteriorate could be targeted at an early stage then this could facilitate intervention to enhance regeneration.

Liver specific therapies to improve outcomes following liver injury have included directly targeting hepatocytes to proliferate using mitogens, supporting liver function using an extracorporeal device, administering hepatocytes or hepatocyte like cells directly or targeting the non-parenchymal cells of the liver to facilitate recovery of the hepatic environment (Figure 1.11).

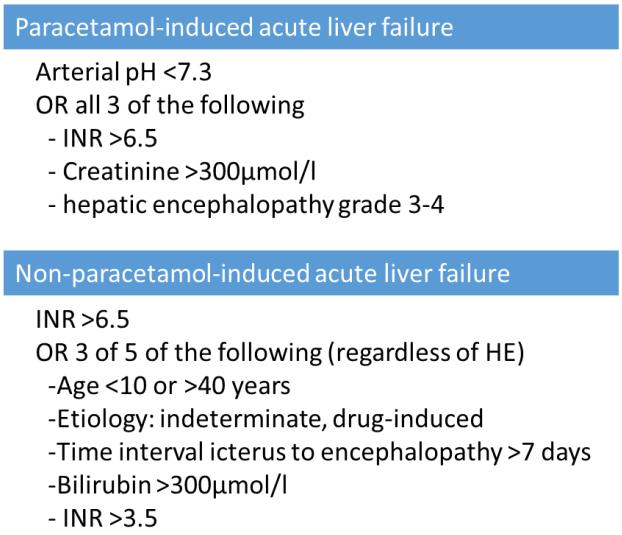


Figure 1.10: Simplified King's college criteria

The King's college criteria serves as a prognostic algorithm to identify those patients who are likely to die from acute liver failure. The criteria are divided into patacetamol and non-paracetamol induced acute liver failure, reflecting differences in progression of acute liver failure in these cohorts.

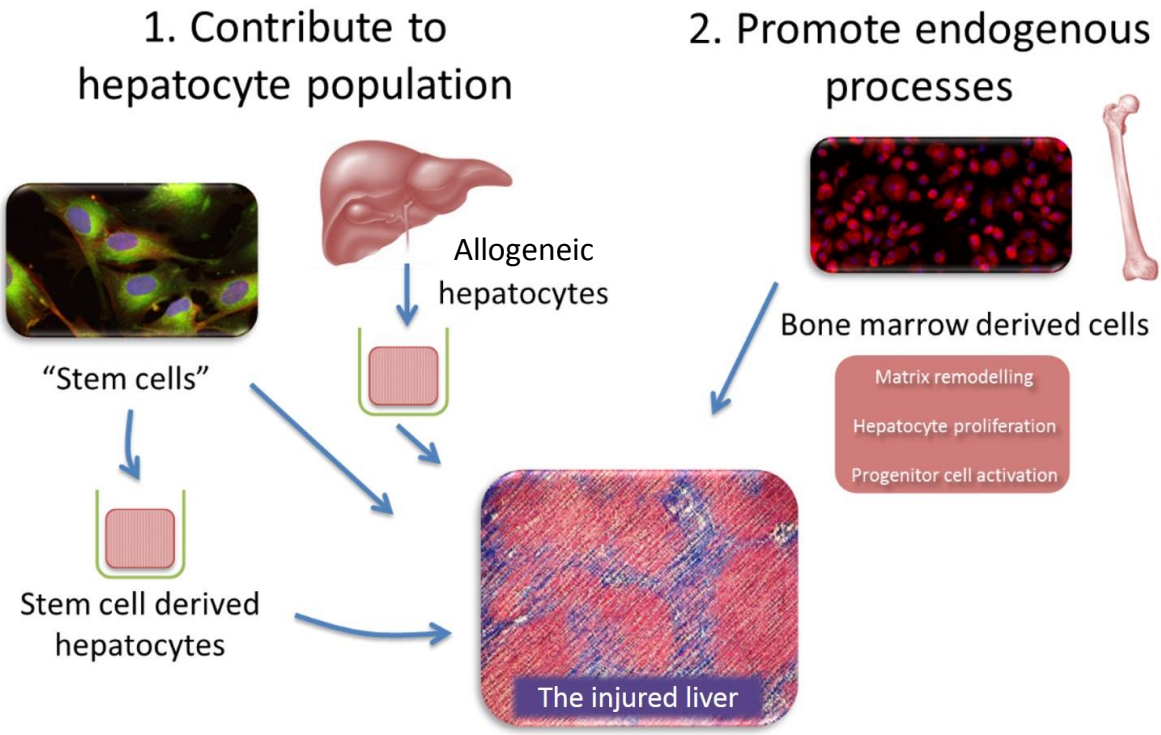


Figure 1.11: Cell therapy based strategies to support the injured liver

Cell therapies to support the injured liver can be broadly grouped into those that contribute to the hepatocyte proliferation, either directly (e.g. allogeneic hepatocytes or stem cell derived hepatocytes) or cell therapies that aim to enhance endogenous processes (e.g. bone marrow derived cells).

### Hepatocyte mitogens

Administration of hepatocyte mitogens (such as HGF) may boost hepatocyte proliferation in preclinical models and safety has been demonstrated in a recent phase I clinical trial[99-101]. However in the context of cancer surgery, growth factor administration could increase risk of recurrence or promote metastasis. In addition the short half-life of these agents, in animal models which have shown benefit, rely upon viral vector gene therapy to upregulate growth factor expression, which is not a translatable model. A range of hormone strategies have been trialled in the clinic including insulin / glucagon infusion and human growth hormone in the settings of acute liver failure and partial hepatectomy with chronic liver injury respectively[102,103]. However neither of these interventions resulted in demonstrable clinical benefit.

### Extracorporeal liver support

Extracorporeal liver support systems have been trialled in settings of acute and acute-on-chronic liver failure with limited success. These systems can either involve an albumin dialysis circuit and charcoal filtration (artificial liver support), or contain functional hepatocyte-like cells, intended to perform both detoxification and synthetic functions (bioartificial liver support). I undertook a meta-analysis of randomised controlled trials involving extracorporeal liver support systems prior to my PhD. This indicated a small survival benefit in acute liver failure, but there was no evidence of survival benefit in acute-on-chronic liver failure[104].

### Cellular therapies

Direct administration of stem cells or even allogeneic or differentiated hepatocytes has had limited success[105]. This is likely due to the unfavourable environment which these cells encounter within the injured liver. Bone marrow derived cells are thought to

contribute to regeneration by promoting endogenous processes and their supplementation (by adoptive transfer) or mobilisation may further promote regeneration of the liver following PH[106]. Beneficial effects of various BM derived cells administered in rodent models of liver regeneration have been reported and this cell source also offers the opportunity to use autologous cells[105]. Favourable effects are likely due to paracrine action, although the mechanisms underlying this are poorly understood[107,108]. It was previously thought that bone marrow derived cells could transdifferentiate into hepatocytes[109-111]. However this has subsequently not been repeatable, with hepatocytes either erroneously identified, likely the result of cell fusion events, or involve animal models with unique selection pressures not directly relevant to clinical practice[107].

Clinical studies administering BM derived cell populations (eg mononuclear cells) mainly in liver cirrhosis have begun with potentially promising results[112]. However these small, generally uncontrolled trials tend to administer mixed cell populations, limiting the understanding of mechanism and risking administration of profibrotic cell populations[106,112]. In the context of liver surgery, evidence from small (poorly controlled) clinical studies suggests that administering enriched bone marrow progenitor cell populations (CD133+ and/or CD34+) to patients at the time of portal vein embolization may further boost future liver remnant volume[113-116].

In chronic liver injury, bone marrow derived macrophages are pivotal to remodelling fibrosis, which is a key requirement for the hepatic progenitor cell (HPC) response.[59,117] With this in mind, preclinical studies have recently demonstrated a therapeutic role for macrophage administration in promoting remodelling of fibrotic liver matrix[87]. There is mounting evidence that the macrophage is a key cell in the control of liver regeneration

following partial hepatectomy also[118-120]. Mechanisms of macrophage action in this context include the production of cytokines and growth factors, regulation of vascular tone, minimising endotoxin mediated systemic inflammation and hepatocyte damage[29,121-123]. With the macrophage functioning as a major mediator of both regeneration and the innate immune system, this cell represents a potential therapeutic target.

## Colony stimulating factors

There are three colony stimulating factors- macrophage colony stimulating factor (MCSF, CSF 1), granulocyte macrophage colony stimulating factor (GMCSF, CSF2) and granulocyte colony stimulating factor (GCSF, CSF3). MCSF has a role in the maintenance of cells of the monocyte macrophage lineage from bone marrow precursor to tissue resident macrophage. GMCSF is involved in both neutrophil and macrophage maintenance and is predominantly produced by inflammatory cells. GCSF is involved maintenance of bone marrow stem cell populations and their release into the blood, as well as neutrophil production and function.

While the importance of CSF1 in liver regeneration was discussed earlier, its therapeutic potential has not been explored in liver disease. However CSF1 supplementation following kidney and neurological injury has shown regenerative benefit [124,125]. In the clinical setting higher CSF1 level has been associated with more rapid liver regrowth following living donor PH[126]. GMCSF (CSF2) has a role in stimulating remodelling of the liver, likely through effects on neutrophils during regeneration and supplementation can facilitate regeneration in normal and cirrhotic rats[127-129]. However, there is evidence that overstimulation of GMCSF can have cytotoxic effects in the presence of lipopolysaccharide, inducing widespread hepatocyte apoptosis[130].

GCSF (CSF3) can mobilise liver sinusoidal progenitor cells (LSECs), which are a rich source of hepatocyte growth factor. GCSF therapy can promote regeneration in rat models of acute liver injury and recent evidence suggests that in patients with acute-on-chronic liver failure, GCSF therapy can improve survival[36,114].

In summary, therapeutic strategies to enhance liver regeneration either focus on enhancing the hepatocyte pool (cell administration or mitogens) or facilitating non parenchymal cell involvement in the regenerative process.

# 1.5 Targeting macrophages

Experimental strategies to enhance liver regeneration have typically focussed on the hepatocellular compartment, neglecting the importance of hepatic immune function. In considering an appropriate strategy to enhance liver regeneration it seems both the effects on hepatocellular regeneration and on innate immunity should be considered.

Given the macrophage predominates in the liver during the steady state, the critical role of the liver macrophage in maintaining homeostasis through innate immune functions and the role of the macrophage in regeneration, the macrophage appears to offer a suitable therapeutic target. To understand the best methods in which to target macrophages, an understanding of tissue macrophage dynamics in the steady state, injury and repair is necessary.

## The origin of liver macrophages

There has been considerable attention on the origin of tissue macrophages over the past 40 years. Liver macrophage origin remains controversial with options including proliferation of mature macrophages, replenishment by circulating monocytes or derivation from a progenitor / stem cell originating from within the liver.

### Historical perspective of liver macrophage origin

Using radiolabelled thymidine[x] to identify cells undergoing mitosis, Crofton et al showed back in the 1970s that tissue resident macrophages in the liver are capable of proliferation in the steady state[131]. However the percentage was low, with just 1% of

[x] The radioactive nucleoside, 3H-thymidine, integrates with new chromosomal DNA during mitosis. DNA is replicated during S-phase of the cell cycle and this where the incorporation occurs.

liver macrophages incorporating 3H-thymidine at 1 hour following injection (approximately 1.4%). To assess whether replenishment of hepatic macrophages was principally due to resident cell proliferation of a long lived population or replenishment of macrophages by bone marrow derived monocytes, this group explored the dynamics of monocytes in the bone marrow and peripheral blood in comparison to labelled cells in the liver. 48 hours following a single injection the authors found that liver macrophage labelling had increased to 10.4% of the population and thereafter this percentage reduced slowly. Monocyte labelling in the blood was much higher however, at up to 60% 48 hours following injection. The authors concluded that the increase in labelled Kupffer cells could not be attributed to proliferation of resident liver macrophages alone and therefore that monocytes must be contributing to the liver macrophage pool. Following this the authors irradiated mouse livers, but protected bone marrow finding that liver macrophages returned rapidly. Crofton concluded that tissue resident macrophage replenishment was not due to proliferation but derived from circulating monocytes.

The results of Crofton et al. contrasted with an earlier parabiosis[xi] experiment (1976) where 3H-thymidine was repeatedly given to one rat in the pair following vascular coupling[132]. The liver of the second rat was then examined at later time points for 3H-thymidine positive macrophages[xii]. While monocytes were labelled in the non-injected rat, hepatic macrophages labelling was minimal suggesting that crossover of labelled monocytes was not contributing to the second rat's liver macrophage populations.

These two early studies have a number of limitations, given they both rely on indirect measures and summations for identification of macrophages (phagocytic ability), cell

[xi] Parabiosis is this context refers to the surgical joining of two animals which then share a circulatory system.
[xii] Labelled monocytes crossed between rats such that labelled monocyte percentage was similar in both animals

labelling (3H-thymidine incorporation) and assessment with a single technique (non-parenchymal liver cell smear and cell count). The use of radiation to deplete tissue macrophages can result in general tissue injury and this undoubtedly influences the monocyte / macrophage response.

In the intervening years there were isolated reports indicating the proliferative capacity of macrophages or "macrophage-like" cells. Such as the depletion experiment by Yamamoto et al.[133]. Here clodronate encapsulated liposomes[xiii] were administered to deplete tissue macrophages. Liver macrophage number returned to normal by day 14 following injection. There appeared to be a population of small, highly proliferative "macrophage-like cells" that the authors suggested could represent a liver macrophage progenitor cell population. Equally, however, these cells may have represented immature monocyte populations induced by the widespread depletion of phagocytic cells.

Overall, given the low proliferation of macrophages in the steady state, it became the widely accepted belief that tissue resident macrophages and inflammatory macrophages are terminally differentiated cells arising from blood monocytes[135].

## Contemporary analysis of liver macrophage origin

30 years on from the experiments of Crofton[131] and Volkman[132] developments in genetic manipulation and cell labelling techniques have enabled the question of macrophage origin to be readdressed. Bouwens et al, labelled liver macrophages with a single

[xiii] Clodronate is a bisphosphonate which, when in solution, does not cross liposomal or cellular phospholipid membranes. However when it is encapsulated in liposomes, the liposome is taken up by phagocytic cells and released intracellularly, impairing mitochondrial function and leading to apoptosis of the phagocytic cell134. Lehenkari, P.P., *et al.* Further insight into mechanism of action of clodronate: inhibition of mitochondrial ADP/ATP translocase by a nonhydrolyzable, adenine-containing metabolite. *Molecular pharmacology* **61**, 1255-1262 (2002).

injection of latex beads[xiv]. They found that the mean number of labelled liver macrophages did not change over a period of 3 months. These results indicate the longevity of the liver macrophage population and could account for the low proliferation rate if this macrophage population was indeed self-renewing. It has subsequently become accepted that macrophages are capable physiologically relevant proliferation under certain stimuli. Jenkins et al recently demonstrated that accumulation of macrophages at inflammatory foci occurs independently of blood monocytes, via a process of self-renewal involving interleukin-4 and CSF1[136]. Subsequently both bone marrow derived and tissue resident macrophages have been shown to be capable of proliferation during inflammation[137].

With regards to the liver resident macrophage in the steady state, Klein et al., exploited the two different alleles of the CD45 gene (CD45.1 and CD45.2) to create chimeric mice. In their experiments CD45.2 mice received CD45.1 bone marrow following irradiation to the hind limbs while shielding the liver[119]. Mice were then examined in the steady state and following liver transplantation. By extracting macrophages and assessing populations by flow cytometry they showed that 4 weeks following bone marrow transplantation 99% of hepatic macrophages were derived from the donated bone marrow. However when assessed by immunohistochemistry, only 54% of hepatic macrophages were found to be derived from the transplanted bone marrow. The reason for this discrepancy was unclear. Klein et al trialled multiple macrophage extraction strategies to try to get at this population by flow cytometry but these were unsuccessful. The group termed this population “sessile macrophages”, in view of the fact that they could not be extracted. They commented that they were unsure where this population of macrophages arose from, but that there was no evidence they were derived from a

[xiv] Latex beads are rapidly phagocytosed by macrophages

progenitor cell population. This discrepancy highlights the problems with relying on a single technique for cell identification and in particular the limitations of cell extraction.

Schulz et al. opted for a genetic strategy whereby haematopoietic stem cells could be ablated without the requirement for radiation via the conditional knock out of the transcription factor *Myb*[138]. This approach meant that tissue macrophages dynamics could be explored without the requirement for radiation, so avoiding the effects of tissue injury on macrophage phenotype, This group found that a population of macrophages arose in the yolk sac, prior to the development of haematopoietic stem cells and that there was evidence that these yolk sac derived macrophages persisted into adulthood as the predominant liver macrophage. Experiments by Yona et al. have since confirmed these findings of a liver macrophage population independent of the bone marrow using a different strategy. Yona et al., exploited the dynamics of the *Cx3Cr1* gene which is expressed by monocytes but not tissue liver macrophages in the adult[139]. Using mice with either conditional or constitutively active Cre recombinase genes in the *Cx3Cr1* they showed that fetal liver macrophages were *Cx3Cr1* positive but adult liver macrophages were not. By labelling fetal liver macrophages with the conditional *Cx3Cr1* reporter (red fluorescent protein) in mice with constitutively expressed *Cx3Cr1* (green fluorescent protein) it was shown that the majority of the liver macrophages were derived from the embryonically labelled macrophages (red fluorescent protein).

These contemporary findings contrast with the historical perspective of replenishment of macrophages in the steady state and demonstrate the importance of adopting different strategies and multiple methods of assessment to address a specific question. The genetic labelling techniques of Schulz[138] and Yona appear the most robust although these groups did not disrupt normal homeostasis by testing macrophage replenishment in

injury or following macrophage loss. In the peritoneal cavity resident macrophages are under the transcriptional control of Gata6, which controls their proliferative renewal both during homeostasis and during inflammation[140]. Recognition of hepatic macrophages as a distinct self-renewing macrophage population is likely to identify specific genes regulating their homeostasis and response to injury and inflammation.

Applying these genetic strategies to models of liver injury and macrophage depletion will be interesting and no doubt demonstrate the plasticity of the system.

## Regulation of cells of the monocyte macrophage lineage

There are two key haemopoetic growth factors which can influence monocyte and macrophage production and phenotype. These are macrophage colony stimulating factor (MCSF or CSF1) and granulocyte-macrophage colony stimulating factor (GMCSF, CSF2).

CSF1 is produced by a wide range of tissues and in the liver can be produced by both parenchymal and non-parenchymal cells[141,142]. Colony stimulating factor 1 is an essential regulator of optimal monocyte- macrophage function, necessary for the generation of monocytes from bone marrow progenitor cells and the maintenance of tissue macrophages[143]. GMCSF has negligible circulating levels, but this can rise in response to an inflammatory stimulus, in particular in response to infection. GMCSF is produced by inflammatory cells rather than epithelial tissue[144]. While GMCSF can influence macrophage phenotype it lacks the capacity to generate mature human monocyte or tissue macrophage populations[145].

There is thought to be competition between CSF1 and GMCSF when both are present at high concentrations, such that macrophage phenotype can be influenced[146]. With tissue

macrophages exposed to CSF1 under normal conditions in the steady state it has been regarded a more anti-inflammatory, "pro-regenerative" macrophage phenotype, whereas GMCSF, which is only present during inflammatory reactions is regarded as inducing a "pro-inflammatory" macrophage phenotype[144]. In vitro classification of macrophages has led to the categories of M1 (more "pro-inflammatory", characterised by TNF alpha and Il6 production) and M2 (more "anti-inflammatory", characterised by high Il10 production) macrophages[147]. However, in vivo the situation is more complex with macrophages displaying a range of activation states and a phenotypic spectrum dependent on the specific microclimate of the individual cell.

CSF1 has a central role in mediating repair following organ damage. In mouse models of injury in both the brain and kidney CSF1 blockade impairs the regenerative response and supplementation of CSF1 can facilitate recovery[148-150]. GMCSF elicits a more proinflammatory, "M1" response to facilitate destruction of invading pathogens[144]. This pro-inflammatory state induced by GMCSF can have negative consequences, with overexpression of GMCSF in the context of lipopolysaccharide administration leading to widespread hepatocyte apoptosis[130].

## The biology of macrophage colony stimulating factor

The macrophage colony stimulating factor (CSF1) deficient mouse (op/op mouse) shows an extremely low number of mononuclear phagocytes, general growth retardation, impaired regenerative capacity and poor fertility, although it is still viable[82,83]. Mice with genetic ablation of the CSF1 receptor (CSF1R) express a more severe phenotype however, and rarely survive to adulthood[151]. Recently a second ligand for the CSF1R was identified which could account for the discrepancy between the ligand and receptor deficiency models. Following a functional screen of a comprehensive set of recombinant

proteins against a range of cell types Lin et al. identified a novel cytokine which interacted specifically with the CSF1 receptor[152]. The authors named this novel cytokine Il-34. Further analysis by other groups has shown that while there is functional overlap between Il34 and CSF1 their tissue expression is more diverse. For example while Il34 mRNA is expressed in the liver, Il34 deficiency had no effect on liver resident macrophage numbers[153]. However Il34 deficiency did result in a marked depletion of Langerhans cells (dendritic cells[xv] of the skin) and microglia (the resident macrophage of the brain and central nervous system).

Antibody blockade of the CSF1 receptor in the steady state markedly reduces macrophage numbers in the liver and also reduces liver size in mice, demonstrating the importance of CSF1R signalling in maintaining homeostasis[80]. Using radiolabelled CSF1 it was shown in the 1980s that liver resident macrophages are the principle regulators of serum CSF1 concentration[84]. This group showed that macrophages selectively cleared CSF1 by receptor mediated endocytosis and subsequent intracellular degradation. The effect of removal of liver tissue on circulating CSF1 level has not previously been established in mouse models. However it was recently shown in humans that patients undergoing living donor partial hepatectomy[xvi], a higher serum CSF1 level was associated with increased rate of liver remnant growth[126]. In chronic liver disease, serum CSF1 levels are elevated but the functional consequences of this are unclear[156].

[xv] Dendritic cells and macrophages are morphologically similar and there has been some controversy as to whether these two cells actually represent subtypes of the same cell rather than distinct cells altogether. Treated as separate cells, macrophages perform a predominantly innate immune reponse, whereas dendritic cells interface with the adaptive immune system through antigen presentation. 154. Ferenbach, D. & Hughes, J. Macrophages and dendritic cells: what is the difference? *Kidney Int* **74**, 5-7 (2008), 155. Hume, D.A. Macrophages as APC and the dendritic cell myth. *J Immunol* **181**, 5829-5835 (2008).

[xvi] Living donor partial hepatectomy is the first part of a liver transplant procedure whereby an individual (usually a relative of the patient requiring liver transplantation) undergoes partial hepatectomy to donate part of their liver to a patient with liver failure.

## Macrophages during liver injury and repair

Macrophage dynamics have been explored in models of liver injury although techniques to define origins have not been as rigorous as that shown in the steady state. Efforts have centred around ablation of specific cells using genetic and toxin based approaches. These have centred around the CD11b-DTR mouse[xvii], clodronate encapsulated liposomes (see Footnote xiii, p40) and limitation of cellular trafficking by chemokine inhibition.

Following chronic liver injury Prakash et al., used adoptive transfer experiments and depletions using the CD11b-DTR mouse to show that monocytes are recruited from the circulation and become macrophages necessary for effective remodelling of hepatic fibrosis[158]. The CD11bDTR mouse depletes cells expressing the CD11b cell surface receptor. While this model is regarded as a model to deplete monocytes and macrophages, a number of other cell types also express this receptor, including neutrophils and eosinophils. However, in a model of lung injury induced by lipopolysaccharide, infiltrating neutrophil numbers did not seem to be affected by CD11b-DTR, despite neutrophil upregulation of CD11b expression in association with injury[159]. In a lung model of sterile inflammation, numbers of eosinophils in the circulation were not affected by CD11b-DTR depletion but there was reduced recruitment of eosinophils to the lung[160]. It seems likely that administration of diphtheria toxin will influence the phenotype of these CD11b expressing cells. Interestingly, although monocytes and some tissue resident macrophages (kidney, peritoneum, lung) are depleted by the administration diphtheria toxin in the CD11b-DTR mouse, liver

[xvii] The CD11b-DTR construct targets cells expressing the CD11b receptor whereby administration of diphtheria toxin (DTR) leads to depletion of these cells. Mice do not otherwise express a receptor for the diphtheria toxin. It is reported that this model preferentially targeting monocytes and macrophages, although other cells do express the CD11b receptor. 157. Duffield, J.S., *et al.* Conditional ablation of macrophages halts progression of crescentic glomerulonephritis. *Am J Pathol* **167**, 1207-1219 (2005).

resident macrophages are not[86]. This is likely to be due to the low CD11b expression of these cells[161].

Thomas et al, showed that adoptive transfer of macrophages during the fibrotic process can enhance the remodelling effects[87]. Following acute liver injury characterised by necrosis (paracetamol intoxication), monocyte macrophage infiltration via the chemokine CCR2, is required for effective clearance of necrotic debris[49,52]. In models of liver regeneration in the absence of liver remnant injury (partial hepatectomy), circulating monocytes are recruited via ICAM-1 and mediate hepatocyte proliferation via the production of tumour necrosis factor and interleukin (IL)-6[28]. Depletion of macrophages in liver regeneration either using the CSF1 deficient mouse or by ablation with clodronate encapsulated liposomes impairs the hepatocyte proliferative response[162]

An understanding of the origin of macrophages and their potential manipulation allows consideration of therapeutic possibilities. Both administration of bone marrow derived macrophages and stimulation of macrophages in vivo via macrophage colony stimulating factor (CSF1) appear to be suitable strategies to explore the effects of macrophage manipulation on liver regeneration. A macrophage based therapy could address a rapidly increasing clinical need by promoting safe resection of liver cancers and facilitate regeneration following acute liver injury.

I therefore aimed to determine whether the positive effects of macrophage therapy seen in mouse models of liver fibrosis can be extended to liver resection and define the mechanisms underpinning this action. In this thesis I go on to explore the effects of macrophage stimulation in vivo using a CSF1 based therapy in surgical models of liver

regeneration and a model of acute toxic liver injury. Finally I explore the dynamics of serum macrophage colony stimulating factor in humans following both partial hepatectomy and acute toxic liver injury.

# Chapter 2. Materials and Methods

## 2.1 Animal experiments

All experiments adhered to the Animals (Scientific Procedures) Act 1986. I obtained ethical approval from the University of Edinburgh ethics committee for partial hepatectomy and partial hepatectomy plus chronic liver injury experiments. The licence to operate was granted by the Home Office. I obtained wild type C57BL/6 mice from Charles River for the liver regeneration, macrophage administration and CSF1-Fc experiments. Mice were randomly distributed to ensure weight and age distribution across groups. Mice were maintained on 12-hr light-dark cycle and had free access to water and food. 8 -12 week old male mice were used for all experiments. Mice from the same batch were used in each experiment.

I obtained MacGreen mice ($Tg(Csf1R\text{-}GFP)_{Hume}$[163] for imaging experiments from the Roslin Institute, University of Edinburgh. I collaborated with Professor Allan Mowat and Calum Bain (Post-doctoral scientist) from the University of Glasgow to undertake experiments using the CCR2-/- mouse. I collaborated with Professor Steve Anderton to obtain Il6-/- mice.

I collaborated with Professor Jeff Pollard who had previously performed lineage tracing experiments using an inducible CSF1R-Cre system to identify CSF1R expressing cells in the liver. These experiments had been performed at the Albert Einstein College of Medicine, USA following ethical approval and according to NIH guidelines for the care of laboratory animals.

In this experiment which had previously been performed, *Tg*(*Csf1r-Mer2iCre)*$_{jwp}$ were crossed to Rosa floxed stop tomato red (obtained from the Jackson labs) at the Albert Einstein College of Medicine and lineage tracing experiments performed[138]. To induce the cre recombinase mice were fed for two weeks with F6370 Rodent Diet formulated with Tamoxifen at 750 mg/k (Bio-Serv). This method had previously been have found to give optimal induction of the cre recombinase, with greater than 90% of monocytes labelled[138]. All mice were bred and maintained under specific pathogen-free conditions.

## 2.2 Reagents

Chronic liver injury was induced by intraperitoneal injection of carbon tetrachloride (Sigma-Aldrich; 99.9%) in solution with olive oil (Sigma-Aldrich; highly refined, low acidity). CSF1-Fc is a conjugate of porcine CSF1 with the Fc region of porcine IgG1A (43.82kD total) produced by Zoetis for D. Hume (UK patent application GB1303537.1). Porcine CSF1 is equally active in mice[164] and the conjugate was formed for increased in vivo stability. CSF1-Fc does not exhibit any endotoxin like activity in murine BM-derived macrophages and phosphate buffered saline (PBS) was used as the control[165]. CSF1 receptor blockade was induced by the CSF1R tyrosine kinase inhibitor, GW2580 (160mg/kg suspended in 0.5% hydroxypropylmethylcellulose and 0.1% Tween 80[165], LC laboratories), or using the antibody AFS98 (produced from hybridoma by BioServ UK). The GW2580 vehicle and rat IgG2a (provided by BioServ UK) were used as control. CSF1-Fc, GW2580 and AFS98 were administered immediately following 2/3 partial hepatectomy or 12 hours following acetaminophen intoxication (point of maximal injury[166]). 5,Bromo-2-deoxyuridine (50mg/kg, Sigma-Aldrich) was administered 1 hour prior to cull by intraperitoneal injection.

# 2.3 Models of liver regeneration

## Partial hepatectomy

I performed 2/3 partial hepatectomy under isofluorane anaesthesia by ligating the left lobe and left and right median lobes as previously described[167]. I performed surgery between 9am and 12pm to minimise the effect of diurnal variation on liver regeneration. I strictly adhered to aseptic technique and conducted animal husbandry according to veterinary advice.

## Partial hepatectomy and chronic liver injury

I induced hepatic fibrosis in mice by intraperitoneal injection of carbon tetrachloride (CCl4) at doses from 0.5mcl/g to 2 mcl/g made up in olive oil in a 1:3 (CCl4:olive oil) solution (see section 3.2 Partial hepatectomy and chronic liver injury, p67 for discussion of dosage choice). I performed partial hepatectomy as per details above at day 3 following the final injection. I selected day 3 as this is the time point of maximal fibrosis[158].

## Paracetamol intoxication

I performed paracetamol intoxication by intraperitoneal administration of 350mg/kg acetaminophen (Sigma Aldrich) dissolved in PBS following an overnight fast as previously described[168]. PBS was warmed to 60 degrees Celsius to facilitate solution and then kept warm until intraperitoneal injection. See section 3.3 Acute toxic liver injury, p81 for explanation of dosage choice.

# 2.4 Therapeutic interventions

## Macrophage generation for direct administration

I extracted bone marrow from syngeneic mouse femurs and cultured in Teflon pots in DMEM/F12 medium conditioned with CSF-1 derived from L929 cells. This method follows protocols well established within this laboratory[87]. Following 7 days culture cells I characterised a sample of these cells according to surface marker expression based on flow cytometry (F4/80; CD209; Ly6C; CD11b) and immunohistochemistry (CD68; MR; INOS).

I initially selected the portal vein as the optimal route of administration of macrophages, following on from previous work within this laboratory[87]. However following partial hepatectomy, portal vein injection resulted in an unacceptably high complication rate. Therefore the route of administration was changed to intrasplenic injection (see section "5.2 Optimising route of cellular injection", p

5.2 Optimising route of cellular injection" page 104).

## CSF1 receptor stimulation with CSF1-Fc

The treatment group received 0.75mcg/g CSF1-Fc[165] administered subcutaneously either in the steady state without injury, immediately following partial hepatectomy or 12 hours following paracetamol intoxication and subsequently every 24 hours for three further doses. 0.75mcg/g dose choice was based on unpublished data by collaborators (D. Hume and D Gow) who had performed dose escalation studies. Control mice received subcutaneous PBS of appropriate volume. I considered whether administering a pure Fc fragment for control was appropriate but after discussion with collaborators and supervisors this was not deemed necessary due to the relatively small number of Fc fragments administered in conjugation and the fact that a true control would require a Fc-conjugation with an inactive protein and this was not available.

## CSF1 receptor inhibition

The antibody against the CSF1 receptor (AFS98) and the small molecule inhibitor (GW2580) were administered immediately following partial hepatectomy or at 12 hours following paracetamol intoxication. Administration was continued until post-operative day 2 with daily administration following partial hepatectomy (peak proliferative time point). In the case of paracetamol intoxication inhibition was commenced 12 hours following injury until day 3.

## 2.5 Terminal procedures

Mice were culled via CO2 inhalation at various time points from the point of injury according to Home Office guidelines and weighed. Following a midline laparotomy blood was aspirated from the inferior vena cava for serum analysis. Mice were perfused slowly through the inferior vena cava with 5mls of PBS and viscera excised and weighed. Liver and other viscera were either fixed in 4% formalin for immunohistochemistry, placed in RNA later® (Life Technologies), or placed in PBS for flow cytometry.

## 2.6 Assessment of hepatic function

### Indocyanine green assay

I developed an assay to assess indocyanine green clearance non-invasively. The development of this assay is discussed in "Functional assessment of liver regeneration", p84. Mice were anaesthetised with isofluorane anaesthesia and placed in the IVIS scanner (Fluorescent imaging camera). Indocyanine green [Sigma] diluted in sterile water was then administered via a peripheral vein. 30 seconds following this serial fluorescent images were taken at 1 minute intervals for up to 30 minutes. Regions of interest were drawn over the left and right hind paws, the liver region and also lower abdomen (control compensation for liver region). Efficiency of fluorescence (ratio of absorbed to emitted photons) was then used to quantify the fluorescent signal.

### Phagocytosis assay

I developed an assay to assess phagocytosis in vivo. The development of this assay is discussed in "Functional assessment of liver regeneration", p84. Mice were anaesthetised with 2% isolfluorane and the inferior vena cava was cannulated. 0.1mls of 5000IU/ml

heparin solution was infused to prevent blockage of the catheter. 100µl of red fluorescent bead solution (1:5 Latex beads 1.0µm, fluorescent red, SIGMA-ALDRICH®) was infused through the cannula (1:2 solution for assay following paracetamol injury[xviii]).

Ex vivo fluorescent quantification was performed at one minute following bead injection and 15mls 0.9% NaCl flush (see Supplementary Figure 5a). For assessment of bead clearance from the circulation 20mcl of blood was removed from the cannula every two minutes starting from 1 minute post injection for 15 minutes. Blood was immediately fixed with 300µl FACS-Lysing solution (BD Biosciences). The cannula was flushed after sample removal and subsequently, dead space aspirated prior to sampling. After the 15 minute timepoint mice were perfused with 15mls 0.9% saline through the IVC cannula after dividing the portal vein enabling outflow. Organs were then removed (Liver, spleen, lungs, kidney, brain) and images captured using a Kodak In-Vivo Multispectral FX image station (Excitation: 550nm; Emission: 600nm; Exposure 1 sec; f-stop 2.8). Subsequently blood samples were analysed using a LSR-Fortessa™ flow cytometer (BD Biosciences) with fluorescent beads detected on the blue channel (B695/40) by a 1 minute sample collection on low flow rate setting. Multiphoton imaging was performed using a Zeiss LSM7 MP with Coherent Chameleon Ti:Sa laser.

## 2.7 Immunohistochemistry

Three µm sections of formalin-fixed tissue were used for immunostains. Ki67, BRDU, pan cytokeratin and CYPD2 required heat mediated antigen retrieval with 0.01M sodium

[xviii] Given the degree of tissue loss was much less that that following partial hepatectomy (approx. 70% following partial hepatectomy versus 10-20% following paracetamol intoxication) I increased dose of fluorescent beads administered in the paracetamol model.

citrate pH 6.0 for 10 minutes. Primary antibodies were used at the following dilutions: Ki67 (Leica) 1:500, BRDU (Abcam) 1:100, F4/80 (clone CI:A3-I, Biolegend) 1:100, CYPD2 (Abcam) 1:100. Appropriate secondary antibody was applied at a 1:250 dilution. Dual immunohistochemistry with F4/80 and BRDU or Ki67 was performed by first developing F4/80 using the Tyramide signal amplification system (PerkinElmer®) with subsequent heat mediated antigen retrieval followed by BRDU or Ki67 staining. Ki67 and F4/80 dual immunohistochemistry was also performed by developing F4/80 with an alkaline phosphatase substrate kit (red, Vector) and following heat mediated antigen retrieval Ki67 was developed with 3,30-diaminobenzidine (Dako) then counterstained with Harris' hematoxylin. Stained slides were blinded and images taken on the Nikon Eclipse E600. For image quantification of F4/80 staining 20 non overlapping images were photographed at x200. The extent of DAB staining quantified using image analysis software (Adobe Photoshop CS6). For CYPD2 quantification images were quantified using image analysis software (Adobe Photoshop CS6). For Ki67 quantification 20 serial non overlapping images were photographed at x400 then hepatocytes identified by assessment of morphology.

## 2.8 Flow cytometry

Liver was digested in 2mg/ml collagenase D (Sigma Aldrich) at 37degC for 30minutes then passed through a 100μm filter. 7 minute 50G spin to remove hepatocytes. Further purification of nonparenchyaml cells using 30% percoll® (Sigma) gradient. Cell stained with fixable viability dye eFluor 780® then incubated with Fc block (TrustainfcX™, Biolegend) prior to staining with CD45 (clone:30F11, AF700, Biolegend), F4/80 (clone:BM8, PECy7, Biolegend), CD11b (clone:RM208, FITC, Invitrogen), Ly6C (clone:HK1.4, PerCP/Cy5.5, Biolegend), dump gate (PE: CD3 (clone:17A2, PE, Biolegend,

CD19 (clone:6D5, PE, Biolegend), Siglec F (clone:E502440, PE, BD Biosciences), Ly6G (clone:IA8,PE, BD Biosciences). For proliferation assay cells were fixed and permeablised using BD Pharminogen BRDU flow kit then stained with antiBRDU (FITC, BD Pharminogen) and Ki67 (eF660, eBioscience). Flow cytometry performed using the LSR Fortessa. Gating strategies for cellular populations are shown in Appendix 2, (p233) and Appendix 3, (p233).

## 2.9 Quantification of Messenger RNA (mRNA) Levels by Real-Time Reverse-Transcription Polymerase Chain Reaction

RNA extraction kits (Qiagen) were used to extract RNA from whole tissue. cDNA was generated from 1 µg of RNA using the Quantitect reverse transcription kit. Predesigned validated primer sets for MARCO (macrophage receptor with collagenous structure), MSR1 (macrophage scavenging receptor 1), MR (mannose receptor), Il6, OSM (oncostatin M), TNF (tumour necrosis factor), IFNg (interferon gamma), Il10 and GAPDH were purchased from Qiagen (Qiagen Quantitect Primers). Quantitative real-time PCR was performed using Express SYBR Green (Qiagen, UK). Gene expression was calculated relative to GAPDH for each sample. Values are shown relative to the mean of the control group, which served as the comparator. Gene array at 6 hours following CSF1-Fc administration was performed using Cytokine and Chemokine array $RT^2$ Profiler PCR arrays and analysed using the online $RT^2$ profiler PCR Array Data Analysis (Version 3.5, Qiagen, UK) and presented by Volcano plot. Affymetrix Mouse gene 1.1 ST Array data were accessed from the Gene Expression Omnibus website and analysed using GEO2R. To take into account the false discovery rate due to multiple comparisons, the Benjamini

& Hochberg (False discovery rate) correction was applied to gene data series. The gene array data is provided in Appendix 1, (p231).

## 2.10 Serum Analyses

Serum biochemistry assays were performed using commercially available kits by a biochemist, including alanine aminotransferase (ALT; Alpha Laboratories), alkaline phosphatase (Alk phos; Roche Diagnostics), total bilirubin (bili; Alpha Laboratories Ltd), albumin (Alb; Alpha Laboratories). Serum cytokines and chemokines were analysed using MILLIPLEX® mouse cytokine/chemokine array (Merck-Millipore). All cytokine/chemokine assays were completed in collaboration with a Merck-Millipore biomarker specialist. Results are presented relative to the mean of the control group. Cytokines/chemokines above background signal are shown in the histograms. Cytokines/chemokines below background signal are listed below histograms.

## 2.11 Human Work

Ethical approval was obtained from the South East Scotland Research Ethics Committee (2) for examination of patient records and for collection of patient serum pre and post partial hepatectomy undertaken at the Hepatobililary Unit, Royal Infirmary of Edinburgh between December 2012 and October 2013. Serum samples were blinded and cytokine analysis completed in a random order. In the partial hepatectomy cohort liver failure was defined according to Schindl et al.[2]. For the acute liver failure cohort ethical approval was granted by the local human research ethics committee and informed consent was obtained from all patients, or the patient's next of kin, before entry into the study. This study builds on previous analysis of this patient cohort by Antoine et al.[97] and represents

84 adult patients admitted to the Royal Infirmary Edinburgh, UK or the University of Kansas Medical Centre, USA with acute liver injury. Serial patient samples were based on a second patient cohort where samples were collected from admission to hospital (as opposed to admission to the specialist liver centre with acute liver failure) some of these patients have been included in analyses previously but again serum CSF1 level had not previously been assessed[97]. Patients were grouped according to outcome, into those with acute liver failure who survived and those who required liver transplantation or died. Serum CSF1 was analysed using the Meso Scale Discovery® CSF1 immunoassay and analysed on a Meso QuickPlex SQ120. Serum acetyl-HMGB1 was previously analysed by mass spectrometry and this was not repeated[97].

## 2.12 Statistics

Statistical analysis was performed on Graphpad Prism V6.0, except logistic regression analyses which were conducted in *R*[169] by a qualified statistician. All data are presented as mean +/- standard error of the mean unless otherwise stated. Two tailed Student's *t* test are used where appropriate to analyse parametric data. Mann-Whitney test was used for non-parametric data. One-way and Two way ANOVA with Bonferroni adjustment for multiple hypothesis testing are stated when used. Kruskal-Wallis test was used to test non-parametric data involving greater than two groups.

Benjamini & Hochberg (False discovery rate) correction was used in analysis of array data. Biomarker analysis and development of the logistic regression models was completed by a qualified statistician. All data were blinded prior to analysis. Data were first plotted irrespective of outcome. While CSF1 showed an appropriate range, many of the acetyl-HMGB1 values were grouped around zero, which leads to difficulty in creating

a combined model. Therefore a logarithmic transformation was performed on the acetyl-HMGB1 variable. Preceding with the logarithmic transformation, a high correlation between CSF1 and acetyl-HMGB1 was seen. Using logistic regression to build a model, the individual models for CSF1 and acetyl-HMGB1 were first calculated. The models were then combined (glm(formula=outcome~log(acetyl-HMGB1)+CSF1, family = "binomial", data=data). Comparison of the combined model and the CSF1 model alone was performed by analysis of deviance of the dual model versus the singular model. Level of significance was set at $p<0.05$ for all analyses.

# Chapter 3. Developing mouse models of liver regeneration

The human liver is a solid organ which can be divided into right, left, quadrate and caudate lobes. However a more clinically relevant segmentation is based on the portal blood supply to the liver originally described by Couinaud in 1957 (Figure 3.1a). Liver surgery is planned according to this segmentation to facilitate tumour removal and minimise damage to remaining tissue.

The murine liver is lobulated, including the left, median, right and caudate lobe (Figure 3.1b) which facilitates surgical removal of liver segments, and subsequent study of the regenerative process. The availability of genetically manipulated mice means this species offers an ideal model to study regenerative processes.

This sections describes the development of the techniques and procedures that I have used for this project.

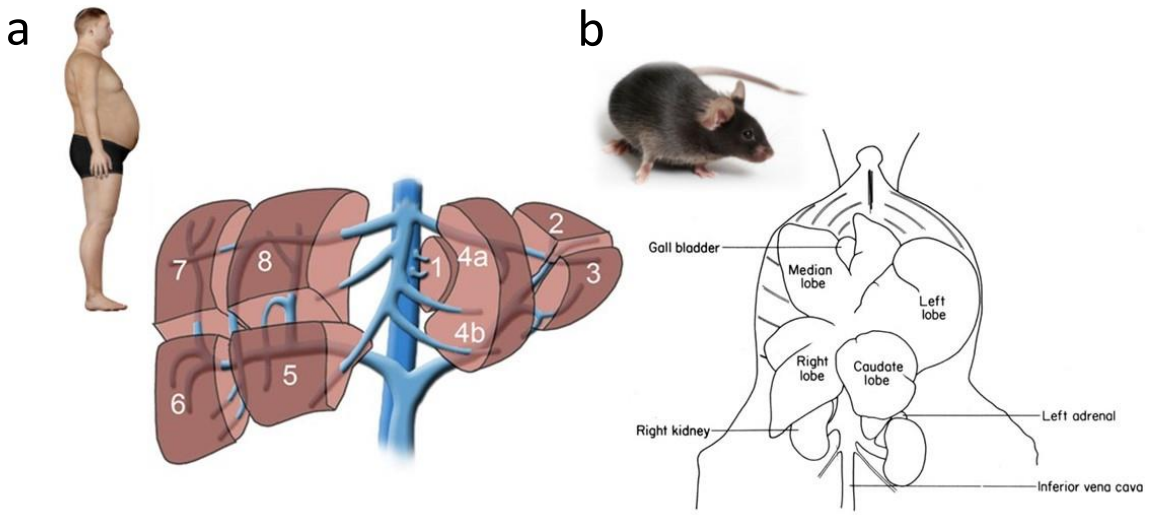


Figure 3.1: Schematic demonstrating the human and mouse liver divided into segments and lobes respectively

a) Couinard classification of liver segments. b) The lobulated mouse liver.

# 3.1 Partial hepatectomy

## Aims

1. Become proficient with 2/3 hepatectomy in mice and optimise operative procedures
2. Characterise baseline regenerative parameters following 2/3 hepatectomy
3. Assess macrophage dynamics following partial hepatectomy

## Results

I performed 2/3 PH on C57Bl6 mice at time points from 1 day to 7 days to assess change in liver weight to body weight ratio change and hepatocyte proliferation (n=8 per time point). The procedure was well tolerated with no mortality. As has previously been well described I found that liver regeneration following 2/3 hepatectomy in mice is rapid. Figure 3.2 shows the regenerative response to 2/3 hepatectomy with liver weight to body weight ratio approaching that of a normal mouse by day 7. Hepatocyte proliferation peaked at day 2 as assessed by Ki67(a nuclear protein associated with proliferation) immunohistochemistry.

I then analysed hepatic macrophage number and following partial hepatectomy, as identified by F4/80 positive cells, at time points from 1 hour to 7 days following surgery (n=4 per group). Figure 3.3 shows an increase in hepatic macrophage numbers following partial hepatectomy. There is also evidence of macrophage proliferation based on dual Ki67 and F4/80 immunohistochemistry which is reduced as a percentage during the early stages following partial hepatectomy.

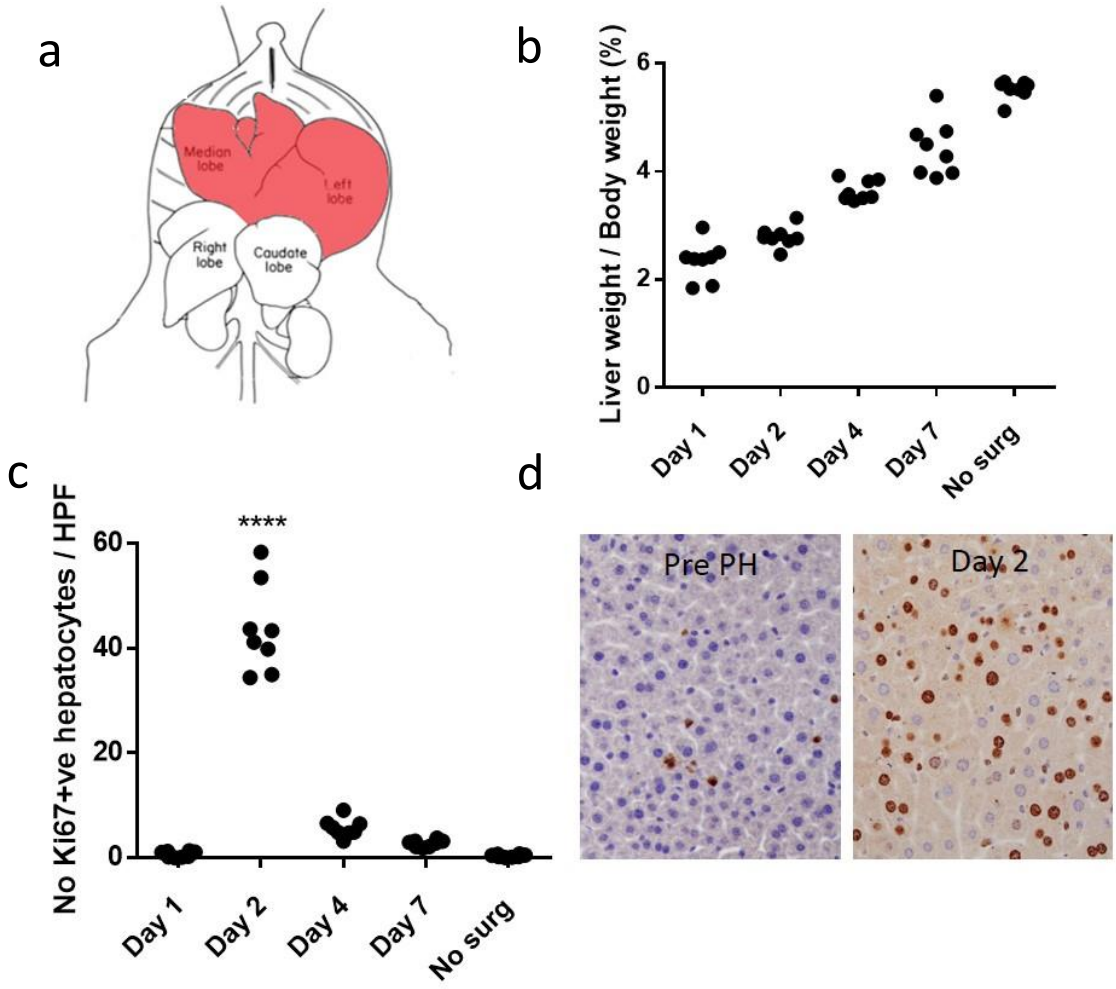


Figure 3.2: Hepatic dynamics following partial hepatectomy.

a) Schematic showing resected lobes in PH. b) Liver weight to body weight ratio following PH (n=8 per timepoint). c) Hepatocyte proliferation following PH based on number of Ki67 positive hepatocytes per high powered field (n=8 per timepoint). One way ANOVA shows Day 2 significantly elevated hepatocyte Ki67 expression compared to other time points (no signif diff between Day 1, 2, 7 and no surg). d) Indicative Ki67 immunohistochemistry pre partial hepatectomy and at Day 2 following partial hepatectomy.

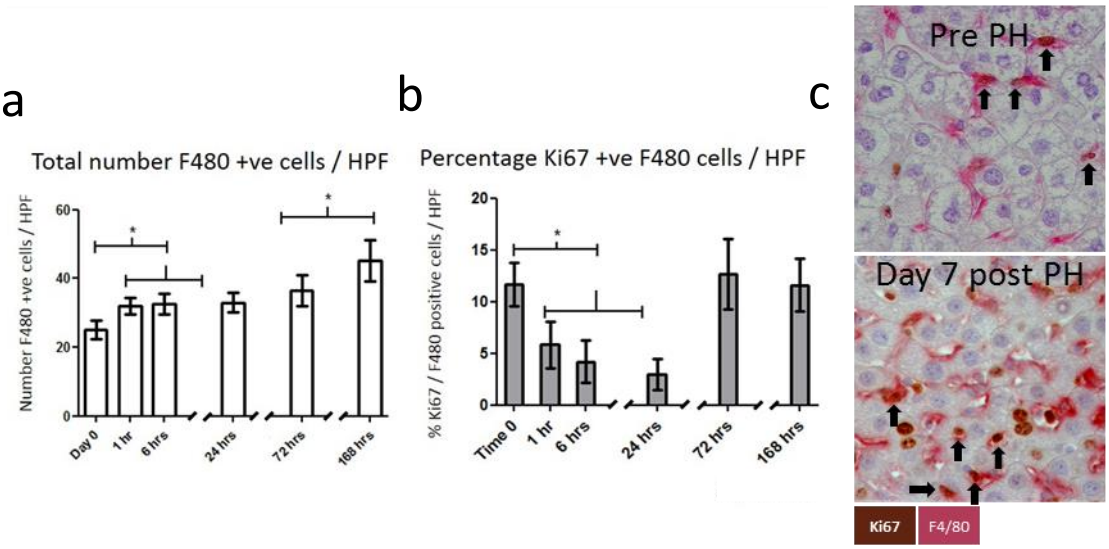


Figure 3.3: Hepatic macrophage numbers following partial hepatectomy.

a) Number of F4/80 positive macrophages per high powered field following PH (n=4 per timepoint; Kruskal-Wallis test; Dunn's test for multiple comparisons; *$p<0.05$ . b) Percentage Ki67 positive macrophages per HPF following PH (n=4 per timepoint; Kruskal-Wallis test; Dunn's test for multiple comparisons; *$p<0.05$). c) Indicative immunohistochemistry for F4/80 (pink) and Ki67 (brown) following PH. Arrows indicate dual positive cells.

## Discussion

The main non-parenchymal cells of the liver include tissue resident macropahges, stellate cells and sinusoidal endothelial cells. A range of other cells including T cells, natural killer cells and neutrophils have also been identified in the regenerating liver. Hepatic macrophages, neutrophils and stellate cells are thought to have a role in the matrix remodelling process through the production of matrix metalloproteinases. In addition to hepatocyte proliferation macrophages were also seen to proliferate following PH. Evidence of mitotic bodies in macrophages post-PH has previously been reported and this is confirmed here by the coexpression of F4/80 and Ki67. It was previously thought that in situ macrophage proliferation accounted for the increase in number of macrophages noted within the liver following PH but this has been questioned by more recent studies suggesting that infiltration of macrophages are important for effective hepatocyte proliferation[28,131]. However, these have been indirect assessments and the existence or role of these two populations remains uncertain. The importance of infiltrating macrophages in liver regeneration would support the idea of therapeutic macrophage administration in the context of PH.

## Conclusion

Consistent with the literature I have shown that partial hepatectomy results in a rapid restoration of volume through hepatocyte proliferation and there is evidence to support an early infiltration of macrophages.

# 3.2 Partial hepatectomy and chronic liver injury

## Aims

1. Establish a model of 2/3 hepatectomy on a background of hepatic fibrosis caused by chronic liver injury
2. Develop a model that demonstrates maximal fibrosis, feasibility and low mortality

### Rationale for approach to fibrosis induction

Carbon tetrachloride (CCl4) was selected to induce chronic liver injury. The resulting fibrosis shows a similar pattern to that seen in human disease and this model of chronic liver injury has previously been well characterised[170]. The use of CCl4 to induce injury plus partial hepatectomy in rodents has previously been reported[61,99,171] . These other groups have used the enteral route, which avoids issues with adhesions caused by intraperitoneal injection (scar tissue forming within the intra-abdominal cavity)[172]. However this route was not sanctioned by the regional Home Office Inspector. The intraperitoneal route was therefore the only available option (subcutaneous administration leads to variable results). In reviewing the literature, the greatest fibrotic response was in a mouse model of CCl4 gavage 3 times per week. However this frequency of IP injection was thought to risk greater potential adhesion formation and increase risk of complications from IP injection. Therefore the strategy of twice weekly injections was decided upon. A time period of 8 weeks was chosen as the length of fibrosis induction based on previous studies, balancing consistency of fibrosis with financial cost of a lengthier model. To modulate degree of fibrosis and achieve a workable model of hepatectomy, three different doses of carbon tetrachloride were selected following literature review and discussion with this and other groups working in the liver fibrosis field. These doses were 2mcl/g, 1mcl/g and 0.5mcl/g of CCl4 per gram mouse weight in

a 1:3 mixture CCl4: low acidity olive oil [supplied Sigma-Aldrich]). These doses were based on literature review and discussion with researchers who have experience of this model.

### Assessment of fibrosis induction regimen

C57Bl/6 mice were weighed prior to each injection and trends in weight loss monitored. If weight loss of over 20% occurred, mice were closely monitored and if weight regain did not occur or the condition of the mouse was deemed to have reached the severity limits of the experiment, the mouse was removed from the protocol and culled. Sirius red stain was used to indicate collagen deposition in the fibrotic liver. Image quantification was then performed using Adobe Photoshop (CS5).

### Partial hepatectomy following carbon tetrachloride

I performed partial hepatectomy 72 hours following the last IP injection of carbon tetrachloride as this is the time point of maximal fibrosis following CCl4 injection[158]. In addition, at this time point the acute effects of carbon tetrachloride administration are limited, potentially increasing the clinical relevance of this model of fibrosis. Age-matched control mice also underwent PH as previously described (termed "Hepatectomy control"). Further control mice underwent the fibrosis induction regimen but did not undergo PH (termed "Fibrosis control").

## Results

I selected three doses of carbon tetrachloride to induce fibrosis 0.5mcl/g, 1mcl/g and 2mcl/g. 2mcl/g CCl4 resulted in rapid weight loss and deterioration in mouse condition such that nearly 20% of mice were either removed from the protocol and were culled or died early on in the protocol. This dosing regimen was therefore terminated. 1mcl/g was generally well tolerated and resulted in a greater degree of fibrosis in comparison with the lower dose of 0.5mcl/g. Mouse body weight, Kaplein Meir plot of survival and fibrosis quantification are shown in Figure 3.4.

I performed partial hepatectomy 3 days following the final dose of carbon tetrachloride. Level of fibrosis reduced rapidly following partial hepatectomy. Interestingly there was no significant difference in level of fibrosis at Day 4 between the higher and lower dose of CCl4 (M-W U 150.0 p=0.12) despite the significantly greater fibrosis at Day 0 (M-W U= 5.0 p=<0.0001) (Figure 3.5). Rate of fibrosis resolution was more rapid following partial hepatectomy than sham surgery (Figure 3.6). Similar increased rate of fibrosis resolution has previously been shown in rats[61].

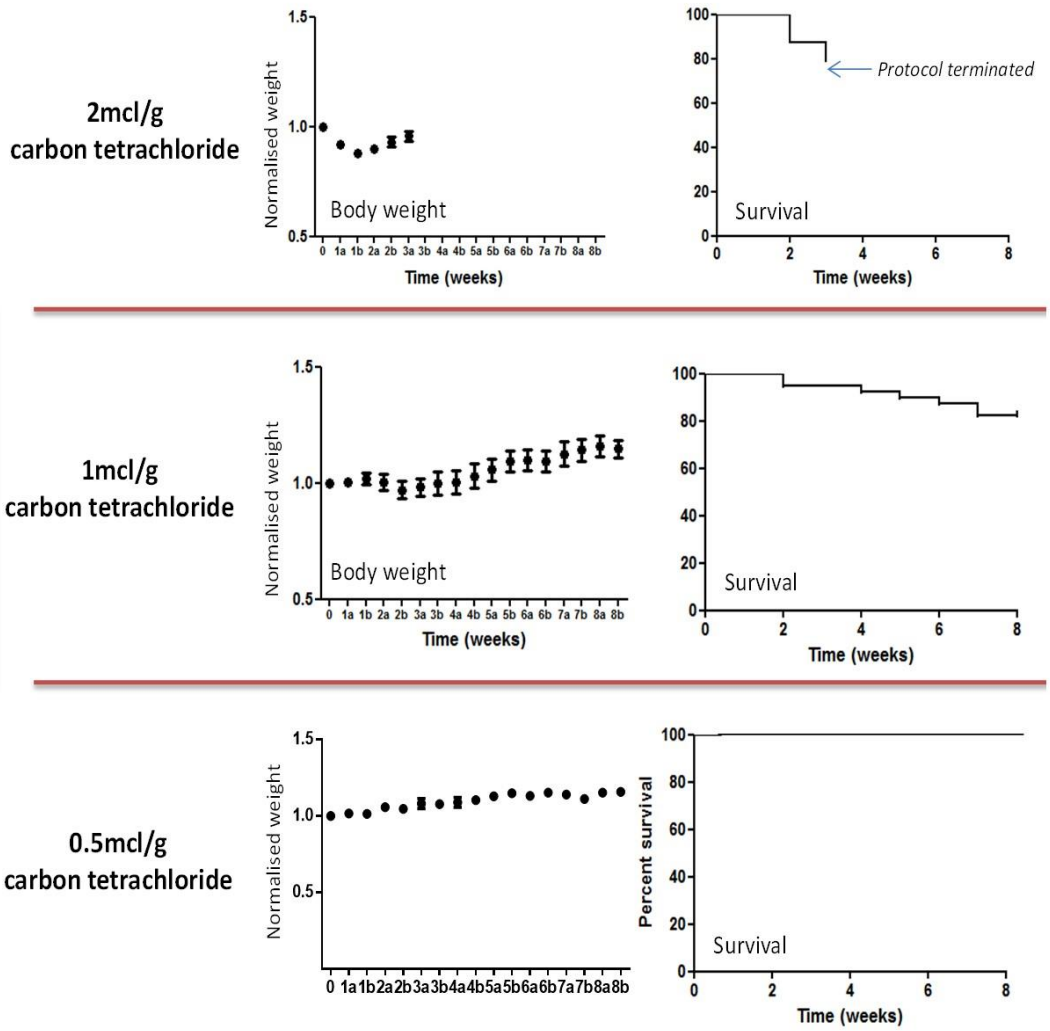


Figure 3.4: Fibrosis induction regimen.

Mouse body weight and Kaplein Meir plot of survival during the 8 week fibrosis induction regime with twice weekly intraperitoneal injection of carbontetrachloride at three doses (0.5mcl/g, n=8; 1mcl/g, n=22; 2mcl/g, n=24). Mouse body weight was taken prior to each injection and the weights expressed relative to the body weight prior to starting the experiment (normalised weight).

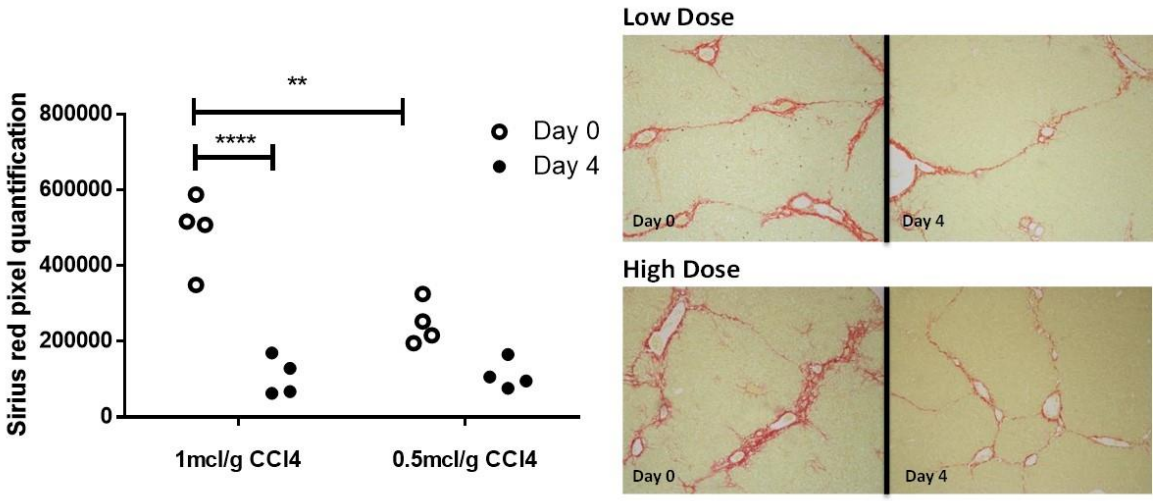


Figure 3.5: CCl4 dose comparison following partial hepatectomy.

Fibrosis quantification via sirius red analysis with representative siruis red staining. 2-way ANOVA showing significant difference between high dose and low dose CC4 at Day 0 and no significant difference between Day 4 values.

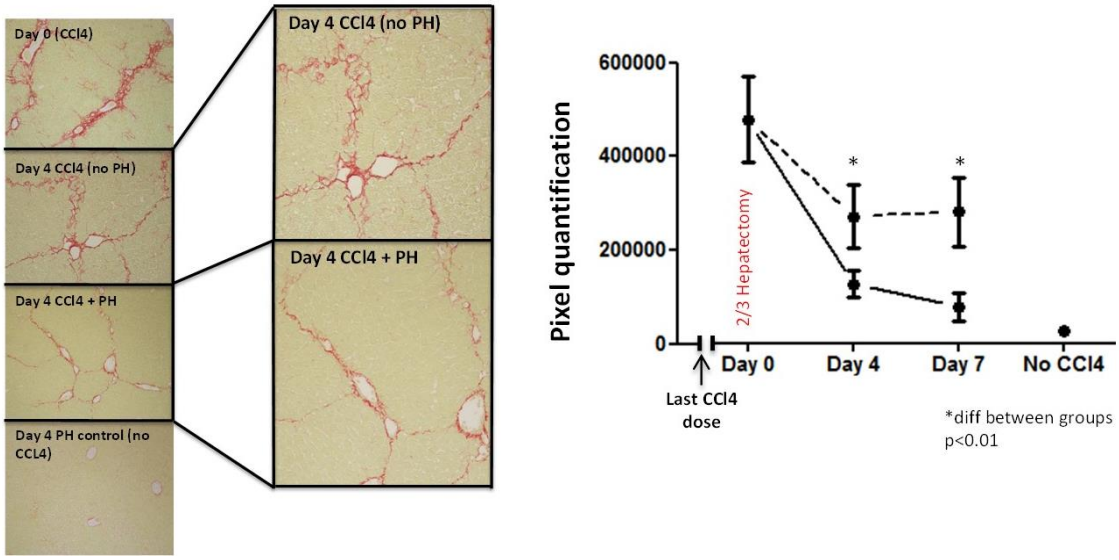


Figure 3.6: Comparison in fibrosis resolution between mice undergoing partial hepatectomy and mice undergoing sham surgery.

Fibrosis quantification via sirius red analysis with representative siruis red staining (n>/=4 per timepoint). Two-way ANOVA with Bonferroni post hoc showing significant difference between PH + fibrosis (solid line) and sham surgery + fibrosis (dotted line) at day 4 and day 7 postoperatively.

I found that liver weight to body weight ratio was higher in CCl4 treated mice compared to uninjured mice at time 0 (i.e. immediately following partial hepatectomy) (Figure 3.7). Rate of liver growth following partial hepatectomy was greater in the uninjured mice compared to those with previous CCl4 induced chronic liver injury (Figure 3.7). Hepatocyte proliferation was significantly reduced following hepatectomy in fibrotic mice compared to age matched controls who did not undergo the fibrosis induction regimen at time points from day 2 to day 7 ($p<0.001$) (Figure 3.8).

Liver progenitor cells were identified by morphological assessment following immunohistochemistry for pan cytokeratin (pan CK) (Figure 3.9). Previously termed oval cells, liver progenitor cells show potential for differentiation into either biliary cells or hepatocytes and stain positive for panCK. As biliary cells also stain positive for panCK morphological assessment was necessary to exclude ductular structures. Following 8 weeks CCl4 injury hepatic progenitor cells (PanCK positive) were evident. The number of these cells fell following partial hepatectomy at a similar rate to that following sham surgery (Figure 3.10).

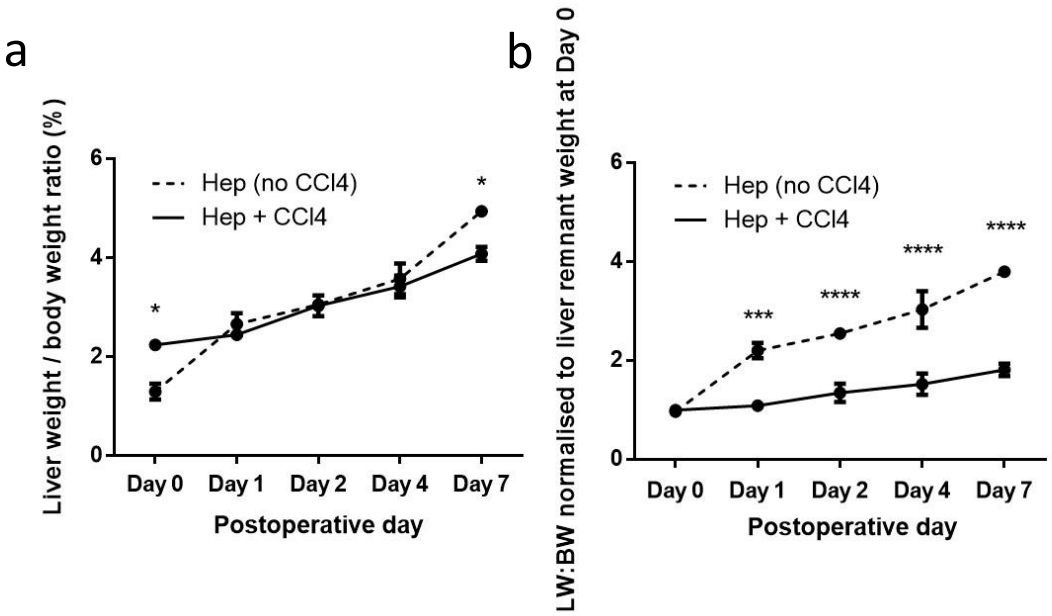


Figure 3.7: Liver weight to body weight ratio following partial hepatectomy with or without CCl4 pretreatment

a) Liver weight to body weight ratio following partial hepatectomy preceded by 8 weeks 1mcl/g carbon tetrachloride via intraperitoneal injection versus no CCl4 pretreatment age matched controls (n>/=4 per group; two-way ANOVA with Bonferroni test). b) Liver weight to body weight ratio relative to liver remnant weight at day 0 comparing CCl4 pretreated and age matched controls (n>/=4 per group; two-way ANOVA with Bonferroni test). (*p<0.05; ***p<0.001, ****p<0.0001)

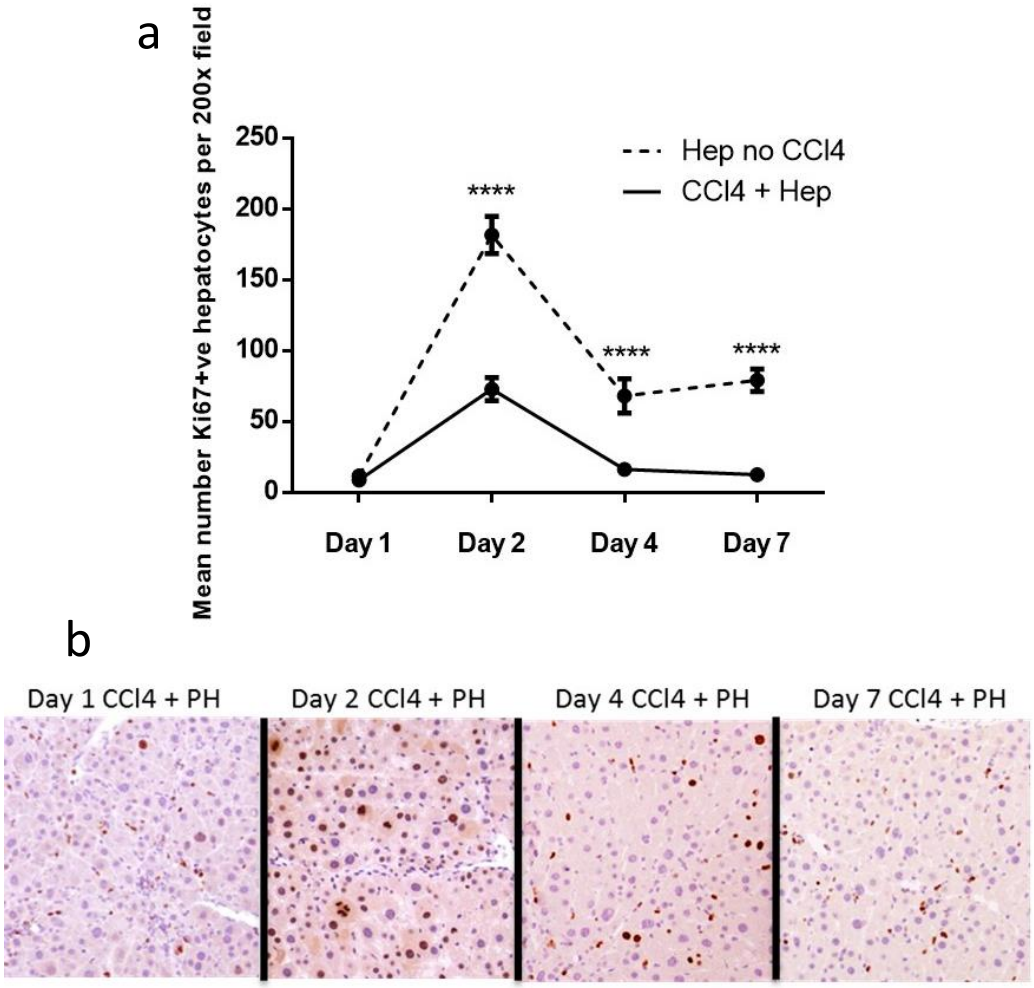


Figure 3.8 Hepatocyte proliferation following partial hepatectomy with or without carbon tetrachloride pretreatment

a) Comparison between hepatocyte Ki67 expression following PH with CCl4 pretreatment and PH hepatectomy only in age matched controls (n=4 per group; comparison with 2-way ANOVA). b) Number of Ki67 positive hepatocytes per 200x field following partial hepatectomy and CCL4 chronic injury or partial hepatectomy alone

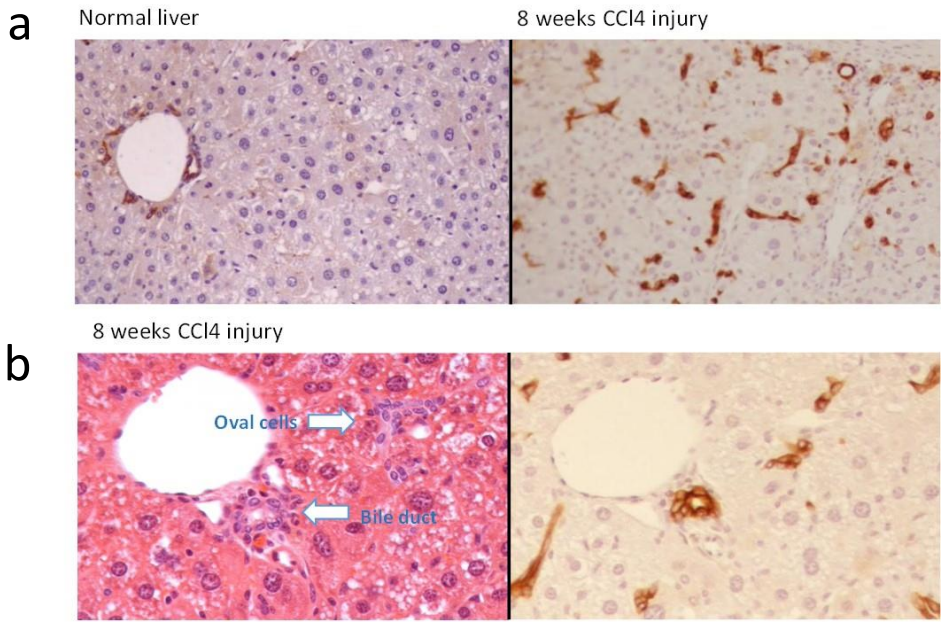


Figure 3.9 Hepatic progenitor cells following chronic liver injury.

a) Pan CK immunohistochemistry (biliary and progenitor cell marker) in the normal age matched control liver and following 8 weeks 1mcl/g CCl4 twice weekly intraperitoneal injection. b) High powered view of haematoxylin and eosin stain showing oval cells (equivalent to hepatic progenitor cells) and pan CK staining

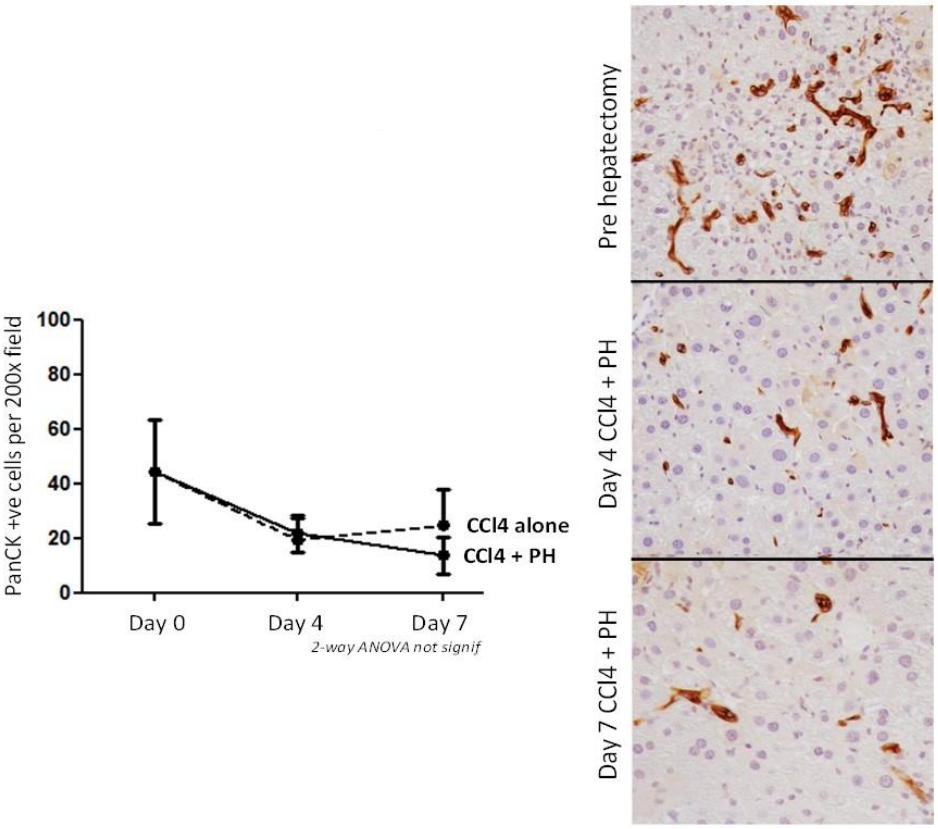


Figure 3.10 Hepatic progenitor cells following partial hepatectomy.

Comparison of hepatic progenitor cell numbers (defined as PanCK positive cells outwith a ductular structure) per high powered field in mice undergoing partial hepatectomy following CCl4 injury and mice who underwent CCl4 injury and sham surgery (two way ANOVA ns)

## Discussion

It is well recognised that regeneration of the fibrotic liver is impaired following partial hepatectomy, and this was demonstrated here in this mouse model of intra-peritoneal carbon tetrachloride and partial hepatectomy. Interestingly the pattern of hepatocyte proliferation was similar to that of normal liver regeneration (i.e. peak proliferation at day 2 following partial hepatectomy). I had anticipated that the requirement for greater hepatocyte proliferation following chronic injury would have resulted in increased hepatocyte proliferation at later time points. However this was not the case and rate of proliferation fell in line with partial hepatectomy of the uninjured liver.

The fibrotic livers were larger than uninjured livers relative to body weight ratio which may then have affected requirement for hepatocyte proliferation. In the human the cirrhotic liver is typically densely fibrotic and shrunken. While the carbon tetrachloride model was able to induce marked fibrosis, it did not result in the shrunken liver seen in humans. Modelling the lengthy fibrosis seen in humans, which occurs following decades of chronic injury, is clearly difficult to replicate in young mice over a limited period of time.

I found that fibrosis resolution was more rapid following partial hepatectomy than following sham surgery. This supports work by Suarez-Cuenca et al., who demonstrated that following partial hepatectomy with chronic liver injury matrix remodelling is markedly upregulated associated with increased collagenase activity[61]

I considered whether hepatic progenitor cells might contribute to regeneration following partial hepatectomy and chronic liver injury. Espanol-Suner et al. recently showed that

following chronic liver injury induced by a dietary liver injury model (choline-deficient diet) liver progenitor cells were able to differentiate into hepatocytes[173]. In this model, following injury induction, 0.78% of hepatocytes were shown to be derived from progenitor cells. Two weeks following cessation of injury this had increased to 2.45% of the hepatocyte population. Following a 4 week carbon tetrachloride model there was no contribution to regeneration from progenitor cells and this was also the case following partial hepatectomy. In my model of partial hepatectomy and chronic liver injury I found that chronic liver injury induced a progenitor cell response. At time points up to 7 days following partial hepatectomy on a background of chronic liver injury and sham surgery there was a reduction in number of progenitor cells. Lineage tracing experiments would be required to test if these cells are differentiating into hepatocytes.

The fact that chronic injury appeared to elicit a progenitor response, which was not seen following partial hepatectomy, it might be speculated that progenitor cell activation does not provide a significant contribution to regeneration in this setting. However, my work contrasts with that of others. Kuramitsu et al., found that liver progenitor cell number increased following partial hepatectomy on a background of chronic liver injury[174]. This group then tested the effects of blockade of progenitor cell proliferation via blockade of the progenitor mitogen TWEAK (tumour necrosis factor-like weak inducer of apoptosis) using a neutralising antibody. Rather than impair regeneration, this progenitor cell targeted intervention actually augmented liver regeneration in their model[xix]. There is evidence that liver progenitor cells can differentiate into hepatocytes and these cells could contribute to hepatic regeneration following liver regeneration, although further work is required to assess how best this system can be manipulated.

[xix] The model of liver fibrosis and partial hepatectomy used by Kuramitsu et al. (2013), involved 6 weeks of three times weekly gavage of carbon tetrachloride.

Given the limitations of the carbon tetrachloride model I trialled thioacetamide[xx] in the drinking water as an alternative form of chronic injury (see section "Thioacetamide", p19). I trialled lengths of administration of up to 18 weeks. A small number of mice did display marked macroscopic fibrosis and a shrunken liver at 18 weeks however this was not consistent. On the basis of this pilot study I decided not to attempt to optimise this further given both time and cost limitations. I decided to focus instead on the carbon tetrachloride method of chronic injury and accept its limitations.

## Conclusion

Partial hepatectomy with chronic injury is feasible. However it is limited by the requirement for repeated intraperitoneal injection, which can cause adhesions, and the rapid fibrosis resolution that occurs following partial hepatectomy.

[xx] Thioacetamide is a organosulphur compoung which is known to induce hepatotoxicity in mice and has been used in chronic model of liver injury by addition to drinking water.

# 3.3 Acute toxic liver injury

## Aims

1. Use a reliable model acute liver injury in mice directly relevant to humans.

## Selecting the appropriate model

Paracetamol to induce acute liver injury in mice has been used widely as a model of acute toxic liver injury. This has direct clinical relevance as paracetamol intoxication is the leading cause of acute liver failure in UK (see Acute liver injury, p6). The response to paracetamol is dependent on a range of factors, including strain of mouse or rat, length of time fasting and dose of paracetamol[48]. After review of the literature I opted for a fasted mouse model with a dose of 350mg/kg of paracetamol[48,168]. This model resulted in a considerable degree of liver injury with minimal mortality. At higher doses mortality rates can reach 50% and death occurs rapidly[168].

## Results

In characterising this model I found that 350mg/kg paracetamol resulted in a considerable degree of injury and no mortality. Figure 3.11 provides an overview of serum alanine transaminase (ALT)[xxi] rise following paracetamol intoxication and also representative histology of liver sections at corresponding time points. Based on these initial sections I developed a method for analysing areas of necrosis in the H&E sections, which is shown in Figure 3.12.

[xxi] Alanine transaminase (ALT) is an enzyme found in hepatocyte, but also other cells such as muscle. It is released following hepatocellular injury and is a clinically accepted marker of liver injury.

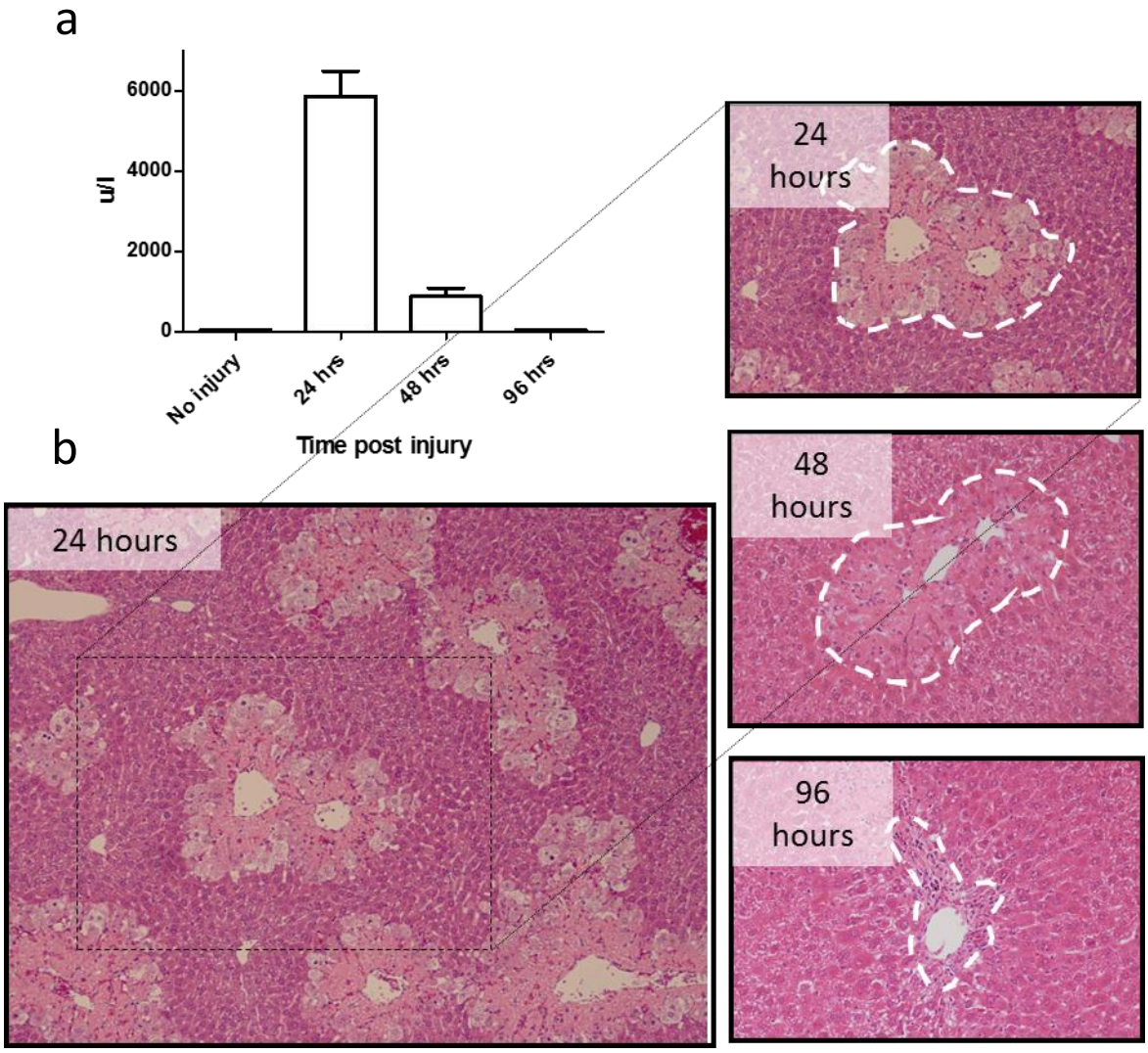


Figure 3.11: Overview of paracetamol intoxication model.

a) Serum ALT following paracetamol intoxication (n>4/group). b) Indicative haematoxylin and eosin histology at time points corresponding with serum ALT level in A. Figure shows x200 image 24 hours following intoxication (right side) and then close up image centred on the hepatic veins (zone 3) at 24 hours, 48 hours and 96hours showing resolution of injured region.

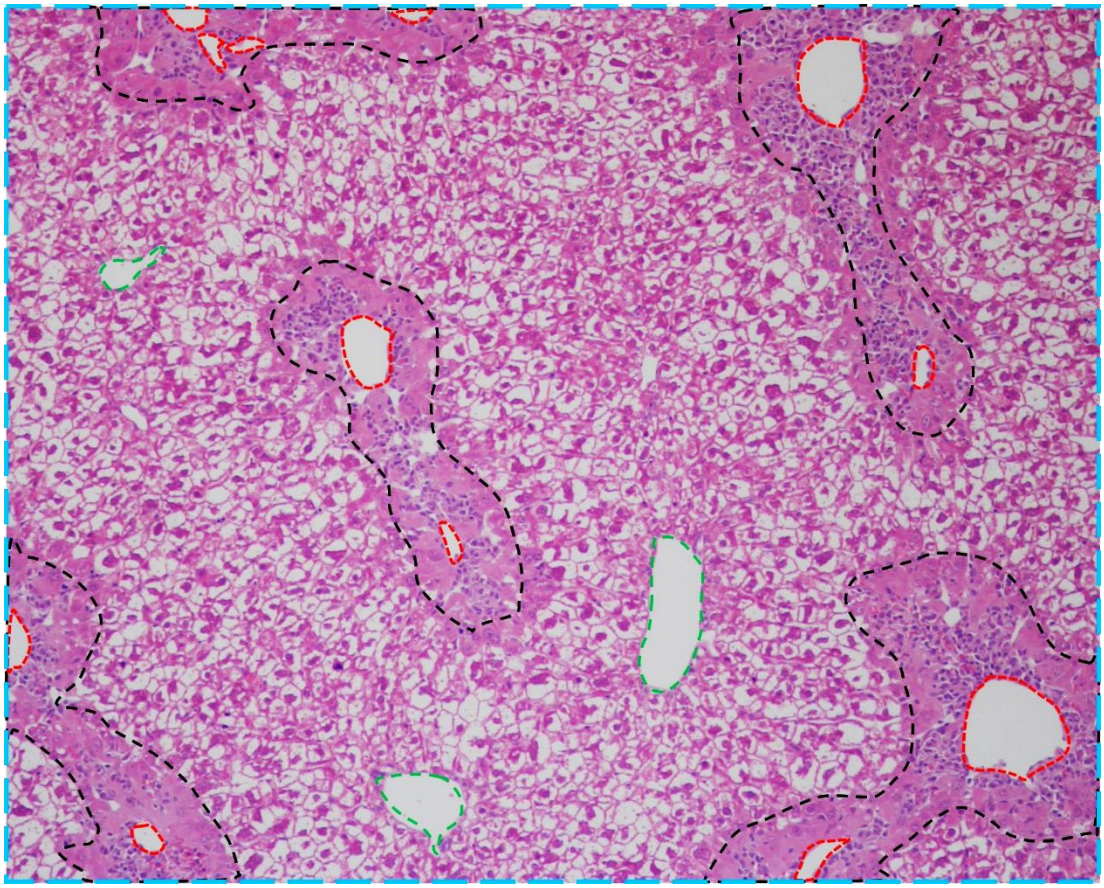

Figure 3.12: Quantification of necrotic area in mice following paracetamol intoxication

Black= perimeter of necrosis; red= hepatic vein; green=portal tracts; blue = total area

Formula for % necrosis=

(black area – red area)/(blue area – (green area + red area)) x 100

# Chapter 4. Functional assessment of liver regeneration

In considering translation of a proposed therapy to the clinic, assessing translational measures of regeneration is important. Assessment of regeneration following PH can involve functional, proliferative, and volumetric parameters. In the preclinical setting, liver weight provides a measure analogous to liver volume assessed by CT scanning in the clinical setting. However size does not necessarily relate to function especially with background chronic liver injury. Effective functional assays are highly desirable.

## 4.1 Hepatocyte function

### Background

Two main techniques have been used to measure dynamic hepatic function, centred on compounds which are eliminated exclusively by hepatocytes. These include mebrofenin, a radio isotope detected by hepatobiliary scintigraphy, and indocyanine green, a fluorescent cyanine dye[175].

Both mebrofenin and ICG rely on similar transporter systems for uptake into hepatocytes. Mebrofenin uptake utilises the organic anion transporter polypeptide (OATP) family (OATP1B1and OATP1B3) while ICG utilises OATP1B3 and the Na+-taurocholate cotransporting polypeptide (NTCP) transporter for uptake into hepatocyte and passage into the bile[176].

Hepatobiliary scintigraphy (HBS) involves the administration of radioisotopes which are taken up by hepatocytes and excreted in the bile enabling imaging of the hepatobiliary system using gamma cameras to create two-dimensional images. Given the tissue penetrance of this technique it is possible to image uptake by the liver in vivo. HBS can provide both a volumetric and functional assessment of regeneration noninvasively, which has been validated in rodent models, showing promise for clinical investigation[177,178].

Indocyanine green has already been used extensively in clinical practice for a range of applications including as an indicator of hepatic function and for assessment of blood flow. The tissue penetrance of fluorescence is far inferior to gamma imaging and so assessment of ICG clearance in humans relies upon fluorescent quantification of blood samples or quantification in the peripheral circulation via pulse spectrophotometry following ICG injection. In some centres ICG clearance is routinely performed to assess patient's suitability for surgery based on liver function[179]. ICG has been criticised for this application based on its dependency on hepatic blood flow. However as liver dysfunction increases, functional hepatocyte mass can become a major limiting factor, with ICG retention rate directly related to postoperative outcome[180].

While HBS can provide an effective non-invasive measure of liver regeneration the involvement of radioisotopes limits its application. Indocyanine green clearance can be performed in the clinical setting by repeat blood sampling (and subsequent near infrared spectroscopy) or by a noninvasive digital pulse densitometry device[181]. However in the preclinical setting repeat blood sampling can significantly deplete intravascular volume of small rodents and noninvasive digital pulse densitometry devices are too large for use

in these small animals. Recent advances in imaging technology have enabled fluorescent imaging of whole animals under anaesthesia to be undertaken. ICG is excited and emitted in the far-red part of the spectrum (absorbance: 600nm-900nm; emittance: 750-950) which shows much better tissue penetrance than lower wavelengths, so enabling in vivo imaging applications[182].

In vivo fluorescent imaging could provide a novel method to assess ICG clearance in rodents as an indication of liver function during liver regeneration.

## Results

Following injection of indocyanine green, the liver region is clearly identified using the fluorescent imaging system and ICG can be seen to pass into the gut (Figure 4.1).

I selected regions of interest over the hind paws to enable assessment of indocyanine green clearance over time. 1mg/kg ICG administered intravenously is rapidly cleared in both the normal mouse and following partial hepatectomy (Figure 4.2). Dose optimisation showed that with increasing concentration of ICG, clearance rate varies considerably, such that at 10mg/kg no clearance phase is seen (Figure 4.3). Following this dose optimisation 2.5mg/kg was selected for further assessment as the system appeared saturated with both 5mg/kg and 10mg/kg. This dose was administered to mice following PH or sham procedure showing no significant difference between mice 1/3 hepatectomy and sham but a significantly delayed clearance with 2/3 PH (Figure 4.4).

In C57Bl6 mice (black skin pigment) the liver region is not visible as the fluorescence is absorbed by skin pigment. However using Balb/c (white) mice a region of interest can be placed over the liver region to assess change in fluorescent signal over time (Figure 4.5). Using this technique both peripheral clearance of ICG and liver uptake of ICG can be obtained.

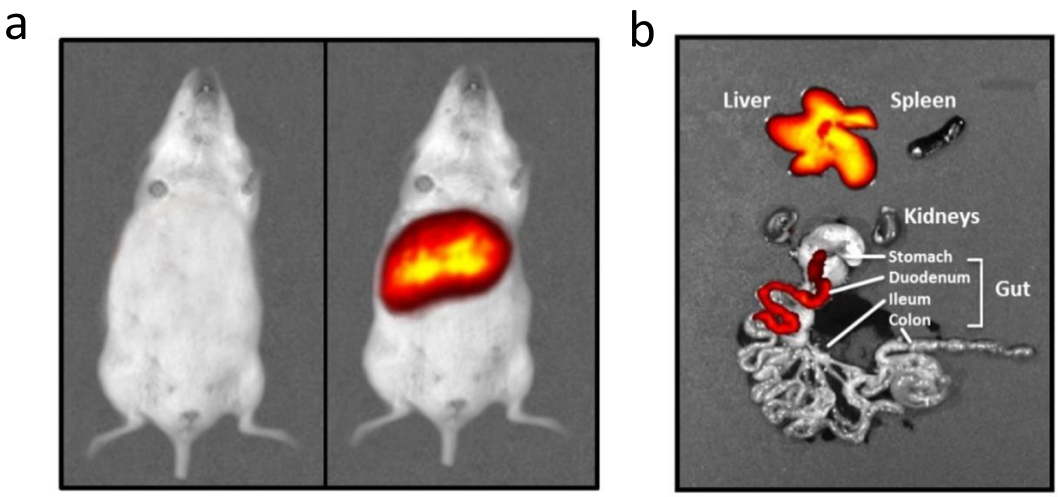


Figure 4.1: In vivo fluorescence following indocyanine green injection

a) Fluorescent image of the Balb/c mouse before and 15 minute following indocyanine green injection. b) Ex vivo viscera demonstrating ICG uptake by liver and passage into gut 15 minutes following ICG injection.

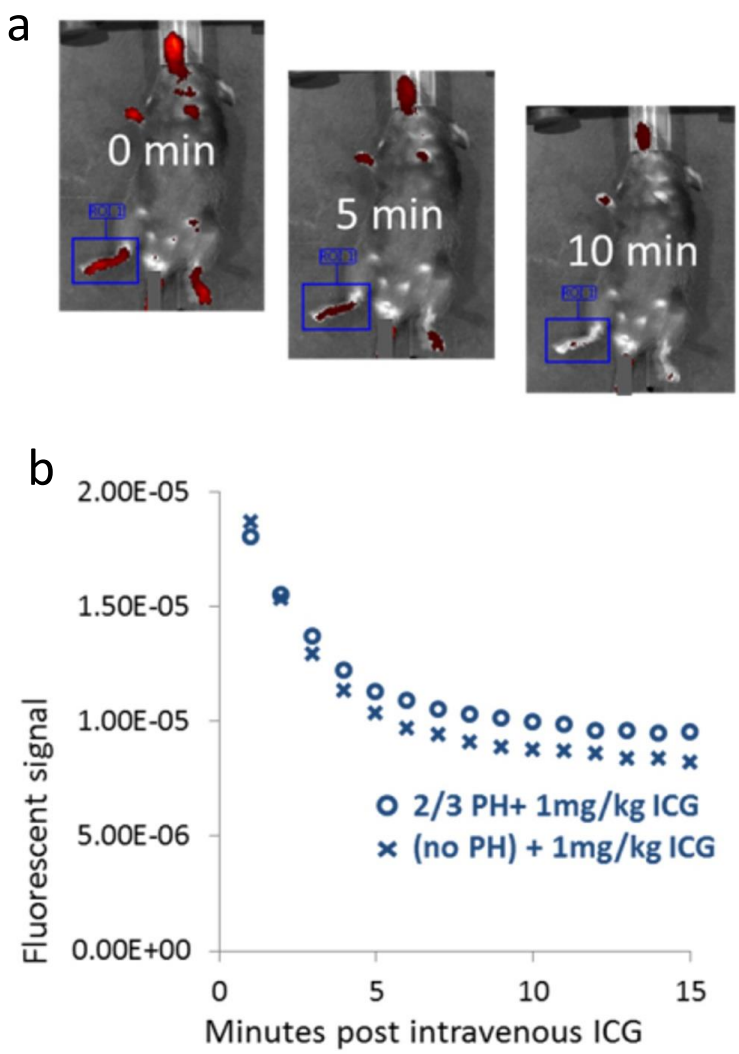


Figure 4.2: Fluorescent intensity following indocyanine green in the C57Bl/6 mouse

a) Representative fluorescent image following ICG administration. Immediately following injection, at 5 minutes and 10 minutes. b) Fluorescent intensity following ICG administration according to region of interest placed over left and right paw.

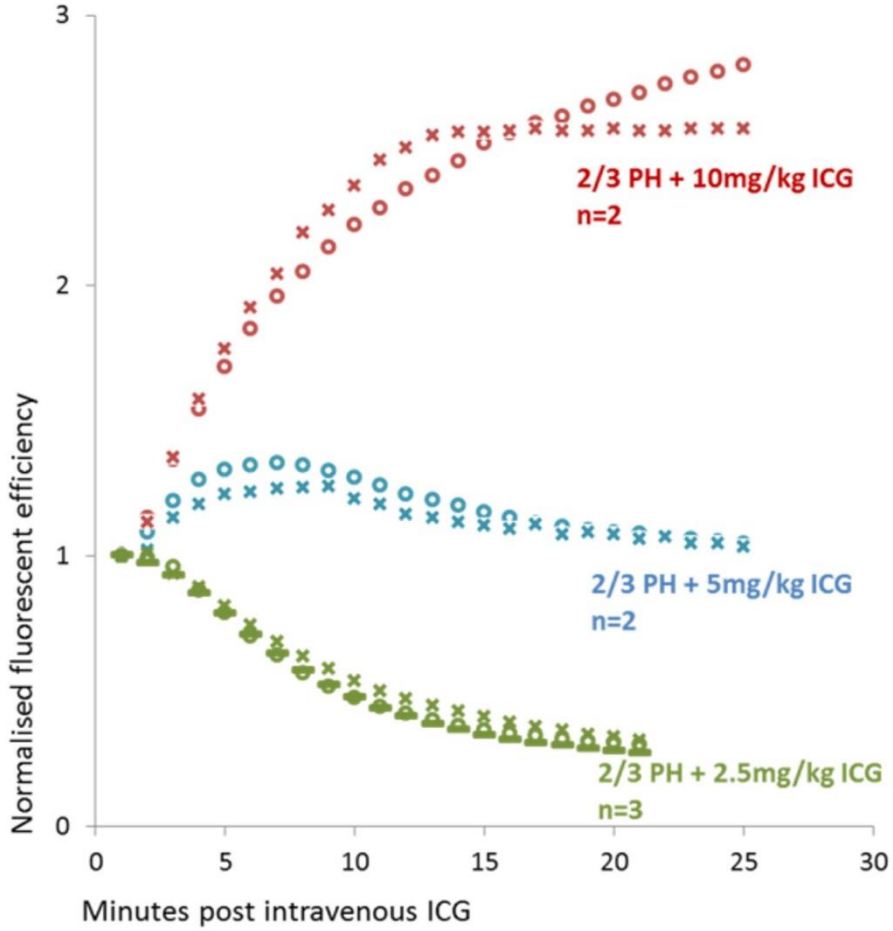


Figure 4.3. Indocyanine green dose comparison following partial hepatectomy

ICG clearance assessed immediately following partial hepatectomy, n=2/group

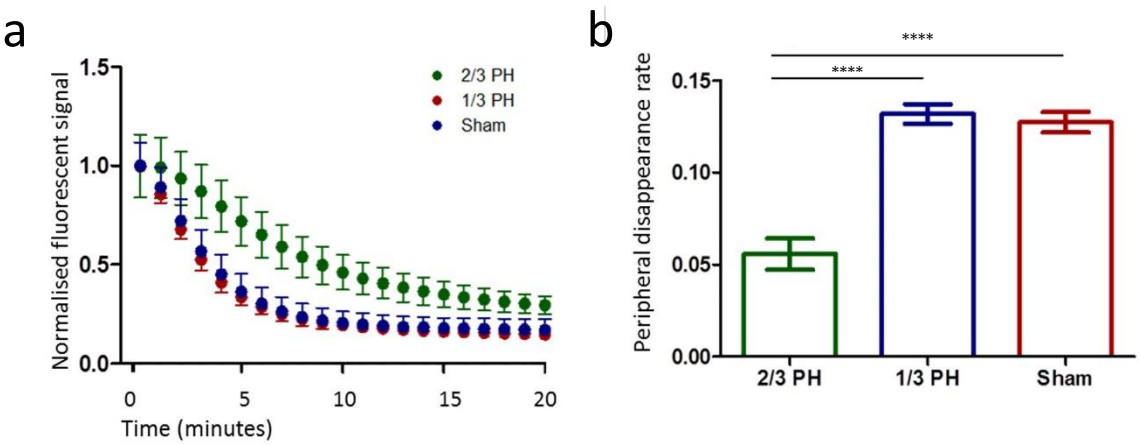


Figure 4.4: Effect of extent of partial hepatectomy (1/3, 2/3 or sham) on ICG clearance (2.5mg/kg) in C57Bl/6 mice.

a) Peripheral disappearance of indocyanine green immediately following 2/3 PH, 1/3 PH or sham (n=3/group, mean +/- std error). b) 5 minute peripheral disappearance rate ICG. Clearance rate significantly reduced following 2/3 PH compared to 1/3 PH or sham (n=3/group, mean +/- std error, one-way ANOVA with Bonferroni post hoc).

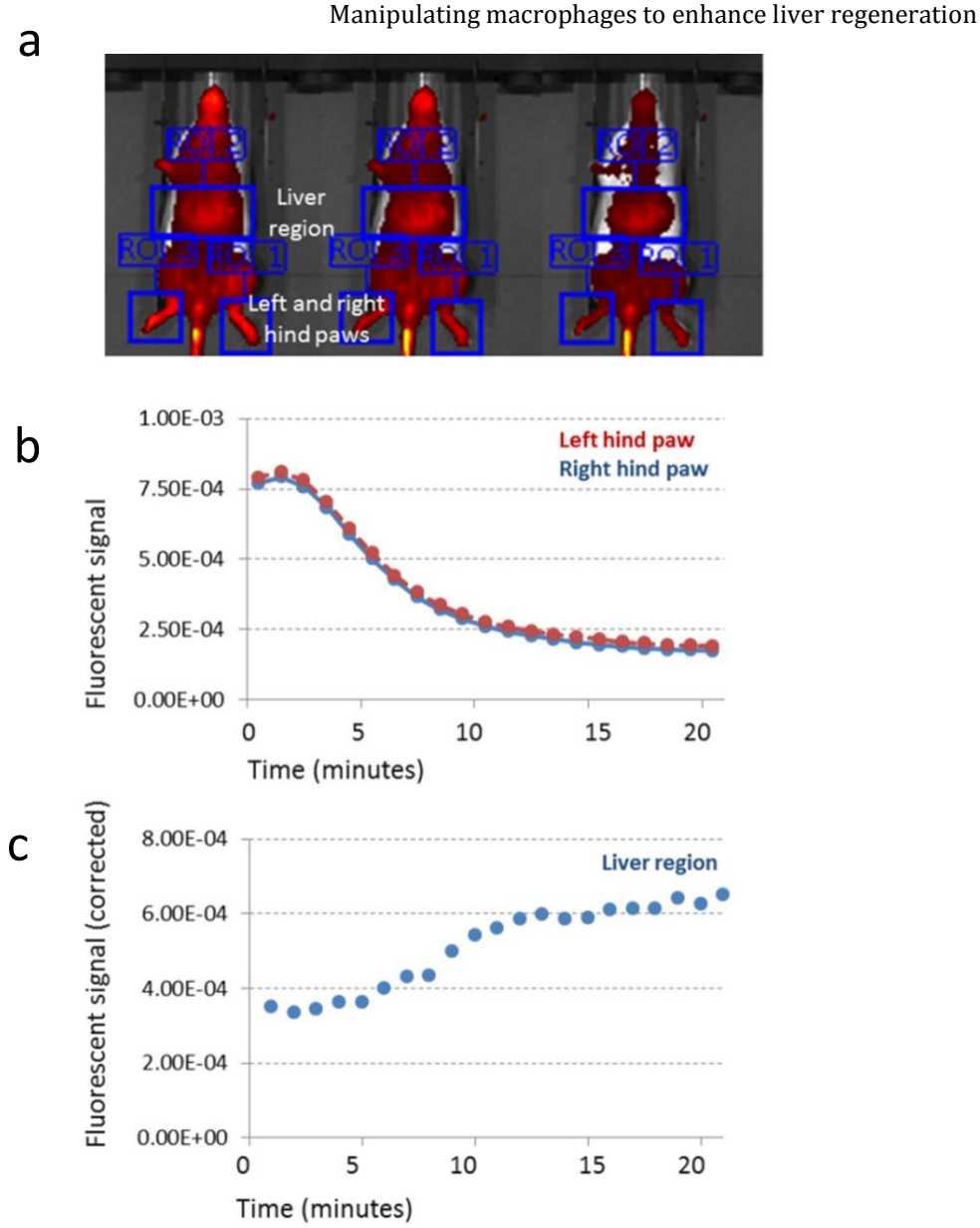


Figure 4.5: Fluorescent intensity following indocyanine green in the Balb/c mouse

a) Representative fluorescent image following ICG administration to Balb/c mouse. Immediately following injection, at 5 minutes and 10 minutes. Blue rectangles show regions of interest over liver region, left and right hind paws. b) Fluorescent intensity following ICG administration according to region of interest placed over left and right paw. c) Fluorescent intensity over liver region of interest corrected according to fluorescent signal in lower abdomen (region of interest in lower abdomen subtracted from region of interest in liver region to remove background)

## Discussion

In this experiment I have demonstrated that indocyanine green clearance can be assessed using fluorescence imaging in mice in vivo. This novel, non-invasive procedure could be performed at repeat time points enabling serial assessment of regeneration in the same animal.

The dose of indocyanine green seems crucial to optimise its discriminative capacity, with a low dose cleared rapidly even with considerable tissue loss. Finding a dose near the saturating level may be key to differentiating between degrees of liver injury. In the clinical setting a dose of 0.5mg/kg is well established to discriminate the most severe forms of chronic liver disease and is used to assess eligibility for liver surgery[179,183]. It may be that a higher dose of indocyanine green would aid discrimination between patients with less severe degrees of liver injury. This measure could potentially form a clinical trial outcome measure, given assessment of liver function in the clinical setting is currently limited. The current low dose that is used for preoperative assessment is unlikely to be beneficial in the trial setting as only severe deficiencies could be noted.

## Conclusion

Indocyanine green clearance can be measured via in vivo fluorescent imaging, which may provide a useful tool to assess functional liver regeneration.

# 4.2 Assessment of hepatic phagocytic function

## Background

Following acute liver injury or major hepatic resection in humans, hepatic innate immune capacity is markedly reduced, with sepsis complicating acute liver failure in over 30% of cases[64,76,77]. Hepatic macrophages are crucial for innate immune integrity and are necessary for effective hepatocyte proliferation during regeneration. Indeed the innate immune system plays a critical role in liver regeneration as macrophages are required to phagocytose necrotic liver tissue and pathogens. I therefore wanted to develop a technique to assess hepatic phagocytic capacity in mice.

In humans, clearance of radiolabelled albumin microspheres has been used to demonstrate impaired hepatic phagocytic capacity following acute liver injury and also following partial hepatectomy[76,77]. However this technique was not feasible in the local animal facility given safety issues and site licences required for working with radioactive agents. Given the experience I developed with fluorescence imaging I investigated whether there was a fluorescent imaging approach which could be used to assess hepatic phagocytic capacity.

## Aims

1. Develop an assessment method for hepatic phagocytic capacity.
2. Assess effects of partial hepatectomy on hepatic phagocytic capacity.

## Results

I found that following injection of fluorescent latex microbeads into the inferior vena cava there was rapid uptake by the liver as evidenced by hepatic fluorescent signal (Figure 4.6a). Uptake by hepatic phagocytes was rapid, with marked hepatic fluorescence detected just one minute following injection. There was minimal uptake of fluorescent beads by phagocytes in the spleen, lung, kidney or brain.

Multiphoton imaging of the exvivo liver from the MacGreen mouse one minute following bead injection showed that there was considerable phagocytosis by hepatic macrophages (Figure 4.6b).

By performing flow cytometry of the blood I was able to assess whether phagocytic cellular populations in the blood also took up fluorescent beads following injection. While there were some beads within gated cellular populations, overall this was minimal and over a period of 15 minutes, as beads were removed from the circulation, this did not increase (Figure 4.7).

By performing flow cytometry of blood sampled at timepoints following injection of fluorescent microbeads I have shown that fluorescent bead clearance is markedly impaired following partial hepatectomy (Figure 4.8).

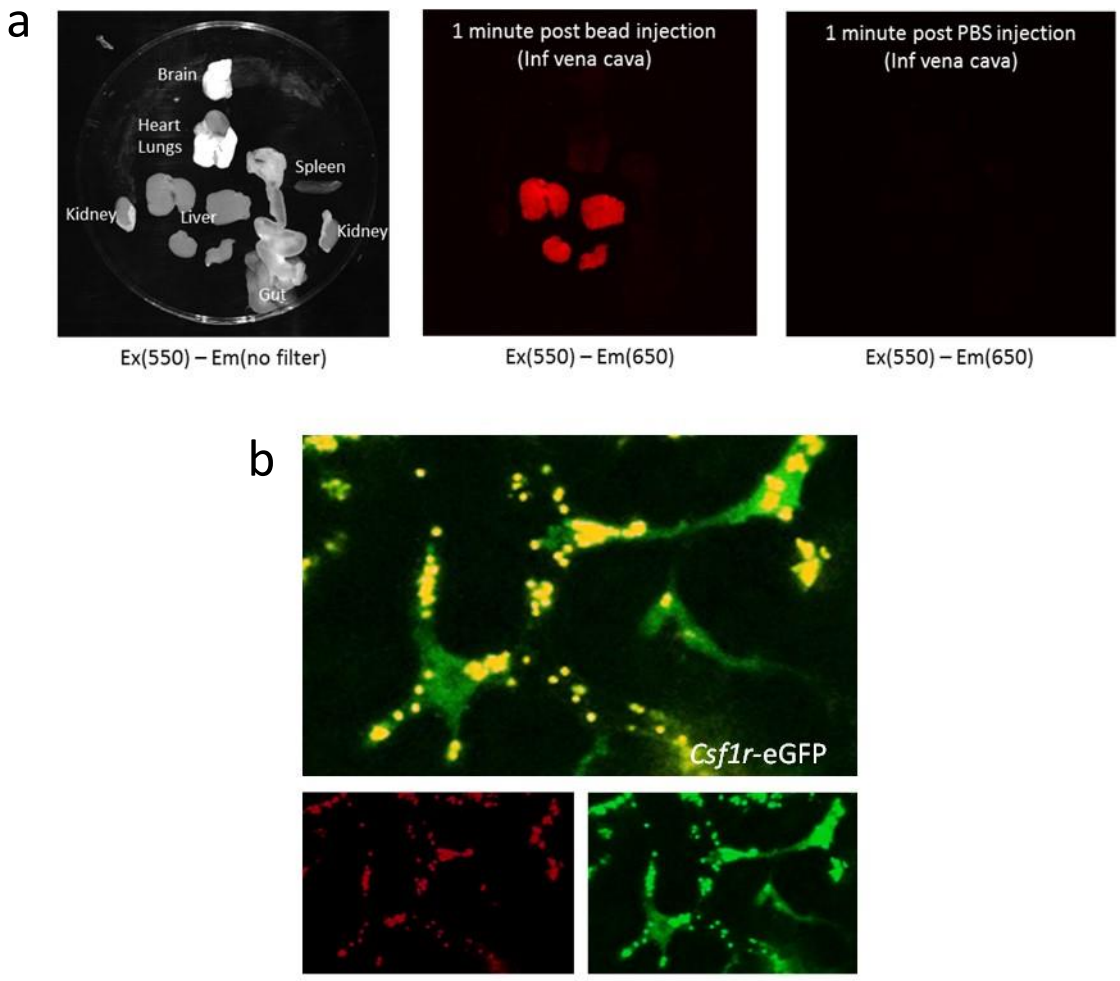


Figure 4.6: Assessment of hepatic phagocytic capacity

a) Assessment of fluorescent signal in ex vivo organs following injection of fluorescent microbeads into the inferior vena cava. Organs were flushed and removed 1 minute following bead injection. b) Multiphoton image of exvivo liver MacGreen mouse 1 minute following injection of fluorescent microbeads and subsequent PBS flush.

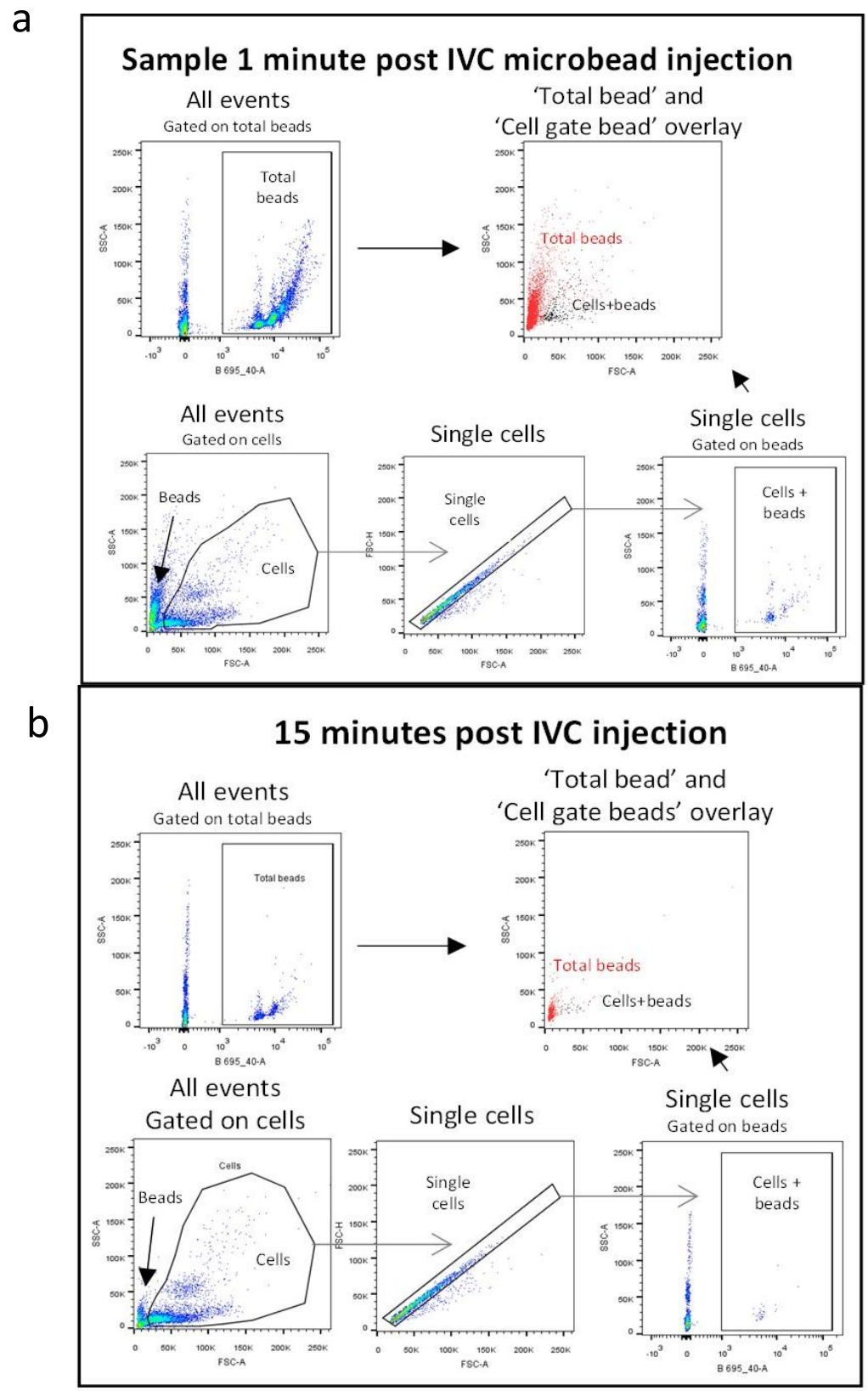


Figure 4.7: Assessment of the blood cellular population following fluorescent bead injection. (PTO for details)

Representative flow plots of blood sampled from the inferior vena cava at 1 minute (a) and 15 minutes (b) following injection of fluorescent microbeads into the circulation. Gating strategies including total fluorescent bead count ("Total beads") and bead count within blood cellular populations ("Cells+beads").

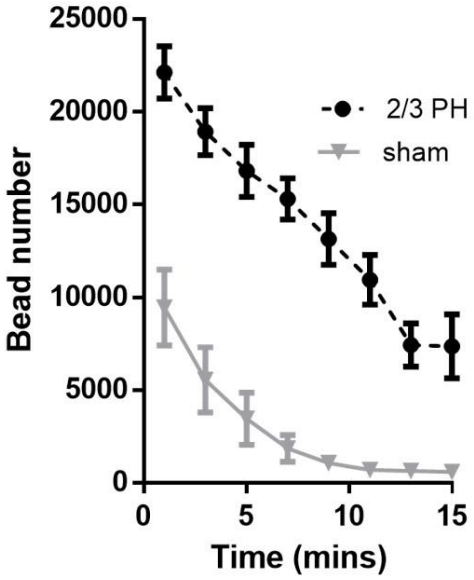


Figure 4.8: Fluorescent bead clearance following partial hepatectomy or sham surgery

Fluorescent bead clearance assessed by flow cytometry of blood samples at Day 2 following 2/3 partial hepatectomy and sham surgery with injection of fluorescent microbeads into the inferior vena cava (n=6/group)

## Discussion

I have shown that by using a combination of flow cytometry of blood samples to identify fluorescent bead clearance from the circulation and also ex vivo fluorescent imaging of viscera to indicate fluorescent bead uptake, I am able to assess hepatic phagocytic capacity.

It is interesting to note that although the spleen is recognised as possessing considerable phagocytic capacity there is minimal uptake at the one minute timepoint following injection. On the other hand the liver shows marked phagocytic capacity with rapid uptake of fluorescent beads by hepatic macrophages. This discrepancy is discussed in more detail in the section "6.4 Focus on the spleen", p147.

Some fluorescent microbeads were taken up by circulating cellular populations although this was minimal. A fluorescent bead technique has been used by others to label monocyte populations in vivo to study their subsequent trafficking[184]. In this study the number of labelled circulating cells decreases at later time points rather than increases, suggesting that these cells are being cleared from the circulation. Based on the ex vivo fluorescent imaging I would hypothesise that these cells are being cleared by the liver. This is not an angle that I have explored further.

## Conclusion

Phagocytic capacity can be assessed in vivo by injection of fluorescent microbeads and subsequent assessment of bead clearance by flow cytometry and quantification of fluorescent signal via ex vivo fluorescent imaging.

# Chapter 5. Macrophage administration in mouse models of liver regeneration

## Aims

1. Optimise administration of macrophages to mice following chronic liver injury and partial hepatectomy
2. Trial macrophage administration to mice following chronic liver injury and partial hepatectomy.

## 5.1 Macrophage generation and limitations

I followed protocols used extensively by my supervisor's laboratory to generate macrophages derived from mouse bone marrow by culture in L929 conditioned media (see Materials and Methods section, "Macrophage generation for direct administration", p52). Following these protocols I generated cells that were consistent with the purity generated by previous researchers in the laboratory (Figure 5.1a). I found that approximately 90% of cells were positive for the macrophage marker F4/80 following 7 days culture (Figure 5.1). Cells also highly expressed CDllb (indicative of myeloid lineage), showed low expression of Ly6-C (monocyte lineage marker) and CD209 (macrophage and dendritic cell marker). Immunohistochemistry showed high expression of CD68 (macrophage marker) and mannose receptor (macrophage marker unpolarised and "M2" type phenotype), without evidence of INOS expression ("M1" type phenotype) (Figure 5.1b). (see section entitled Regulation of cells of the monocyte macrophage lineage, p43).

This macrophage generation technique is limited by use of L929 media which although contains macrophages colony stimulating factor, which is required for macrophage generation, also contains a multitude of other factors (VEGF, MCP-1, KC, and MIG, and low amounts of FGF-beta, Eotaxin, IL-10, IL-9, and IL-12) which have the potential to alter macrophage phenotype[185]. As with any conditioned media there is likely to be batch to batch variation in the constituent cytokines of L929 conditioned media which could then influence macrophage generation. Rather than altering protocols (ie changing to pure macrophage colony stimulating factor) at this stage I decided to acknowledge the limitations of the technique and continue with the established protocol.

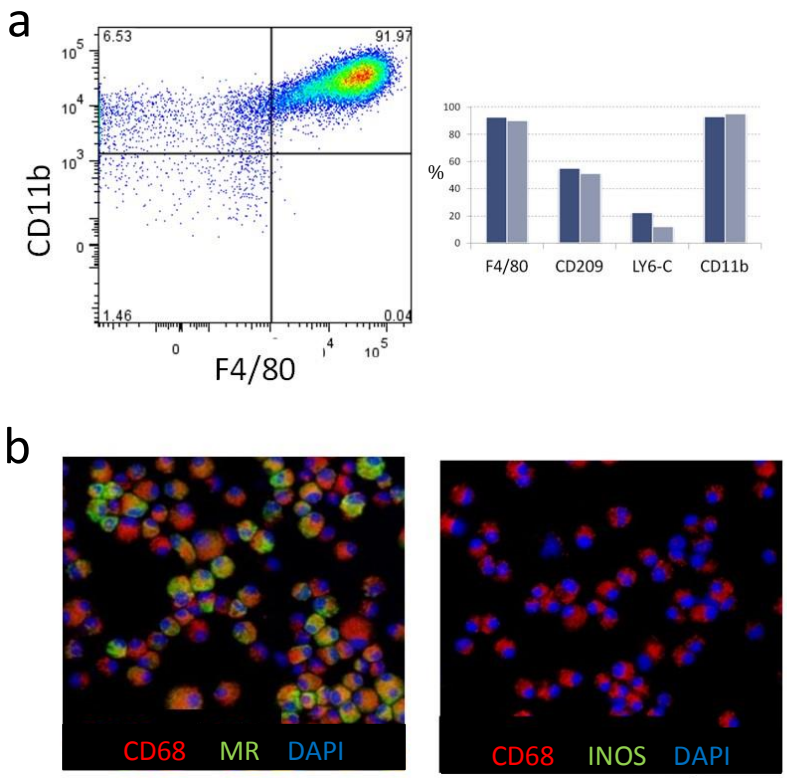


Figure 5.1: Characterisation of bone marrow derived cells cultured in L929 media

a) Flow cytometry dot plot showing representative F4/80 and CD11b expression with histogram showing percentage F4/80, CD209, Ly6C and CD11b expression (n=2 per surface marker). b) Immunohistochemsitry of generated macrophages for CD68, MR (mannose receptor) and INOS.

# 5.2 Optimising route of cellular injection

## Intraportal injection

The planned route of cellular injection was via the portal vein. However it became apparent that portal vein application of cells was poorly tolerated, with issues occurring either at the time of injection, prior to terminating the anaesthetic and following recovery from anaesthetic. These issues were exacerbated by partial hepatectomy and chronic liver injury

At the time of surgery, I injected cells into the portal vein using a 30G needle with clear visualisation using a microscope. I used a cotton bud with haemostatic agent (Surgicel®) to apply pressure and achieve haemostasis following intraportal injection. This technique was previously performed by others in this group[87]. While this was often effective at controlling the bleeding it was often difficult resulting in mice being needing to be culled. After seeking technical assistance from experienced animal surgeons both in this centre and in other centres, it became apparent that this is generally the case and not an issue unique to me. I tried a number of methods in an attempt to optimise portal vein injection.

Tachosil® (an alternative haemostatic agent) was trialled as an alternative haemostatic agent which in clinical practice is one of the most effective agents around. However in this group, livers appeared markedly pale, indicating impaired blood flow. This suggested that portal vein thrombosis may have occurred potentially related to the effectiveness of thrombotic agent. I trialled slinging the portal vein upstream and downstream of the injection site with suture material at the time of injection, but this

was time consuming and introduced further risk given manipulation of the vein. I trialled needles from a different manufacturer but this did not improve the situation.

After discussion with supervisors I decided that to continue to pursue the strategy of portal vein injection in this context was not appropriate. I considered moving to surgery in rats where the greater size of the portal vein might enable more effective haemostasis. However given the more limited number of reagents available for rats and lack of genetically modified animals for elucidation of potential mechanism I decided in discussion with my supervisors that continuing with investigations in mice would be the best option. I therefore considered alternative routes of injection.

### Selecting the intrasplenic route

Injection routes used by others have included direct hepatic injection, tail vein (or other peripheral vein) or intrasplenic (venous drainage of spleen passes straight to liver). Direct hepatic injection is limited as it only affects a small portion of the liver and is of limited translational relevance as no therapies are currently delivered via this route.
Unpublished data from the Forbes lab (undertaken by C. Pope, A Mackinnon and others) suggests that peripheral administration of macrophages via the portal vein does not reduce fibrosis (as opposed to the intraportal injection route used in the Thomas et al.[87] paper).

As proof of principle therefore I worked with A Mackinnon (Senior Post Doc, Forbes lab) who labelled murine bone marrow derived macrophage with CSFE (this provides a stable nuclear stain which can be detected by flow cytometry). I then injected these cells into the spleen at doses of $1x10^6$ and $5x10^6$. We performed flow cytometry of the liver

staining for macrophage marker F4/80 and also gating on CFSE positive cells (488nm) to assess if injected macrophages were trafficking to the liver.

Intrasplenic injection was well tolerated with infusion of both $1x10^6$ and $5x10^6$ macrophages. There was evidence of cells passing to the liver following intrasplenic injection as assessed by flow cytometry of hepatic cellular populations (Figure 5.2). Following this proof of principle experiment I selected the intrasplenic route for further experimentation.

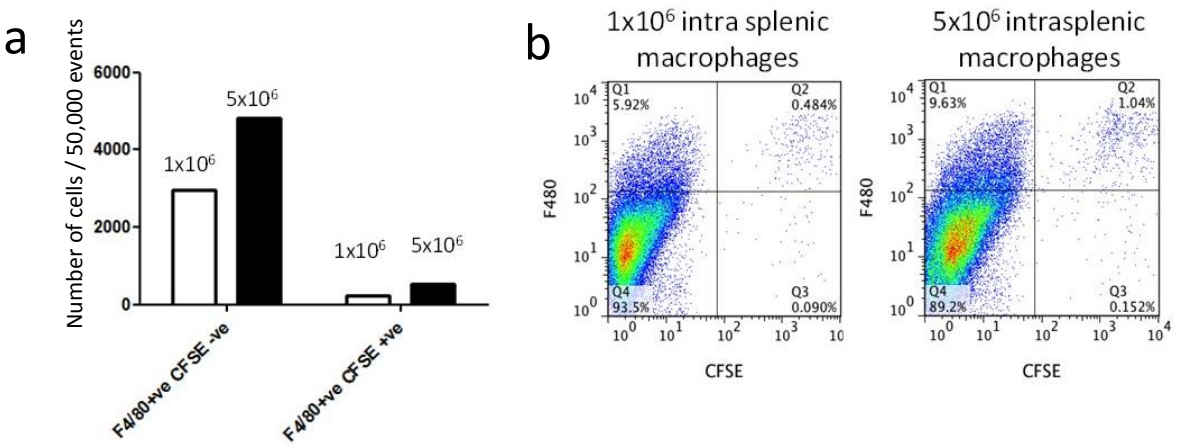


Figure 5.2: Hepatic macrophage populations following intrasplenic injection of CSFE labelled macrophages

a) Quantification of number of F4/80 positive, CFSE negative cells (the recipient's native macrophages) and number of F4/80 positive, CFSE positive cells (donor derived macrophages). b) Representative flow plots showing F480 populations and F4/80, CFSE dual positive cells.

## Limitations of the intrasplenic route

While I selected the intrasplenic route for further experimentation I was aware of a number of potential issues with this method of cell administration.

Firstly many of the injected cells may remain intrasplenic. There may be a high rate of phagocytosis by macrophages in the spleen. The phenotype of injected macrophages could be altered during transit through the spleen and this may influence subsequent effects on the liver. I decided that first I would investigate the effect of administration of these cells and if this approach were to be successful I planned to then go on and further characterise the phenotype of these cells. All experiments were performed using the same batch of L929 conditioned media with cells pooled prior to administration to limit effects of variation within the batch.

# 5.3 Administration of macrophages following partial hepatectomy and chronic liver injury

## Results

Following macrophage administration ($5x10^6$) by intrasplenic injection, I found no effect on survival (Figure 5.3) and no effect on liver weight to body weight ratio (Figure 5.4). Intrasplenic injection did not increase spleen weight to body weight ratio at this Day 4 time point (Figure 5.5). I used Sirius red stain and image quantification to assess degree of fibrosis but there was no reduction in fibrosis following intrasplenic injection of macrophages (Figure 5.6).

I planned on first assessing if macrophage administration via the intrasplenic route would influence regeneration. I did not want to label macrophages in this experiment to assess effect as there was a possibility that labelled cells might behave differently to unlabelled macrophages. If I had found a difference between groups I then planned on assessing macrophage dynamics in detail. This would have included location of the administered macrophages assessed by immunohistochemistry of labelled cells within the liver and also macrophage phenotype assessed by flow cytometry and immunohistochemistry.

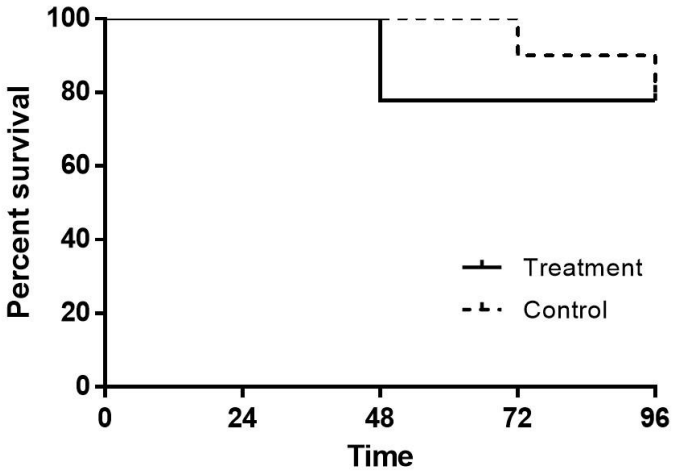


Figure 5.3: Kaplein Meir survival analysis following chronic liver injury, partial hepatectomy and intrasplenic macrophage injection.

(treatment n=7, control n=9)

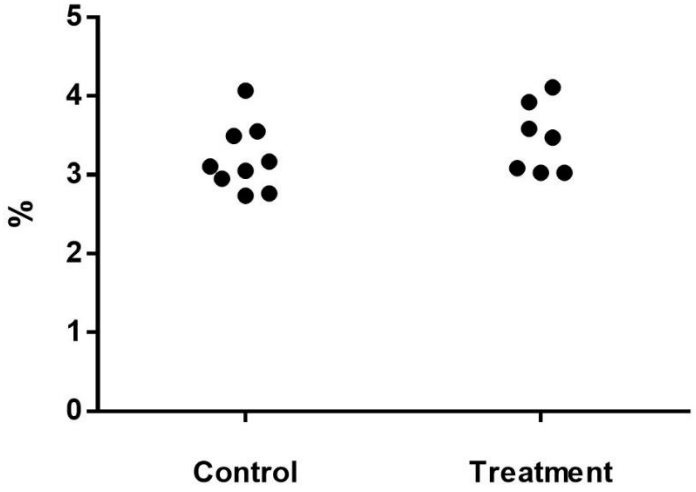


Figure 5.4: Liver weight to body weight ratio at Day 4 following chronic liver injury, partial hepatectomy and intrasplenic macrophage injection

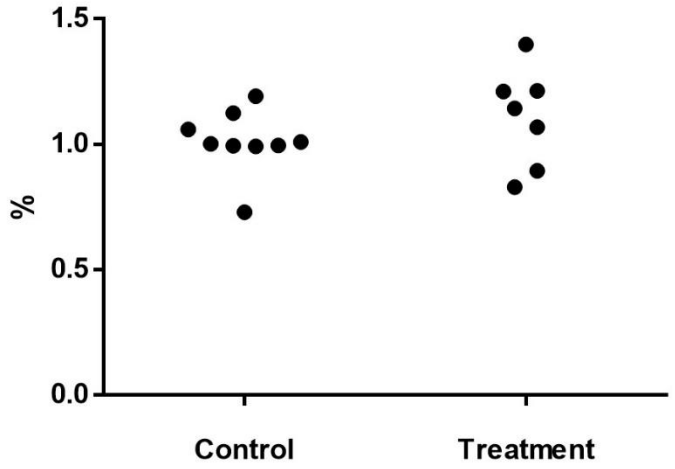


Figure 5.5: Spleen weight to body weight ratio at Day 4 following chronic liver injury, partial hepatectomy and intrasplenic macrophage injection

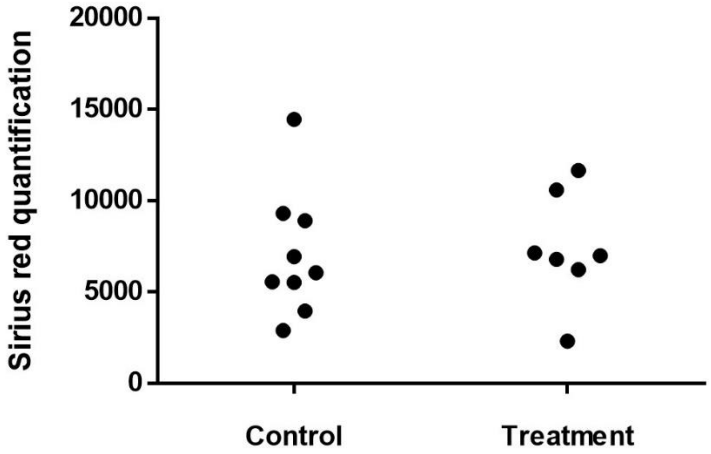


Figure 5.6: Sirius red quantification of fibrosis at Day 4 following chronic liver injury, partial hepatectomy and intrasplenic macrophage injection

## Discussion

Based on these outcome measures I did not find benefit with intrasplenic administration of macrophages. This contrasts with previous work from this group which found a single injection of macrophages via the intraportal route 4 weeks following injection improved fibrosis is a mouse model of chronic liver injury[87]. The mechanism of effect of this previous study was based on recruiting host macrophages to the liver by increased hepatic chemokine expression. The administered macrophages engrafted transiently.

There are a number of differences between this previous study and my work, including model, route of administration and number of cells which could account for the difference. Certainly remodelling of the fibrotic matrix is markedly upregulated following partial hepatectomy without further intervention (Figure 3.6). It may be that any potential effect of additional bone marrow derived macrophages is overwhelmed by the endogenous response to partial hepatectomy. In order to assess this would require an additional control group of sham surgery to assess the rate of remodelling. However due to time constraints (it was not feasible to run a further contemporaneous group)

Given the extensive optimisation I had already performed for this experiment and while there were other options for further optimisation (ie. alter macrophage administration technique, increase cell number (although others in the group report mortality with injection of greater cell numbers), alter macrophages culture conditions, alter model) I decided the most appropriate next step would be to examine alternative intervention options.

There was an opportunity to work with a novel compound to stimulate macrophages in the host. A CSF1-Fc conjugate had been developed by D Gow and D Hume (Roslin

Institute, University of Edinburgh) and Zoetis. When administered to mice they found that liver size was significantly increased and there was extensive hepatocyte proliferation. This appeared an ideal candidate to test in models of liver regeneration.

## Conclusion

In this model of partial hepatectomy on a background of chronic liver injury intrasplenic macrophage administration did not enhance the regenerative response.

# Chapter 6. Macrophage stimulation in mouse models of regeneration

## 6.1 Background

Macrophage colony stimulating factor (CSF1) is the principal macrophage growth factor. It has a central role in macrophage development and homeostasis from bone marrow stem cell to tissue resident macrophage. Clinical trials of recombinant CSF1 were first conducted in the late 1980's / early 1990's following antitumour effects of CSF1 seen in preclinical models relating to macrophage mediated phagocytosis of tumour cells[186]. Recombinant CSF1 administration was found to be safe, although the dose limiting toxicity related to thrombocytopenia in some patients[186-189]. These early phase I / II studies were not followed up by further trials. There is no clear reason for this in the literature. CSF1 facilitates macrophage mediated tissue growth[190]. This finding led to the hypothesis that supplementation of CSF1 could be used to enhance neonatal growth of livestock for commercial benefit.

### Fc conjugation of CSF1

However serum CSF1 has a short half-life (several hours) and undergoes rapid receptor mediated endocytosis, principally by hepatic macrophages but it is also eliminated via renal excretion[84]. Given these rapid pharmacokinetics, in the clinical setting, trials involve repeated infusions of CSF1. CSF1-Fc was developed with the aim of enhancing CSF1 half-life so facilitating administration to test potential growth promoting effects in weaner pigs. CSF1-Fc was generated by D. Hume and D. Gow in collaboration with Pfizer animal health (now Zoetis).

Fc conjugation is a well-recognised strategy to increase the pharmacokinetics of a protein. It is thought to increase half-life both through an increase in the size of the protein, which can limit renal excretion and also through its effects on endosomal recycling[191]. Regarding the latter point, under normal circumstances immunoglobulins can be recycled after cellular uptake by first binding to the "neonatal Fc receptor"[xxii] (FcRn). The immunoglobulin-FcRn complex then passes to the cell surface where the immunoglobulin is released, so preventing lysosomal degradation[192]. By fusing a protein to an Fc fragment, the resulting conjugate may be treated in the same way as an immunoglobulin. Therefore the protein-Fc conjugate is released back into the circulation after activating the relevant receptor mediated pathways[191]. A number of Fc-fusion based drugs are in clinical use, including etanercept (TNF receptor – Fc fragment of IgG1 fusion) and rilonacept (Il-1R –Fc fragment of IgG1 fusion)[193,194].

This compound consists of porcine CSF1 protein bound to a porcine Fc fragment. This Fc modification substantially increased half-life of CSF1 and exhibits considerable potency in terms of stimulating monocyte / macrophage populations in vivo[165]. In weaner pigs CSF1-Fc did not enhance rate of growth, however profound effects were noted on cells of monocyte macrophages lineage. Porcine CSF1 is equally active in mice[164]. When administered to mice it was noted that marked hepatosplenomegaly occurred. This was associated with extensive proliferation of hepatocytes after 4 days of daily treatment. These findings raised the prospect that CSF1-Fc could be used to enhance liver regeneration in mouse models of liver injury.

[xxii] The neonatal Fc receptor (FcRc) was first discovered due to its role in transporting IgG derived from the mother's milk across the gut and into the newborns blood stream192. Jones, E.A. & Waldmann, T.A. The mechanism of intestinal uptake and transcellular transport of IgG in the neonatal rat. *J Clin Invest* **51**, 2916-2927 (1972).

# 6.2 CSF1 receptor stimulation in the steady state

## Aims

1. Assess hepatic effects of CSF1R stimulation on the steady state
2. Assess extrahepatic effects of CSF1R stimulation on the steady state

## Results

### CSF1R stimulation induces hepatic macrophage accumulation

I used the Macgreen mouse *Tg(Csf1r-GFP)$_{Hume}$* to assess CSF1 receptor expression under physiological conditions. Figure 6.1a shows that CSF1 receptor expression was restricted to cells of macrophage morphology in the liver using multiphoton microscopy. I collaborated with Professor J Pollard who had generated the *Csf1r-Mer2iCre$_{JWP}$* crossed with the rosa floxed stop tomato red. In this mouse CSF1R positive cells are then labelled with the tomato reporter following tamoxifen induction. Review of liver sections from this mouse shows complete co-localisation with the macrophage marker F4/80 in the steady state (Figure 6.1b).

I then administered CSF1-Fc to mice without injury, to test hepatic effects of CSF1R signalling in the steady state. Six hours following CSF1-Fc administration there was a greater than 4-fold upregulation in gene expression of CCR2 ligands- CCl2, CCl7 and CCl12 (Figure 6.2a). Marked macrophage accumulation was seen within the liver over four days of CSF1-Fc administration (Figure 6.2b). I performed FACS analysis of hepatic macrophages which revealed extensive macrophage infiltration (F480$^{lo}$/CD11b/$^{hi}$, Ly6C/$^{hi}$) accompanied by expression of markers associated with proliferation (ki67 and

BRDU) in both resident ($F4/80^{hi}$;red) and infiltrating macrophages ($F4/80^{lo}$; blue) (Figure 6.3a-c).

This macrophage accumulation increased hepatic size in wild type (WT) mice after just 2 days of administration (Figure 6.4a). Given the marked infiltrating macrophage phenotype and upregulation of CCR2 ligands, we explored the effects of CSF1-Fc administration in CCR2-/- mice. Liver weight to body weight ratio was not increased in CCR2-/- mice given CSF1-Fc (Figure 6.4a) and infiltrating macrophage accumulation ($F480^{lo}/CD11b^{hi}/Ly6C^{hi}$) was reduced compared to WT mice (Figure 6.4b). While CCR2-/- mice have markedly reduced circulating numbers of Ly6C high monocytes in the steady state (Figure 6.4c) and this deficit was overcome by CSF1-Fc treatment, with resulting Ly6C profile similar to CSF1-Fc treated WT mice (Figure 6.4d). This marked monocytosis following CSF1-Fc treatment is likely driving the extensive macrophage infiltration occurring in both WT and CCR2-/- (Figure 6.4d).

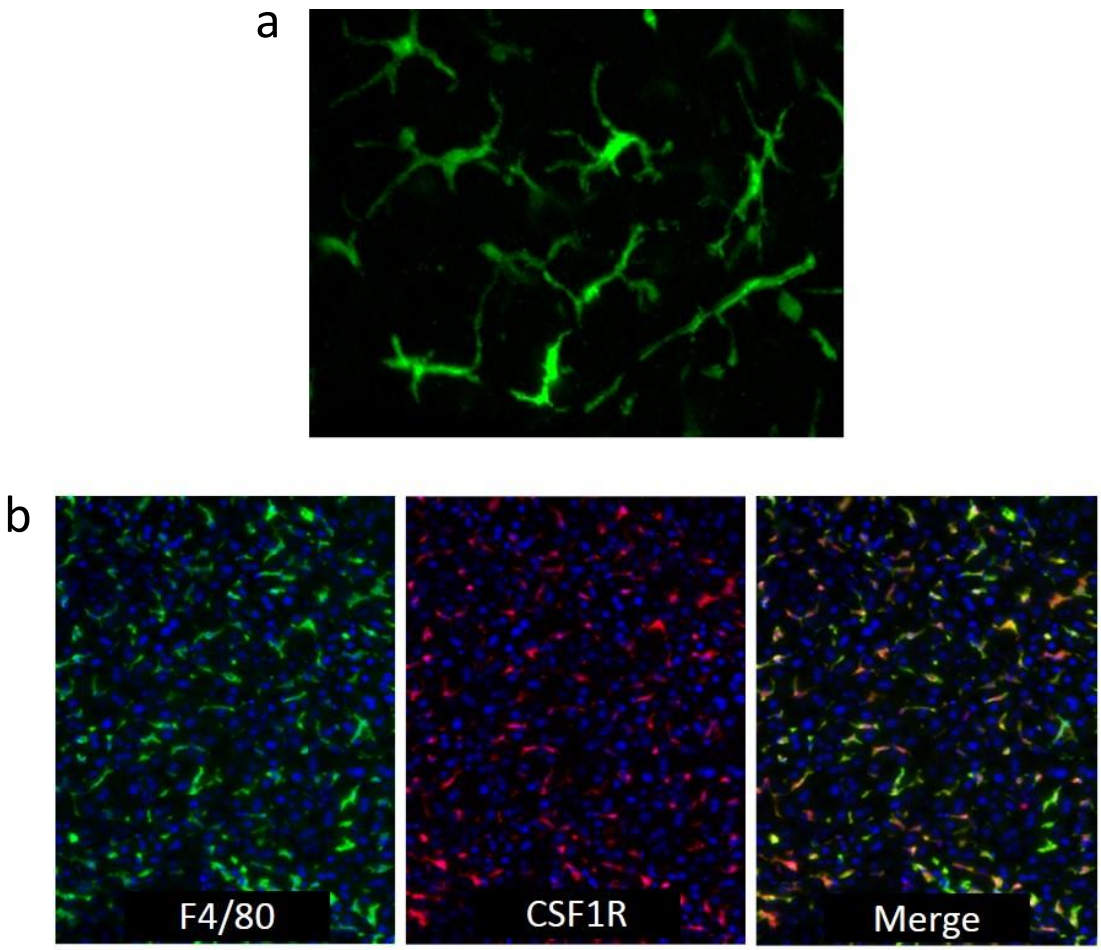


Figure 6.1: Hepatic CSF1 receptor expression

a) Representative multiphoton image of ex vivo liver (MacGreen mouse *Tg(CSF1r-GFP)*$_{Hume}$); b) Representative immunofluorescence images of *Csf1r-Mer2iCre*$_{JWP}$ x Rosa floxed stop tomato red following induction (F4/80 (green), CSF1R (red) and merged images).

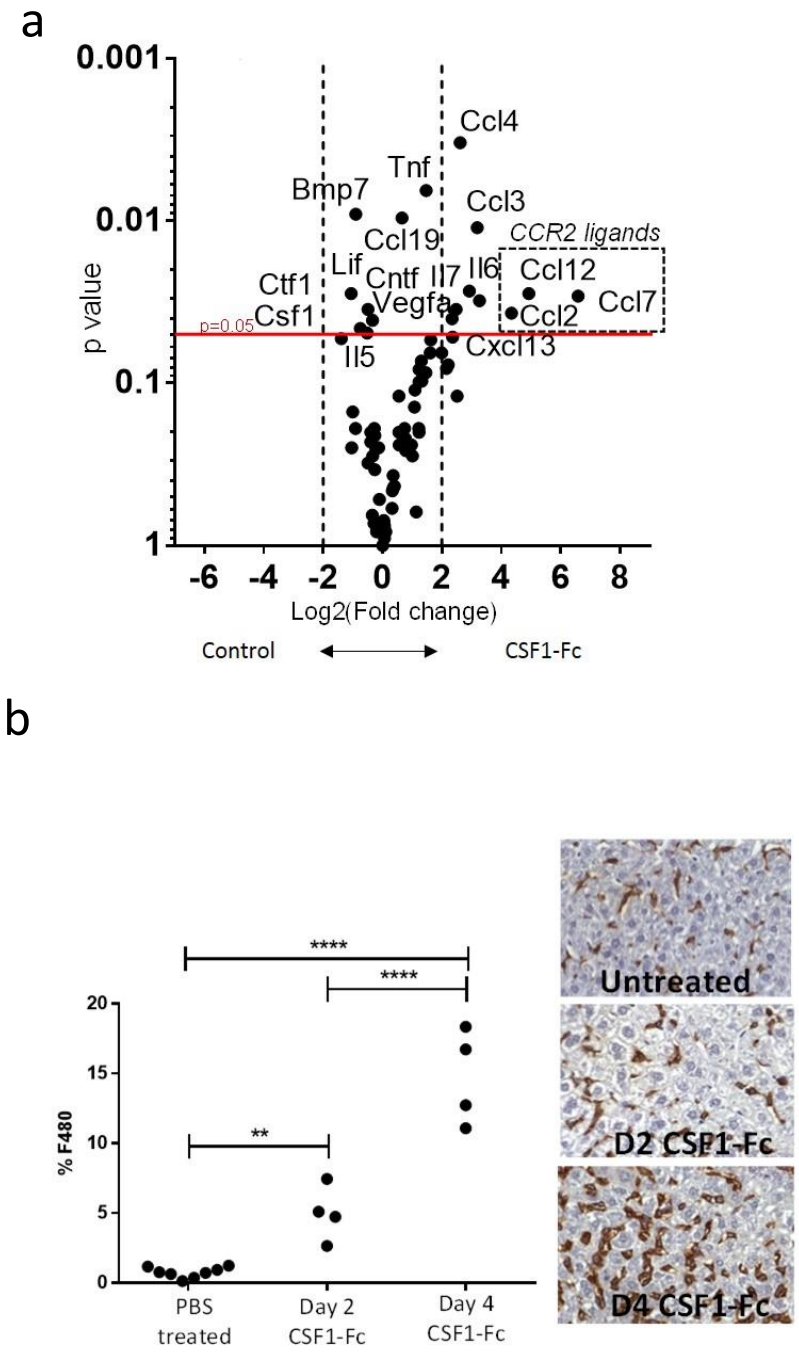


Figure 6.2: Effects of CSF1-Fc on hepatic macrophages

a) Cytokine/Chemokine array of liver tissue 6 hours following CSF1-Fc treatment versus control (n=4/group). (see Appendix 1, p231 for gene list). Quantification of hepatic F4/80 immunohistochemistry in PBS control treated (n=8) and mice treated with CSF1-Fc for 2 or 4 days (n=4/group).

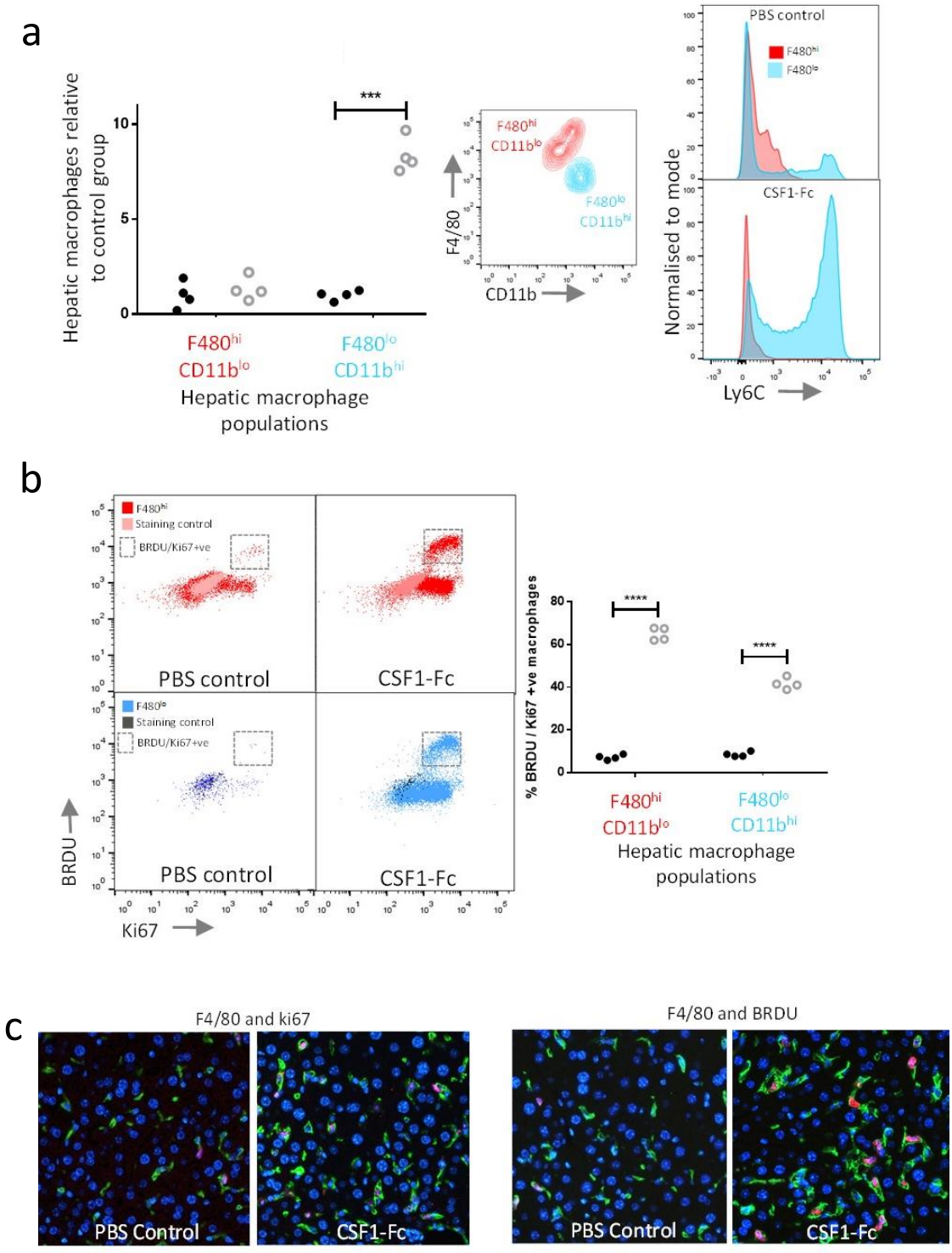


Figure 6.3: Hepatic macrophage characteristics following CSF1-Fc administration

a) Relative number of hepatic macrophage populations ($F480^{hi}/CD11b^{lo}$ and $F480^{lo}/CD11b^{hi}$) day 2 following CSF1-Fc administration or control (n=4/group; CSF1-

Fc= solid circles; control= hollow circles) and representative Ly6C profile of $F480^{hi}$ (red) and $F480^{lo}$ (blue) populations (two way ANOVA with Bonferroni post hoc). b) Representative dot plots of Ki67 expression and BRDU incorporation of $F480^{hi}$ and $F480^{lo}$ hepatic macrophage populations day 2 following CSF1-Fc (solid circles) or Control (hollow circles). Quantitative analysis of BRDU and Ki67 dual positive cell populations (n=4/group) (two way ANOVA with Bonferroni post hoc). c) Representative dual immunohistochemistry F4/80 (green) and BRDU or Ki67 (red) Day 2 following CSF1-Fc administration or control.

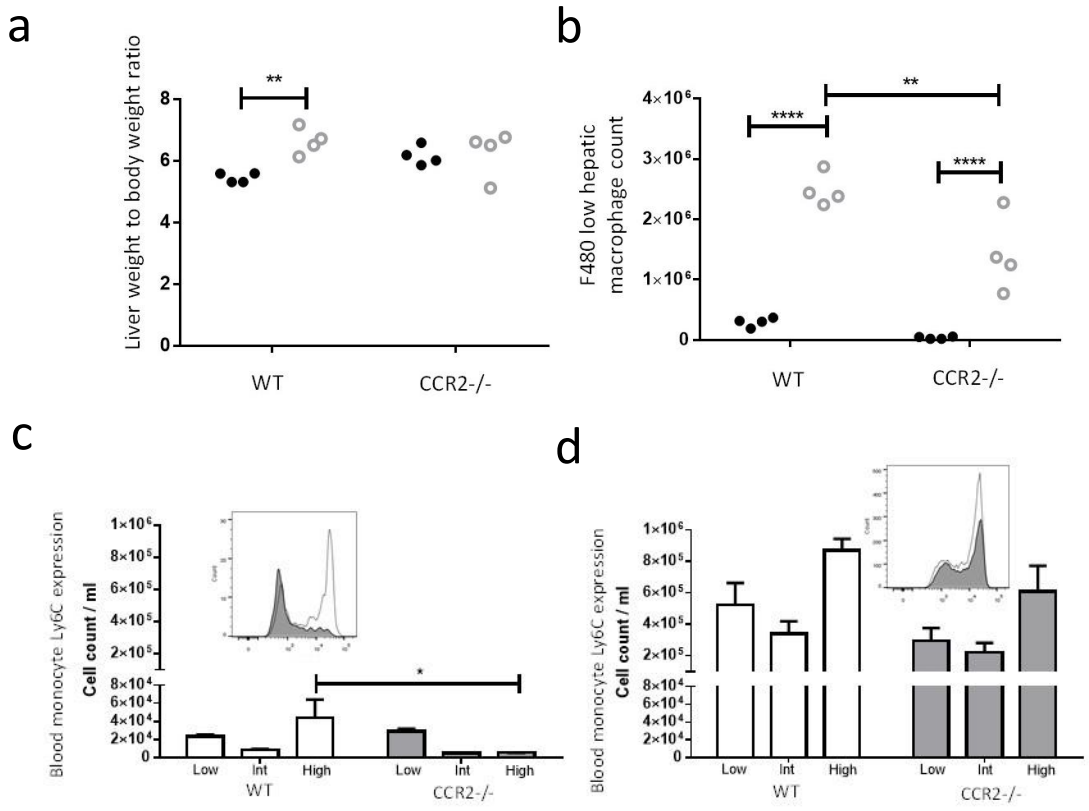


Figure 6.4: CSF1-Fc and the CCR2-/- mouse

a) Liver weight to body weight ratio following 2 days control (black) or CSF1-Fc administration (grey) in wild type and CCR2-/- mice. b) Number of F480$^{lo}$/CD11b$^{hi}$ macrophages following CSF1-Fc administration in WT and CCR2-/- mice (n=4/group). *p<0.05, **p<0.01, ***p<0.001, ****p<0.0001. c) Blood monocyte Ly6C profile in PBS treated controls in WT (clear bars) and CCR2-/- mice (shaded bars) (monocytes identified by flow cytometry for CSF1R positivity) (2-way ANOVA with Bonferroni post hoc). d) Blood monocyte Ly6C profile in WT (clear bars) and CCR2-/- (shaded bars) following 2 days treatment with CSF1-Fc (n=4/group; 2-way ANOVA ns).

## CSF1R stimulation indirectly induces hepatocyte proliferation

I then examined the effects of CSF1-Fc induced macrophage accumulation on hepatocyte activity. Continued CSF1-Fc administration led to extensive hepatocyte proliferation by day 4 (Figure 6.5a and Figure 6.5b). Given early upregulation of Il6 following CSF1-Fc administration (Figure 6.2), and its recognised role in inducing hepatocyte proliferation[26,28], I examined the impact of Il6-deficiency on hepatocyte proliferation following CSF1-Fc administration. Following four days of CSF1-Fc administration liver weight increased equally in WT and Il6$^{-/-}$ mice. Hepatocyte proliferation was not inhibited but impaired with Il6 deficiency (Figure 6.6a and Figure 6.6b).

Given this I examined other factors previously implicated in hepatocyte proliferation by analysis of Affymetrix gene array[xxiii] data of livers following CSF1-Fc or PBS control in WT mice[20,21]. Factors including TNF, matrix remodelling (MMP9) and growth factor activation (urokinase activity) were elevated (Figure 6.7a and Figure 6.7b)[17,195]. Growth factor expression remained relatively unchanged although notably *Tgfb1* gene expression was elevated (Figure 6.7b). This was not accompanied by an increase in TGF beta receptor expression and there was no evidence of apoptosis assessed by TUNEL staining (Figure 6.8a and Figure 6.8b). This was accompanied by a reduction in classic markers of hepatocyte injury (ALT and Alk phos) (Figure 6.8c).

Based on whole liver gene expression CSF1-Fc induces a mixed macrophage phenotype, with elevation of genes associated with "M1" type and "M2" type macrophages[196] (Figure 6.9).

xxiii: This Affymetrix gene array was completed by collaborators D. Hume and D Gow and published online. I downloaded the raw data and analysed this accordingly.

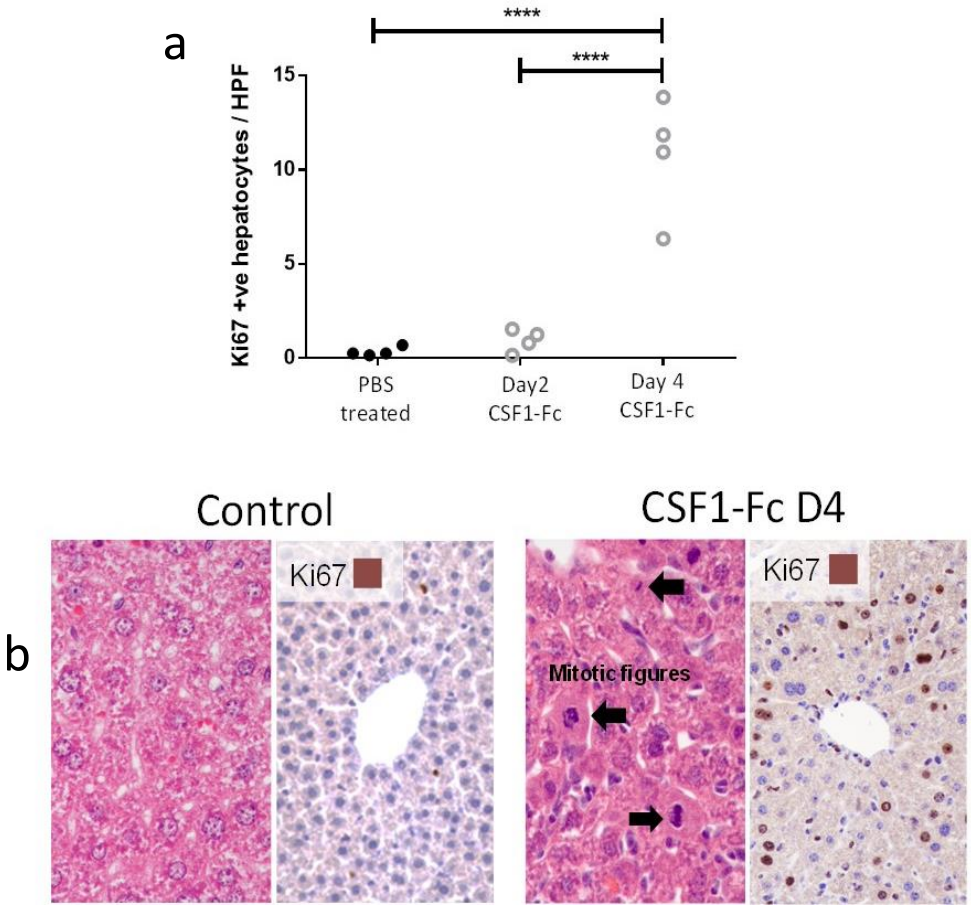


Figure 6.5: Hepatocyte proliferation following CSF1-Fc administration

a) Quantification of hepatocyte proliferation at Day 2 and Day 4 following CSF1-Fc administration (20 HPF/mouse). b) Representative images of HE stain and Ki67 immunohistochemistry in control and D4 CSF1 treated animals

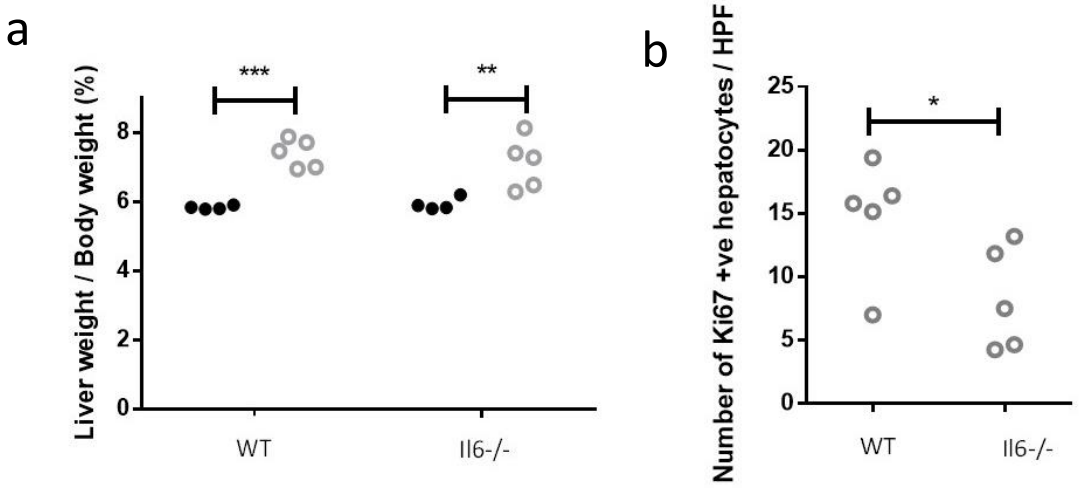


Figure 6.6: CSF1-Fc and the Il6-/- mouse

a) Liver weight to body weight ratio in wild type and Il6-/- mice following PBS control (n=4/group) or CSF1-Fc treatment in WT or Il6-/- mice (n=5/group) 2-way ANOVA with Bonferroni post hoc. b) Hepatocytes proliferation in WT or Il6-/- mice at Day 4 following CSF1-Fc administration (n=5/group).

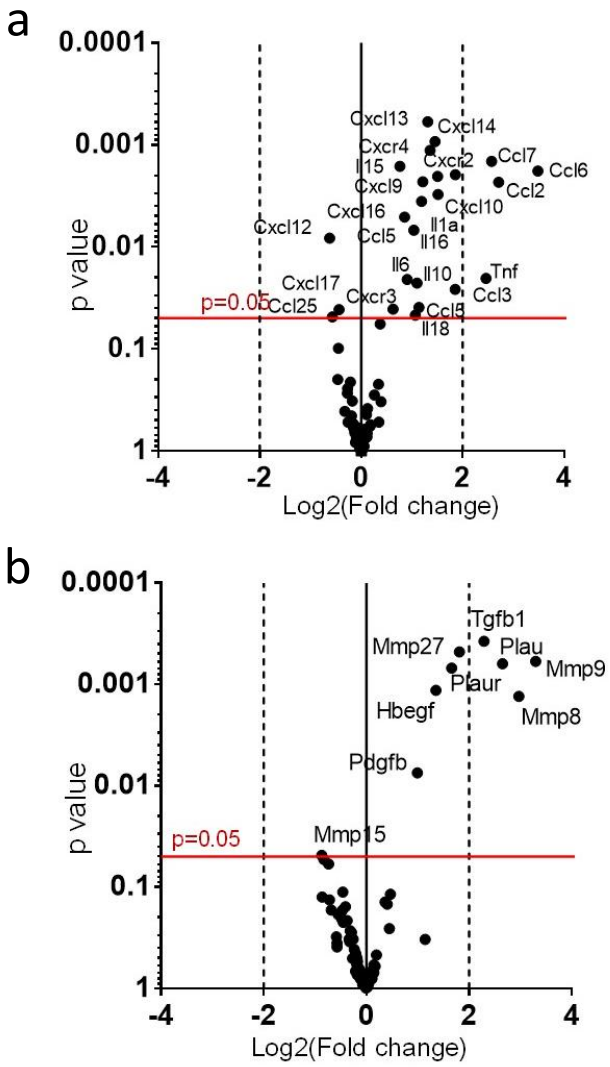


Figure 6.7: Gene array analysis whole liver

a) Cytokine and chemokine profile extracted from Affymetrix gene array[20] showing expression of genes significantly elevated following CSF1-Fc administration (number of genes assessed n=73; Gene list Supplementary Fig. 9b). b) Growth factors and matrix metalloproteinases extracted from Affymetrix gene array[20] showing expression of genes significantly elevated following CSF1-Fc administration (number of genes assessed n=82; Gene list Supplementary Fig. 9c). c)

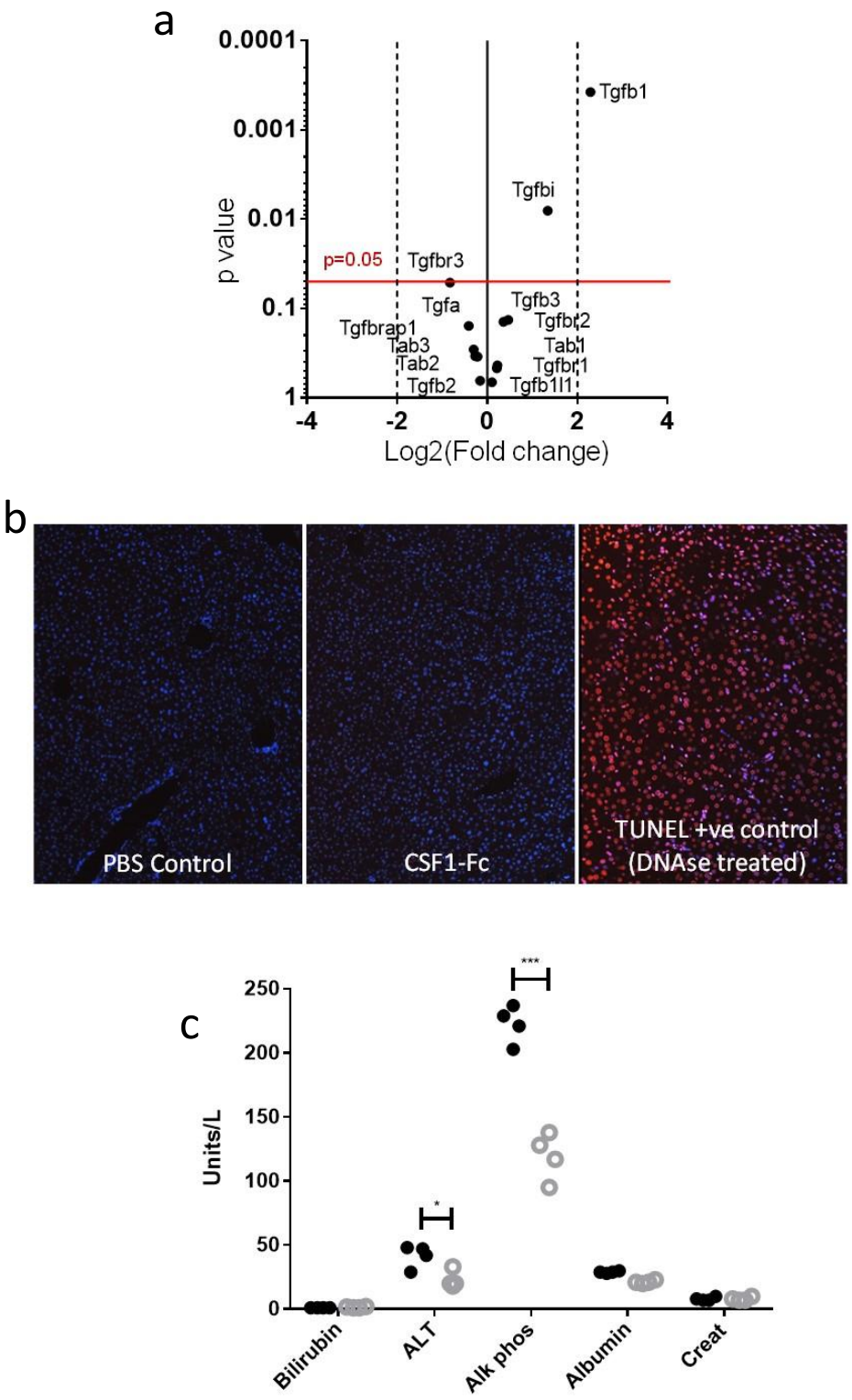


Figure 6.8: TGF beta pathway and markers of hepatic injury

a) Funnel plot showing TGF beta related gene expression extracted from Affymetrix gene array[20]. b) TUNNEL immunohistochemistry following PBS control or CSF1-Fc

administration (positive control DNAse treated section). c) Serum liver associated biochemistry tests following PBS control or CSF1-Fc treatment for 4 days (n=4/group) 2-way ANOVA (Control= solid black dots; CSF1-Fc treatment= hollow grey dots)

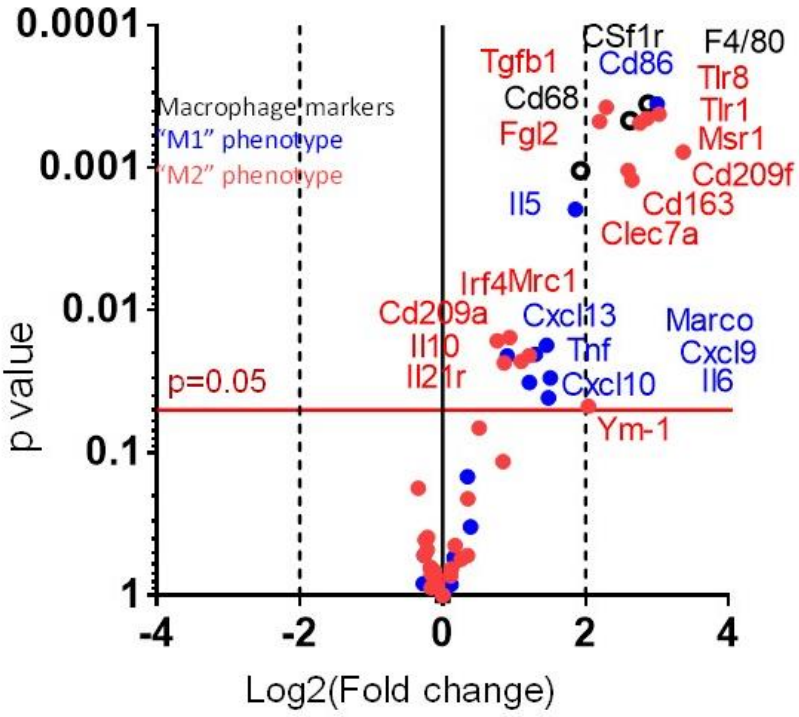


Figure 6.9: Macrophage polarisation markers

Macrophage markers and markers of macrophage polarisation extracted from Affymetrix gene array[20] showing expression of genes significantly elevated following CSF1-Fc administration compared to PBS control (number of genes assessed n=61; Appendix 1, p231).

## Effect on extrahepatic organs

I also examined spleen, lung, kidney and brain following CSF1-Fc injection. Most notably spleen size increased following CSF1-Fc administration associated with increase in red pulp macrophages and BRDU incorporation (Figure 6.10).

There is evidence of increased macrophage numbers and BRDU incorporation in the lung and kidney although the brain appeared unaffected but weights of these organs were not affected (
Figure 6.11).

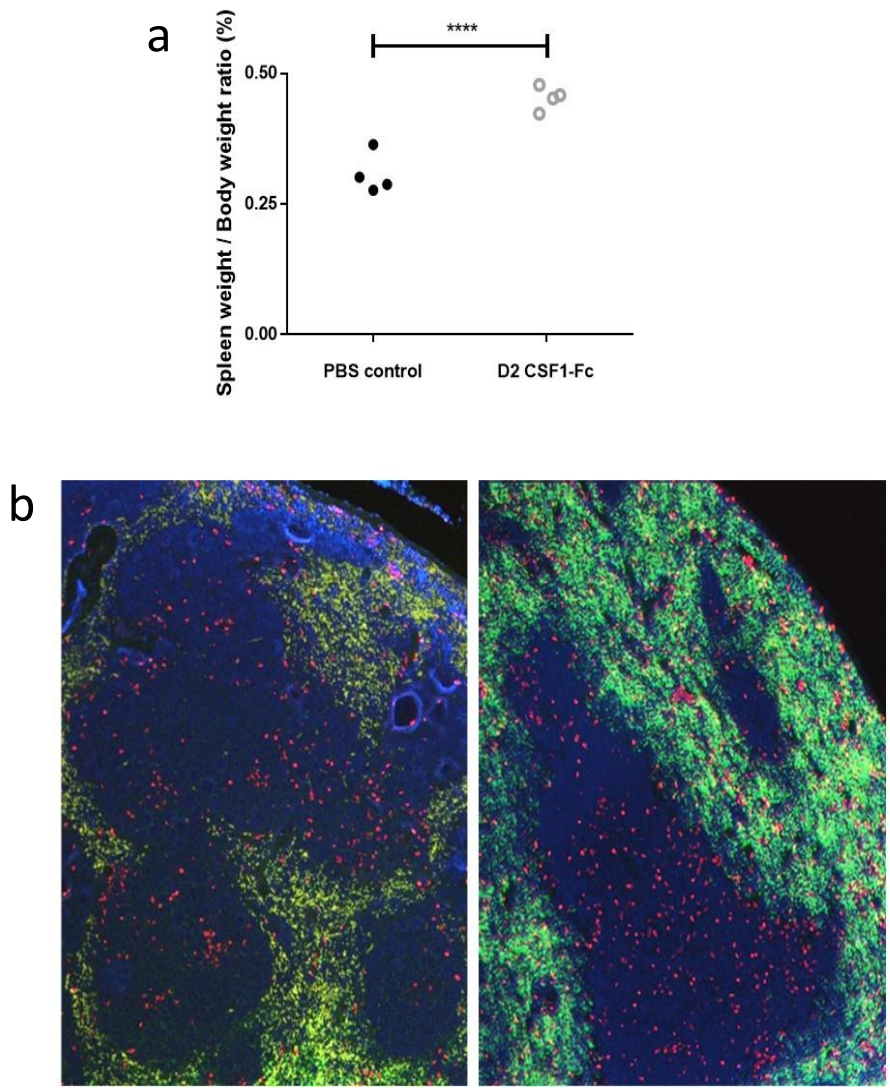


Figure 6.10: Effect of CSF1-Fc administration on the spleen

a) Spleen weight to body weight ratio 2 days following CSF1-Fc or PBS control to WT mice (n=4/group; t test). b) Indicative immunofluorescence of WT spleen showing F4/80 (green) and BRDU incorporation (red) following 2 days PBS control or CSF1-Fc administration.

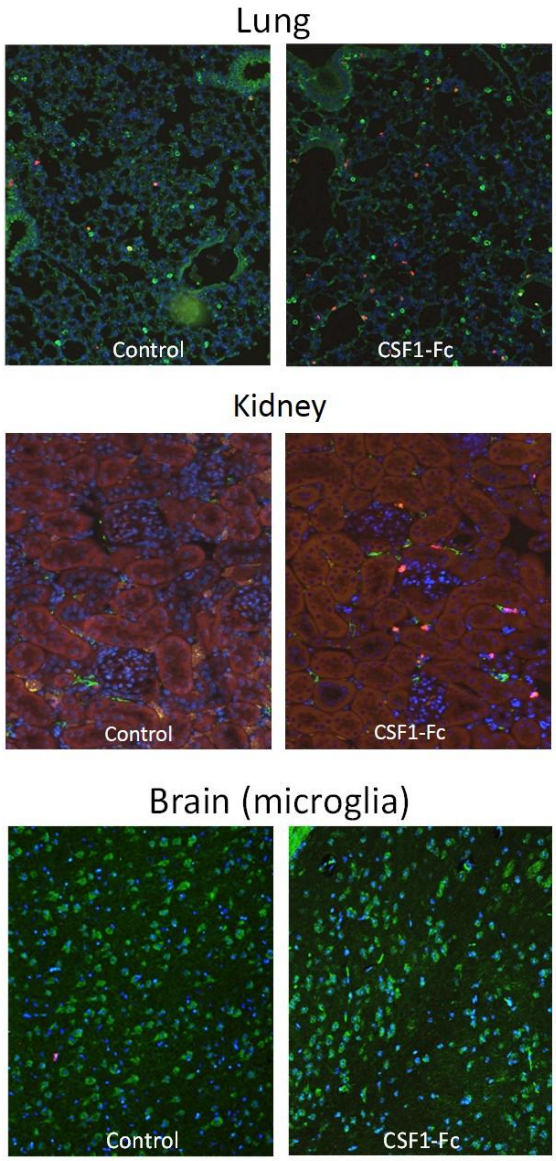


Figure 6.11: BRDU and F4/80 immunohistochemistry lung, kidney and brain

Indicative immunofluorescence of WT lung, kidney and brain showing F4/80 (green) and BRDU incorporation (red) following 2 days PBS control or CSF1-Fc administration.

## Discussion

I have shown that CSF1-Fc administration to uninjured mice led to an early upregulation of hepatic CCR2 ligand gene expression. This supports previous work showing CSF1 induced CCR2 dependent monocyte trafficking during placental growth[197]. Although hepatic macrophage infiltration was reduced in CCR2 -/- mice following CSF1-Fc compared to control, the infiltrate was still considerable demonstrating the functionality of other chemokine receptors. Interestingly CSF1-Fc can overcome the blood Ly6C high monocyte deficit in the CCR2-/- mouse and this warrants further investigation.

Macrophage accumulation is recognised as an important feature of hepatic regeneration following injury[28,49]. Here we show that even in the absence of injury, hepatocyte proliferation was induced following macrophage accumulation. Indeed serum injury markers (ALT and Alk phos) were actually reduced in this setting, supporting a role for the clearance of these enzymes by hepatic macrophages[28,198]. I targeted the IL6 pathway as a potential mechanism for hepatocyte proliferation based on early gene changes and published work indicating the role of Il6 in hepatocyte proliferation[26]. Hepatocyte proliferation was not prevented but was impaired in $Il6^{-/-}$, indicating a multifactorial mechanism supported by the multitude of other regeneration associated hepatic gene changes. Given the different dynamics of macrophage accumulation and hepatocyte proliferation (rapid and early versus late) it is likely that the former is the main contributor to hepatic size increase. Supporting this is the finding that despite reduced hepatocyte proliferation hepatic size increase was similar to WT controls following CSF1-Fc.

The array analyses shows that both TGF-beta and Il-10 are both elevated at the gene level following CSF1-Fc administration. These cytokines can have immunosuppressive

functions, acting in particular through T regulatory cells[199]. Effect on T cell phenotype has not been explored during this thesis but certainly warrants further investigation. Kupffer cells responding to fulminant hepatitis are also known to upregulate Il-10 and TGF-beta, which plays an important role in attenuating the inflammatory injurious process[200].

Hepatic gene expression revealed no clear macrophage "M1" or "M2" activation bias following CSF1R stimulation, rather a spectrum of pro and anti-inflammatory macrophage markers. Relating whole liver analysis to a specific cell is clearly limited but the alternative of extracting macrophages for gene analysis is limited by the effect of the extraction process on cell function. While macrophage accumulation was also seen in the kidney and lung, there was no evidence of deleterious effects. Indeed this may be beneficial in injury given CSF1 administration in mouse models can support renal regeneration and CSF1-deficiency in sepsis leads to early death associated with phagocytic impairment[148,201,202].

## Conclusion

CSF1 receptor stimulation with CSF1-Fc induces marked hepatic macrophage accumulation involving both infiltration and proliferation, which increases hepatic size. After continued administration there is evidence of hepatocyte proliferation which is likely due to macrophages.

# 6.3 CSF1 receptor stimulation following partial hepatectomy

## Aims

1. Assess effects of CSF1R stimulation on hepatocellular regeneration following PH
2. Assess effects of CSF1R stimulation on macrophage phagocytic function following PH

## Results

Following PH I found that effects of CSF1-Fc were similar to the uninjured mouse with an increase in liver size and overall enhanced hepatocyte proliferation (Figure 6.12a and Figure 6.12b). Peak hepatocyte proliferation (Day 2) was not increased by CSF1-Fc treatment. However CSF1 dependence was supported by the inhibitory actions of CSF1R kinase inhibition (GW2580) and antibody against the CSF1 receptor (AFS98) (Figure 6.12c).

The liver is the dominant clearance site for insoluble material, as demonstrated earlier ("4.2 Assessment of hepatic phagocytic function", p94). CSF1-Fc treatment increased hepatic macrophage density following PH (Figure 6.13a) with corresponding elevation in phagocytic genes MARCO (macrophage receptor with collagenous structure) and MSR1 (macrophage scavenger receptor 1) (Figure 6.13b). PH leads to a marked impairment in fluorescent microbead clearance from the circulation and I found that this deficit was substantially improved by CSF1-Fc treatment (Figure 6.14a). By assessing whole liver fluorescence I show that CSF1-Fc treatment also augmented hepatic phagocytic capacity (Figure 6.14b).

Elevation in genes associated with matrix remodelling and cytokine gene profiles are similar to that seen in uninjured mice with reciprocal change given CSF1R inhibition (Figure 6.15a and Figure 6.15b). Serum cytokine multiplex showed increased circulating Il5, CXCl9 and CXCL10 (Figure 6.15c)

Immunohistochemistry for hepatocyte marker CYPD2 showed a reduction at day 4 (Figure 6.16a) suggestive of non-parenchymal cell accumulation. Extracted macrophages show a predominance of $F480^{lo}/CD11b^{hi}/Ly6C^{hi}$ macrophages (Figure 6.16b and Figure 6.16c). Macrophage proliferation was seen in both infiltrating and resident populations, with increase following CSF1-Fc treatment (Figure 6.17).

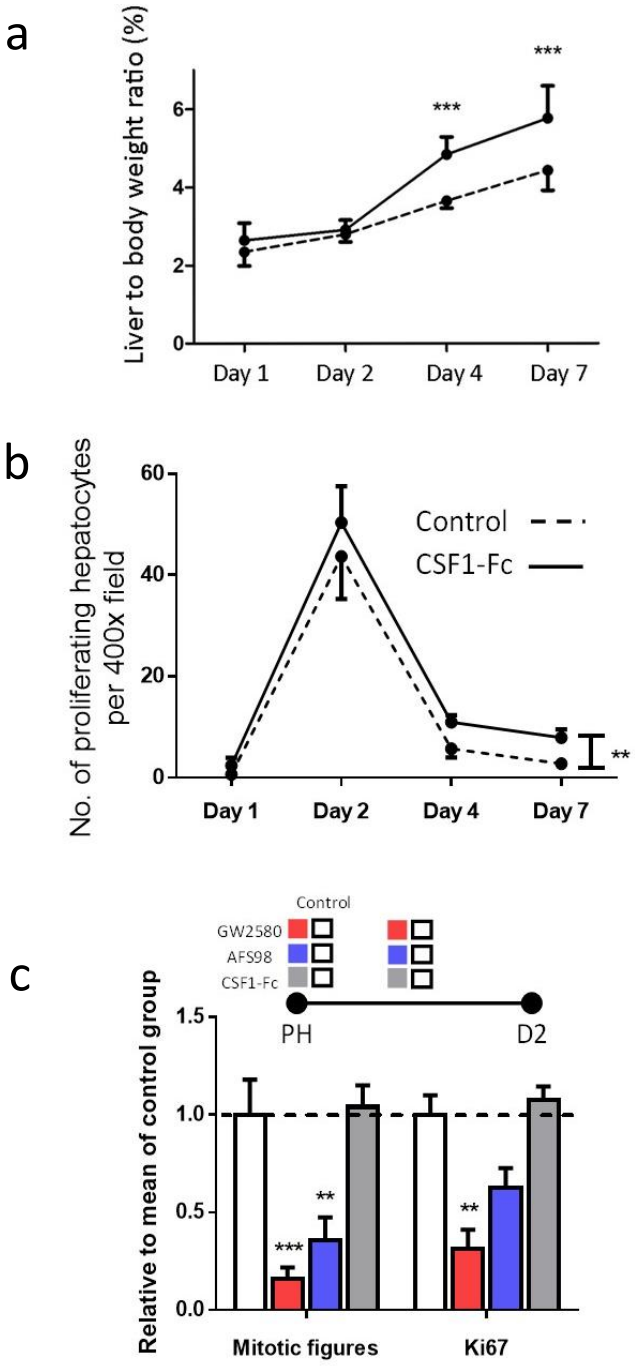


Figure 6.12: Effects of CSF1-Fc on regenerative parameters following partial hepatectomy

a) Liver weight to body weight ratio following partial hepatectomy (PH) with CSF1-Fc or control (2 way ANOVA; n=8/group). b) Ki67positive hepatocytes per HPF following PH (2 way ANOVA, Bonferroni post-test; n=8/group). c) Mitotic figures and Ki67 positive

hepatocytes per HPF following CSF1 receptor inhibitor (GW2580, red, n=8), CSF1R antibody blockade (AFS98, blue, n=7) or CSF1-Fc (grey, n=8). Compared to vehicle gavage (n=8), Rat IgG2A (n=8) and PBS (n=8) respectively; 2-way ANOVA with Bonferroni post-hoc).

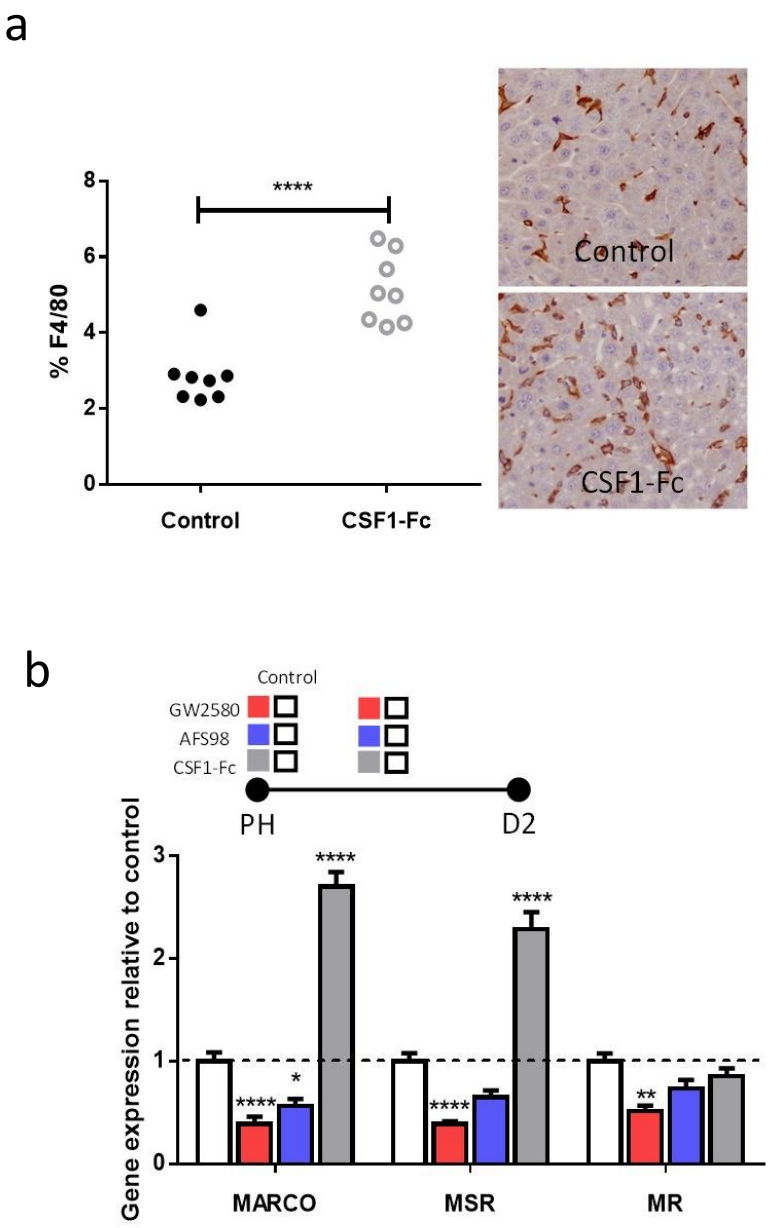


Figure 6.13: Hepatic macrophage density and markers of phagocytosis

a) Whole liver gene expression of phagocytic markers MARCO (macrophage receptor with collagenous structure), MSR1 (macrophage scavenger receptor 1) and MR (mannose receptor) versus relevant control (2-way ANOVA, Bonferroni post-test). b) Hepatic macrophage accumulation by F4/80 immunohistochemistry at Day 2 (t test) and representative F4/80 immunohistochemistry

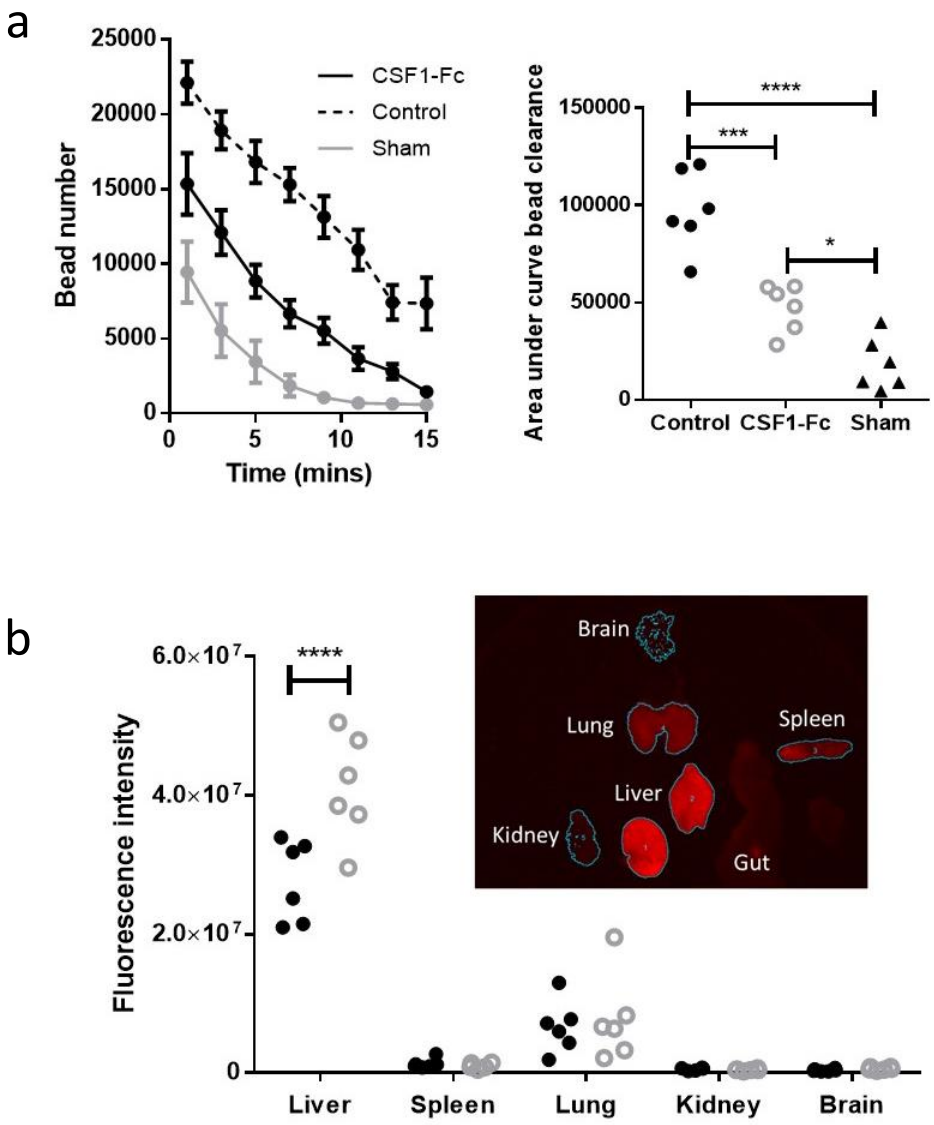


Figure 6.14: Phagocytosis assay following partial hepatectomy and CSF1-Fc

a) Clearance of microbeads from the circulation following sham or 2/3 PH with control or CSF1-Fc (n=6/group/timepoint) with area under the curve (one-way ANOVA, Bonferroni post-hoc, n=6/group). b) Net fluorescence liver, spleen, lung, kidney and brain Day 2 following PH and CSF1-Fc or control. (2 way repeated measures ANOVA with Bonferroni post test, n=6 per group). *p<0.05, **p<0.01, ***p<0.001, ****p<0.0001.

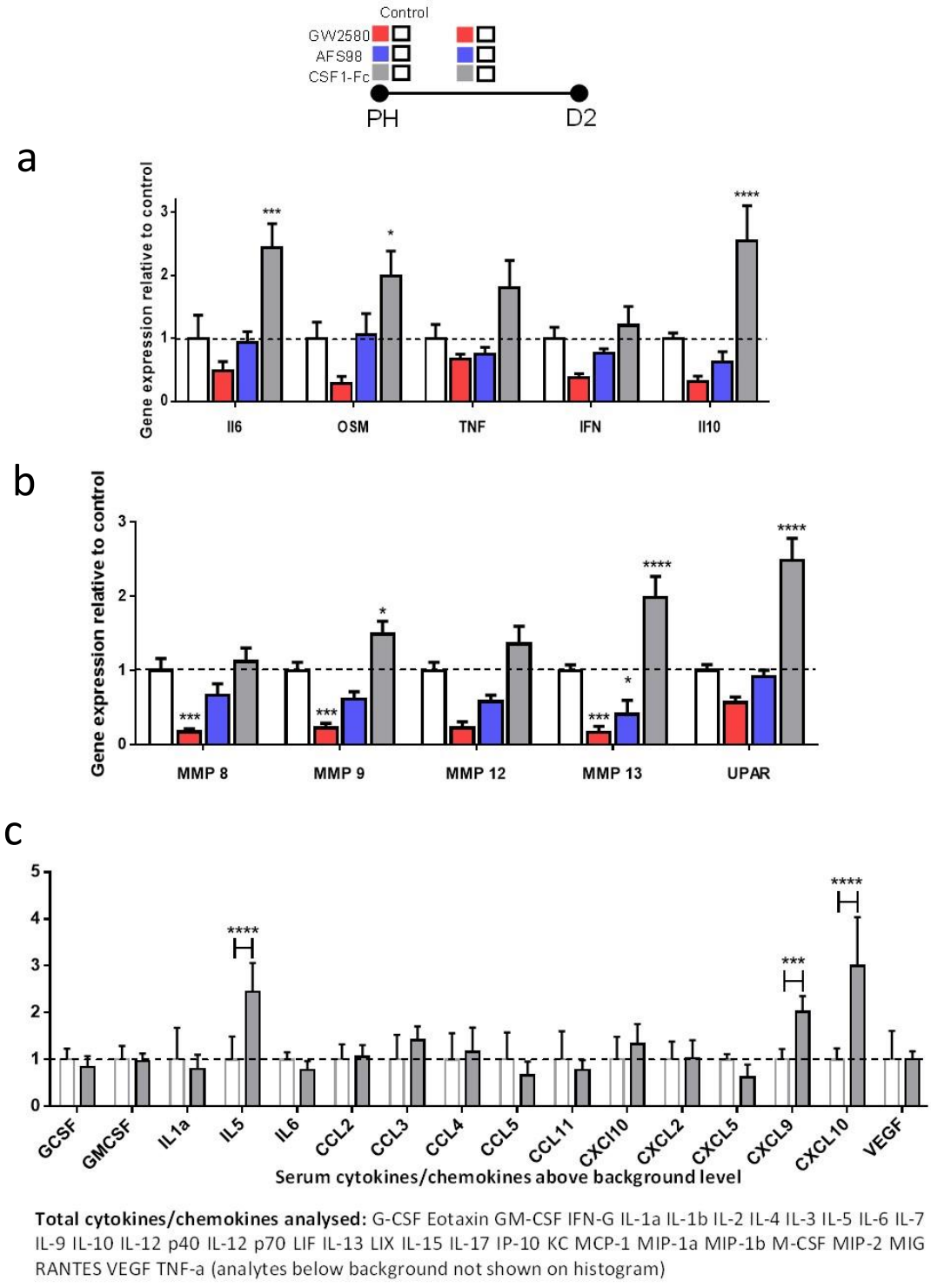


Figure 6.15: Hepatic gene and serum cytokine expression profiles following partial hepatectomy and CSF1-Fc administration

a) Hepatic gene cytokine expression at Day 2 following partial hepatectomy and either GW2580, AFS98 or CSF1-Fc administration versus control (vehicle gavage, rat IgG2a,

PBS; n=8/group; 2-way ANOVA comparing intervention with relevant control, Bonferroni post hoc). b) Hepatic MMP and UPAR (urokinase plasminogen activator receptor) gene expression Day 2 following partial hepatectomy and either GW2580, AFS98 or CSF1-Fc administration versus control (vehicle gavage, rat IgG2a, CSF1-Fc; n=8/group; 2-way ANOVA comparing intervention with relevant control, Bonferroni post hoc). c) Serum cytokine array Day 4 following partial hepatectomy and either PBS control or CSF1-Fc treatment (2-way ANOVA and Bonferroni post hoc).

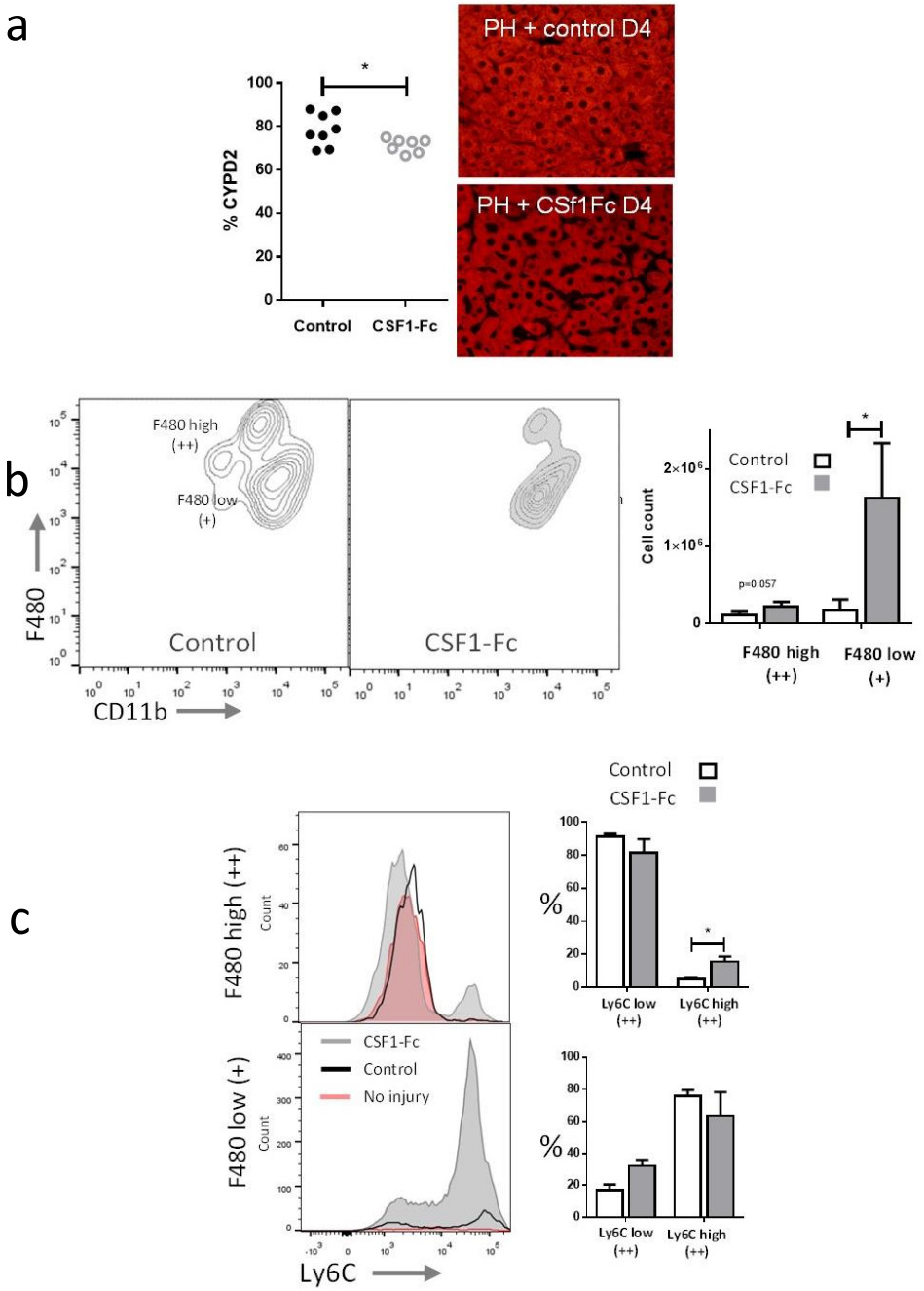


Figure 6.16: Macrophage accumulation following partial hepatectomy and CSF1-Fc.

a) Quantification CYPD2 immunofluorescence (red) per 20x HPF/mouse (control n=8; CSF1-Fc n=7; t test). b) Hepatic macrophage populations at Day 4 following partial hepatectomy and either PBS control or CSF1-Fc administration with quantification of F4/80++ and F4/80+ populations (2-way ANOVA). c) Ly6C profile of F4/80 + and ++ populations with quantification (n=4/group).

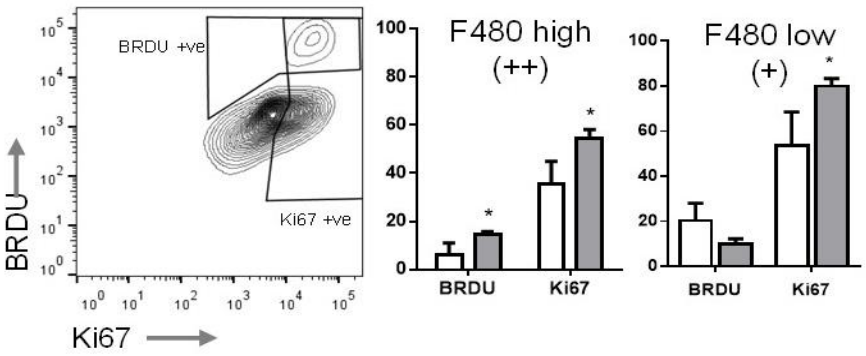


Figure 6.17: Macrophage proliferation following partial hepatectomy and CSF1-Fc

BRDU and Ki67 quantification F4/80 ++ and F4/80 + populations at Day 4 following partial hepatectomy with CSF1-Fc (grey) or control (white) (n=4/group; 2-way ANOVA).

## Discussion

I have found that following PH, CSF1-induced macrophage accumulation led to an overall increase in hepatocyte proliferation. However at the peak proliferative time point (Day 2) hepatocyte proliferation was not increased over control. This early stage of regeneration is the most clinically relevant time period, aiming to restore hepatic volume as rapidly as possible. As regeneration in mice is rapid, improving hepatocyte proliferation over and above what is already highly effective may not necessarily be advantageous. The requirement for CSF1 signalling to enable effective regeneration is demonstrated by the impaired regeneration following CSF1R blockade. This is consistent with findings in the CSF1 deficient mouse[162]. Liver weight to body weight was increased at later time points (Day 4 and Day 7) following CSF1-Fc administration, however this most likely relates, at least in part, to the marked macrophage accumulation.

Comparing both CSF1 receptor stimulation and inhibition there is an elevation and reciprocal reduction respectively in cytokines associated with liver regeneration and matrix remodelling. This supports a multifactorial mechanism by which macrophage exert their proregenerative effects.

I have shown that the impairment in hepatic phagocytic capacity following PH is considerable. This is consistent with work in humans where clearance of circulating radiolabelled albumin microbeads was impaired following partial hepatectomy to a similar extent as patients with severe chronic liver disease[76]. The liver represents the first line of defence from gut derived pathogens, receiving around 75% of its blood from the portal system[203]. Infection rate is increased following major PH[204] therefore enhancing hepatic innate capacity is desirable. CSF1-induced macrophage accumulation

markedly improved both rate of phagocytosis assessed by clearance of beads from the circulation and phagocytic capacity assessed by hepatic fluorescent bead uptake.

## Conclusion

CSF1R signalling is crucial for effective regeneration. Partial hepatectomy results in a marked impairment in innate immune capacity which can be ameliorated by CSF1-Fc therapy.

# 6.4 Focus on the spleen

## Aims

1. Assess splenic dynamics following partial hepatectomy and CSF1R stimulation
2. Assess splenic macrophage dynamics following partial hepatectomy and CSF1R stimulation

## Results

In the spleen, macrophages reside predominantly in the splenic red pulp. I assessed splenic macrophage morphology using multiphoton imaging of the MacGreen mouse spleen ex vivo. Macrophages are abundant in the splenic red pulp with distinct morphology as compared to hepatic macrophages (Figure 6.18a and Figure 6.18b).

I found that spleen size increased following partial hepatectomy in control treated mice and this was significantly increased further by CSF1-Fc treatment (Figure 6.19a and Figure 6.19b). Following PH, enhanced red pulp Ki67 expression co-stains with macrophage marker F4/80 and this was further increased following CSF1-Fc administration indicating macrophage proliferation (Figure 6.19c).

I considered whether, given this increase in size, there would be an effect on splenic cytokine and chemokine gene expression. However, I found that splenic cytokine gene profiles were not markedly influenced by CSF1-Fc treatment (Figure 6.20).

Given the abundance of macrophages in the spleen, I analysed the effects of the fluorescent microbead assay on the spleen and compared this to the liver. I found that microbead uptake of the spleen was markedly inferior to the liver both overall and per unit area (Figure 6.21).

Given the increase in splenic macrophage populations, I considered whether there was evidence of trafficking of these cells between the liver and spleen in addition to bone marrow production. I therefore analysed the number and percentage of monocytes in the portal blood (which directly drains the spleen and also gut) and compared this to the inferior vena cava (which is down-stream of the femoral bone marrow- a major blood monocyte producer) and tail vein (a site upstream of the major monocyte producing regions). I found an increase in monocytes in the portal blood, immediately downstream of the spleen, greatly enhanced by CSF1-Fc treatment (Figure 6.22). This suggests that the spleen is also a site of monocyte production with trafficking of monocyte/macrophages between spleen and liver. This is likely to occur in addition to local proliferation and bone marrow production of monocytes/macrophages.

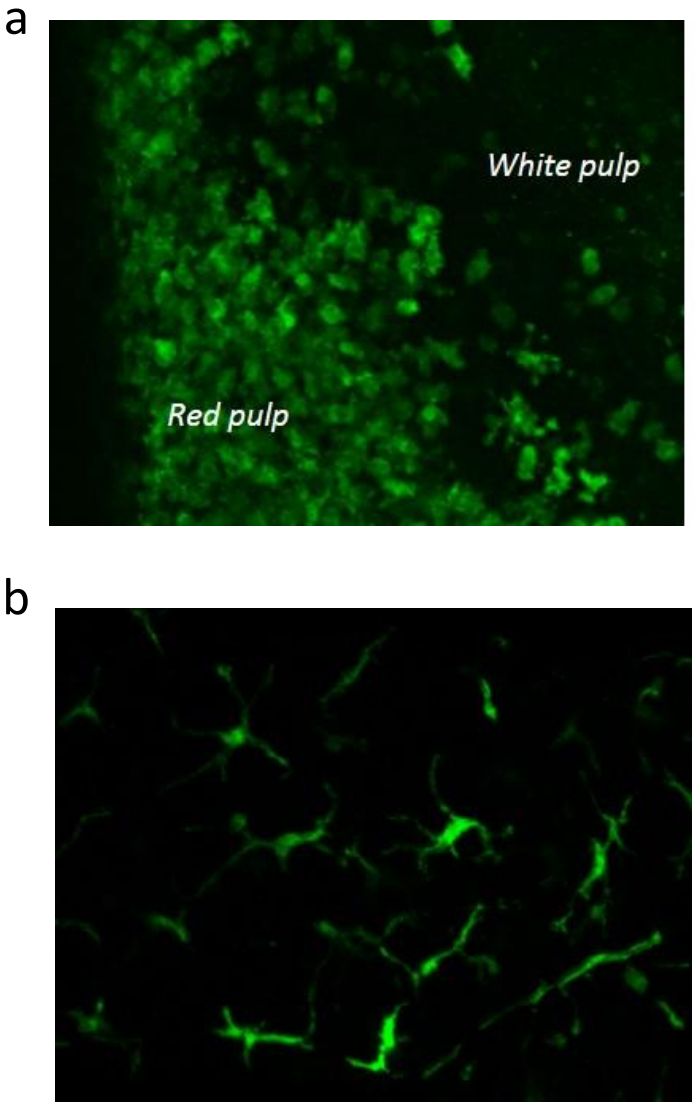


Figure 6.18: Comparison of splenic and hepatic macrophage morphology

a) Multiphoton image MacGreen mouse spleen in the steady state; b) Multiphoton image MacGreen mouse liver in the steady state (Note: this liver image is also shown in "Figure 6.1: Hepatic CSF1 receptor expression". It is repeated here for comparison with the splenic image)

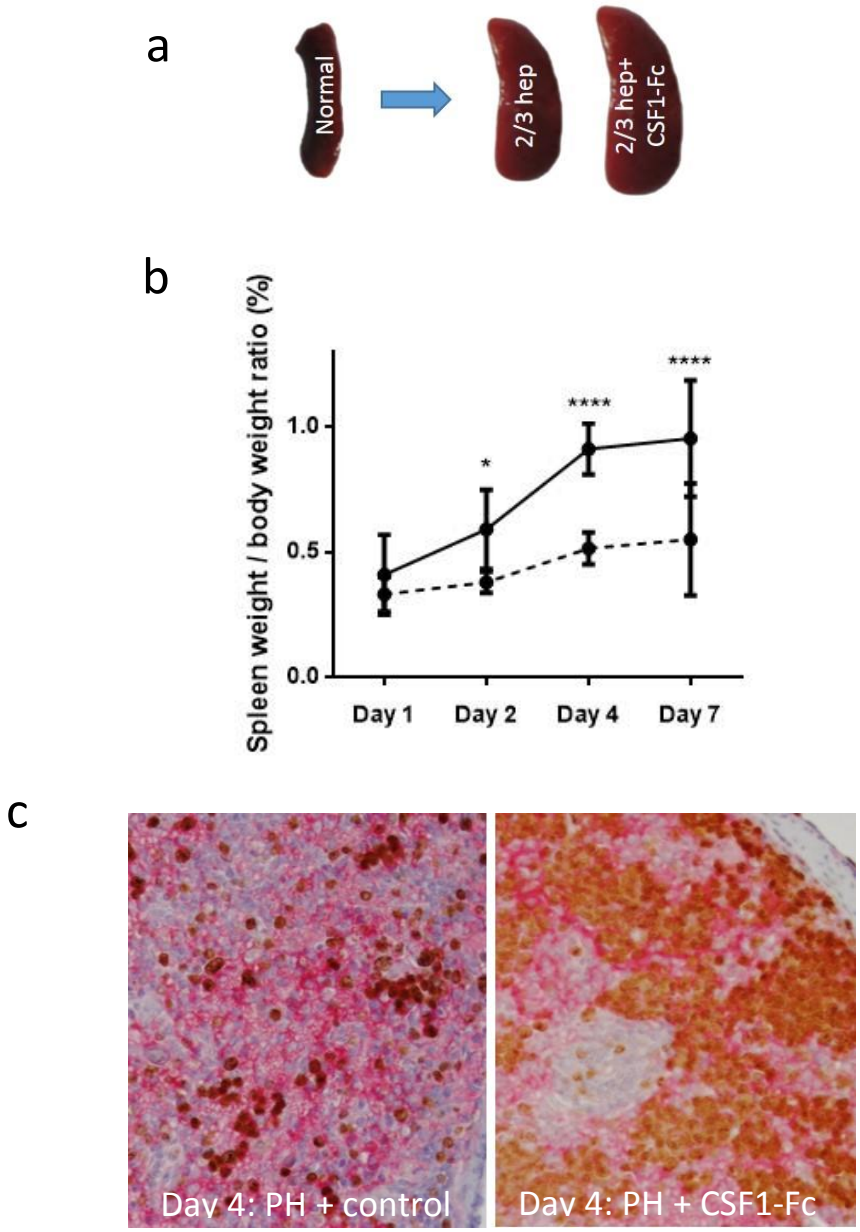


Figure 6.19: Splenic size following partial hepatectomy +/- CSF1-Fc

a) Representative image demonstrating change in spleen size following partial hepatectomy and partial hepatectomy with CSF1-Fc treatment. b) Change in spleen weight to body weight ratio following partial hepatectomy with PBS control (dotted line) and CSF1-Fc treatment (solid line). Compared using two way ANOVA with Bonferroni post-hoc analysis. *$p<0.05$, ****$p<0.0001$. c) Dual immunohistochemistry for macrophage marker F4/80 (pink) and Ki67 (brown) in mice at Day 4 following PH +/- CSF1-Fc treatment.

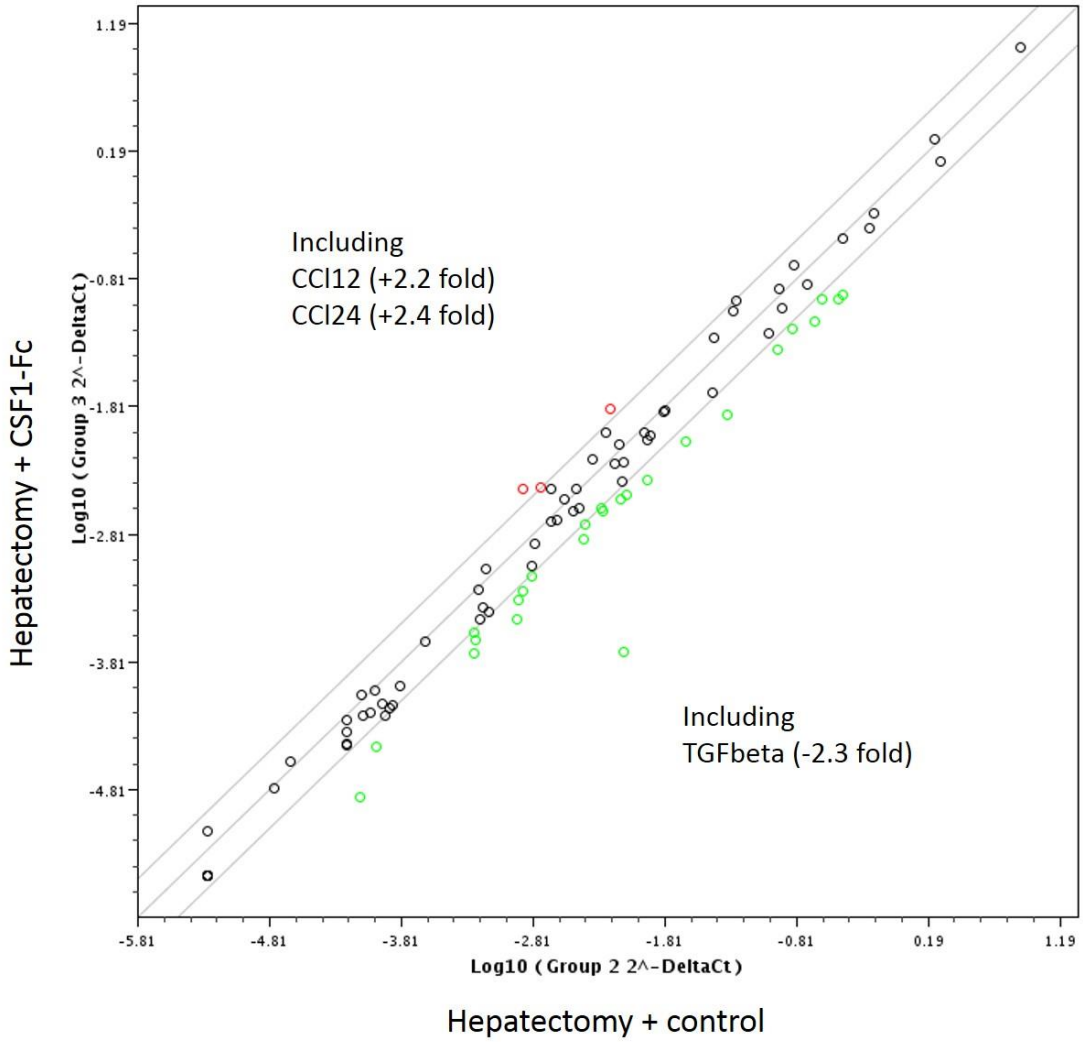


Figure 6.20: Pooled sample cytokine/chemokine array whole spleen

Comparison between partial hepatectomy plus CSF1-Fc and partial hepatectomy plus PBS control. (n=4 per group, samples pooled following RNA extraction)

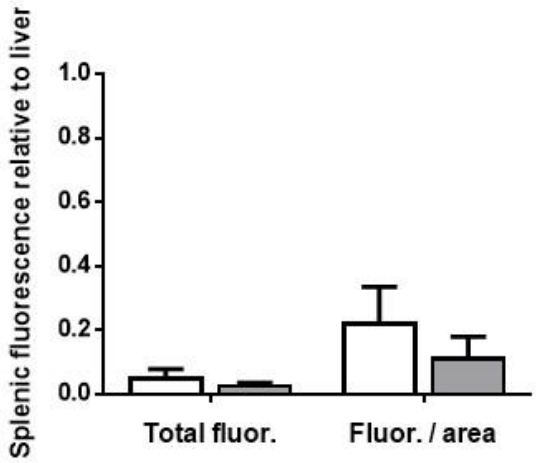


Figure 6.21: Fluorescence of spleen compared to liver following fluorescent microbead injection

Explanation: Here I injected mice with fluorescent microbeads via the inferior vena cava at Day 2 following partial hepatectomy with PBS control (white bar) or CSF1-Fc treatment (grey bar) as per analysis shown in "Figure 6.14: Phagocytosis assay following partial hepatectomy and CSF1-Fc". I then compared the relative fluorescence of the spleen compared to the liver for each mouse ([liver fluorescence] / [splenic fluorescence]; n=6 per group). This includes both the total fluorescence of each organ (Total fluor.) and fluorescence per area (Fluor. / area).

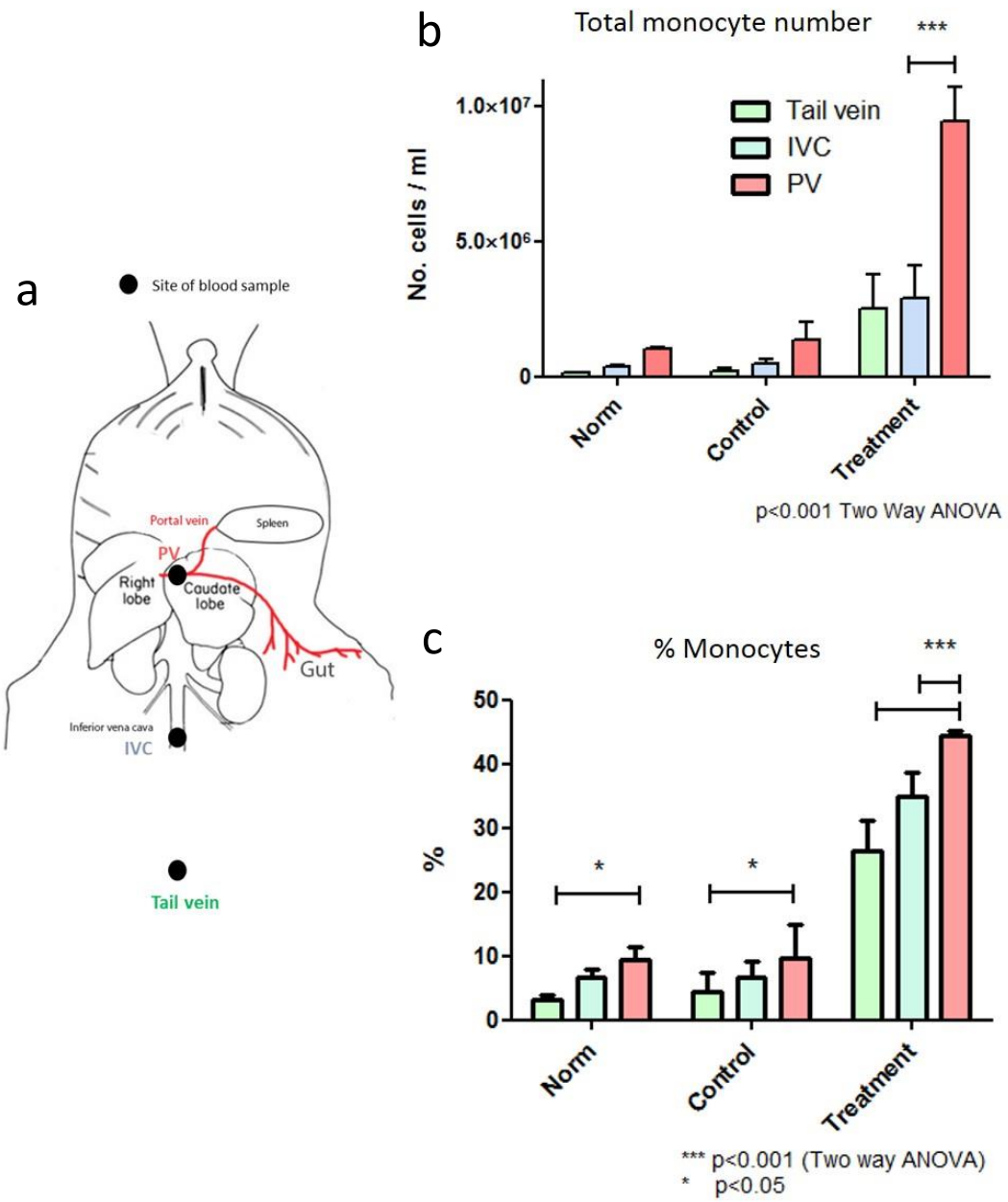


Figure 6.22: Splenic monocyte trafficking

a) Diagram illustrating sampling sites for assessment of blood monocyte content (tail vein= green; inferior vena cava (blue) and portal vein (red). b) Total monocyte number at each sampling site in untreated/uninjured mice (Norm), PBS control treated mice at Day 2 following partial hepatectomy (Control) and CSF1-Fc treated mice at Day 2 following partial hepatectomy. c) Percentage monocytes out of total cellular blood populations at each sampling site. Note: Monocytes identified by CSF1R expression.

## Discussion

I have shown that the spleen increases in size following partial hepatectomy in mice and that spleen size is increased further by CSF1-Fc treatment. In the clinical setting an increase in spleen size is noted following partial hepatectomy for colorectal liver metastasis with a greater than 40% increase in splenic size evident 6 months following surgery[205]. Portal pressure does increase transiently following partial hepatectomy of greater 30% (as assessed using an indirect ultrasonography method)[206,207] and this may be in part responsible for the increase in spleen size, but as this pressure increase is short-lived it might be that circulating growth factors contribute to splenic size increase.

Despite the spleen's reputation as the "body's largest filter of blood"[208], microbead uptake was markedly inferior to the liver. Anatomically the liver's far superior phagocytic capacity makes sense given that it is situated immediately downstream from the gut. The percentage cardiac output that the liver receives is also far superior to the spleen, with the spleen receiving approximately 2.2% and the liver (via its dual supply of portal vein and hepatic artery) receiving approximately 27.3%[209]. The functional reason behind splenic size increase does not appear to be to increase phagocytic capacity.

It has been shown that in other injury models, such as cardiac ischemia, that splenomegaly also occurs. In these models the spleen can act as a monocyte reservoir, supporting trafficking of monocytes to sites of distant injury[210]. I assessed blood monocyte content of the portal vein, directly downstream from the spleen and found that blood monocyte content was markedly increased compared to blood sampled from either the tail vein or inferior vena cava. This finding indicates that there is likely to be a

degree of monocyte trafficking from the spleen to the liver. This may serve to provide sufficient monocyte numbers during repair and regeneration.

The literature on effects of splenectomy on regeneration following partial hepatectomy is mixed with some investigators finding that splenectomy impaired regeneration in mice via its effects on t cells and Il17 production (monocyte/macrophage dynamics not assessed)[211], with others finding that splenectomy enhanced liver regeneration in rats by removing the splenic source of TGF beta[212]. Studying the effects of splenectomy on monocyte and macrophage dynamics following partial hepatectomy is required.

## Conclusion

Spleen size increases following partial hepatectomy with further increase following CSF1-Fc treatment. Macrophage populations within the splenic red pulp expand and there is evidence to support monocyte/macrophage trafficking from the spleen to the liver.

# 6.5 CSF1 receptor stimulation, partial hepatectomy and chronic liver injury

## Aims

Assess the effects of CSF1R stimulation on outcomes following partial hepatectomy and chronic liver injury

## Results

Following partial hepatectomy and chronic liver injury CSF1-Fc treatment led to a non-significant trend to improved survival (p=0.08) (Figure 6.23). Subsequent results reflect analysis of survivors (Day 4: control n=5, treatment n=7; Day 7: control n=6, treatment n=7). Liver weight to body weight ratio was significantly increased from Day 3 onwards (Figure 6.24). Hepatocyte proliferation was not enhanced at the Day 4 time point but was significantly increased at Day 7 (Figure 6.26). I used indocyanine green (ICG) as an indicator of hepatocyte function. I found no difference in ICG clearance between CSF1-Fc and control treated mice although both these groups had significantly impaired ICG clearance compared to control at postoperative day 4 (Figure 6.27) (n=8 per group at each time point). These ICG data are the almagmation of two sets of experiments; n= 4 per group randomly selected from the mice prior to cull; and n=4 per group at day 4 of mice that were then recovered and continued to the Day 7 time point).

Figure 6.28 shows Ki67 and F4/80 dual immunohistochemistry of mouse liver from the Day 4 timepoint, with macrophage clustering around the scar area. I did not find a reduction in degree of fibrosis following CSF1-Fc treatment by quantification of Sirius

red staining (Figure 6.29). There was a significant reduction in serum ALT and serum bilirubin at Day 4 postoperatively (Figure 6.30; Figure 6.31). Serum albumin was decreased at both Day 4 and Day 7 time points (Figure 6.32). There was no significant difference in serum creatinine at either day 4 or day 7 (Figure 6.33).

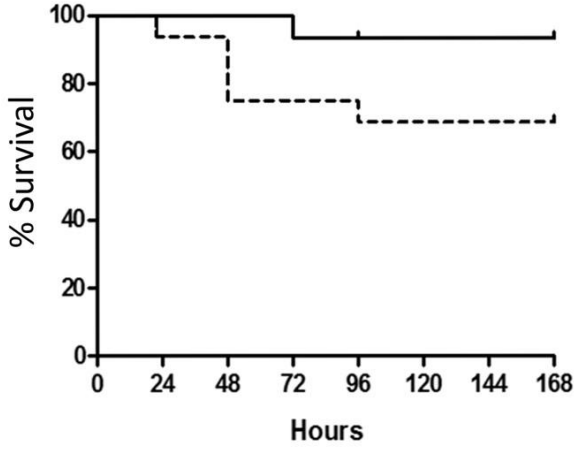


Figure 6.23: Kaplan-Meier survival plot following partial hepatectomy and chronic liver injury with CSF1-Fc or control

Log rank test p=0.08

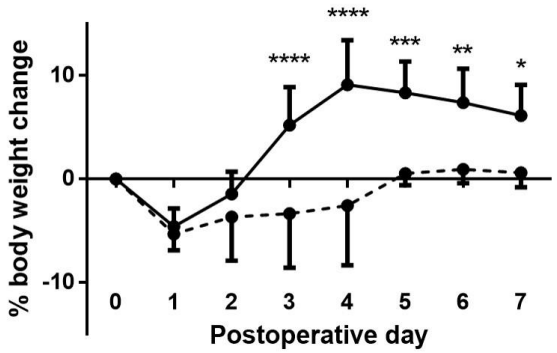


Figure 6.24: Mouse body weight following partial hepatectomy and chronic liver injury with CSF1-Fc or control

2 way ANOVA with Bonferroni post hoc. *p<0.05, **p<0.01, ***p<0.001, ****p<0.0001

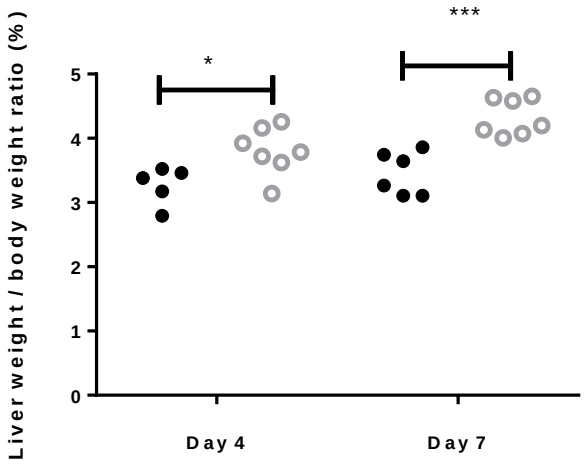


Figure 6.25: Liver weight to body weight ratio following partial hepatectomy and chronic liver injury with control (solid circles) or CSF1-Fc (hollow circles) assessed by hepatocyte Ki67 expression. 2 way ANOVA with Bonferroni post hoc. *p<0.05, ***p<0.001

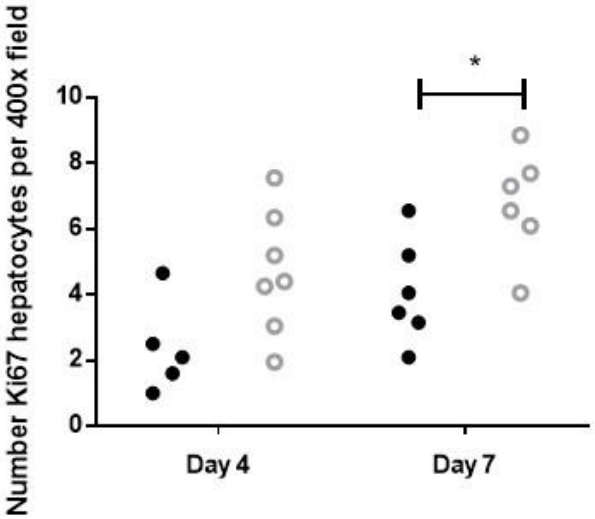


Figure 6.26: Hepatocyte proliferation following partial hepatectomy and chronic liver injury with control (solid circles) or CSF1-Fc (hollow circles) assessed by hepatocyte Ki67 expression. 2 way ANOVA with Bonferroni post hoc. *p<0.05

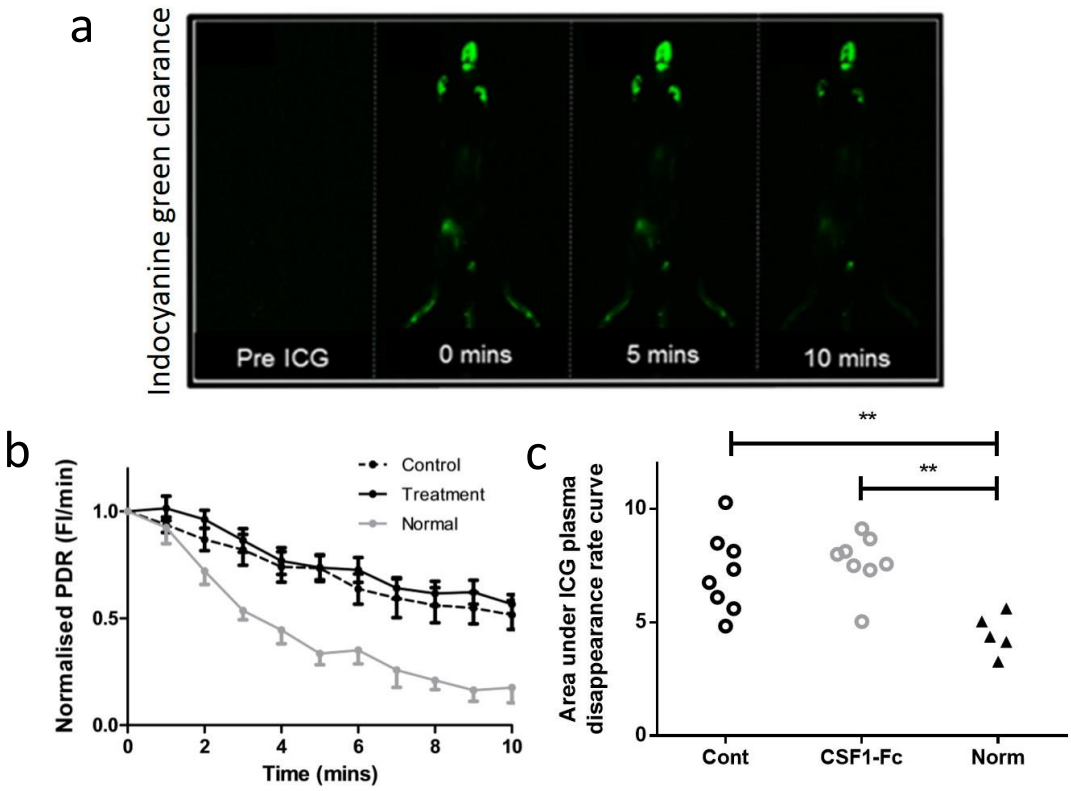


Figure 6.27: Indocyanine green clearance following partial hepatectomy and chronic liver injury with CSF1-Fc or control

a) Indicative ICG clearance images including fluorescent images taken prior to ICG injection (Pre ICG), at 0 mins (immediately following injection), at 5 and 10 minutes post injection. b) ICG plasma disappearance rate in control (PH + chronic liver injury with PBS control, dotted line, n=8), treatment (PH+ chronic liver injury with CSF1-Fc, solid black line, n=8) and normal (uninjured untreated mice, solid grey line n=6). c) Area under ICG plasma disappearance rate curve. One-way ANOVA with Bonferroni post hoc, **p<0.05

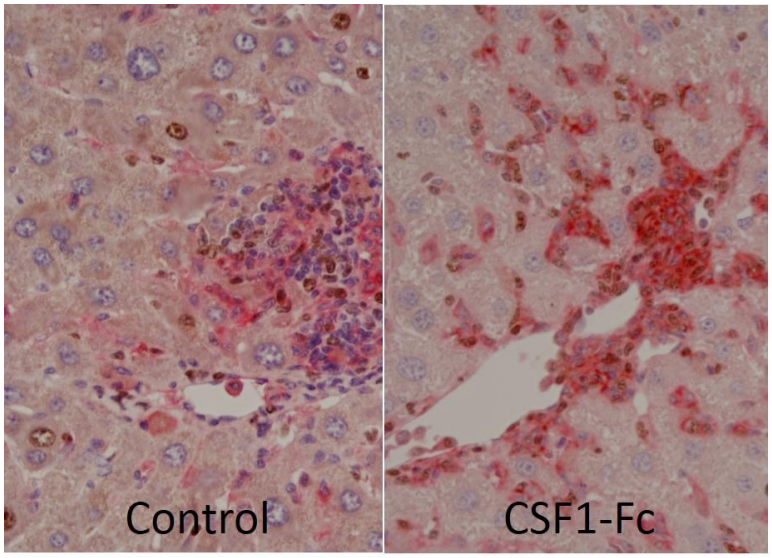


Figure 6.28: Ki67 and F4/80 immunohistochemistry following partial hepatectomy and chronic liver injury with CSF1-Fc or control

Pink= F4/80; brown (DAB) = Ki67

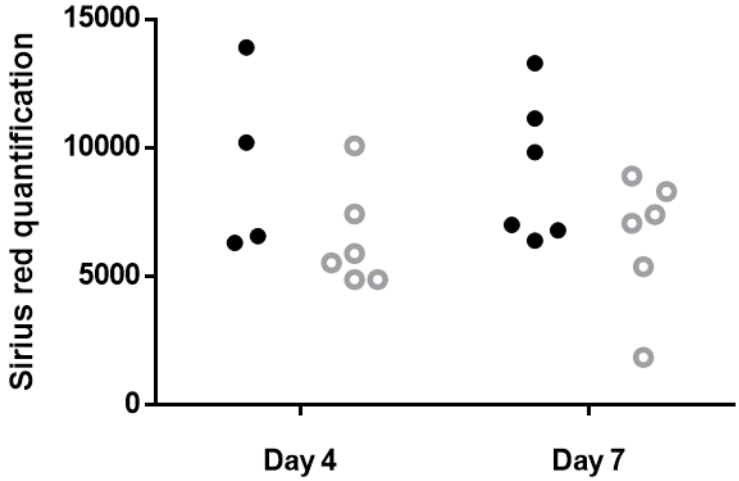


Figure 6.29: Fibrosis quantification via Sirius red image analysis following partial hepatectomy and chronic liver injury with control (solid circles) or CSF1-Fc (hollow circles). (NB. n=1 from day 4 timepoint 0 was not suitable for Sirius red analysis (despite repeated attempts) and so was discarded)2-way ANOVA; p=0.35

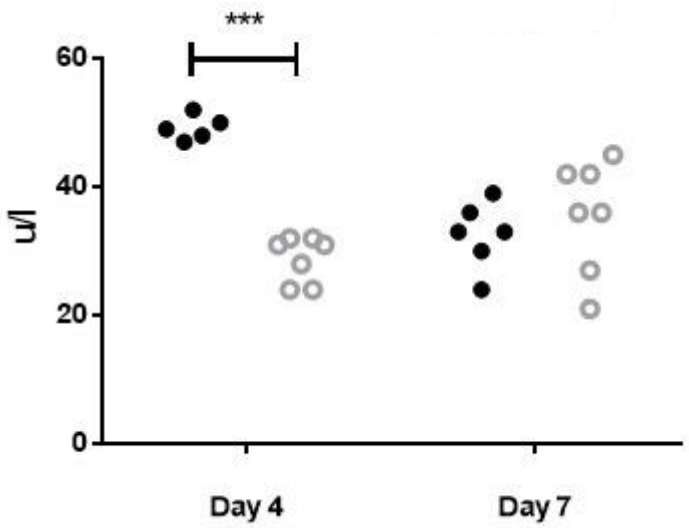


Figure 6.30: Serum ALT following partial hepatectomy and chronic liver injury with control (solid circles) or CSF1-Fc (hollow circles).

2 way ANOVA with Bonferroni post hoc. ***p<0.001

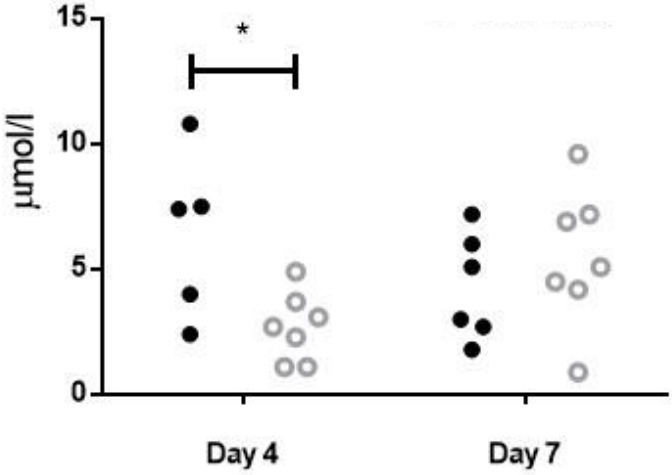


Figure 6.31: Serum bilirubin following partial hepatectomy and chronic liver injury with control (solid circles) or CSF1-Fc (hollow circles).

2 way ANOVA with Bonferroni post hoc. *p<0.05

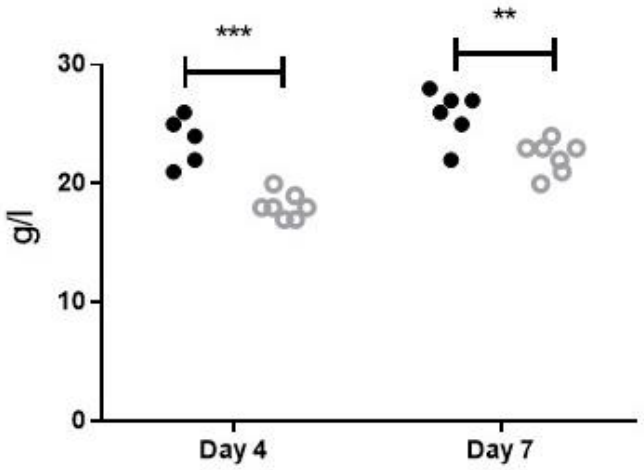


Figure 6.32: Serum albumin following partial hepatectomy and chronic liver injury with control (solid circles) or CSF1-Fc (hollow circles).

2 way ANOVA with Bonferroni post hoc.. ** p<0.01; ***p<0.001

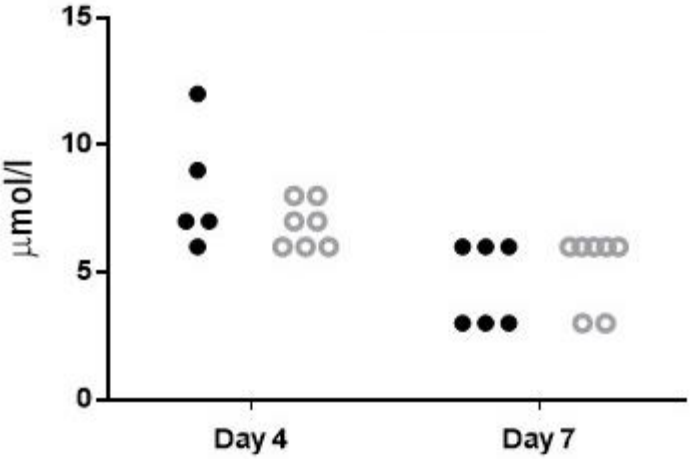


Figure 6.33: Serum creatinine following partial hepatectomy and chronic liver injury control (solid circles) or CSF1-Fc (hollow circles). 2 way ANOVA with Bonferroni post hoc. ns

## Discussion

While survival was not significantly enhanced with CSF1-Fc treatment there was a significant increase in body weight suggestive of improved postoperative course. Liver weight to body weight was increased but as in the partial hepatectomy model (without chronic liver injury) this was not accompanied by a significant increase in hepatocyte proliferation indicating that macrophage accumulation accounted for much of this size increase. I used the ICG clearance assay to provide a dynamic assessment of hepatocyte function. The lack of difference between groups despite the increased liver size further indicates that this increase in liver size is likely to be due to macrophage accumulation. It should also be noted that ICG clearance was not impaired by the macrophage accumulation in this model.

Fibrosis as assessed by Sirius red was reduced by CSF1 therapy. As shown previously ("Figure 3.6: Comparison in fibrosis resolution between mice undergoing partial hepatectomy and mice undergoing sham surgery." p 72) fibrosis remodelling following partial hepatectomy on a background of chronic liver injury is already rapid.

Serum analyses show some differences between control and CSF1-Fc treated groups including a lower bilirubin and ALT at Day 4, although serum albumin is also reduced. (this is discussed in more detail in the following section ("6.6 CSF1 receptor stimulation and Paracetamol toxicity "; p 176)

## Conclusion

CSF1-Fc treatment in this model led to a trend to improved survival, increased body weight and increased liver weight to body weight ratio, likely due to hepatic macrophage accumulation.

# 6.6 CSF1 receptor stimulation and Paracetamol toxicity

## Aims

1. Assess effects of CSF1R stimulation on hepatocyte mediated regeneration following paracetamol intoxication
2. Assess effects of CSF1R stimulation on macrophage phagocytic function following paracetamol intoxication

## Results

### Treatment post injury

I treated male C57/Bl6 mice with CSF1-Fc or PBS control 12 hours following acetaminophen intoxication (n=8 per group). This delayed treatment time point was chosen to enable injury to develop without the effects of CSF1-Fc intervention. Between 12 and 24 hours are recognised as the time of maximal injury[166]. I had thought that delaying treatment further would limit potential effects of the intervention given the rapid regenerative process in mice.

Liver weight to body weight ratio was significantly increased with CSF1-Fc administration (Figure 6.34a) although I found that hepatocyte proliferation was not enhanced at clinically relevant early time points (Figure 6.34b). There was no significant difference in area of necrosis following CSF1-Fc administration (Figure 6.34c). CSF1-Fc treatment resulted in marked hepatic macrophage accumulation at the area of necrosis and this accumulation persisted at later timepoints (Figure 6.35a). Despite profound macrophage changes, serum cytokines were unaffected by CSF1-Fc at Day 4 (Figure

6.35b). Hepatic cytokine profile following CSF1R stimulation and inhibition is shown in Figure 6.36.

This macrophage expansion was paralleled by a reduction in serum injury markers, with a reciprocal increase following CSF1R blockade (Figure 6.37). Serum albumin level was reduced with CSF1-Fc treatment (Figure 6.37) although hepatic albumin gene expression was not reduced by CSF1-Fc treatment (Figure 6.38).

Hepatic phagocytic genes MARCO and MSR1 were elevated with CSF1-Fc administration with a reciprocal decrease following CSF1R inhibition (Figure 6.39). Clearance of microbeads from the circulation remained effective in both groups likely due to the much reduced liver loss compared to PH (Figure 6.40a). Overall liver fluorescence increased following microbead injection with CSF1-Fc treatment (Figure 6.40a).

I found that CSF1-Fc increased blood monocyte count following paracetamol intoxication, with continued CSF1R stimulation increasing both Ly6C-high and Ly6C-low populations (Figure 6.41a and Figure 6.41b; gating strategy: Appendix 3, p233). Prolonged stimulation also increased neutrophil count but T cell, B cell and eosinophils were unchanged (Figure 6.42).

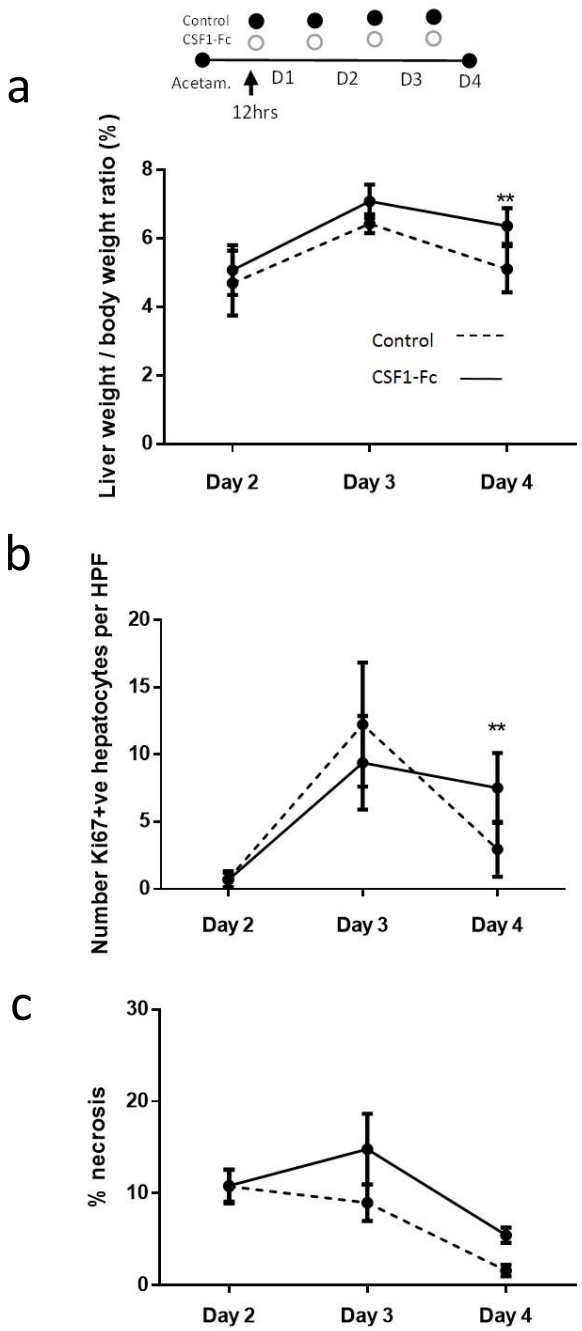


Figure 6.34: Regenerative parameters following paracetamol intoxication and CSF1-Fc

a) Liver weight to body weight ratio with CSF1-Fc or control (2 way ANOVA with Bonferroni post-test). b) Quantification of Ki67 positive hepatocytes at days 2, 3 and 4 following acetaminophen intoxication (one way ANOVA with Bonferroni post hoc). c) Quantification of area of necrosis and cellular infiltrate at Day 2, 3 and 4 following acetaminophen intoxication (see Figure 3.12: Quantification of necrotic area, p83).

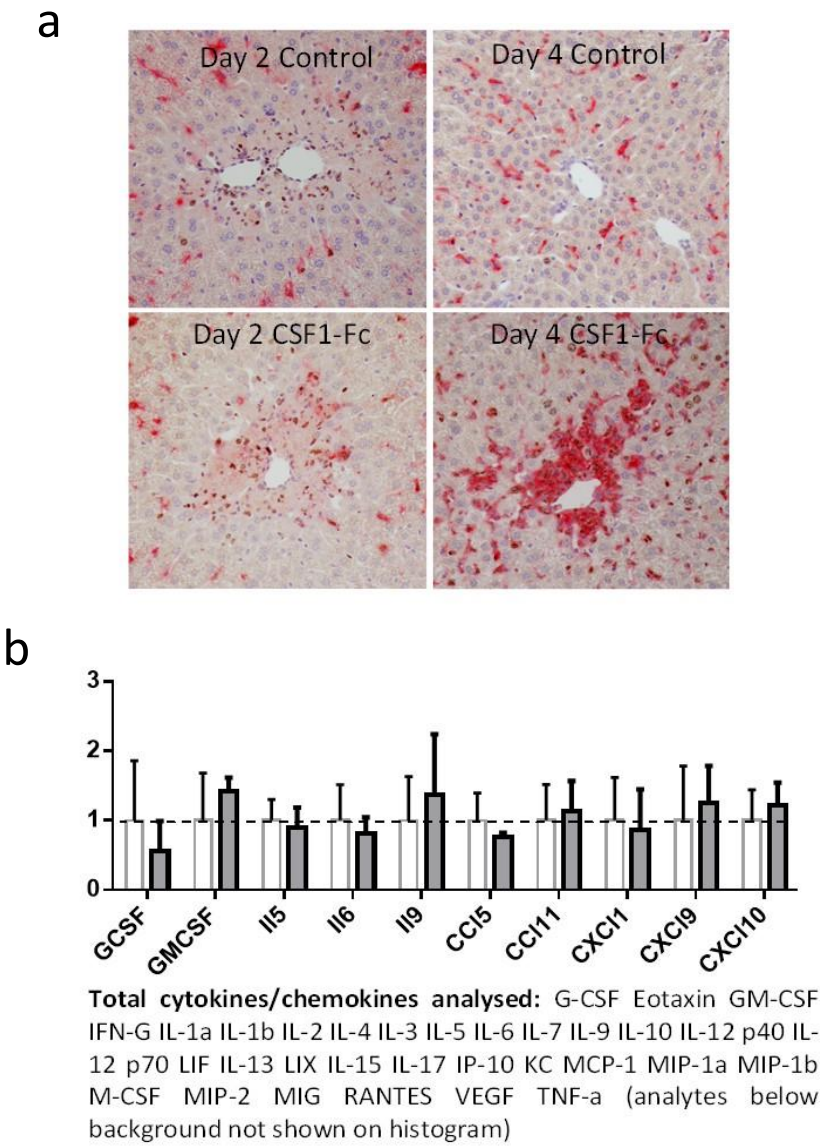


Figure 6.35: Effects of CSF1-Fc on regeneration following paracetamol intoxication

a) Representative immunohistochemistry F4/80 (red) and Ki67 (DAB) at Day 2 and Day 4 following acetaminophen with PBS control or CSF1-Fc. b) Serum cytokine array Day 4 following partial hepatectomy and either PBS control (white bar) or CSF1-Fc treatment (grey bar) (2-way ANOVA and Bonferroni post hoc ns).

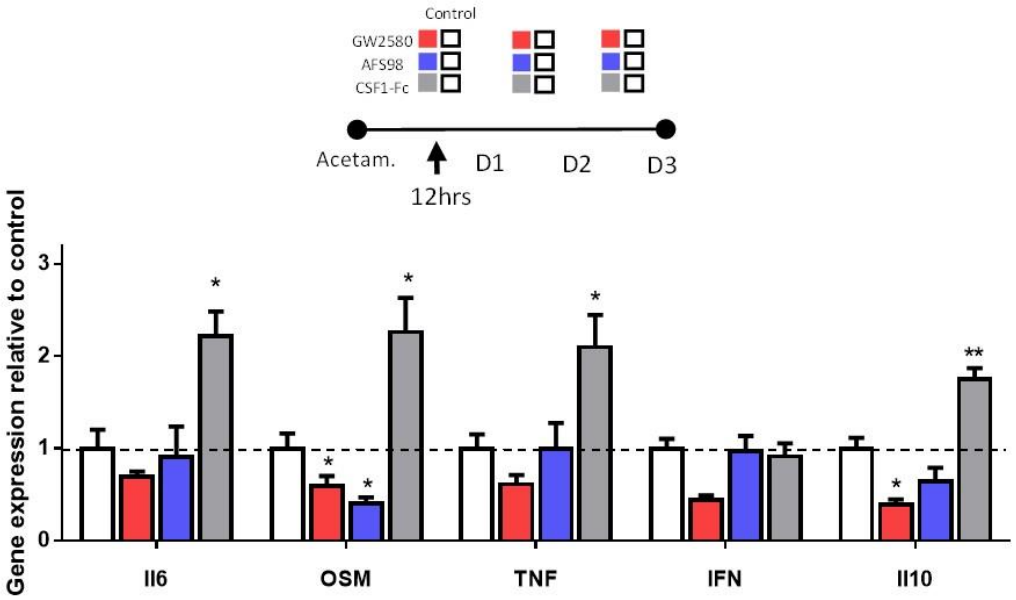


Figure 6.36: Hepatic cytokine expression

Hepatic gene cytokine expression at Day 3 following paracetamol intoxication and either GW2580, AFS98 or CSF1-Fc administration versus control (vehicle gavage, rat IgG2a, PBS; n=8/group; 2-way ANOVA comparing intervention with relevant control, Bonferroni post hoc).

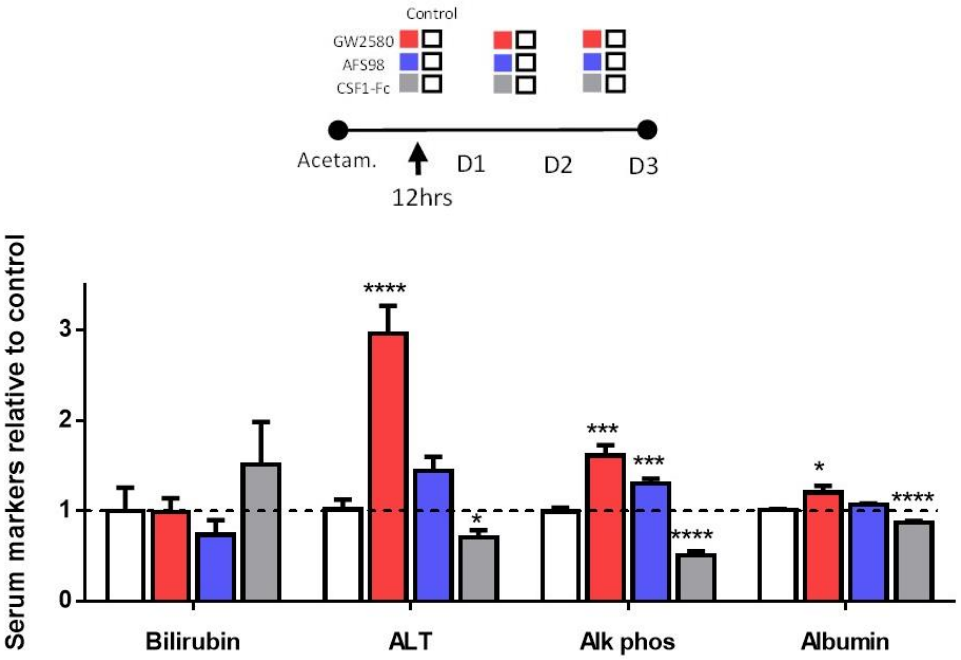


Figure 6.37: Serum biochemistry following CSF1R blockade or stimulation

Serum liver associated biochemistry tests relative to mean of control group at day 3 following acetaminophen intoxication and either GW2580 (red), AFS98 (blue) or CSF1-Fc (grey) compared to control (vehicle, rat IgG2a, PBS respectively; 2-way ANOVA with Bonferroni post-test).

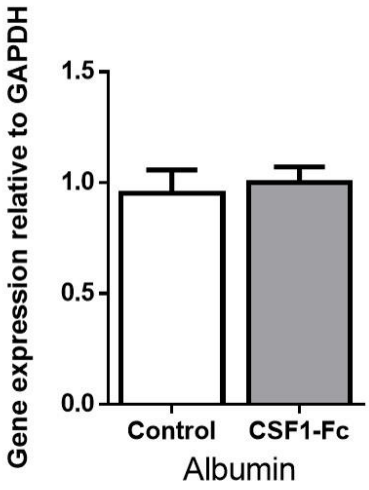


Figure 6.38: Hepatic albumin gene expression

Whole liver, n=8/group

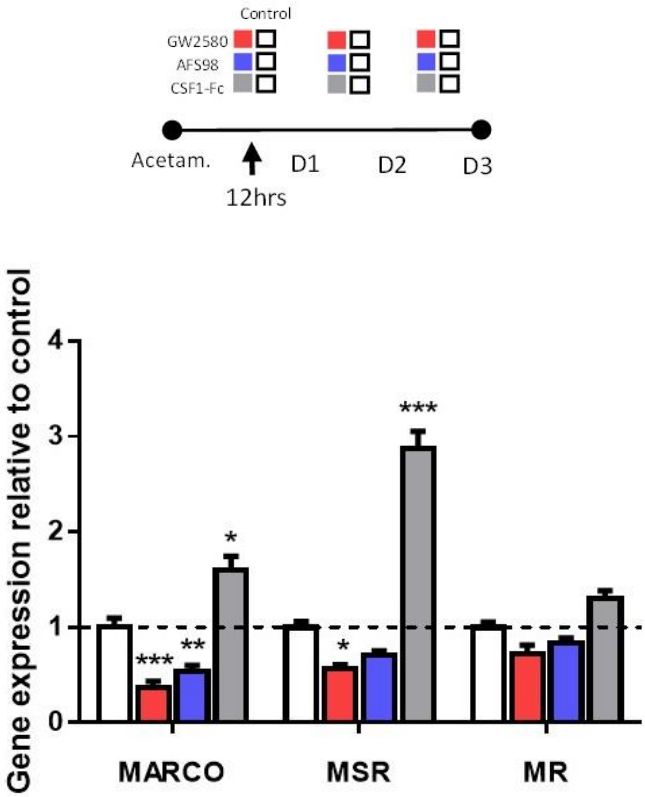


Figure 6.39: Hepatic phagocytosis related gene expression

Hepatic phagocytic related gene expression at Day 3 following paracetamol intoxication and either GW2580, AFS98 or CSF1-Fc administration versus control (vehicle gavage, rat IgG2a, PBS; n=8/group; 2-way ANOVA comparing intervention with relevant control, Bonferroni post hoc).

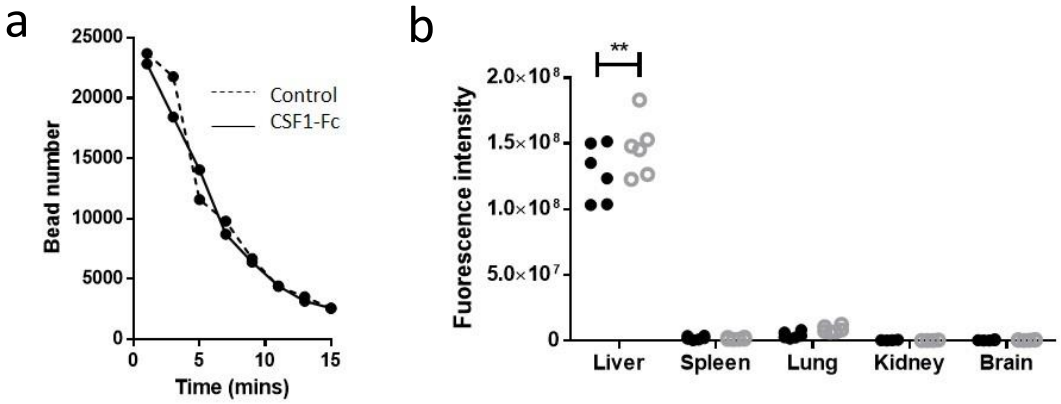


Figure 6.40: Phagocytosis assay

a) Bead clearance at Day 2 following acetaminophen intoxication with PBS control or CSF1-Fc. b) Net ex vivo liver fluorescence 15 minutes following injection of fluorescent beads at Day 2 following acetaminophen intoxication with PBS control (solid circle) or CSF1-Fc (hollow circle) (2-way ANOVA with Bonferroni post-test).

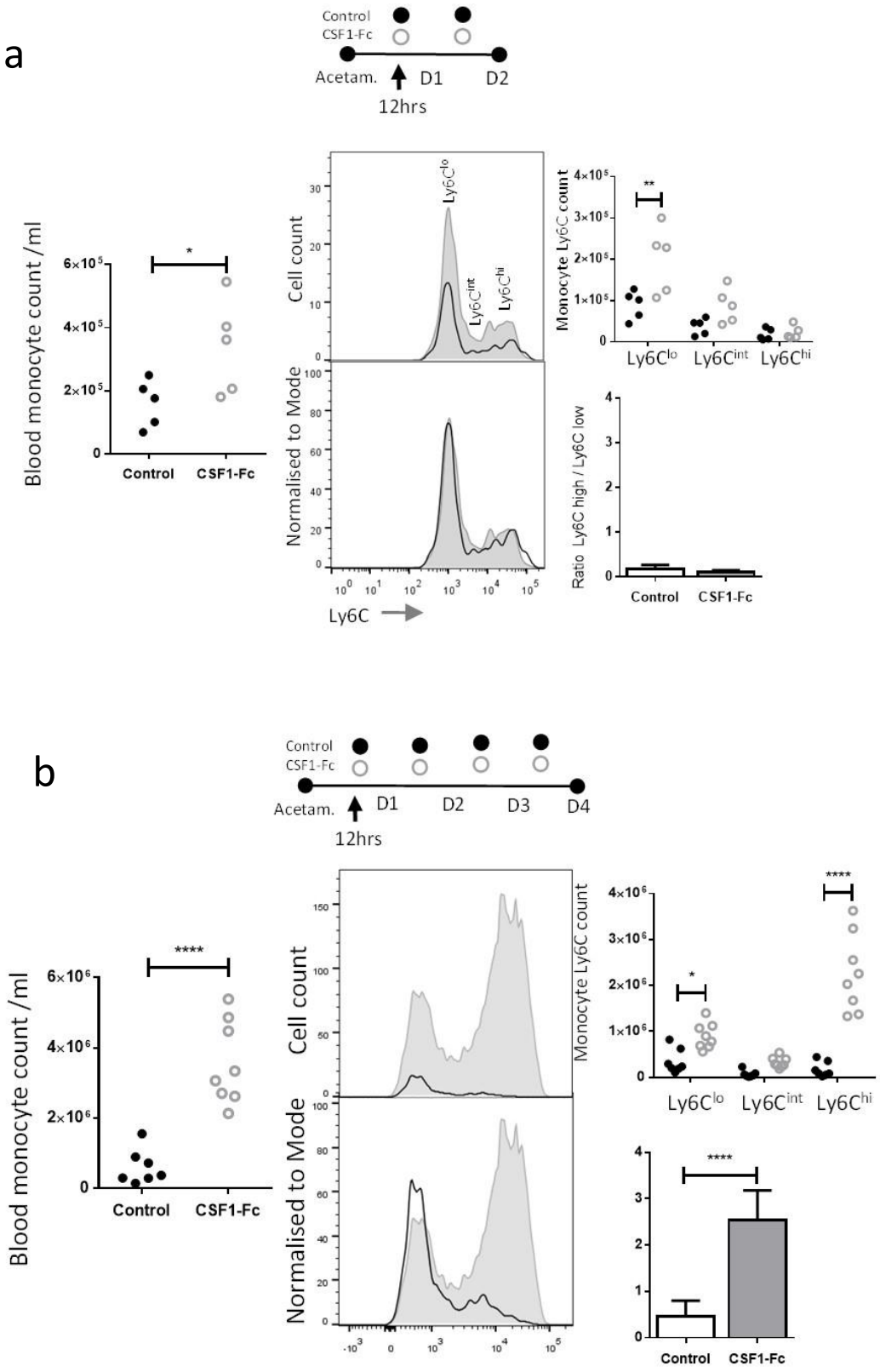


Figure 6.41: Blood monocyte profile following CSF1-Fc administration

a) Blood monocyte count (Student *t* test, *p<0.05) and Ly6C profile (2 way ANOVA with Bonferroni post test) day 2 following acetaminophen intoxication and CSF1-Fc or control (gating strategy Supplementary Fig. 7a). b) Blood monocyte count (*t* test) and Ly6C profile (2 way ANOVA with Bonferroni post-test) day 4 following paracetamol intoxication and CSF1-Fc or control.

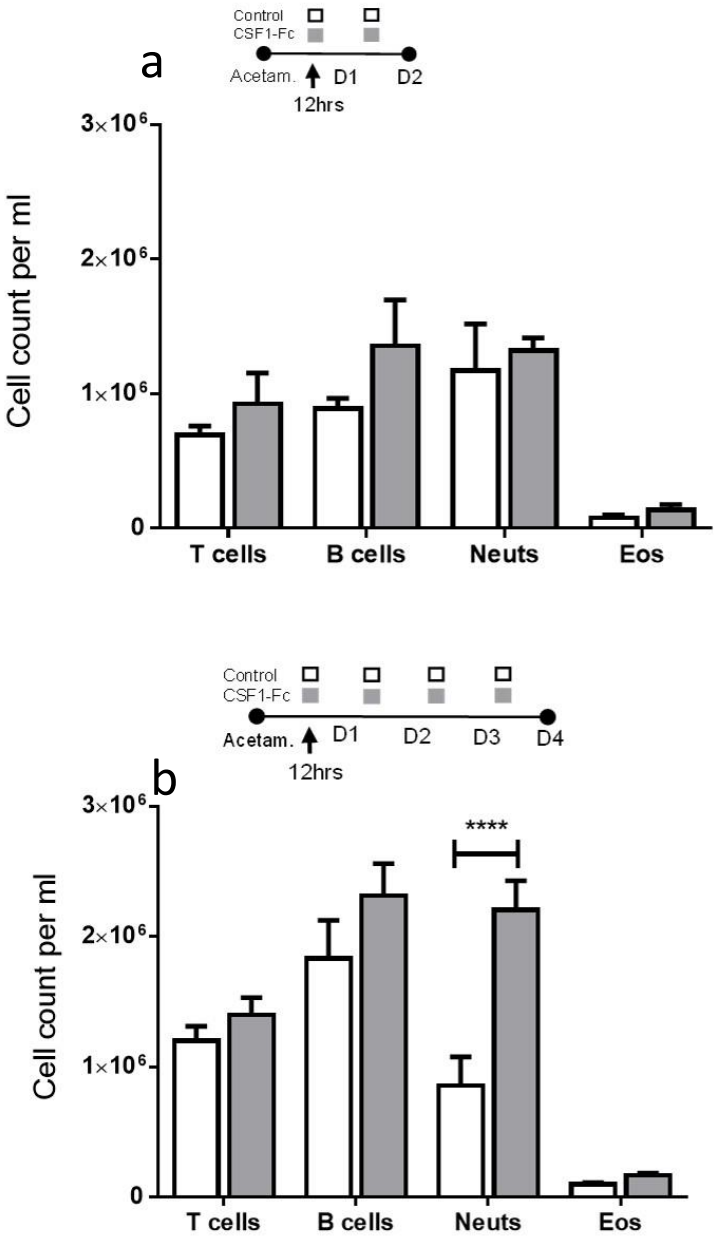


Figure 6.42: Blood cellular populations following paracetamol intoxication

Quantification of T cells, B cells, neutrophils and eosinophils Day 2 (a) and 4 (b) following acetaminophen intoxication with PBS control or CSF1-Fc.

## Discussion

The effects seen in the PH model with enhanced phagocytosis prompted me to investigate the effects of CSF1-induced macrophage expansion in a mouse model of paracetamol intoxication where liver tissue loss is characterised by hepatocyte death through both necrotic and apoptotic mechanisms[48].

Mice do not develop the same protracted clinical deterioration as humans and at high paracetamol doses death in mice is rapid, limiting study of the regenerative process[168]. I therefore used a mouse model leading to marked injury but not associated with death so enabling study of regeneration and resolution. CSF1R stimulation or inhibition was commenced at 12 hours after injury to limit effects on the injurious process.

Liver size increased with CSF1-Fc treatment and in the absence of increased hepatocyte proliferation this likely relates to enhanced macrophage accumulation. Extent of tissue loss by necrosis was much less than 2/3PH and microbead clearance from the circulation remained effective. Nevertheless, overall liver fluorescence was increased by CSF1-Fc consistent with increase in phagocytosis associated genes. In the clinical setting a marked impairment in microbead clearance occurs, consistent with degree of injury[77]. A higher dose of paracetamol would have led to a greater extent of liver injury in this mouse model but this is associated with high mortality (up to 50%[168]), which was not feasible given Home Office Animal Welfare restrictions.

Following prolonged CSF1-Fc administration (4days), macrophages continued to accumulate in the area of previous necrosis whereas in control mice macrophage accumulation reduced in line with a fall in hepatic CSF1 gene expression. It is evident

that hepatic CSF1 production drives macrophage accumulation during the early post injury phase when phagocytosis is essential to clear dying hepatocytes.

Treatment with CSF1-Fc reduced traditional injury markers, with a reciprocal increase following CSF1R blockade. Since CSF1-Fc was administered after peak injury this likely indicates enhanced macrophage related clearance of these enzymes[198]. Serum albumin level was reduced following 4 days of CSF1-Fc treatment. This is likely a reflection of the pro-inflammatory state given hepatic albumin gene expression was unchanged from control. Despite profound changes in macrophage trafficking serum cytokines were unaffected by CSF1-Fc, indicating that the context rather than simply the presence of macrophages drives systemic inflammatory cytokine expression.

CSF1-Fc increased blood monocyte count, with continued CSF1R stimulation increasing both Ly6C-high and Ly6C-low populations. As is well documented in the literature CSF1 administration boosted blood monocyte levels, but also increased neutrophil count at the later time point (Day 4). This is consistent with reports of CSF1 responsive granulocyte progenitors within bone marrow[213].

## Conclusion

CSF1-Fc administration enhances hepatic macrophage accumulation and markers of phagocytosis following paracetamol intoxication in mice.

# Chapter 7. Serum macrophage colony stimulating factor in humans following liver injury

## 7.1 Partial hepatectomy in humans

### Aims

1. Identify cohort of patients where serum has been collected prior to and following partial hepatectomy
2. Assess serum CSF1 level in these patients

### Results

Relating these findings to the clinical setting I assessed serum CSF1 level in patients undergoing PH. Following ethical approval I collaborated with a surgical colleague (M. Hughes, Surgical Registrar, Royal Infirmary of Edinburgh) who was collecting serum samples from patients prior to and at days 1 and 3 following partial hepatectomy[xxiv]. Figure 7.1 details the characteristics of this group. Two patients developed postoperative liver failure and their details are provided in Figure 7.2. Healthy control data was provided by D. Antoine, University of Liverpool (Appendix 4, p234).

I trialled several methods of serum CSF1 assessment including ELISA and cytometric bead array technology however these attempts were unsuccessful. Serum CSF1 level is

[xxiv] Samples were collected by M. Hughes (a collaborator) and I amended and submitted the ethical documentation to enable CSF1 analysis on these samples

apparently notoriously difficult to analyse. I then collaborated with D. Antoine (Principal Investigator, Centre for Translational Medicine, Liverpool) who has extensive experience of biomarker usage and development. D. Antoine analysed the samples using the Mesoscale Discovery platform[xxv] blinded to patient and time point and then sent results back to me for analysis. This was successful.

I found that preoperative serum CSF1 in this patient cohort was higher than healthy volunteers (Figure 7.3a). Initial reduction in serum CSF1 following partial hepatectomy was followed by a marked increase at postoperative Day 3 (Figure 7.3a). The two patients who developed postoperative liver failure (Figure 7.2) had serum CSF1 levels below the 25$^{th}$ percentile (Figure 7.3c).

Although more extensive resection may increase blood loss there was no correlation between serum CSF1 and blood loss at either time point (Figure 7.4a and Figure 7.4b). Monocyte count increased proportionate to extent of resection, although there was no direct correlation between monocyte count and serum CSF1 level (Figure 7.6).

Given the increase in serum CSF1 level we looked to assess hepatic CSF1 gene expression during regeneration. Liver biopsy following PH in humans carries significant clinical risk so we therefore analysed mouse liver following PH. CSF1 gene expression in total liver in mice did not increase following PH (Figure 7.7).

[xxv] This platform uses electrochemiluminescence detection to detect binding events on patterned arrays

| Extent resection | n | Mean age (SD) | M:F | BMI (SD) | ASA | Diagnosis | Post op hepatic failure | Blood loss Mean (SD) | Mortality |
|---|---|---|---|---|---|---|---|---|---|
| >5 segments | 10 | 60.6 (16.2) | 5:5 | 27.7 (3.9) | 2 | CLM (6) Carcin (1) HCC (2) Cholangio (1) | 1 | 1915 (1543) | 0/10 |
| 3-5 segments | 28 | 61.5 (10.4) | 14:14 | 27.4 (5.7) | 2 | CLM (22) Cyst (3) Carcin. (2) Abscess (1) | 1 | 1063 (1425) | 0/28 |
| <3 segments | 17 | 63.9 (10.3) | 17:3 | 29.9 (5.2) | 2 | CLM (10) HCC (4) Haemang. (2) Mets ?prim (1) | 0 | 1011 (777) | 0/17 |
| *Overall* | *55* | *62.1* | *18:11* | *28.3* | *2* | *CLM (38) Carcin. (3) HCC (6) Haemang. (2) Cholangio (1) Abscess (1) Mets ?prim (1)* | *2* | *1202 (1294)* | *0/55* |

Figure 7.1: Details of patients undergoing partial hepatectomy categorised according to extent of resection

| | Age | Sex | BMI | ASA | Diagnosis | Extent of resection | Blood loss (mls) | Post op hepatic failure | Outcome |
|---|---|---|---|---|---|---|---|---|---|
| 1 | 65 | F | 30.5 | 2 | Carcinoid | 6 segments (1,4,5,6,7,8) | 2500 | Bilirubin >54 and hepatic encephalopathy (grade 3) | Improved with supportive care |
| 2 | 63 | M | 29 | 2 | Colorectal liver metastasis | 4 segments (5,6,7,8) | 500 | Bilirubin >54, ascites and hepatic encephalopathy (grade 1) | Improved with supportive care |

Figure 7.2: Details of patients developing postoperative liver failure (n=2)

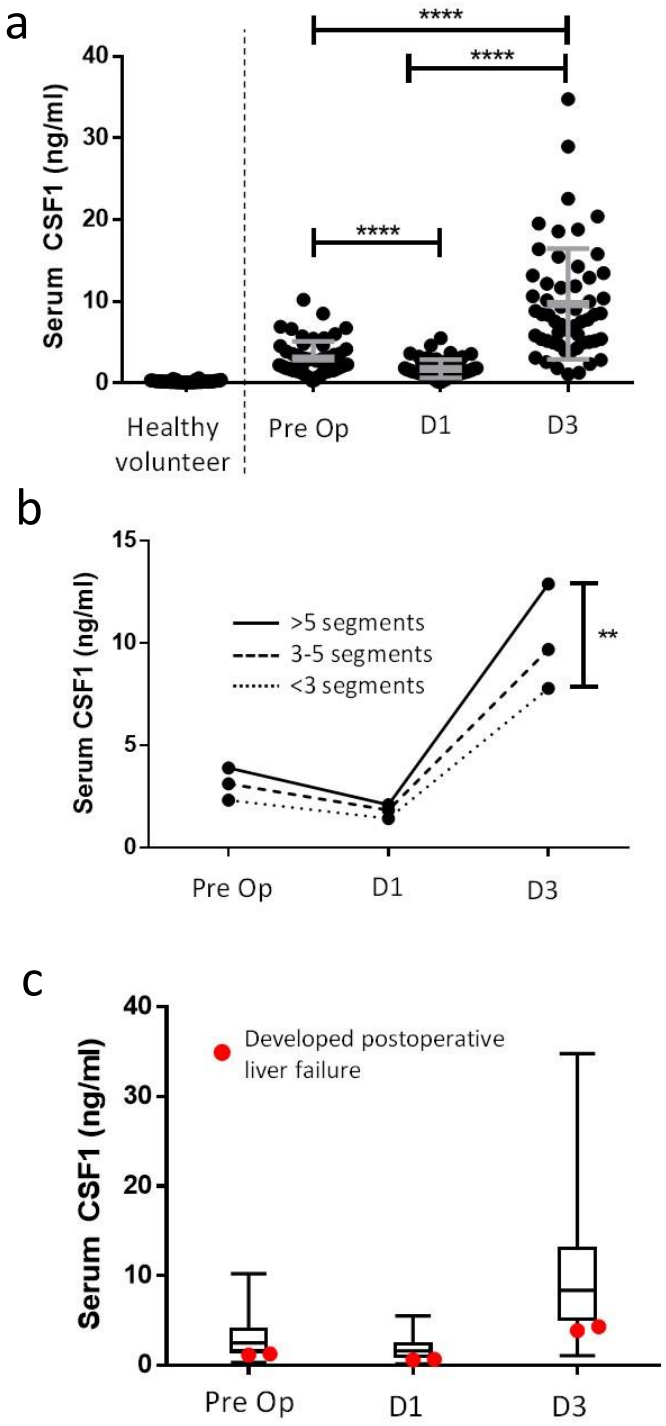


Figure 7.3: Serum CSF1 increases following partial hepatectomy in humans proportional to extent of resection.

a) Serum CSF1 in healthy volunteers and patients undergoing partial hepatectomy to remove cancer at preoperative, Day 1 postoperative and Day 3 postoperative time points

(One-way repeated measures ANOVA with Bonferroni post hoc). b) Mean serum CSF1 categorised according to extent of resection (<3 liver segments, 3-5 liver segments and >5 liver segments resected; Two-way RM ANOVA with Tukey's post hoc). c) Box and whisker plots showing minimum to maximum values per time point with patients developing postoperative liver failure overlaid with red dots. *p<0.05, **p<0.01, ***p<0.001, ****p<0.0001.

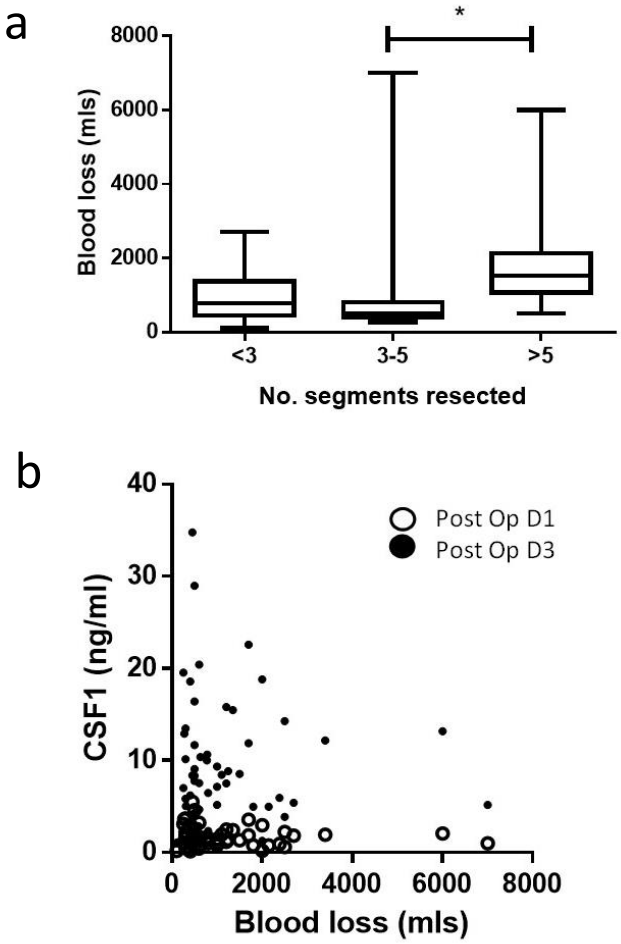


Figure 7.4: Serum CSF1 level versus blood loss

a) Blood loss according to extent of resection. b) Dot plot showing blood loss versus serum CSF1 (no relationship between these variables).

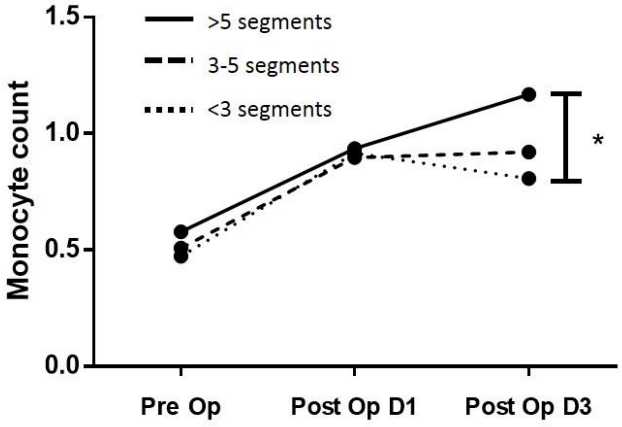


Figure 7.5: Blood monocytes following partial hepatectomy.

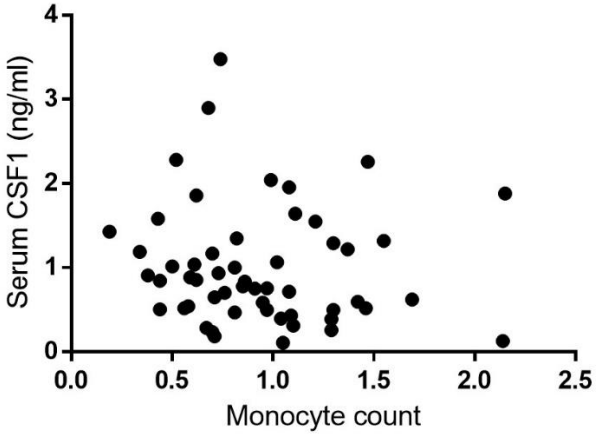


Figure 7.6: Correlation between serum CSF1 and monocyte count on Day 3 post op.

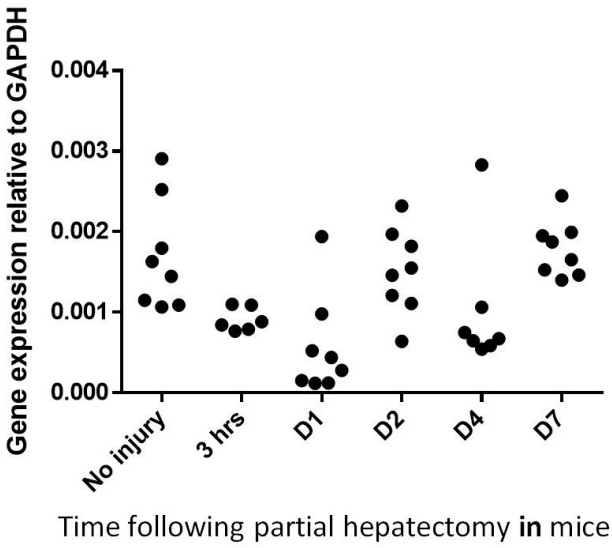


Figure 7.7: Hepatic CSF1 gene expression following partial hepatectomy in mice.

## Discussion

In humans, I found a marked increase in CSF1 level following PH, proportionate with the extent of resection. It has previously been reported that hepatic macrophages are the main clearance source of CSF1 from the circulation[84]. I therefore considered whether this postoperative rise related to extent of resection was either due to reduced clearance of serum CSF1 given the smaller liver remnant or whether the liver remnant was producing a greater quantity of CSF1 following surgery. I considered whether obtaining liver biopsies following surgery in humans would be appropriate. However, given the high risks associated with liver biopsy this would not be ethical in the postoperative period. I therefore analysed hepatic CSF1 gene expression in mice following partial hepatectomy. I found that hepatic CSF1 gene expression was not increased in mice following PH, indicating that the rise in serum CSF1 likely relates to reduced CSF1 clearance capacity.

In my analysis two patients with low serum CSF1 levels developed postoperative liver failure. Recent work in living liver donors undergoing PH showed that a higher serum CSF1 level was associated with more rapid liver regrowth[126]. Together, this could suggest a potential role for supplementary CSF1 to enhance liver regeneration in humans but the numbers in my study are too low to draw clear conclusions.

In my series the serum CSF1 level was higher preoperatively than normal controls, and actually reduced Day 1 following surgery. This is consistent with the production of CSF1 by the malignant process. The majority of these patients were undergoing surgery for metastatic colorectal cancer. The production of CSF1 has been linked with aggressiveness of cancers, metastasis and poor outcome[214,215]. Indeed the link between CSF1 and tumour growth has led to work inhibiting this pathway[215]. Following this patient cohort up so as to identify those patients whose cancer recurs may enable

prediction of those patients with particularly aggressive cancer that are at high risk of subsequently recurring. If this was the case, a patient group could be targeted for subsequent chemotherapy.

Although blood monocyte count rise follows a similar pattern at Day 3 following partial hepatectomy as that of serum CSF1, the lack of association between these two variables likely reflects the multifactorial nature of inflammatory response stimuli.

In the mouse model CSF1-Fc was administered following PH when the cancer in humans would have been resected. While theoretically the patient may be cancer free, up to 50% of patients may recur within 2 years[216]. Therefore it is crucial that any potential effects of CSF1 therapy on recurrence are thoroughly explored. Routine use of a CSF1 based therapy following partial hepatectomy might seem inappropriate. However perhaps in the context of a patient with low serum CSF1 level and a failing liver postoperatively, a CSF1 based therapy could have a therapeutic role, by boosting hepatic macrophage accumulation, facilitating regeneration and phagocytic capacity.

## Conclusion

Serum CSF1 is raised in patients prior to partial hepatectomy to remove liver cancer. Following an initial reduction, CSF1 level rebounds most likely related to reduced CSF1 clearance by the liver.

# 7.2 Paracetamol intoxication in humans

## Aims

1. Identify cohort of patients where serum has been collected following paracetamol intoxication
2. Assess serum CSF1 level in these patients

I collaborated with K. Simpson (Senior lecturer, Liver Transplantation, University of Edinburgh) who has an established collaboration with D. Antoine (Principal Investigator, Centre for Translational Medicine, University of Liverpool). Together they have established a series of 84 patients who presented to a specialist liver centre with acute liver failure induced by paracetamol intoxication. This cohort has been well characterised and previous work assessing markers of injury has been published on this series[97]. A second group of patients where serum samples were collected from first presentation to hospital was also analysed.

D. Antoine analysed the samples using the Mesoscale Discovery platform[xxvi] blinded to patient and time point and then sent results back to me for analysis.

[xxvi] This platform uses electrochemiluminescence detection to detect binding events on patterned arrays

## Results

Patient cohort characteristics are shown in Figure 7.8 and Figure 7.9. Serum CSF1 level was significantly elevated in survivors compared with patients who subsequently died or required liver transplantation (Figure 7.10a). The receiver operator characteristic curve indicates biomarker potential, with area under the curve of 0.84 (Figure 7.10b). Serial samples in a further cohort of patients (patient characteristics in Figure 7.9), this time from first presentation to hospital, showed serum CSF1 level continued to increase after presentation in survivors (Figure 7.10c). Due to the prohibitive risks of liver biopsy hepatic CSF1 gene expression was assessed in mice, revealing increased expression following acetaminophen intoxication, peaking at Day 2 (Figure 7.11).

Given previously published work demonstrating the prognostic value of the injury marker acetyl-HMGB1[97], I considered whether combining CSF1 and acetyl-HMGB1 could enhance prognostic ability using logistic regression analysis. For this section I collaborated with B. Francis (Statistician, Centre for Translational Medicine, University of Liverpool). B. Francis undertook the logistic regression analysis using the software package R[169].

Analysis of acetyl-HMGB1 levels from serial samples from admission to hospital showed a marked increase in patients who subsequently died or required liver transplantation (Figure 7.12a). We then reviewed the patient cohort from admission to the specialist liver unit again. Many acetyl-HMGB1 values in this cohort were close to zero so a log transformation was performed (Appendix 5). A high inverse correlation existed between serum acetyl-HMGB1 and serum CSF1, with a similar relationship shown in both the survivors of acute liver failure and those who died or subsequently required liver transplantation (Figure 7.12b).

When combined in a logistic regression model, only CSF1 showed significance (Figure 7.14a; Details of the logistic regression modelling are provided in Appendix 6 (p236), Appendix 7 (p236), Appendix 8 (p236)). Analysis of deviance showed no significant difference between the combined model and CSF1 alone indicating that the addition of acetyl-HMGB1 did not further enhance the model (Figure 7.14b). This can be visually represented by receiver operator characteristic curves (Figure 7.13c). Figure 7.14 provides example CSF1 values with risk of death based on the 'CSF1 alone' logistic regression model.

| Outcome | n | Age | M:F | ALT (U/L) | PT (Sec) | Creatinine (µmol/L) | Acetyl-HMGB1 (ng/ml) | **CSF1 (ng/ml)** |
|---|---|---|---|---|---|---|---|---|
| Survived | 47 | 37 (13) | 21:26 | 4412 (3764) | 38.7 (30.0) | 129.8 (120.1) | 0.46 (1.52) | 7.81 (2.82) |
| Died/Liver transplantation | 31 | 42 (15) | 10:21 | 4814 (3060) | 70.0 (38.8) | 213.8 (112.8) | 4.49 (5.70) | 3.69 (2.49) |

Figure 7.8: Details of acetaminophen intoxication patients presenting to the specialist liver unit with acute liver failure grouped according to survivors versus those who subsequently required liver transplantation or died.

Patient cohort and acetyl-HMGB1 values as per Antoine et al.[24]

| Outcome | n | Age | M:F | ALT (U/L) | Bilirubin (mg/dl) | Acetyl-HMGB1 (ng/ml) | **CSF1 (ng/ml)** |
|---|---|---|---|---|---|---|---|
| Survived | 10 | 39 (9) | 2:3 | 1370 (1104) | 3.1 (1.8) | 0.33 (0.29) | 1.84 (1.33) |
| Died/Liver transplantation | 10 | 41 (14) | 2:3 | 3873 (1902) | 3.5 (1.9) | 2.06 (2.59) | 1.25 (1.08) |

Figure 7.9: Details of patients from first presentation to hospital following acetaminophen intoxication

n=10 per group; patients randomly selected from patient cohort as per Antoine et al.[24]

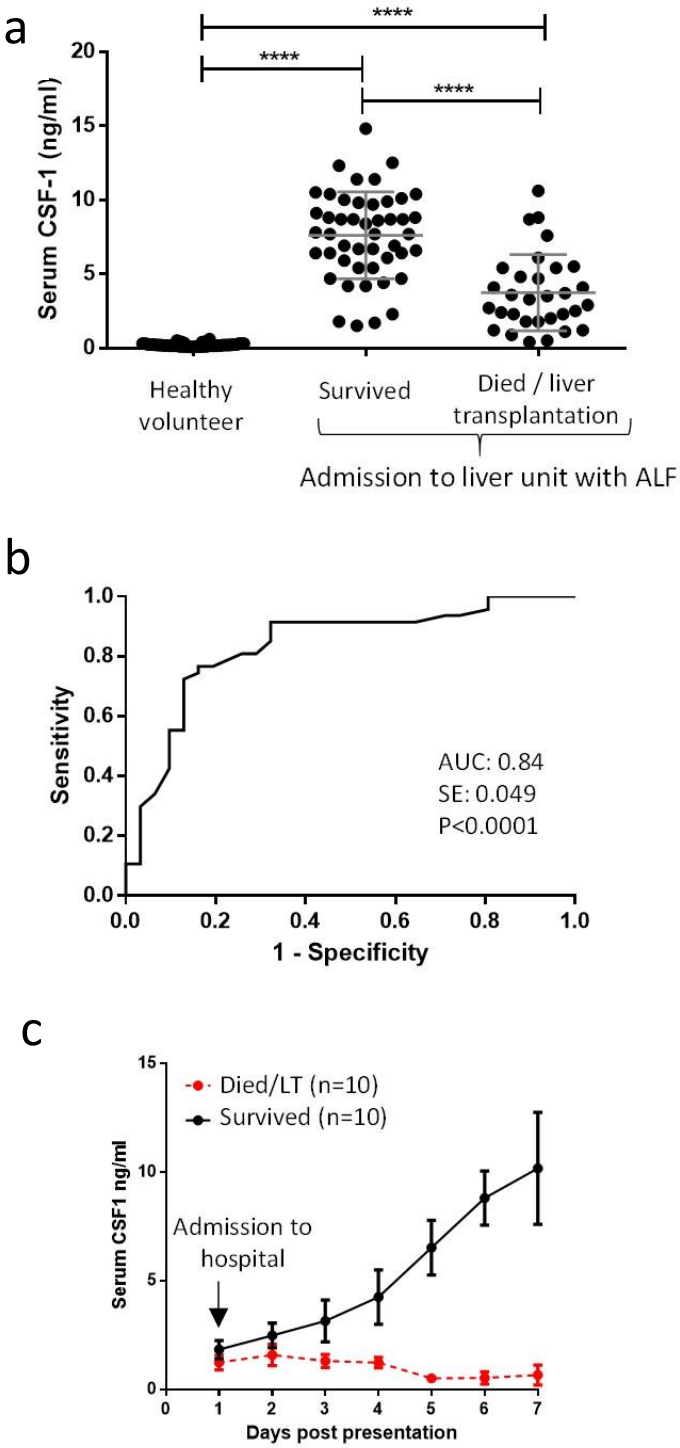


Figure 7.10: Serum CSF1 level is associated with survival in acute liver failure in humans. a) Serum CSF1 level in healthy volunteers and in patients following paracetamol intoxication on arrival to a specialist liver unit grouped according to outcome (mean and standard deviation; survived n=47; Died/Liver transplantation n=37; One way ANOVA,

Bonferroni post-hoc). b) Receiver operator characteristic based on serum CSF1 level in patients who subsequently survived or died/required liver transplantation corresponding to cohort shown in (a). c) Serial CSF1 samples of patients on first presentation to hospital following acetaminophen intoxication categorised into survived or died/required liver transplantation (n=10/group). *p<0.05, **p<0.01, ***p<0.001, ****p<0.0001.

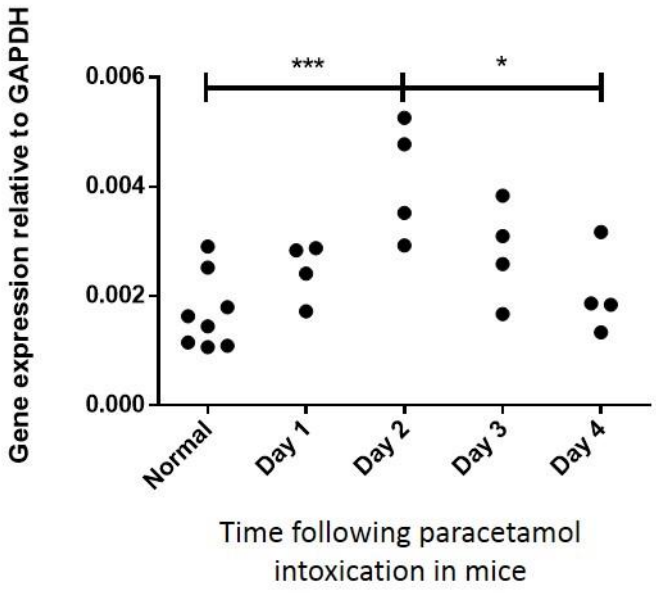


Figure 7.11: Hepatic CSF1 gene expression in mice following paracetamol intoxication at time points including normal (uninjured mice, (n=8)), Day 1 (n=4), Day 2, (n=4), Day 3 (n=4) and Day 4 (n=4)

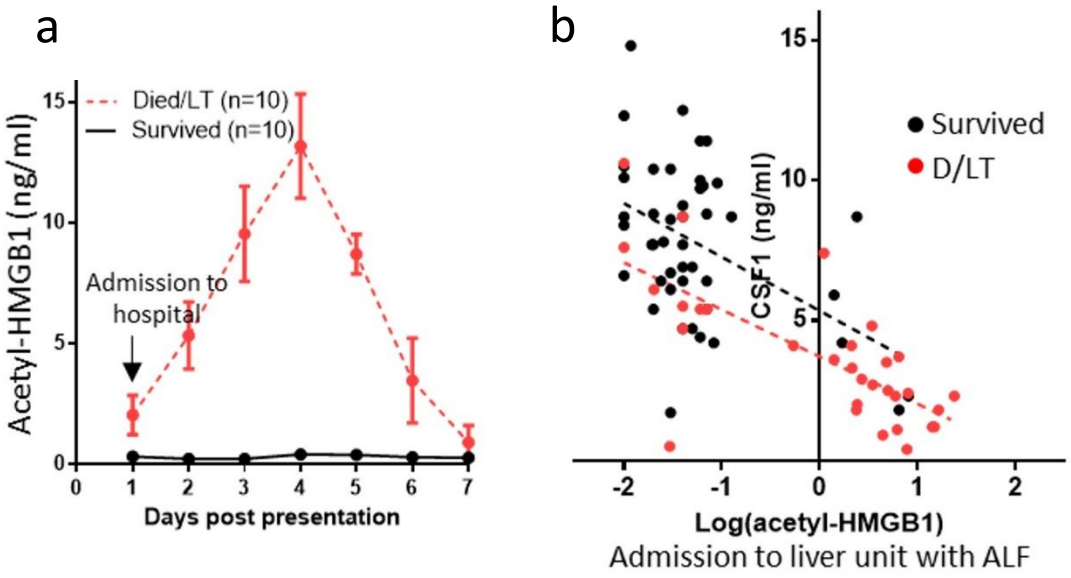


Figure 7.12: Serum CSF1 versus acetyl-HMGB1

a) Serial acetyl-HMGB1 samples of patients first presenting to hospital following acetaminophen intoxication categorised into survived or died/required liver transplantation (n=10/group). b) Dot plots of serum CSF1 level versus log(serum acetyl-HMGB1) on presentation to the specialist liver centre (survived= black; died/required liver transplantation=red) with line of best fit (survived: $r^2$ 0.22, p=0.0008; Died/liver transplantation: $r^2$ 0.52, p<0.0001; slope difference: F=0.15, p=0.70; Intercept difference: F=8.03, p=0.006).

a

**Components of combined logistic regression model**

| | Estimate | Std Error | Z value | p | False +ve rate | False -ve rate |
|---|---|---|---|---|---|---|
| **(Intercept)** | 2.6536 | 0.7047 | 3.765 | <0.0001 | | |
| **Log(acetyl -HMGB1)** | 0.3092 | 0.1671 | 1.851 | 0.06420 | 0.1064 | 0.7097 |
| **CSF1** | -0.3642 | 0.1427 | -2.552 | 0.01072 | 0.1702 | 0.7419 |

b

**Analysis of Deviance**

| | | Degrees freedom | Residual deviance | p |
|---|---|---|---|---|
| **Model 1** | Log(acetyl HMGB1) + CSF1 | 75 | 67.299 | 0.0657 |
| **Model 2** | CSF alone | 76 | 70.687 | |

c

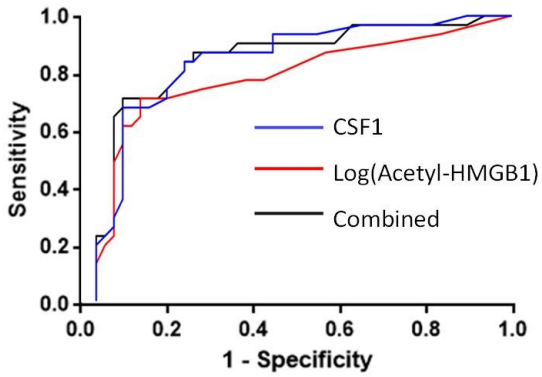


Figure 7.13: Details of the combined logistic regression model involving Log(serum acetyl-HMGB1) + serum CSF1. b) Analysis of deviance comparing combined Log(acetyl-HMGB1) + CSF1 model (Model 1) and CSF1 alone (Model 2). c) Receiver operator characteristic curves for CSF1 alone model, log(acetyl-HMGB1) and combined (CSF1+acetyl-HMGB1) models.

**Logistic regression model for CSF1**

| CSF1 value | Logit(p) | Chance of death |
|---|---|---|
| 1 | 2.11 | 89% |
| 5 | -0.05 | 49% |
| 10 | -2.75 | 6% |

Logit(p)=intercept coeffic.-CSF1 coeffic. x (CSF1 value)
P=exp(logit(p)/(1+exp(logit(p)))

Figure 7.14: Logistic regression model

a) Example serum values and predicted chance of death based on logistic regression involving CSF1 alone (Model 2).

I then sought to examine the serum level levels of the other main regulator of macrophage phenotype, GMCSF. As discussed in "Regulation of cells of the monocyte macrophage lineage", (p43), GMCSF can influence macrophage phenotype to generate a more pro inflammatory cell and in the presence of lipopolysaccharide (found in the outer membrane of gram negative bacteria) GMCSF predominance can lead to wide spread hepatocyte apoptosis[130,144]. In this cohort of patients, GMCSF was significantly elevated in patients with acute liver failure who either died or required liver transplantation (Figure 7.15a). The receiver operator characteristic curve indicates that serum GMCSF has more limited discriminative ability than serum CSF1 (Figure 7.15b). There was no relationship between serum CSF1 and GMCSF levels (Figure 7.16).

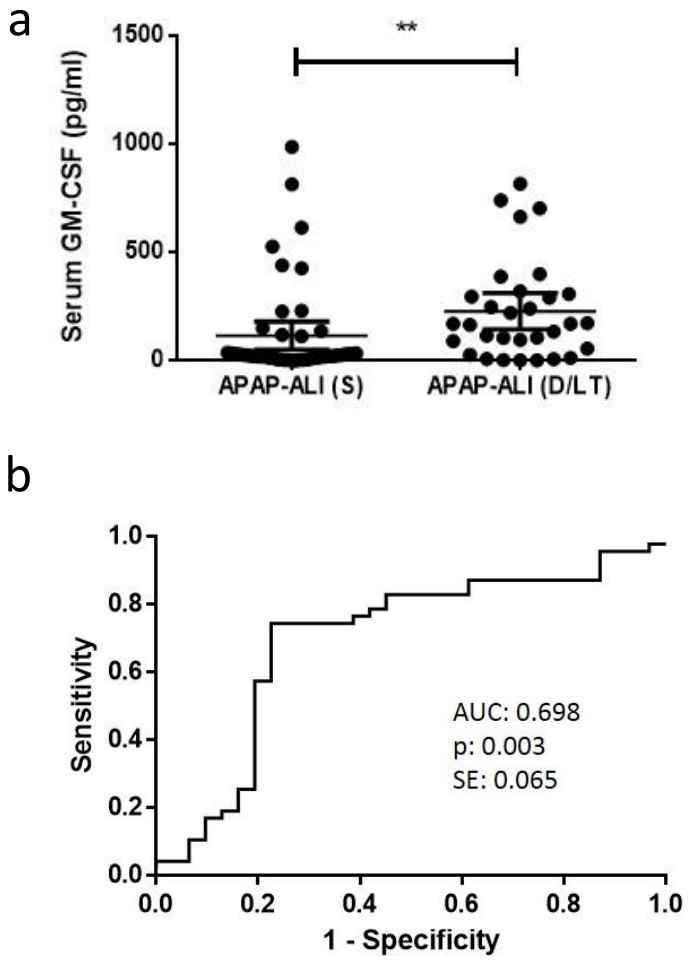


Figure 7.15: Serum GMCSF in acute liver failure

a) Serum GMCSF in patients presenting with acute liver failure due to paracetamol intoxication who either survived or died following admission to liver unit with acute liver failure (median; Mann-Whitney test). b) Receiver operator characteristic based on serum GMCSF level in patients who subsequently survived or died/required liver transplantation corresponding to cohort shown in (a).

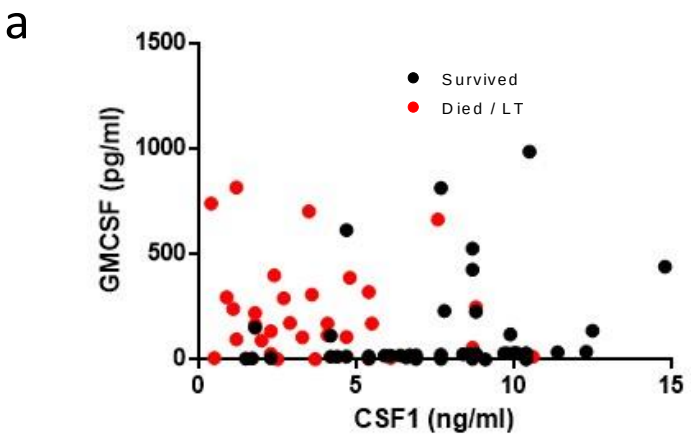


Figure 7.16: Relating serum GMCSF and CSF1 in acute liver failure

Serum GMCSF versus serum CSF1 in patients who either survived or died due to acute liver failure following paracetamol intoxication (survivors (black): $r^2$=0.038, p=0.19; died/LT (red): $r^2$=0.029, p=0.36).

## Discussion

In humans, I found that serum CSF1 level was elevated in all patients with acute liver failure induced by paracetamol intoxication. However serum CSF1 level was highest in those who survived compared with those who died or required liver transplantation. Given the ethical concerns regarding liver biopsy in humans I turned to the mouse model to assess hepatic CSF1 production. Here hepatic CSF1 gene expression increased following hepatic injury, peaking at Day 2. It is evident that hepatic CSF1 production drives macrophage accumulation during the early post injury phase when phagocytosis is essential to clear dying hepatocytes. Falling CSF1 levels in the non-survivor group therefore indicates worsening hepatic function. Falling CSF1 levels may also influence tissue macrophage phenotype[51], reduce monocyte survival[217] and potentially contributing to organ dysfunction at extrahepatic sites. The serum CSF1 reduction is consistent with the monocytopenia described in acute liver failure[51,52] particularly given the persistence of bone marrow monocyte precursors[52].

Others have shown that remaining monocytes express low levels of HLA-DR which can impair response to sepsis[51]. Supplementary CSF1 therapy in this setting might facilitate regeneration by increasing monocyte numbers, facilitate a proregenerative macrophage phenotype, increase monocyte HLA-DR expression[217] and enhance phagocytic capacity.

We tested whether the combination of serum CSF1 level, with the previous best biomarker of injury (acetyl-HMGB1[97]) could improve prognostic capacity. However, within the combined logistic regression model only serum CSF1 was significant, with no significant difference between the combined model and CSF1 alone. Given there is no clear advantage of combining CSF1 and acetyl-HMGB1 it would suggest that serum CSF1 is the maximal predictor of eventual death in this cohort.

The ability to stratify patients on admission to the specialist liver centre would be highly advantageous, potentially enabling earlier listing for transplantation in those predicted to die and even avoiding transplantation in those with a high chance of survival. This data provides a platform on which to power prospective studies and develop a validation cohort for the current observations.

The finding that serum GMCSF was significantly elevated in patients who died or required liver transplantation might reflect the more polarised inflammatory environment in patients with the severest liver injury. Animal models that demonstrate hepatocyte apoptosis in the presence of raised GMCSF indicate the potentially negative consequences of this situation[130]. The presence of competition between CSF1 and GMCSF for resulting cell phenotype may indicate that supplementary CSF1 could alter the cellular effects of this in a favourable direction.

## Conclusion

Serum CSF1 level is raised in patients with acute liver failure induced by paracetamol intoxication and demonstrates discriminative capacity in identifying those at the greatest risk of requirement for liver transplantation or death.

# Chapter 8. Overview and Opportunities

## 8.1 Overview

The objective of this project was to explore whether macrophages could be manipulated to enhance liver regeneration following acute injury. Hepatic macrophages perform a multitude of functions critical to maintaining homeostasis. Following hepatic injury, macrophage mediated innate immunity is compromised, associated with a high risk of sepsis. Given the role of hepatic macrophages in inducing hepatocyte proliferation, the link between innate immunity and regeneration is clear. The ability to enhance hepatic macrophage function could offer a therapeutic strategy to improve outcomes following liver injury.

I found that, following partial hepatectomy, macrophage number in the liver increases markedly, mainly via infiltration in the early stages and then subsequent proliferation. I trialled direct administration of macrophages in a clinically relevant model of chronic liver injury and partial hepatectomy. Experiments were hampered initially by technical difficulties with the fibrosis induction regimen and safe administration of the cells. After extensive optimisation I did not find a benefit with macrophage administration in this model.

I went on to explore the effects of macrophage stimulation in vivo. Here I used a potent CSF1 receptor stimulator, CSF1-Fc. CSF1-Fc resulted in marked upregulation of chemokines within the liver, via direct hepatic macrophage signalling. In particular the CCR2 ligands, CCl2, CCl7 and CCl12, were elevated. In the CCR2 -/- mouse there was a reduction in monocyte trafficking to the liver and liver size increase was less marked

following CSF1-Fc administration. As has been previously well characterised, CSF1 receptor stimulation can induce macrophage proliferation. I found that CSF1-Fc administration caused both a marked monocytosis and also stimulated tissue resident macrophages in the liver and spleen to proliferate. After 4 days of CSF1-Fc administration liver size had increased markedly. By assessment of F4/80 staining it was apparent that this was mainly due to macrophage accumulation, however there was evidence of hepatocyte proliferation. With an early increase in Il6 and evidence that Il6 can induce hepatocyte proliferation I found that this proliferation was reduced in the Il6 -/- mouse potentially implicating Il6 in this mechanism. A multitude of other factors changed based on analysis of gene array data, in particular matrix remodelling genes which are likely to also influence hepatocyte proliferation. The mechanism of hepatocyte proliferation is likely multifactorial, but given this occurs late and at a time of massive macrophage accumulation, this enhanced hepatocyte proliferation is likely to be of little clinical relevance.

It was interesting to note that the marked macrophage accumulation induced by CSF1-Fc did not appear detrimental to the mice, indeed injury markers were not elevated and systemic cytokine profile showed minimal disruption. Together these data indicate that it is the context which these inflammatory cells are in, rather than the simply the presence of these inflammatory cells, that drives the injurious response.

In the models of liver regeneration, the overwhelming phenotype following CSF1-Fc administration was that of macrophage accumulation involving both proliferation of resident macrophages and infiltration of circulating monocytes. There was an effect on hepatocyte proliferation at later time points, however this occurred at a timepoint when regeneration in the control treated mouse was effectively complete. The most clinically

relevant effect of CSF1-Fc on hepatic injury models was the enhanced innate immune capacity of the liver. This was as a direct consequence of the increased macrophage density within the liver. The fluorescent microbead assay that I developed demonstrated just how effective the liver macrophage is at clearing insoluble material.

Relating these preclinical findings to the clinical setting I have shown that serum CSF1 level rises following partial hepatectomy in humans. Given hepatic gene expression of CSF1 did not rise in mice following partial hepatectomy it is most likely that this increase in serum CSF1 related to extent of liver resection is due, at least in part, to impaired clearance by the reduced liver remnant size. Following paracetamol intoxication in humans a high CSF1 level was associated with survival in acute liver failure. I went on to examine biomarker potential using logistic regression models and show that serum CSF1 outperforms the previous best indicator of outcome in this model. These findings require validation in a prospective cohort of patients to assess potential use as a biomarker.

My work has identified a number of potential future studies, with both therapeutic and prognostic opportunities.

## 8.2 Therapeutic opportunities

The ability to enhance the innate immune capacity of the liver with CSF1-Fc could have number of possible applications in liver disease. Certainly the enhanced clearance of necrotic material following paracetamol intoxication and support for innate immune capacity could improve outcomes in the most severe liver injury. Of course the profound immune stimulation caused by CSF1-Fc could have deleterious effects. Therefore studying the effects of CSF1-Fc in a more clinically relevant model of acute liver injury would be an appropriate next step. The pig may offer an appropriate intermediary to the clinic given similarities between the pig and human mononuclear-phagocytic systems[218]. A porcine model of paracetamol intoxication has been established in Edinburgh and discussions are underway to trial CSF1-Fc in this model[219].

CSF1-Fc could have a role in boosting hepatic innate immune function following partial hepatectomy in humans. However, the effects of CSF1 on any residual cancer (given partial hepatectomy is mainly performed for malignant disease) are unclear. Concerns over the growth promoting effects of CSF1-Fc on cancer require further investigation. This could include studying the effects of CSF1-Fc on a mouse model of colorectal liver metastasis.

## 8.3 Prognostic opportunities

The ability to stratify patients according to predicted outcome prior to clinical deterioration would be highly advantageous. My results suggest that serum CSF1 could serve as a prognostic marker in acute liver failure, which could indicate which patients would benefit from supplementary CSF1 therapy. However this prognostic finding in retrospective cohort requires validation in a second cohort. If this validation reveals similar results then testing the prognostic capacity of CSF1 against current clinical criteria in a prospective trial will be required. This is an avenue that I am currently exploring.

Serum CSF1 level was raised in patients prior to partial hepatectomy and subsequently reduced when the cancer had been resected. In other cancers there has been an association between raised serum CSF1 and more aggressive malignancy. Therefore following this patient cohort over the next 5 years and relating perioperative CSF1 level to incidence of cancer recurrence may provide a tool to predict which cancers are most likely to recur. Stratifying patients in this way at an early stage could facilitate the administration of chemotherapeutics to patients with the greatest clinical need.

## 8.4 Conclusions

Macrophages have a central role in regeneration and manipulating macrophages can enhance regeneration of the injured liver. Providing a cellular therapy by stimulating a specific effector cell in vivo can induce profound effects, offering an alternative to direct cellular administration. The immune and regenerative responses are highly evolved to facilitate rapid recovery and identifying those factors which govern the response at a cellular level may provide an effective therapeutic strategy.

# References

1. Lombard, M. Liver disease and primary care: a briefing paper. Vol. 2014 (2011).

2. Schindl, M.J., Redhead, D.N., Fearon, K.C., Garden, O.J. & Wigmore, S.J. The value of residual liver volume as a predictor of hepatic dysfunction and infection after major liver resection. *Gut* **54**, 289-296 (2005).

3. UK, C.R. Liver cancer rates by age, UK 1975-2010. Vol. 2014 (2013).

4. Capocaccia, R.*, et al.* Hepatocellular carcinoma: trends of incidence and survival in Europe and the United States at the end of the 20th century. *Am J Gastroenterol* **102**, 1661-1670; quiz 1660, 1671 (2007).

5. Altekruse, S.F., McGlynn, K.A. & Reichman, M.E. Hepatocellular carcinoma incidence, mortality, and survival trends in the United States from 1975 to 2005. *J Clin Oncol* **27**, 1485-1491 (2009).

6. Takamoto, T.*, et al.* Recovery of liver function after the cessation of preoperative chemotherapy for colorectal liver metastasis. *Ann Surg Oncol* **17**, 2747-2755 (2010).

7. Berry, P.A.*, et al.* Admission levels and early changes in serum interleukin-10 are predictive of poor outcome in acute liver failure and decompensated cirrhosis. *Liver Int* **30**, 733-740 (2010).

8. Khuroo, M.S. & Kamili, S. Aetiology and prognostic factors in acute liver failure in India. *J Viral Hepat* **10**, 224-231 (2003).

9. Rantala, M. & van de Laar, M.J. Surveillance and epidemiology of hepatitis B and C in Europe - a review. *Euro surveillance : bulletin Europeen sur les maladies transmissibles = European communicable disease bulletin* **13**(2008).

10. Hawton, K.*, et al.* UK legislation on analgesic packs: before and after study of long term effect on poisonings. *BMJ* **329**, 1076 (2004).

11. Bretherick, A.D.*, et al.* Acute liver failure in Scotland between 1992 and 2009; incidence, aetiology and outcome. *QJM : monthly journal of the Association of Physicians* **104**, 945-956 (2011).

12. Bernal, W., Auzinger, G., Dhawan, A. & Wendon, J. Acute liver failure. *Lancet* **376**, 190-201 (2010).

13. Zamora Nava, L.E., Aguirre Valadez, J., Chavez-Tapia, N.C. & Torre, A. Acute-on-chronic liver failure: a review. *Therapeutics and clinical risk management* **10**, 295-303 (2014).

14. Kohler, J.J.*, et al.* Approaches to hepatitis C treatment and cure using NS5A inhibitors. *Infection and drug resistance* **7**, 41-56 (2014).

15. Pellicoro, A., Ramachandran, P. & Iredale, J.P. Reversibility of liver fibrosis. *Fibrogenesis & tissue repair* **5**, S26 (2012).

16. Godwin, J.W., Pinto, A.R. & Rosenthal, N.A. Macrophages are required for adult salamander limb regeneration. *Proc Natl Acad Sci U S A* **110**, 9415-9420 (2013).

17. Michalopoulos, G.K. Liver regeneration after partial hepatectomy: critical analysis of mechanistic dilemmas. *Am J Pathol* **176**, 2-13 (2010).

18. Mars, W.M.*, et al.* Immediate early detection of urokinase receptor after partial hepatectomy and its implications for initiation of liver regeneration. *Hepatology* **21**, 1695-1701 (1995).

19. Sokabe, T.*, et al.* Differential regulation of urokinase-type plasminogen activator expression by fluid shear stress in human coronary artery endothelial cells. *Am J Physiol Heart Circ Physiol* **287**, H2027-2034 (2004).

20. Michalopoulos, G.K. Liver regeneration. *J Cell Physiol* **213**, 286-300 (2007).

21. Yeh, C.C.*, et al.* Shear stress modulates macrophage-induced urokinase plasminogen activator expression in human chondrocytes. *Arthritis research & therapy* **15**, R53 (2013).

22. Gu, J.M.*, et al.* Urokinase plasminogen activator receptor promotes macrophage infiltration into the vascular wall of ApoE deficient mice. *J Cell Physiol* **204**, 73-82 (2005).

23. Kim, T.H., Mars, W.M., Stolz, D.B. & Michalopoulos, G.K. Expression and activation of pro-MMP-2 and pro-MMP-9 during rat liver regeneration. *Hepatology* **31**, 75-82 (2000).

24. LaMarre, J.*, et al.* An alpha 2-macroglobulin receptor-dependent mechanism for the plasma clearance of transforming growth factor-beta 1 in mice. *J Clin Invest* **87**, 39-44 (1991).

25. Yamada, Y., Kirillova, I., Peschon, J.J. & Fausto, N. Initiation of liver growth by tumor necrosis factor: deficient liver regeneration in mice lacking type I tumor necrosis factor receptor. *Proc Natl Acad Sci U S A* **94**, 1441-1446 (1997).

26. Cressman, D.E.*, et al.* Liver failure and defective hepatocyte regeneration in interleukin-6-deficient mice. *Science* **274**, 1379-1383 (1996).

27. Huang, W.*, et al.* Nuclear receptor-dependent bile acid signaling is required for normal liver regeneration. *Science* **312**, 233-236 (2006).

28. Selzner, N.*, et al.* ICAM-1 triggers liver regeneration through leukocyte recruitment and Kupffer cell-dependent release of TNF-alpha/IL-6 in mice. *Gastroenterology* **124**, 692-700 (2003).

29. Abshagen, K., Eipel, C., Kalff, J.C., Menger, M.D. & Vollmar, B. Loss of NF-kappaB activation in Kupffer cell-depleted mice impairs liver regeneration after partial hepatectomy. *Am J Physiol Gastrointest Liver Physiol* **292**, G1570-1577 (2007).

30. Tiberio, G.A.*, et al.* IL-6 Promotes compensatory liver regeneration in cirrhotic rat after partial hepatectomy. *Cytokine* **42**, 372-378 (2008).

31. Lesurtel, M.*, et al.* Platelet-derived serotonin mediates liver regeneration. *Science* **312**, 104-107 (2006).

32. Borude, P.*, et al.* Hepatocyte-specific deletion of farnesoid X receptor delays but does not inhibit liver regeneration after partial hepatectomy in mice. *Hepatology* **56**, 2344-2352 (2012).

33. Goh, Y.P.*, et al.* Eosinophils secrete IL-4 to facilitate liver regeneration. *Proc Natl Acad Sci U S A* **110**, 9914-9919 (2013).

34. DeAngelis, R.A.*, et al.* A complement-IL-4 regulatory circuit controls liver regeneration. *J Immunol* **188**, 641-648 (2012).

35. Oben, J.A. & Diehl, A.M. Sympathetic nervous system regulation of liver repair. *The anatomical record. Part A, Discoveries in molecular, cellular, and evolutionary biology* **280**, 874-883 (2004).

36. Wang, L.*, et al.* Liver sinusoidal endothelial cell progenitor cells promote liver regeneration in rats. *J Clin Invest* **122**, 1567-1573 (2012).

37. Olsen, P.S., Poulsen, S.S. & Kirkegaard, P. Adrenergic effects on secretion of epidermal growth factor from Brunner's glands. *Gut* **26**, 920-927 (1985).

38. Ochoa, B.*, et al.* Hedgehog signaling is critical for normal liver regeneration after partial hepatectomy in mice. *Hepatology* **51**, 1712-1723 (2010).

39. Dong, J.*, et al.* Elucidation of a universal size-control mechanism in Drosophila and mammals. *Cell* **130**, 1120-1133 (2007).

40. Sakamoto, T.*, et al.* Mitosis and apoptosis in the liver of interleukin-6-deficient mice after partial hepatectomy. *Hepatology* **29**, 403-411 (1999).

41. Braun, L.*, et al.* Transforming growth factor beta mRNA increases during liver regeneration: a possible paracrine mechanism of growth regulation. *Proc Natl Acad Sci U S A* **85**, 1539-1543 (1988).

42. Sanderson, N.*, et al.* Hepatic expression of mature transforming growth factor beta 1 in transgenic mice results in multiple tissue lesions. *Proc Natl Acad Sci U S A* **92**, 2572-2576 (1995).

43. Apte, U.*, et al.* Enhanced liver regeneration following changes induced by hepatocyte-specific genetic ablation of integrin-linked kinase. *Hepatology* **50**, 844-851 (2009).

44. Rahman, T.M. & Hodgson, H.J. Animal models of acute hepatic failure. *Int J Exp Pathol* **81**, 145-157 (2000).

45. Lee, W.M. & Seremba, E. Etiologies of acute liver failure. *Current opinion in critical care* **14**, 198-201 (2008).

46. Nelson, S.D. Molecular mechanisms of the hepatotoxicity caused by acetaminophen. *Semin Liver Dis* **10**, 267-278 (1990).

47. Zakowski, J.J. & Tappel, A.L. Purification and properties of rat liver mitochondrial glutathione peroxidase. *Biochim Biophys Acta* **526**, 65-76 (1978).

48. Antoine, D.J., Williams, D.P., Kipar, A., Laverty, H. & Park, B.K. Diet restriction inhibits apoptosis and HMGB1 oxidation and promotes inflammatory cell recruitment during acetaminophen hepatotoxicity. *Molecular medicine* **16**, 479-490 (2010).

49. Dambach, D.M., Watson, L.M., Gray, K.R., Durham, S.K. & Laskin, D.L. Role of CCR2 in macrophage migration into the liver during acetaminophen-induced hepatotoxicity in the mouse. *Hepatology* **35**, 1093-1103 (2002).

50. Hogaboam, C.M.*, et al.* Exaggerated Hepatic Injury Due to Acetaminophen Challenge in Mice Lacking C-C Chemokine Receptor 2. *The American Journal of Pathology* **156**, 1245-1252 (2000).

51. Antoniades, C.G.*, et al.* Reduced monocyte HLA-DR expression: a novel biomarker of disease severity and outcome in acetaminophen-induced acute liver failure. *Hepatology* **44**, 34-43 (2006).

52. Antoniades, C.G.*, et al.* Source and characterization of hepatic macrophages in acetaminophen-induced acute liver failure in humans. *Hepatology* **56**, 735-746 (2012).

53. Brattin, W.J., Glende, E.A., Jr. & Recknagel, R.O. Pathological mechanisms in carbon tetrachloride hepatotoxicity. *Journal of free radicals in biology & medicine* **1**, 27-38 (1985).

54. Clawson, G.A. Mechanisms of carbon tetrachloride hepatotoxicity. *Pathology and immunopathology research* **8**, 104-112 (1989).

55. Chieli, E. & Malvaldi, G. Role of the microsomal FAD-containing monooxygenase in the liver toxicity of thioacetamide S-oxide. *Toxicology* **31**, 41-52 (1984).

56. Xie, G.*, et al.* Role of differentiation of liver sinusoidal endothelial cells in progression and regression of hepatic fibrosis in rats. *Gastroenterology* **142**, 918-927 e916 (2012).

57. Pellicoro, A., Ramachandran, P., Iredale, J.P. & Fallowfield, J.A. Liver fibrosis and repair: immune regulation of wound healing in a solid organ. *Nature reviews. Immunology* **14**, 181-194 (2014).

58. Ruddell, R.G.*, et al.* A role for serotonin (5-HT) in hepatic stellate cell function and liver fibrosis. *Am J Pathol* **169**, 861-876 (2006).

59. Duffield, J.S.*, et al.* Selective depletion of macrophages reveals distinct, opposing roles during liver injury and repair. *J Clin Invest* **115**, 56-65 (2005).

60. Bourbonnais, E.*, et al.* Liver fibrosis protects mice from acute hepatocellular injury. *Gastroenterology* **142**, 130-139 e134 (2012).

61. Suarez-Cuenca, J.A.*, et al.* Partial hepatectomy-induced regeneration accelerates reversion of liver fibrosis involving participation of hepatic stellate cells. *Exp Biol Med (Maywood)* **233**, 827-839 (2008).

62. Moreau, R.*, et al.* Acute-on-chronic liver failure is a distinct syndrome that develops in patients with acute decompensation of cirrhosis. *Gastroenterology* **144**, 1426-1437, 1437 e1421-1429 (2013).

63. Arvaniti, V.*, et al.* Infections in patients with cirrhosis increase mortality four-fold and should be used in determining prognosis. *Gastroenterology* **139**, 1246-1256, 1256 e1241-1245 (2010).

64. Vaquero, J.*, et al.* Infection and the progression of hepatic encephalopathy in acute liver failure. *Gastroenterology* **125**, 755-764 (2003).

65. Rolando, N.*, et al.* The systemic inflammatory response syndrome in acute liver failure. *Hepatology* **32**, 734-739 (2000).

66. Bjerring, P.N., Eefsen, M., Hansen, B.A. & Larsen, F.S. The brain in acute liver failure. A tortuous path from hyperammonemia to cerebral edema. *Metabolic brain disease* **24**, 5-14 (2009).

67. Stravitz, R.T. & Larsen, F.S. Therapeutic hypothermia for acute liver failure. *Critical care medicine* **37**, S258-264 (2009).

68. Gao, B., Jeong, W.I. & Tian, Z. Liver: An organ with predominant innate immunity. *Hepatology* **47**, 729-736 (2008).

69. Mogensen, T.H. Pathogen recognition and inflammatory signaling in innate immune defenses. *Clinical microbiology reviews* **22**, 240-273, Table of Contents (2009).

70. Krueger, P.D., Lassen, M.G., Qiao, H. & Hahn, Y.S. Regulation of NK cell repertoire and function in the liver. *Critical reviews in immunology* **31**, 43-52 (2011).

71. Balmer, M.L.*, et al.* The liver may act as a firewall mediating mutualism between the host and its gut commensal microbiota. *Science translational medicine* **6**, 237ra266 (2014).

72. Wiest, R., Lawson, M. & Geuking, M. Pathological bacterial translocation in liver cirrhosis. *J Hepatol* **60**, 197-209 (2014).

73. Tuomisto, S.*, et al.* Changes in gut bacterial populations and their translocation into liver and ascites in alcoholic liver cirrhotics. *BMC Gastroenterol* **14**, 40 (2014).

74. Verbeke, L., Nevens, F. & Laleman, W. Bench-to-beside review: acute-on-chronic liver failure - linking the gut, liver and systemic circulation. *Crit Care* **15**, 233 (2011).

75. Wang, X.D., Soltesz, V., Andersson, R. & Bengmark, S. Bacterial translocation in acute liver failure induced by 90 per cent hepatectomy in the rat. *Br J Surg* **80**, 66-71 (1993).

76. Schindl, M.J.*, et al.* The adaptive response of the reticuloendothelial system to major liver resection in humans. *Ann Surg* **243**, 507-514 (2006).

77. Canalese, J.*, et al.* Reticuloendothelial system and hepatocytic function in fulminant hepatic failure. *Gut* **23**, 265-269 (1982).

78. Stutchfield, B.M. & Forbes, S.J. Liver sinusoidal endothelial cells in disease - And for therapy? *J Hepatol* **58**, 178-180 (2013).

79. Corbitt, N.*, et al.* Gut bacteria drive Kupffer cell expansion via MAMP-mediated ICAM-1 induction on sinusoidal endothelium and influence preservation-reperfusion injury after orthotopic liver transplantation. *Am J Pathol* **182**, 180-191 (2013).

80. MacDonald, K.P.*, et al.* An antibody against the colony-stimulating factor 1 receptor depletes the resident subset of monocytes and tissue- and tumor-associated macrophages but does not inhibit inflammation. *Blood* **116**, 3955-3963 (2010).

81. Hume, D.A., Pavli, P., Donahue, R.E. & Fidler, I.J. The effect of human recombinant macrophage colony-stimulating factor (CSF-1) on the murine mononuclear phagocyte system in vivo. *J Immunol* **141**, 3405-3409 (1988).

82. Wiktor-Jedrzejczak, W.*, et al.* Total absence of colony-stimulating factor 1 in the macrophage-deficient osteopetrotic (op/op) mouse. *Proc Natl Acad Sci U S A* **87**, 4828-4832 (1990).

83. Stanley, E.R.*, et al.* Biology and action of colony--stimulating factor-1. *Molecular reproduction and development* **46**, 4-10 (1997).

84. Bartocci, A.*, et al.* Macrophages specifically regulate the concentration of their own growth factor in the circulation. *Proc Natl Acad Sci U S A* **84**, 6179-6183 (1987).

85. Sauter, K.A.*, et al.* Pleiotropic effects of extended blockade of CSF1R signaling in adult mice. *J Leukoc Biol* (2014).

86. Devey, L.*, et al.* Tissue-resident macrophages protect the liver from ischemia reperfusion injury via a heme oxygenase-1-dependent mechanism. *Mol Ther* **17**, 65-72 (2009).

87. Thomas, J.A.*, et al.* Macrophage therapy for murine liver fibrosis recruits host effector cells improving fibrosis, regeneration and function. *Hepatology* (2011).

88. Abu-Tair, L.*, et al.* Natural killer cell-dependent anti-fibrotic pathway in liver injury via Toll-like receptor-9. *PLoS One* **8**, e82571 (2013).

89. Gao, B. Natural killer group 2 member D, its ligands, and liver disease: good or bad? *Hepatology* **51**, 8-11 (2010).

90. Proctor, W.R.*, et al.* Eosinophils mediate the pathogenesis of halothane-induced liver injury in mice. *Hepatology* **57**, 2026-2036 (2013).

91. Bjornsson, E., Kalaitzakis, E. & Olsson, R. The impact of eosinophilia and hepatic necrosis on prognosis in patients with drug-induced liver injury. *Aliment Pharmacol Ther* **25**, 1411-1421 (2007).

92. Chan, A.C.*, et al.* Liver transplantation for acute-on-chronic liver failure. *Hepatol Int* **3**, 571-581 (2009).

93. O'Grady, J. Liver transplantation for acute liver failure. *Best practice & research. Clinical gastroenterology* **26**, 27-33 (2012).

94. O'Grady, J.G., Alexander, G.J., Hayllar, K.M. & Williams, R. Early indicators of prognosis in fulminant hepatic failure. *Gastroenterology* **97**, 439-445 (1989).

95. Avery, R.K. Recipient screening prior to solid-organ transplantation. *Clinical infectious diseases : an official publication of the Infectious Diseases Society of America* **35**, 1513-1519 (2002).

96. O'Grady, J. Timing and benefit of liver transplantation in acute liver failure. *J Hepatol* **60**, 663-670 (2014).

97. Antoine, D.J.*, et al.* Molecular forms of HMGB1 and keratin-18 as mechanistic biomarkers for mode of cell death and prognosis during clinical acetaminophen hepatotoxicity. *J Hepatol* **56**, 1070-1079 (2012).

98. Antoine, D.J.*, et al.* Mechanistic biomarkers provide early and sensitive detection of acetaminophen-induced acute liver injury at first presentation to hospital. *Hepatology* (2013).

99. Xue, F.*, et al.* Hepatocyte growth factor gene therapy accelerates regeneration in cirrhotic mouse livers after hepatectomy. *Gut* **52**, 694-700 (2003).

100. Ozawa, S.*, et al.* Combination gene therapy of HGF and truncated type II TGF-beta receptor for rat liver cirrhosis after partial hepatectomy. *Surgery* **139**, 563-573 (2006).

101. Ido, A.*, et al.* Safety and pharmacokinetics of recombinant human hepatocyte growth factor (rh-HGF) in patients with fulminant hepatitis: a phase I/II clinical trial, following preclinical studies to ensure safety. *Journal of translational medicine* **9**, 55 (2011).

102. Harrison, P.M.*, et al.* Failure of insulin and glucagon infusion to stimulate liver regeneration in fulminant hepatic failure. *J Hepatol* **10**, 332-336 (1990).

103. Luo, S.M., Liang, L.J. & Lai, J.M. Effects of recombinant human growth hormone on remnant liver after hepatectomy in hepatocellular carcinoma with cirrhosis. *World J Gastroenterol* **10**, 1292-1296 (2004).

104. Stutchfield, B.M., Simpson, K. & Wigmore, S.J. Systematic review and meta-analysis of survival following extracorporeal liver support. *Br J Surg* **98**, 623-631 (2011).

105. Stutchfield, B.M., Forbes, S.J. & Wigmore, S.J. Prospects for stem cell transplantation in the treatment of hepatic disease. *Liver Transpl* **16**, 827-836 (2010).

106. Stutchfield, B.M., Rashid, S., Forbes, S.J. & Wigmore, S.J. Practical barriers to delivering autologous bone marrow stem cell therapy as an adjunct to liver resection. *Stem Cells Dev* **19**, 155-162 (2010).

107. Thorgeirsson, S.S. & Grisham, J.W. Hematopoietic cells as hepatocyte stem cells: a critical review of the evidence. *Hepatology* **43**, 2-8 (2006).

108. Wang, L., Wang, X., Xie, G., Hill, C.K. & Deleve, L.D. Liver sinusoidal endothelial cell progenitor cells promote liver regeneration in rats. *J Clin Invest* **122**, 1567-1573 (2012).

109. Theise, N.D.*, et al.* Derivation of hepatocytes from bone marrow cells in mice after radiation-induced myeloablation. *Hepatology* **31**, 235-240 (2000).

110. Lagasse, E.*, et al.* Purified hematopoietic stem cells can differentiate into hepatocytes in vivo. *Nat Med* **6**, 1229-1234 (2000).

111. Pittenger, M.F.*, et al.* Multilineage potential of adult human mesenchymal stem cells. *Science* **284**, 143-147 (1999).

112. Moore, J.K., Stutchfield, B.M. & Forbes, S.J. Systematic review: the effects of autologous stem cell therapy for patients with liver disease. *Aliment Pharmacol Ther* **39**, 673-685 (2014).

113. Zocco, M.A.*, et al.* CD133+ stem cell mobilization after partial hepatectomy depends on resection extent and underlying disease. *Digestive and Liver Disease* **43**, 147-154 (2011).

114. Garg, V.*, et al.* Granulocyte-Colony Stimulating Factor Mobilizes CD34+ Cells and improves Survival of Patients with Acute-On-Chronic Liver Failure. *Gastroenterology* (2011).

115. Furst, G.*, et al.* Portal vein embolization and autologous CD133+ bone marrow stem cells for liver regeneration: initial experience. *Radiology* **243**, 171-179 (2007).

116. am Esch, J.S., 2nd*, et al.* Portal application of autologous CD133+ bone marrow cells to the liver: a novel concept to support hepatic regeneration. *Stem Cells* **23**, 463-470 (2005).

117. Lorenzini, S.*, et al.* Characterisation of a stereotypical cellular and extracellular adult liver progenitor cell niche in rodents and diseased human liver. *Gut* **59**, 645-654 (2010).

118. Aldeguer, X.*, et al.* Interleukin-6 from intrahepatic cells of bone marrow origin is required for normal murine liver regeneration. *Hepatology* **35**, 40-48 (2002).

119. Klein, I.*, et al.* Kupffer cell heterogeneity: functional properties of bone marrow derived and sessile hepatic macrophages. *Blood* **110**, 4077-4085 (2007).

120. Meijer, C.*, et al.* Kupffer cell depletion by CI2MDP-liposomes alters hepatic cytokine expression and delays liver regeneration after partial hepatectomy. *Liver* **20**, 66-77 (2000).

121. Prins, H.A.*, et al.* Kupffer cell-depleted rats have a diminished acute-phase response following major liver resection. *Shock* **21**, 561-565 (2004).

122. Prins, H.A.*, et al.* The role of Kupffer cells after major liver surgery. *JPEN J Parenter Enteral Nutr* **29**, 48-55 (2005).

123. Abshagen, K., Eipel, C., Kalff, J.C., Menger, M.D. & Vollmar, B. Kupffer cells are mandatory for adequate liver regeneration by mediating hyperperfusion via modulation of vasoactive proteins. *Microcirculation* **15**, 37-47 (2008).

124. Luo, J.*, et al.* Colony-stimulating factor 1 receptor (CSF1R) signaling in injured neurons facilitates protection and survival. *J Exp Med* **210**, 157-172 (2013).

125. Alikhan, M.A.*, et al.* Colony-stimulating factor-1 promotes kidney growth and repair via alteration of macrophage responses. *Am J Pathol* **179**, 1243-1256 (2011).

126. Matsumoto, K.*, et al.* Serial changes of serum growth factor levels and liver regeneration after partial hepatectomy in healthy humans. *International journal of molecular sciences* **14**, 20877-20889 (2013).

127. Meng, F.*, et al.* Role of stem cell factor and granulocyte colony-stimulating factor in remodeling during liver regeneration. *Hepatology* **55**, 209-221 (2012).

128. Vassiliou, I.*, et al.* The combined effect of erythropoietin and granulocyte macrophage colony stimulating factor on liver regeneration after major hepatectomy in rats. *World J Surg Oncol* **8**, 57 (2010).

129. Eroglu, A.*, et al.* Effect of granulocyte-macrophage colony-stimulating factor on hepatic regeneration after 70% hepatectomy in normal and cirrhotic rats. *HPB (Oxford)* **4**, 67-73 (2002).

130. Hirano, K.*, et al.* Overexpression of granulocyte-macrophage colony-stimulating factor in mouse liver enhances the susceptibility of lipopolysaccharide leading to massive apoptosis of hepatocytes. *Liver Int* **25**, 1027-1035 (2005).

131. Crofton, R.W., Diesselhoff-den Dulk, M.M. & van Furth, R. The origin, kinetics, and characteristics of the Kupffer cells in the normal steady state. *J Exp Med* **148**, 1-17 (1978).

132. Volkman, A. Disparity in origin of mononuclear phagocyte populations. *J Reticuloendothel Soc* **19**, 249-268 (1976).

133. Yamamoto, T.*, et al.* Repopulation of murine Kupffer cells after intravenous administration of liposome-encapsulated dichloromethylene diphosphonate. *Am J Pathol* **149**, 1271-1286 (1996).

134. Lehenkari, P.P.*, et al.* Further insight into mechanism of action of clodronate: inhibition of mitochondrial ADP/ATP translocase by a nonhydrolyzable, adenine-containing metabolite. *Molecular pharmacology* **61**, 1255-1262 (2002).

135. Auffray, C., Sieweke, M.H. & Geissmann, F. Blood monocytes: development, heterogeneity, and relationship with dendritic cells. *Annual review of immunology* **27**, 669-692 (2009).

136. Jenkins, S.J.*, et al.* Local macrophage proliferation, rather than recruitment from the blood, is a signature of TH2 inflammation. *Science* **332**, 1284-1288 (2011).

137. Davies, L.C.*, et al.* Distinct bone marrow-derived and tissue-resident macrophage lineages proliferate at key stages during inflammation. *Nature communications* **4**, 1886 (2013).

138. Schulz, C.*, et al.* A lineage of myeloid cells independent of Myb and hematopoietic stem cells. *Science* **336**, 86-90 (2012).

139. Yona, S.*, et al.* Fate mapping reveals origins and dynamics of monocytes and tissue macrophages under homeostasis. *Immunity* **38**, 79-91 (2013).

140. Rosas, M.*, et al.* The transcription factor Gata6 links tissue macrophage phenotype and proliferative renewal. *Science* **344**, 645-648 (2014).

141. Ezure, T., Ishiwata, T., Asano, G., Tanaka, S. & Yokomuro, K. Production of macrophage colony-stimulating factor by murine liver in vivo. *Cytokine* **9**, 53-58 (1997).

142. Stanley, E.R., Berg, K.L., Einstein, D.B., Lee, P.S. & Yeung, Y.G. The biology and action of colony stimulating factor-1. *Stem Cells* **12 Suppl 1**, 15-24; discussion 25 (1994).

143. Chitu, V. & Stanley, E.R. Colony-stimulating factor-1 in immunity and inflammation. *Current opinion in immunology* **18**, 39-48 (2006).

144. Hamilton, J.A. Colony-stimulating factors in inflammation and autoimmunity. *Nature reviews. Immunology* **8**, 533-544 (2008).

145. Li, Y.*, et al.* Induction of functional human macrophages from bone marrow promonocytes by M-CSF in humanized mice. *J Immunol* **191**, 3192-3199 (2013).

146. Phillips, W.A. & Hamilton, J.A. Colony stimulating factor-1 is a negative regulator of the macrophage respiratory burst. *J Cell Physiol* **144**, 190-196 (1990).

147. Martinez, F.O., Sica, A., Mantovani, A. & Locati, M. Macrophage activation and polarization. *Frontiers in bioscience : a journal and virtual library* **13**, 453-461 (2008).

148. Zhang, M.Z.*, et al.* CSF-1 signaling mediates recovery from acute kidney injury. *J Clin Invest* **122**, 4519-4532 (2012).

149. Nandi, S.*, et al.* The CSF-1 receptor ligands IL-34 and CSF-1 exhibit distinct developmental brain expression patterns and regulate neural progenitor cell maintenance and maturation. *Developmental biology* **367**, 100-113 (2012).

150. Menke, J.*, et al.* CSF-1 signals directly to renal tubular epithelial cells to mediate repair in mice. *J Clin Invest* **119**, 2330-2342 (2009).

151. Dai, X.M.*, et al.* Targeted disruption of the mouse colony-stimulating factor 1 receptor gene results in osteopetrosis, mononuclear phagocyte deficiency, increased primitive progenitor cell frequencies, and reproductive defects. *Blood* **99**, 111-120 (2002).

152. Lin, H.*, et al.* Discovery of a cytokine and its receptor by functional screening of the extracellular proteome. *Science* **320**, 807-811 (2008).

153. Wang, Y.*, et al.* IL-34 is a tissue-restricted ligand of CSF1R required for the development of Langerhans cells and microglia. *Nature immunology* **13**, 753-760 (2012).

154. Ferenbach, D. & Hughes, J. Macrophages and dendritic cells: what is the difference? *Kidney Int* **74**, 5-7 (2008).

155. Hume, D.A. Macrophages as APC and the dendritic cell myth. *J Immunol* **181**, 5829-5835 (2008).

156. Itoh, Y.*, et al.* Serum levels of macrophage colony stimulating factor (M-CSF) in liver disease. *J Hepatol* **21**, 527-535 (1994).

157. Duffield, J.S.*, et al.* Conditional ablation of macrophages halts progression of crescentic glomerulonephritis. *Am J Pathol* **167**, 1207-1219 (2005).

158. Ramachandran, P.*, et al.* Differential Ly-6C expression identifies the recruited macrophage phenotype, which orchestrates the regression of murine liver fibrosis. *Proc Natl Acad Sci U S A* **109**, E3186-3195 (2012).

159. Dhaliwal, K.*, et al.* Monocytes control second-phase neutrophil emigration in established lipopolysaccharide-induced murine lung injury. *American journal of respiratory and critical care medicine* **186**, 514-524 (2012).

160. Medoff, B.D.*, et al.* CD11b+ Myeloid Cells Are the Key Mediators of Th2 Cell Homing into the Airway in Allergic Inflammation. *The Journal of Immunology* **182**, 623-635 (2008).

161. Movita, D.*, et al.* Kupffer cells express a unique combination of phenotypic and functional characteristics compared with splenic and peritoneal macrophages. *J Leukoc Biol* **92**, 723-733 (2012).

162. Amemiya, H., Kono, H. & Fujii, H. Liver Regeneration is Impaired in Macrophage Colony Stimulating Factor Deficient Mice After Partial Hepatectomy: The Role of M-CSF-Induced Macrophages. *J Surg Res* (2009).

163. Sasmono, R.T.*, et al.* A macrophage colony-stimulating factor receptor-green fluorescent protein transgene is expressed throughout the mononuclear phagocyte system of the mouse. *Blood* **101**, 1155-1163 (2003).

164. Gow, D.J.*, et al.* Cloning and expression of porcine Colony Stimulating Factor-1 (CSF-1) and Colony Stimulating Factor-1 Receptor (CSF-1R) and analysis of the species specificity of stimulation by CSF-1 and Interleukin 34. *Cytokine* **60**, 793-805 (2012).

165. Jenkins, S.J.*, et al.* IL-4 directly signals tissue-resident macrophages to proliferate beyond homeostatic levels controlled by CSF-1. *J Exp Med* **210**, 2477-2491 (2013).

166. McGill, M.R.*, et al.* The mechanism underlying acetaminophen-induced hepatotoxicity in humans and mice involves mitochondrial damage and nuclear DNA fragmentation. *J Clin Invest* **122**, 1574-1583 (2012).

167. Mitchell, C. & Willenbring, H. A reproducible and well-tolerated method for 2/3 partial hepatectomy in mice. *Nature protocols* **3**, 1167-1170 (2008).

168. Henderson, N.C.*, et al.* Critical role of c-jun (NH2) terminal kinase in paracetamol-induced acute liver failure. *Gut* **56**, 982-990 (2007).

169. R Development Core Team. R: A language and environment for statistical computing. (R Foundation for Statistical Computing, Vienna, Austria, 2010).

170. Starkel, P. & Leclercq, I.A. Animal models for the study of hepatic fibrosis. *Best practice & research. Clinical gastroenterology* **25**, 319-333 (2011).

171. Colakoglu, T., Keskek, M., Colakoglu, S., Can, B. & Sayek, I. Serum endostatin levels and regenerative capacities of normal and cirrhotic livers following partial hepatectomy in mice: the response to different resection sizes. *J Surg Res* **143**, 337-343 (2007).

172. Fujii, T.*, et al.* Mouse model of carbon tetrachloride induced liver fibrosis: Histopathological changes and expression of CD133 and epidermal growth factor. *BMC Gastroenterol* **10**, 79 (2010).

173. Espanol-Suner, R.*, et al.* Liver progenitor cells yield functional hepatocytes in response to chronic liver injury in mice. *Gastroenterology* **143**, 1564-1575 e1567 (2012).

174. Kuramitsu, K.*, et al.* Failure of fibrotic liver regeneration in mice is linked to a severe fibrogenic response driven by hepatic progenitor cell activation. *Am J Pathol* **183**, 182-194 (2013).

175. de Graaf, W.*, et al.* Quantitative assessment of hepatic function during liver regeneration in a standardized rat model. *J Nucl Med* **52**, 294-302 (2011).

176. de Graaf, W.*, et al.* Transporters involved in the hepatic uptake of (99m)Tc-mebrofenin and indocyanine green. *J Hepatol* **54**, 738-745 (2011).

177. de Graaf, W., Bennink, R.J., Vetelainen, R. & van Gulik, T.M. Nuclear imaging techniques for the assessment of hepatic function in liver surgery and transplantation. *J Nucl Med* **51**, 742-752 (2010).

178. de Graaf, W.*, et al.* Assessment of future remnant liver function using hepatobiliary scintigraphy in patients undergoing major liver resection. *J Gastrointest Surg* **14**, 369-378 (2010).

179. Fan, S.T. Liver functional reserve estimation: state of the art and relevance for local treatments: the Eastern perspective. *J Hepatobiliary Pancreat Sci* **17**, 380-384 (2010).

180. Lam, C.M., Fan, S.T., Lo, C.M. & Wong, J. Major hepatectomy for hepatocellular carcinoma in patients with an unsatisfactory indocyanine green clearance test. *Br J Surg* **86**, 1012-1017 (1999).

181. Faybik, P.*, et al.* Comparison of invasive and noninvasive measurement of plasma disappearance rate of indocyanine green in patients undergoing liver transplantation: a prospective investigator-blinded study. *Liver Transpl* **10**, 1060-1064 (2004).

182. Yuan, L., Lin, W., Zheng, K., He, L. & Huang, W. Far-red to near infrared analyte-responsive fluorescent probes based on organic fluorophore platforms for fluorescence imaging. *Chemical Society reviews* **42**, 622-661 (2013).

183. Manizate, F., Hiotis, S.P., Labow, D., Roayaie, S. & Schwartz, M. Liver functional reserve estimation: state of the art and relevance to local treatments. *Oncology* **78 Suppl 1**, 131-134 (2010).

184. Potteaux, S.*, et al.* Suppressed monocyte recruitment drives macrophage removal from atherosclerotic plaques of Apoe-/- mice during disease regression. *J Clin Invest* **121**, 2025-2036 (2011).

185. Gersuk, G.M., Razai, L.W. & Marr, K.A. Methods of in vitro macrophage maturation confer variable inflammatory responses in association with altered expression of cell surface dectin-1. *J Immunol Methods* **329**, 157-166 (2008).

186. Bukowski, R.M., *et al.* Phase I trial of subcutaneous recombinant macrophage colony-stimulating factor: clinical and immunomodulatory effects. *J Clin Oncol* **12**, 97-106 (1994).

187. Weiner, L.M., *et al.* Phase I trial of recombinant macrophage colony-stimulating factor and recombinant gamma-interferon: toxicity, monocytosis, and clinical effects. *Cancer Res* **54**, 4084-4090 (1994).

188. Momin, F.A., *et al.* Phase II trial of recombinant human macrophage colony-stimulating factor in metastatic soft tissue sarcoma. *Journal of immunotherapy with emphasis on tumor immunology : official journal of the Society for Biological Therapy* **16**, 224-228 (1994).

189. Cole, D.J., *et al.* Phase I trial of recombinant human macrophage colony-stimulating factor administered by continuous intravenous infusion in patients with metastatic cancer. *Journal of the National Cancer Institute* **86**, 39-45 (1994).

190. Pollard, J.W. Role of colony-stimulating factor-1 in reproduction and development. *Molecular reproduction and development* **46**, 54-60; discussion 60-51 (1997).

191. Marshall, S.A., Lazar, G.A., Chirino, A.J. & Desjarlais, J.R. Rational design and engineering of therapeutic proteins. *Drug discovery today* **8**, 212-221 (2003).

192. Jones, E.A. & Waldmann, T.A. The mechanism of intestinal uptake and transcellular transport of IgG in the neonatal rat. *J Clin Invest* **51**, 2916-2927 (1972).

193. Goldenberg, M.M. Etanercept, a novel drug for the treatment of patients with severe, active rheumatoid arthritis. *Clin Ther* **21**, 75-87; discussion 71-72 (1999).

194. Hoffman, H.M., *et al.* Efficacy and safety of rilonacept (interleukin-1 Trap) in patients with cryopyrin-associated periodic syndromes: results from two sequential placebo-controlled studies. *Arthritis Rheum* **58**, 2443-2452 (2008).

195. Gow DJ, S.K., Hume DA. NCBI GEO database, accession: PRJNA229512 ID:229512. (2013).

196. Murray, P.J. & Wynn, T.A. Protective and pathogenic functions of macrophage subsets. *Nature reviews. Immunology* **11**, 723-737 (2011).

197. Tagliani, E.*, et al.* Coordinate regulation of tissue macrophage and dendritic cell population dynamics by CSF-1. *J Exp Med* **208**, 1901-1916 (2011).

198. Radi, Z.A.*, et al.* Increased serum enzyme levels associated with kupffer cell reduction with no signs of hepatic or skeletal muscle injury. *Am J Pathol* **179**, 240-247 (2011).

199. Sakaguchi, S., Wing, K., Onishi, Y., Prieto-Martin, P. & Yamaguchi, T. Regulatory T cells: how do they suppress immune responses? *International immunology* **21**, 1105-1111 (2009).

200. Zhang, M., Xu, S., Han, Y. & Cao, X. Apoptotic cells attenuate fulminant hepatitis by priming Kupffer cells to produce interleukin-10 through membrane-bound TGF-beta. *Hepatology* **53**, 306-316 (2011).

201. Ogiku, M., Kono, H., Ishii, K., Hosomura, N. & Fujii, H. Role of macrophage colony-stimulating factor in polymicrobial sepsis according to studies using osteopetrotic (op/op) mice. *J Surg Res* **169**, 106-116 (2011).

202. Feltis, B.A., Jechorek, R.P., Erlandsen, S.L. & Wells, C.L. Bacterial translocation and lipopolysaccharide-induced mortality in genetically macrophage-deficient op/op mice. *Shock* **2**, 29-33 (1994).

203. Leevy, C.M., Smith, F., Longueville, J., Paumgartner, G. & Howard, M.M. Indocyanine green clearance as a test for hepatic function. Evaluation by dichromatic ear densitometry. *JAMA* **200**, 236-240 (1967).

204. Schindl, M.J.*, et al.* The value of residual liver volume as a predictor of hepatic dysfunction and infection after major liver resection. *Gut* **54**, 289-296 (2005).

205. Jacobs, K.E., Visser, B.C. & Gayer, G. Changes in spleen volume after resection of hepatic colorectal metastases. *Clinical radiology* **67**, 982-987 (2012).

206. Nagasue, N., Yukaya, H., Ogawa, Y. & Higashi, T. Portal pressure following partial to extensive hepatic resection in patients with and without cirrhosis of the liver. *Annales chirurgiae et gynaecologiae* **72**, 18-22 (1983).

207. Zoli, M., Melli, A., Viti, G., Marra, A. & Marchesini, G. Sonographic evaluation of liver, spleen, and splanchnic vessels following partial liver resection. *Journal of ultrasound in medicine : official journal of the American Institute of Ultrasound in Medicine* **5**, 563-567 (1986).

208. Mebius, R.E. & Kraal, G. Structure and function of the spleen. *Nature reviews. Immunology* **5**, 606-616 (2005).

209. McDevitt, D.G. & Nies, A.S. Simultaneous measurement of cardiac output and its distribution with microspheres in the rat. *Cardiovasc Res* **10**, 494-498 (1976).

210. Swirski, F.K.*, et al.* Identification of splenic reservoir monocytes and their deployment to inflammatory sites. *Science* **325**, 612-616 (2009).

211. Furuya, S.*, et al.* Interleukin-17A plays a pivotal role after partial hepatectomy in mice. *J Surg Res* **184**, 838-846 (2013).

212. Ueda, S.*, et al.* Transforming growth factor-beta1 released from the spleen exerts a growth inhibitory effect on liver regeneration in rats. *Lab Invest* **83**, 1595-1603 (2003).

213. Rothstein, G.*, et al.* Stimulation of neutrophil production in CSF-1-responsive clones. *Blood* **72**, 898-902 (1988).

214. Aharinejad, S.*, et al.* Elevated CSF1 serum concentration predicts poor overall survival in women with early breast cancer. *Endocrine-related cancer* **20**, 777-783 (2013).

215. Webster, J.A.*, et al.* Variations in stromal signatures in breast and colorectal cancer metastases. *J Pathol* **222**, 158-165 (2010).

216. de Jong, M.C.*, et al.* Rates and patterns of recurrence following curative intent surgery for colorectal liver metastasis: an international multi-institutional analysis of 1669 patients. *Ann Surg* **250**, 440-448 (2009).

217. Becker, S., Warren, M.K. & Haskill, S. Colony-stimulating factor-induced monocyte survival and differentiation into macrophages in serum-free cultures. *J Immunol* **139**, 3703-3709 (1987).

218. Bode, G.*, et al.* The utility of the minipig as an animal model in regulatory toxicology. *J Pharmacol Toxicol Methods* **62**, 196-220 (2010).

219. Newsome, P.N.*, et al.* Development of an invasively monitored porcine model of acetaminophen-induced acute liver failure. *BMC Gastroenterol* **10**, 34 (2010).

# Appendices

a

| Symbol | $Log_2$(FC) | p Value |
|---|---|---|
| Adipoq | 1.22 | 1.9E-01 |
| Bmp2 | 0.04 | 7.0E-01 |
| Bmp4 | 0.32 | 5.9E-01 |
| Bmp6 | 0.06 | 9.0E-01 |
| Bmp7 | -0.90 | 9.1E-03 |
| Ccl1 | -0.23 | 2.5E-01 |
| Ccl11 | 1.32 | 9.7E-02 |
| Ccl12 | 4.92 | 2.8E-02 |
| Ccl17 | -0.20 | 8.2E-01 |
| Ccl19 | 0.65 | 9.6E-03 |
| Ccl2 | 4.34 | 3.7E-02 |
| Ccl20 | -0.11 | 5.2E-01 |
| Ccl22 | -1.39 | 5.3E-02 |
| Ccl24 | 0.78 | 2.6E-01 |
| Ccl3 | 3.19 | 1.1E-02 |
| Ccl4 | 2.61 | 3.3E-03 |
| Ccl5 | -0.26 | 3.4E-01 |
| Ccl7 | 6.58 | 2.9E-02 |
| Cd40lg | 0.74 | 1.9E-01 |
| Cd70 | -0.23 | 2.5E-01 |
| Cntf | 2.34 | 4.0E-02 |
| Csf1 | -0.75 | 4.6E-02 |
| Csf2 | -0.23 | 2.5E-01 |
| Csf3 | -0.23 | 2.5E-01 |
| Ctf1 | -1.06 | 2.8E-02 |
| Cx3cl1 | -0.29 | 7.3E-01 |
| Cxcl1 | 2.51 | 1.2E-01 |
| Cxcl10 | 1.46 | 8.6E-02 |
| Cxcl11 | 1.23 | 2.0E-01 |
| Cxcl12 | -0.33 | 2.8E-01 |
| Cxcl13 | 2.48 | 3.5E-02 |
| Cxcl16 | 0.55 | 1.2E-01 |
| Cxcl3 | -0.23 | 2.5E-01 |
| Cxcl5 | 0.40 | 4.3E-01 |
| Cxcl9 | 2.15 | 8.1E-02 |
| Fasl | 1.00 | 2.8E-01 |
| Gpi1 | -1.01 | 1.5E-01 |
| Hc | 1.60 | 6.5E-02 |
| Ifna2 | -0.28 | 1.9E-01 |
| Ifng | 0.97 | 2.4E-01 |
| Il10 | 1.23 | 9.8E-02 |
| Il11 | -0.23 | 2.5E-01 |
| Il12a | 0.35 | 3.7E-01 |
| Il12b | 1.62 | 5.4E-02 |
| Il13 | 0.05 | 7.3E-01 |
| Il15 | 1.09 | 1.1E-01 |
| Il16 | 0.06 | 7.6E-01 |
| Il17a | -0.23 | 2.5E-01 |
| Il17f | -0.40 | 2.0E-01 |
| Il18 | 1.23 | 8.2E-02 |
| Il1a | 2.21 | 7.7E-02 |
| Il1b | 1.99 | 6.5E-02 |
| Il1rn | 0.77 | 2.2E-01 |
| Il2 | -0.23 | 2.5E-01 |
| Il21 | -0.23 | 2.5E-01 |
| Il22 | -0.23 | 2.5E-01 |
| Il23a | 0.55 | 2.0E-01 |
| Il24 | -0.23 | 2.5E-01 |
| Il27 | 0.33 | 4.6E-01 |
| Il3 | -0.23 | 2.5E-01 |
| Il4 | 0.56 | 2.4E-01 |
| Il5 | -0.52 | 4.9E-02 |
| Il6 | 2.92 | 2.7E-02 |
| Il7 | 3.26 | 3.1E-02 |
| Il9 | -0.23 | 2.5E-01 |
| Lif | -0.49 | 3.5E-02 |
| Lta | -0.26 | 2.1E-01 |
| Ltb | -0.91 | 1.9E-01 |
| Mif | -0.40 | 2.3E-01 |
| Mstn | -0.23 | 2.5E-01 |
| Nodal | -0.35 | 6.5E-01 |
| Osm | -0.49 | 3.1E-01 |
| Pf4 | 1.30 | 7.3E-02 |
| Ppbp | 1.13 | 6.2E-01 |
| Spp1 | 2.36 | 5.2E-02 |
| Tgfb2 | 0.11 | 8.2E-01 |
| Thpo | -1.04 | 2.5E-01 |
| Tnf | 1.47 | 6.5E-03 |
| Tnfrsf11b | -0.13 | 2.5E-01 |
| Tnfsf10 | 1.07 | 1.4E-01 |
| Tnfsf11 | 0.72 | 2.3E-01 |
| Tnfsf13b | 0.36 | 4.4E-01 |
| Vegfa | -0.34 | 4.1E-02 |
| Xcl1 | 1.09 | 1.1E-01 |

b

| Symbol | $Log_2$(FC) | p Value |
|---|---|---|
| Ccl1 | 0.002385 | 0.995794 |
| Ccl11 | -0.168240 | 0.536477 |
| Ccl12 | 0.340998 | 0.222394 |
| Ccl17 | 0.350058 | 0.523640 |
| Ccl2 | 2.709541 | 0.002325 |
| Ccl20 | -0.257800 | 0.522280 |
| Ccl22 | -0.003820 | 0.991413 |
| Ccl24 | 4.451104 | 0.000773 |
| Ccl25 | -0.567320 | 0.048705 |
| Ccl26 | 0.111996 | 0.726955 |
| Ccl28 | -0.125580 | 0.668265 |
| Ccl3 | 1.853422 | 0.026058 |
| Ccl4 | 0.047096 | 0.882061 |
| Ccl5 | 1.067192 | 0.046863 |
| Ccl6 | 3.482285 | 0.001805 |
| Ccl7 | 2.569480 | 0.001451 |
| Ccl8 | 0.389965 | 0.329903 |
| Ccl9 | 1.035653 | 0.006856 |
| Cx3cl1 | -0.174560 | 0.325000 |
| Cx3cr1 | 2.630355 | 0.0000173 |
| Cxcl1 | 0.259143 | 0.284000 |
| Cxcl10 | 1.504879 | 0.002040 |
| Cxcl11 | -0.046100 | 0.747000 |
| Cxcl12 | -0.624460 | 0.008220 |
| Cxcl13 | 1.454787 | 0.000929 |
| Cxcl14 | 1.312222 | 0.000592 |
| Cxcl16 | 0.857306 | 0.005100 |
| Cxcl17 | -0.437610 | 0.041200 |
| Cxcl2 | 0.126631 | 0.385000 |
| Cxcl3 | -0.214340 | 0.212000 |
| Cxcl5 | -0.033550 | 0.801000 |
| Cxcl9 | 1.213310 | 0.002300 |
| Cxcr1 | 0.102748 | 0.442000 |
| Cxcr2 | 1.359056 | 0.001130 |
| Cxcr3 | 0.629190 | 0.040800 |
| Cxcr4 | 0.763783 | 0.001620 |
| Cxcr5 | 0.373911 | 0.057100 |
| Cxcr6 | 0.072390 | 0.614000 |
| Cxcr7 | -0.071870 | 0.592000 |
| Il10 | 1.098651 | 0.022699 |
| Il11 | 0.051655 | 0.911474 |
| Il12a | -0.021180 | 0.950502 |
| Il12b | -0.112150 | 0.828744 |
| Il13 | -0.273940 | 0.272598 |
| Il15 | 1.856345 | 0.001956 |
| Il16 | 1.187241 | 0.003583 |
| Il17a | -0.084110 | 0.739953 |
| Il17b | -0.091550 | 0.815429 |
| Il17c | -0.463920 | 0.200050 |
| Il17c | 0.010033 | 0.981785 |
| Il17f | -0.192430 | 0.454471 |
| Il18 | 1.137145 | 0.039239 |
| Il19 | -0.186460 | 0.447878 |
| Il1a | 1.515215 | 0.003066 |
| Il1b | 0.022323 | 0.963081 |
| Il2 | -0.160390 | 0.585434 |
| Il20 | -0.129630 | 0.631845 |
| Il21 | -0.010280 | 0.979687 |
| Il23a | 0.175548 | 0.572363 |
| Il24 | -0.144800 | 0.553631 |
| Il25 | -0.450970 | 0.098911 |
| Il27 | 0.117625 | 0.669325 |
| Il3 | -0.266650 | 0.245468 |
| Il31 | -0.167720 | 0.526649 |
| Il33 | 0.182980 | 0.553712 |
| Il34 | -0.096760 | 0.772368 |
| Il4 | -0.026460 | 0.936779 |
| Il5 | 0.103314 | 0.737716 |
| Il6 | 0.905786 | 0.020833 |
| Il7 | -0.325000 | 0.410956 |
| Il8 | -0.030550 | 0.919070 |
| Il9 | 0.038919 | 0.894045 |
| Tnf | 2.459398 | 0.020345 |

c

| | | |
|---|---|---|
| Egr3 | -0.291400 | 0.280588 |
| Egr4 | -0.376980 | 0.213341 |
| Eps15 | 0.107026 | 0.797723 |
| Eps15l1 | 0.040064 | 0.906857 |
| Eps8 | -0.075380 | 0.906857 |
| Figf | -0.485030 | 0.204820 |
| Gh | 0.012867 | 0.972631 |
| Hbegf | 1.352622 | 0.001149 |
| Hdgf | -0.127120 | 0.656973 |
| Hdgfl1 | -0.131720 | 0.672690 |
| Hdgfrp2 | -0.010030 | 0.979734 |
| Hgf | -0.450120 | 0.222047 |
| Hgfac | -0.238740 | 0.411344 |
| Igf1 | -0.097930 | 0.729274 |
| Igf1r | -0.117700 | 0.801570 |
| Igf2 | -0.056340 | 0.843021 |
| Negr1 | -0.086150 | 0.766151 |
| Ngf | -0.460200 | 0.111945 |
| Ngfr | -0.736200 | 0.059311 |
| Pdgfa | 0.465977 | 0.117691 |
| Pdgfb | 0.991616 | 0.007461 |
| Pdgfc | -0.211820 | 0.675008 |
| Pdgfd | -0.197900 | 0.537439 |
| Pdgfra | -0.572180 | 0.355846 |
| Pdgfrb | -0.861800 | 0.125556 |
| Pdgfrl | -0.258090 | 0.326537 |
| Pdgfrl | -0.572030 | 0.388097 |
| Pgf | -0.000710 | 0.998317 |
| Tbrg1 | 0.108164 | 0.727556 |
| Tbrg3 | -0.178770 | 0.733905 |
| Tbrg4 | -0.197680 | 0.482563 |
| Tdgf1 | -0.149860 | 0.632217 |
| Tdgf1 | 0.143482 | 0.698228 |
| Tgfa | -0.410510 | 0.156402 |
| Tgfb1 | 2.289855 | 0.000376 |
| Tgfb1l1 | 0.103577 | 0.671180 |
| Tgfb2 | -0.159720 | 0.644567 |
| Tgfb3 | 0.361496 | 0.140552 |
| Vegfa | -0.828610 | 0.053316 |
| Vegfb | -0.271860 | 0.503342 |
| Vegfc | -0.323240 | 0.345173 |
| Vgf | -0.095750 | 0.813812 |
| mmp10 | -0.042620 | 0.906141 |
| Mmp11 | -0.158150 | 0.681161 |
| Mmp12 | -0.084730 | 0.805337 |
| Mmp13 | 0.446693 | 0.256490 |
| Mmp14 | -0.686370 | 0.167780 |
| Mmp15 | -0.872020 | 0.048521 |
| Mmp16 | -0.102840 | 0.689880 |
| Mmp17 | 0.145901 | 0.583675 |
| Mmp19 | -0.470300 | 0.170145 |
| Mmp1a | 0.004525 | 0.990216 |
| Mmp1b | -0.115430 | 0.708046 |
| Mmp2 | -0.583840 | 0.309094 |
| Mmp20 | -0.180910 | 0.505194 |
| Mmp21 | -0.183850 | 0.587209 |
| Mmp23 | -0.339780 | 0.326083 |
| Mmp24 | -0.145820 | 0.673170 |
| Mmp25 | 0.196496 | 0.465701 |
| Mmp27 | 1.811892 | 0.000480 |
| Mmp28 | -0.032310 | 0.916099 |
| Mmp3 | -0.188470 | 0.570204 |
| Mmp7 | -0.173460 | 0.541824 |
| Mmp8 | 2.969730 | 0.001315 |
| Mmp9 | 3.296842 | 0.000596 |
| Plat | -0.206960 | 0.453605 |
| Plau | 2.652202 | 0.000628 |
| Plaur | 1.661674 | 0.000692 |
| Hgf | -0.450120 | 0.222047 |
| Hgfac | -0.238740 | 0.411344 |
| Egf | -0.317090 | 0.268757 |
| Igf1 | -0.097930 | 0.729274 |
| Igf1r | -0.117700 | 0.801570 |
| Igf2 | -0.056340 | 0.843021 |

d

| Symbol | $Log_2$(FC) | p Value |
|---|---|---|
| "M1" macrophage associated genes | | |
| Ccl20 | -0.257800 | 0.522280 |
| Ccl8 | 0.389965 | 0.329903 |
| Ccr7 | 0.349207 | 0.146326 |
| Cd86 | 3.004163 | 0.000357 |
| Cxcl10 | 1.504879 | 0.029807 |
| Cxcl11 | -0.046100 | 0.887823 |
| Cxcl13 | 1.454787 | 0.017555 |
| Cxcl9 | 1.213310 | 0.032081 |
| Il5 | 1.856345 | 0.001956 |
| Il1b | 0.022323 | 0.963081 |
| Il23 | 0.175548 | 0.572363 |
| Il6 | 0.905786 | 0.020833 |
| Ccl19 | 0.115345 | 0.838495 |
| Tnf | 1.298305 | 0.020345 |
| Ido1 | -0.067330 | 0.884483 |
| Il12 | -0.112150 | 0.828744 |
| Marco | 1.480924 | 0.041149 |
| Nos2 | 0.161927 | 0.538278 |
| Cox2 | -0.011760 | 0.975532 |
| Socs3 | -0.268260 | 0.824650 |
| "M2" macrophage associated genes | | |
| Ccl17 | 0.350058 | 0.523640 |
| Ccl26 | 0.111996 | 0.726955 |
| Cd209a | 0.763811 | 0.016345 |
| Cd209b | -0.244000 | 0.406381 |
| Cd209c | -0.171900 | 0.634459 |
| Cd209d | -0.210780 | 0.391446 |
| Cd209e | -0.069370 | 0.842254 |
| Cd209f | 3.367643 | 0.000773 |
| Cd209g | 0.509477 | 0.066775 |
| Clec7a | 2.650960 | 0.001220 |
| Igf1 | -0.097930 | 0.729274 |
| Mrc1 | 0.939408 | 0.015454 |
| Mrc2 | -0.156000 | 0.705061 |
| Sra1 | -0.157280 | 0.646825 |
| Tgfb1 | 2.289855 | 0.000376 |
| Ccl1 | 0.002385 | 0.995794 |
| Ccl20 | -0.257800 | 0.522280 |
| Cxcl1 | 0.259143 | 0.556753 |
| Cxcl2 | 0.126631 | 0.649036 |
| Cxcl3 | -0.214340 | 0.478363 |
| Il10 | 1.098651 | 0.022699 |
| Cd163 | 2.597270 | 0.001044 |
| Il21r | 0.861225 | 0.023289 |
| Tlr1 | 3.029518 | 0.000420 |
| Tlr8 | 2.857926 | 0.000450 |
| Chia | 0.003217 | 0.993376 |
| Fgl2 | 2.195027 | 0.000472 |
| Irf4 | 1.212479 | 0.020706 |
| Klf4 | 0.352448 | 0.209271 |
| Mrc2 | -0.156000 | 0.705061 |
| Relma | -0.114580 | 0.672062 |
| Socs2 | -0.157730 | 0.878418 |
| Sra1 | -0.157280 | 0.646825 |
| F4/80 | 2.874018 | 0.000357 |
| CSf1r | 1.929132 | 0.001049 |
| Cd68 | 2.621014 | 0.000467 |
| Ym-1 | 2.038519 | 0.047152 |
| Arginase | -0.339890 | 0.176144 |
| Lyve-1 | 0.844508 | 0.114706 |
| Fr | 0.177723 | 0.447043 |
| Msr1 | 2.760593 | 0.000485 |

Appendix 1: Gene array data

a) Array data 6 hours following CSF1-Fc administration in uninjured mice (n=4/group).

b) Cytokine / chemokine gene data extracted from Affymetrix gene array comparing

CSF1-Fc treatment (n=3) or PBS control at day 4. c) Growth factor and matrix remodelling associated gene data extracted from Affymetrix gene array comparing CSF1-Fc treatment (n=3) or PBS control at day 4. d) Macrophage phenotype data extracted from Affymetrix gene array comparing CSF1-Fc treatment (n=3) or PBS control at day 4 (blue= M1 associated genes; red=M2 associated genes).

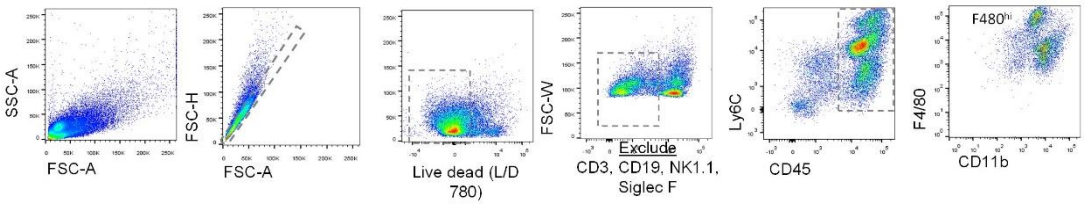


Appendix 2: Gating strategy for hepatic macrophage identification

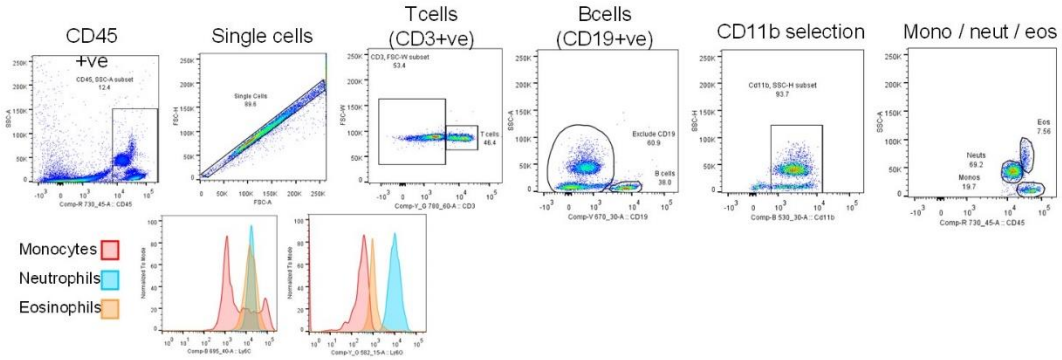


Appendix 3: Gating strategy for T cells , B cells, monoyctes, neutrophils and eosinophils.

| Healthy controls | | | | |
|---|---|---|---|---|
| n | Age | M:F | Acetyl-HMGB1 (ng/ml) | CSF1 (ng/ml) |
| 50 | 35 (10) | 4/5 | 0.06 (0.09) | 0.22 (0.12) |

Appendix 4: Healthy control details

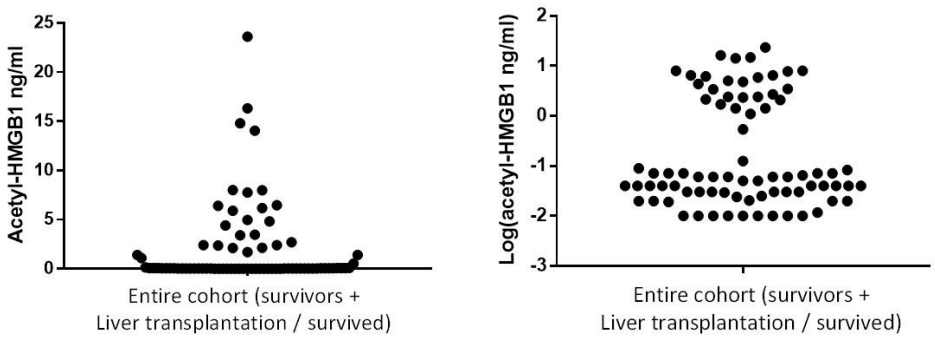


Appendix 5: Dot plots showing acetyl-HMG1 level in entire cohort and log(acetyl-HMGB1) in entire cohort.

**Logistic regression model for CSF1 alone**

| | Estimate | Std Error | Z value | p |
|---|---|---|---|---|
| **(intercept)** | 2.6536 | 0.7047 | 3.765 | <0.0001 |
| **CSF1** | -0.5449 | 0.1214 | -4.489 | <0.0001 |

Appendix 6: Details of logistic regression models for CSF1 alone.

**Logistic regression model for acetyl-HMGB1 alone**

| | Estimate | Std Error | Z value | p |
|---|---|---|---|---|
| **(intercept)** | 0.5623 | 0.3619 | 1.554 | 0.12 |
| **Log(acetyl -HMGB1)** | 0.5952 | 0.1284 | 4.637 | <0.0001 |

Appendix 7: Details of logistic regression models for acetyl-HMGB1 alone.

**Deviance residuals**

| | Min | 1Q | Median | 3Q | Max |
|---|---|---|---|---|---|
| **CSF1** | -1.9447 | -0.7227 | -0.3097 | 0.6767 | 2.5161 |
| **Log(acetyl-HMGB1)** | -1.9763 | -0.6779 | -0.5125 | 0.6470 | 2.1382 |
| **Combined model** | -2.1060 | -0.6573 | -0.3428 | 0.5701 | 2.8091 |

Appendix 8: Deviance residuals for logistic regression models.